NUREG/CR-0458
SAND78-0029
RW

Risk Methodology for Geologic Disposal of Radioactive Waste: Interim Report

James E. Campbell, Richard T. Dillon, Martin S. Tierney, Herbert T. Davis, Peter E. McGrath, F. Joe Pearson, Jr., Herbert R. Shaw, Jon C. Helton, Fred A. Donath

Printed October 1978

Sandia Laboratories

SF 2900-Q(7-73)

407 101

Prepared for

U. S. NUCLEAR REGULATORY COMMISSION

256 44

Issued by Sandia Laboratories, operated for the United States Department of Energy by Sandia Corporation.

Printed in the United States of America

Available from
National Technical Information Service
U. S. Department of Commerce
5285 Port Royal Road
Springfield, VA 22161

Price: Printed Copy $10.75; Microfiche $3.00

NUREG/CR-0458
SAND78-0029
RW

RISK METHODOLOGY FOR GEOLOGIC DISPOSAL OF RADIOACTIVE WASTE: INTERIM REPORT

James E. Campbell
Richard T. Dillon
Martin S. Tierney
Herbert T. Davis
Peter E. McGrath
Sandia Laboratories

F. Joe Pearson, Jr. and Herbert R. Shaw
U. S. Geological Survey

Jon C. Helton
Arizona State University

Fred A. Donath
University of Illinois

Date Published: October 1978

Sandia Laboratories
Albuquerque, New Mexico 87185
operated by
Sandia Corporation
for the
U. S. Department of Energy

Prepared for
Office of Nuclear Regulatory Research
Probabilistic Analysis Staff
U. S. Nuclear Regulatory Commission
Washington, DC 20555
Under Interagency Agreement DOE 40-550-75
NRC Fin No. A1192

ACKNOWLEDGMENTS

We thank the many people who have contributed to the work represented in this report. The following people deserve special recognition: (1) J. P. Brannen (Sandia) for his many contributions in the initial stages of the project; (2) L. Konikow and D. Grove (USGS Water Resources Division, Denver) for their guidance during development of the Radionuclide Transport Model; (3) R. Lantz and S. Pahwa (INTERA Environmental Consultants, Houston) for development of the Radionuclide Transport Model and assistance in its use; (4) L. Hearne and D. Posson (USGS Water Resources Division, Albuquerque) for their assistance in establishing groundwater flow conditions in the Reference System; (5) Ann Frazier (Sandia) for her work in adapting the Transport Model to Sandia's computing system; (6) Ron Iman (Sandia) for his work in developing a statistical design for use of the models presented in this report; (7) G. Apostolakis (UCLA) and J. Conover (Texas Tech) for their assistance in probabilistic modeling; (8) E. Appel, R. McCurley, and F. Lusso (Sandia) for their assistance in data compilation, computer programming and report editing, (9) M. Cullingford (Nuclear Regulatory Commission) for many constructive suggestions and (10) D. J. McCloskey (Sandia) for his continuing strong managerial support.

ABSTRACT

The Fuel Cycle Risk Analysis Division of Sandia Laboratories is funded by the Nuclear Regulatory Commission (NRC) to develop a methodology for assessment of the long-term risks from radioactive waste disposal in deep, geologic media. The first phase of this work, which is documented in this report, involves the following: (1) development of analytical models to represent the processes by which radioactive waste might leave the waste repository, enter the surface environment and eventually reach humans and (2) definition of a hypothetical "reference system" to provide a realistic setting for exercise of the models in a risk or safety assessment. The second phase of this work, which will be documented in a later report, will involve use of the analytical models in a demonstration risk or safety assessment of the reference system. The analytical methods and data developed in this study are expected to form the basis for a portion of the NRC repository licensing methodology.

CONTENTS

CONTENTS (cont)

403 001

CONTENTS (cont)

CONTENTS (cont)

403 009

CONTENTS (cont)

403 010

CONTENTS (cont)

403 011

FIGURES

FIGURES (cont)

403 013

TABLES

INTRODUCTION

The Fuel Cycle Risk Analysis Division of Sandia Laboratories is funded by the Nuclear Regulatory Commission (NRC) to develop a methodology for assessment of the long-term risks from radioactive waste disposal in deep, geologic media. The first phase of this work, which is documented in this report, involves the following: (1) development of analytical models to represent the processes by which radioactive waste may leave the waste repository, enter the surface environment and eventually reach humans and (2) definition of a hypothetical "reference system" to provide a realistic setting for exercise of the models in a risk or safety assessment. The second phase of this work, which will be documented in a later report, will involve use of the analytical models in a demonstration risk or safety assessment of the reference system. The analytical methods and data developed in this study are expected to form the basis for a portion of the NRC repository licensing methodology.

The long-term risk from radioactive waste results from the possibility of a release of previously contained wastes to the human environment. The risk may be expressed as a time-dependent probability of consequences such as somatic or genetic health effects which arise from a release of radioactive waste. The magnitude of this risk, and its time dependence, have not been completely assessed. A complete assessment would take into consideration all mechanisms which could result in, or contribute to, movement of waste from the repository to the biosphere. Once the waste enters the biosphere, its long-term distribution, accumulation, and uptake by man must be analyzed. Finally, the human health effects that are implied by such a distribution of waste in the biosphere need to be quantified.

The models and limited data bases supplied in this report are only the first steps toward an assessment of the levels of risks. However, it is expected that the insight derived from the construction of the analytical models and the compilation of a data base will, ultimately, lead to the placing of bounds on the risk. In view of the lack of experience with deep, geologic disposal systems, such insight and data will be indispensable in the evaluation of proposed repositories against waste management regulations.

The major elements and the organization of our methodology for the analysis of deep, geologic repositories are shown in Figure 1. The "site description" and "radioactive waste description" blocks represent information and numerical data that must be supplied to the analytical models, which are shown as the four, central blocks of the diagram. These models are treated in self-contained chapters of the present report.

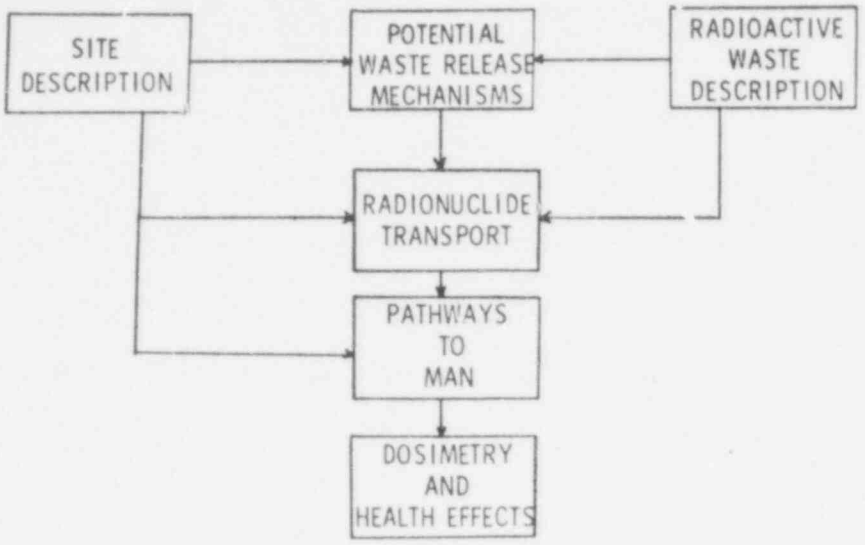

Figure 1. Structure of the Methodology

Parts of the site description and radioactive waste description are presented in Chapter 1. Because a real repository in deep geologic media does not presently exist, we have defined a hypothetical facility, called the reference repository. The reference repository definition includes design specifications of the repository, a description of the wastes contained in the repository, summary statements of the local stratigraphy and hydrology, and assumptions about the topographic setting of the waste disposal site. Other information required for the analysis of the reference repository is supplied, as necessary, in each of the chapters devoted to the models. The numerical values quoted for the parameters that describe the reference site in this report should be considered exemplary and not as final values. An important part of risk assessment is the study of the sensitivity of the risk to the waste facility characteristics. Thus, many of the site, waste, and facility parameters introduced in the report will be varied over reasonable but perhaps large ranges in the course of sensitivity studies.

Models of the potential waste release mechanisms that may operate at the reference repository are discussed in Chapter 2. These models attempt to provide insight into the evolution of the repository site and to estimate the time-dependent probability of local release of radioactivity from the immediate surroundings of the repository. Included in this study are those processes that are initiated by excavation and waste emplacement (the self-induced release mechanisms) and those processes that are, roughly speaking, independent of the presence of the repository (the external release mechanisms). The evolution of the repository site in the presence of thermally hot wastes and the consequences for self-induced release are studied by means of computer simulation of the waste/host rock and mine/host rock interactions. The basis for the simulation and some results are presented in an extensive appendix to Chapter 2. The external release mechanisms are studied in Chapter 2 by means of direct, probabilistic modeling of the phenomena.

A model for the transport of radionuclides in circulating groundwater and the hydrology of the reference site are discussed in Chapter 3. The transport model described in that chapter calculates the movement of waste-derived radionuclides dissolved in groundwater from the time of their release at the repository, to the time of their appearance in surface waters or in ground water used by humans. During transport by groundwater, radioactive decay and production of daughter radionuclides are calculated. The model also accounts for sorption of the nuclides in the geologic media. The output of the radionuclide transport model is radionuclide discharge rates at preselected points in the biosphere.

The transport of radionuclides by ground water through the subsurface to the biosphere is the most likely process for bringing the waste into contact with man. There are, however, certain other potential modes of release (e.g., volcanism, meteorite impact, and very large explosions) that might produce prompt and substantial ejection of waste material to the atmosphere and surrounding soils. As yet, no effort has been made to model the ejection and subsequent atmospheric transport of waste that follows these types of release. If further study shows that these release modes are significant contributors to risk, models for atmospheric transport of radioactive materials are available.

A pathways-to-man model is presented in Chapter 4. Starting with radionuclide discharge rates from the groundwater transport model (Chapter 3), or the fallout pattern from an atmospheric transport model, the pathways model first calculates time-dependent concentrations of radionuclides in environmental components such as soil, surface waters, or sediments. These concentrations are then used to estimate the rates of radionuclide inhalation or ingestion by human beings who use water or food products derived from the affected environmental components.

The pathways-to-man model is constructed to handle a variety of environmental scenarios in which the waste radionuclides could come in contact with humans. Such flexibility is necessary because we are unable to predict the social and climatological variables that might characterize a region affected by a release at some future time. Thus, it is necessary that we consider different environments and use the pathways model to study the rates of human uptake in each environment to gain insight into the potential risk from waste disposal.

The models for dosimetry and human health effects are described in Chapter 5. The rate of radionuclide intake provided by the pathways model in a given scenario is translated by the dosimetry model into radiation dose to specific body organs. A health effects model then converts the radiation dose to probabilities of specific latent somatic effects and genetic effects. Only latent somatic effects are addressed in the health effects model because we believe that the radiation doses arising from release of waste material preclude any early somatic effects.

A final Chapter 6 provides a brief description of the manner in which the models represented in this report might be used in the assessment of a radioactive waste repository.

RISK METHODOLOGY FOR GEOLOGIC DISPOSAL OF RADIOACTIVE WASTE:
INTERIM REPORT

CHAPTER 1. THE REFERENCE SITE AND REFERENCE REPOSITORY

1.1 Introduction

A comparison of the merits and demerits of any system requires a thorough knowledge of the parts of the system and the ways in which those parts interact. Thus it has been necessary in the present study to postulate a detailed but entirely hypothetical system -- a disposal facility for nuclear waste in bedded salt -- to serve as a guide for constructing the requisite models, and to provide a consistent set of data for testing the models. The present chapter contains a brief summary description of the hypothetical system, herein called the reference site in the geographical and geological context, or the reference repository in the engineered structure context.

Some of the physiographic, geologic, and hydrologic aspects of the reference site are mentioned in Section 1.2. Other physical properties of the site, particularly those elements bearing on the site's long-term capacity for waste containment, are described in later chapters as they are needed for analysis. The reference repository mentioned in Section 1.3 is taken from a design for a waste isolation facility in bedded salt; the subject matter of Section 1.3 is concerned more with the means by which the design isolation facility could be realistically converted to serve in the disposal mode. Finally, in Section 1.4, assumptions are made about the kinds and amounts of nuclear waste that are placed in the reference repository.

The background provided by this chapter and its referenced material will be used and supplemented throughout the remainder of this report.

1.2 The Reference Site

The reference site is entirely hypothetical, yet its physiographic setting and geologic and hydrologic properties are analogous to several regions of the continental USA. Such a relatively complicated reference site was used to exercise the several models developed in this study. The ultimate purpose of the models is to analyze the behavior of real, potential repository sites.

The site is located in a symmetrical upland valley, half of which is shown schematically in Figure 1.2.1. The crest of the ridge surrounding the valley is at an elevation of 6000 feet: the crest is a surface and groundwater divide so that only water moving in the valley falls in the

valley itself. The valley is drained by a major river, River L, which is at elevation 2500 feet opposite the surface structures of the repository. Stream valleys tributary to River L exist, such as River U, but these are normally dry. The valley receives a mean annual rainfall of 40 inches per year of which 16 inches are lost by evapotranspiration and the remaining 24 inches recharge the groundwater system.

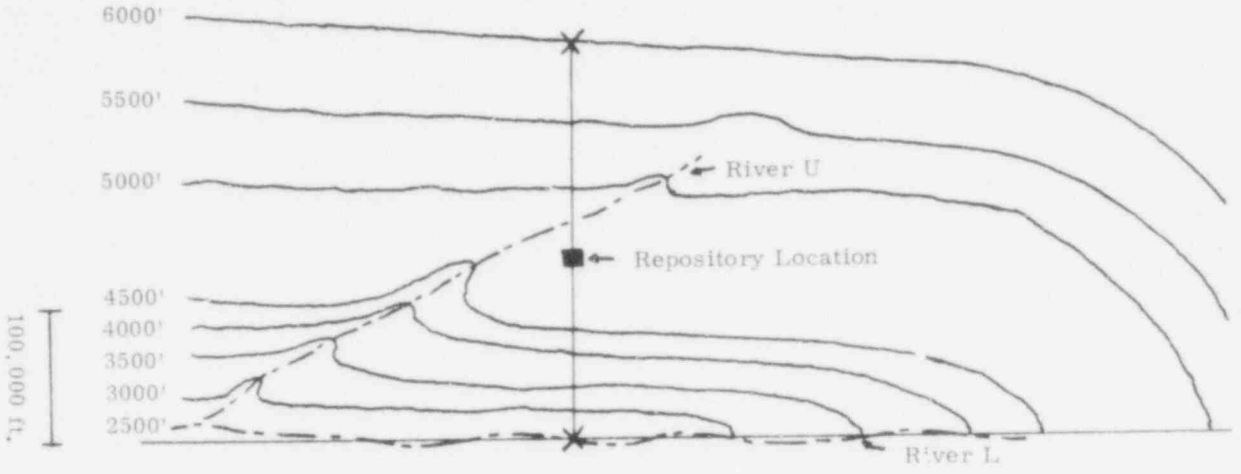

Figure 1.2.1 Physiographic Setting for Reference Site
(One-Half of Parabolic Basin Shown)

The geology of the area near the site is shown in cross section in Figure 1.2.2. The valley is underlain by crystalline bedrock which crops out only over a narrow strip lying at the ridge crest surrounding the valley. This bedrock is assumed impermeable to groundwater flow. Above the bedrock is the sequence of sedimentary rocks roughly sketched in Figure 1.2.2. A more detailed petrographic description of the sedimentary sequence is not necessary at this point. Values of hydraulic parameters, and assumed values of rock thermal-elastic parameters, are provided in tables appearing later in this report, as needed. The thermal-elastic parameters have been used in preliminary calculations of the response of the site's host rocks to thermal loading; these parameters are listed in Section 2.4 of Chapter 2. The hydraulic parameters used in preliminary calculations of groundwater flow and radionuclide transport are provided in the appropriate sections of Chapter 3.

As stated in the introduction to this chapter, the other assumptions about the geologic setting of the site (these generally relate to site location within a geologic province, regional tectonics, and man-made alterations of rock structure) are made in the chapters where such material is required; but usually they are made in a way that is consistent with the structures postulated in Figures 1.2.1 and 1.2.2.

403 019

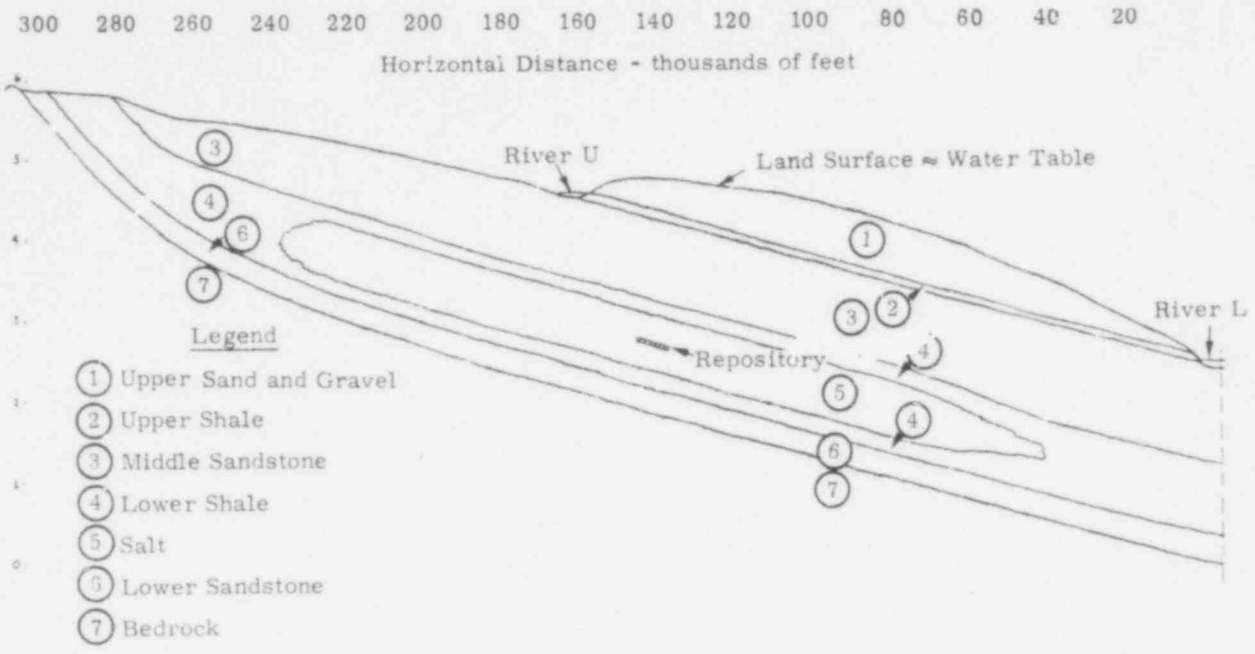

Figure 1.2.2 Geologic Cross Section at Reference Site
(Vertical Exaggeration X20)

1.3 The Reference Repository

Like the choice of reference site, the choice of a reference repository for analysis is entirely hypothetical. The repository is a waste isolation facility designed for the Office of Waste Isolation, Union Carbide Corporation, at Oak Ridge, Tennessee.[1.1] A perspective of this facility is shown in Figure 1.3.1.

The facility consists of (1) service structures located at the surface of the site and (2) the single, working level of the repository located in the middle of the bedded salt layer at a depth of 625 meters (2050 ft) below the surface. For the study of the long-term effects of such a facility, the details of the service structures are immaterial. However, details of the repository at the working level are important. Some of these are shown schematically in the mine master plan of Figure 1.3.2, which also exhibits the sectors of the repository reserved for high-level waste (HLW), intermediate-level waste and cladding waste (ILW and CW), and low-level waste (LLW). Most of the relevant dimensions of the underground repository can be read from the mine master plan in Figure 1.3.2. Other dimensions (drift widths and lengths, etc.) can be found in the engineering specifications.[1.1] The working level of the repository has access to the surface during operational phase through four shafts: a men and materials shaft 7.9 meters (26 ft) inside diameter; an LL waste loading shaft 3 meters (10 ft) ID; a HL waste loading shaft 1.8 meters (6 ft) ID; and a ventilation shaft 6.1 meters (20 ft) inside diameter. All access shafts are lined with 12 inches of 3000 psi concrete.

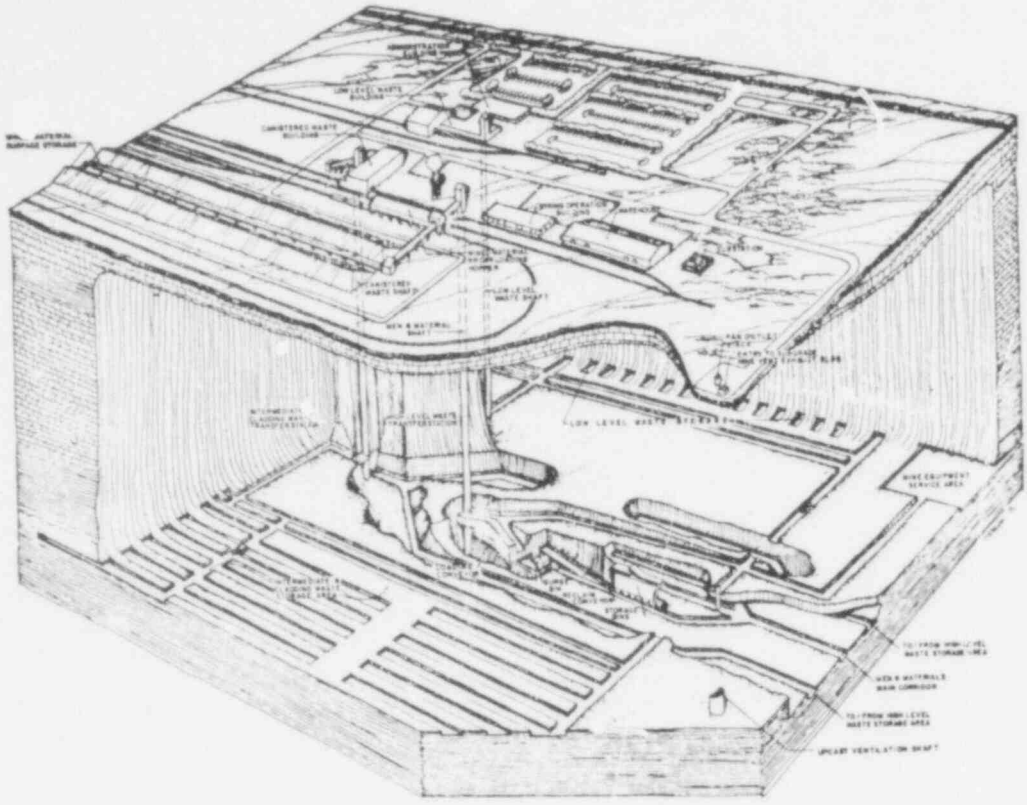

Figure 1, 3, 1 Waste Isolation Facility - Perspective

Figure 1, 3, 2 Mine Master Plan and Waste Storage Sectors

403 021

Assumptions About Conversion from Isolation to Disposal

It is necessary to make assumptions about the techniques to be used in converting the isolation facility just described into the mode of permanent disposal. The facility design provided in Reference 1.1 says nothing about plans for conversion to a disposal mode, and other references[1.2] only suggest some possible techniques.

First of all, a summary description of the encapsulation and local storage procedures for the several waste forms is needed. The more detailed assumptions about the amount and form of the waste to be placed in the repository are treated in the following Section, 1.4, of this chapter.

It is assumed that solidified HL waste is formed in stainless steel containers about 12 inches outside diameter and 10 feet long. Each such container is to be placed in a hole bored in the floor of waste drifts located in the HL sectors of the mine. The holes for the cannisters are 20 inches in diameter and 20 feet deep, lined with a carbon steel sleeve. The void between the sleeve and cannister is filled with crushed salt. During the operational phase the openings of the cannister holes in the floor of the drifts are closed with concrete plugs. The encapsulation and storage of cladding hulls and the ILW-TRU waste is assumed to be the same as that just described for the HL waste. These latter wastes are stored in their appropriate sectors.

The LL waste is stored in 55-gallon, carbon steel drums in the LL waste sectors. The drums are stacked in the LL chambers and the interstices are filled with crushed salt.

At the time of conversion from the isolation (operational) mode to the disposal mode, it is assumed that:

1. The cement plugs covering the HL, ILW-TRU cannister holes would be removed and the remaining voids would be filled with crushed salt up to floor level.
2. The drums of LL waste would be rearranged and the salt fill would be compacted to a high density compatible with the structural integrity of the containers.
3. All HL, ILW-TRU waste chambers, LL waste storage rooms, passageways, equipment storage vaults, and the access shafts up to the top of the salt level, would be filled with crushed salt and compacted to 70% density of the undisturbed salt density (about 2.2 gm cm^{-3}).
4. The concrete liners surrounding the access shafts above the salt level (those portions of the access shafts that pass through the other rocks in the sedimentary sequences) would be removed and the open shafts would be filled with a suitable, impermeable material up to the ground level.
5. The service structures at ground level above the repository would be removed, the site would be decontaminated, and an area surrounding the site would be fenced off to define an exclusion area over which some agency or firm could exercise control for an indefinite time.

The assumption about plugging the access shafts in item (4) is vague because, at present, there is no proven technology for sealing such large holes in a way that guarantees their impermeability for the long times required by waste disposal.

1.4 Description of the Waste Stored in the Reference Repository

The quantities and types of radioactive waste assumed placed in the reference repository are based on the "low growth" projections of Blomeke and Kee.[1.3] In the "low growth" case, it is assumed that the installed nuclear electric generating capacity rises from 70 GW(e) in 1980 to 625 GW(e) in the year 2000. The accumulated isotopic inventories calculated with the ORIGEN[1.4] computer program were provided by C. W. Kee of the Oak Ridge National Laboratory for use in this study.[1.5]

Based on these projections, the reference repository is assumed to accept all the HLW generated by the nuclear power industry through 1995 and shipped to the repository by 2005. In addition, all the cladding, ILW and low-level transuranium wastes generated through 2000 are assumed shipped to the repository by 2005.

1.4.1 High-Level Wastes

High-level wastes are composites of all liquid waste streams from reprocessing spent fuels. They contain more than 99.9 percent of nonvolatile fission products, 0.5 percent of the uranium and plutonium plus other actinides produced by transmutation of uranium and plutonium. The final volume of solidified HLW is assumed to be 0.085 m^3/MT reprocessed fuel. The solidified HLW is shipped to the repository 10 years after reprocessing.

1.4.2 Intermediate-Level Wastes

Intermediate-level wastes consist of solid or solidified materials (excluding HLW and cladding) which contain greater than 10 n Ci/gm long-lived alpha emitters and after packaging, have surface dose rates between 10 and 1000 mrem/yr from fission product contamination. About 283 m^3 of ILW is generated at reprocessing plants per ton of plutonium processed. ILW is assumed reduced in volume by factors of 3 to 7.5 between 1976 and 1987 and by a factor of 10 thereafter. ILW is shipped to a repository 5 years after generation.

1.4.3 Cladding Wastes

Cladding wastes consist of solid fragments of Zircaloy and stainless steel cladding and other structural components of the fuel assemblies that remain after the fuel cores have been dissolved. Cladding wastes are assumed to contain 0.05 percent of the actinides and 0.05 percent of the nonvolatile fission products in addition to neutron-induced activity. The cladding wastes are assumed compacted to 70 percent theoretical density and stored at the reprocessing plant before being shipped to the repository.

403 023

1.4.4 Low-Level Transuranium Waste

These wastes are defined as solid or solidified materials which are known or suspected to contain long-lived alpha emitters in concentrations greater than 10 n Ci/gm while having sufficiently low external radiation dose levels after packaging that they can be handled directly. Low-level transuranium waste is assumed to undergo the same volume reduction as ILW. Low-level TRU wastes are shipped to the repository 5 years after operation.

For this study the HLW form is assumed to be glass. The LL and ILW are assumed fixed in concrete.

The quantities of wastes accumulated at the reference repository through 2005 (the assumed year of decommissioning of the repository) are shown in Table 1.4.1.

TABLE 1.4.1

Volume Accumulated at the Repository Through End of Year

	(Thousands of m^3)			
Year	High Level Waste	Cladding Waste	Intermediate Level Waste	Low-Level TRU Waste
1983	-0-	0.04	0.3	0.
1984	-0-	0.11	1.0	0.
1985	-0-	0.24	2.3	1.
1986	-0-	0.39	4.0	4.
1987	-0-	0.54	5.4	8.
1988	0.04	0.69	6.5	15.
1989	0.13	0.87	7.8	18.
1990	0.28	1.10	9.2	22.
1991	0.46	1.35	10.7	26.
1992	0.64	1.68	12.4	31.
1993	0.82	1.98	13.6	36.
1994	1.04	2.32	15.0	41.
1995	1.30	2.70	16.6	46.
1996	1.61	3.12	18.4	51.
1997	1.99	3.58	20.5	58.
1998	2.35	4.09	22.7	65.
1999	2.76	4.65	25.2	72.
2000	3.21	5.26	27.9	80.
2001	3.71	5.93	30.9	89.
2002	4.26	6.66	34.3	99.
2003	4.87	7.45	38.0	110.
2004	5.53	8.31	42.1	124.
2005	6.25	9.24	46.8	140.

The most likely mode of entry of radionuclides into the environment is by transport through groundwater. Thus an initial screening has been performed, based on injestion toxicity index, to select the most important isotopes for each waste type. Ingestion toxicity for a given isotope is defined as isotopic quantity in microcuries divided by the maximum permissible concentration ($\mu ci/m^3$) in water for that isotope.[1,6] The screening procedure used here was to keep the isotopes comprising the upper 99 percent of the total ingestion toxicity for each waste type. Two time periods were considered: 0 to 1000 years and 1000 to 10^6 years. The thermal output of the waste is important because of its potential adverse effect on the ability of the repository to isolate wastes from groundwater. Therefore, a similar screening procedure based on thermal outputs was applied to the high-level waste. Thermal screening was not applied to other waste types because their thermal output is small compared to that of the high-level waste. The results of this preliminary screening are shown in Tables 1.4.2 through 1.4.5. Figures 1.4.1 and 1.4.2 show the ingestion toxicity and thermal output for the total high-level waste inventory. Figures 1.4.3 through 1.4.5 show the ingestion toxicity for the total cladding, intermediate and low-level TRU waste inventories.

TABLE 1.4.2

Important Isotopes in High-Level Wastes

$0 - 10^3$ Years		$10^3 - 10^6$ Years	
Ingestion Toxicity	Thermal Output	Ingestion Toxicity	Thermal Output
SR 90	SR 90	TC 99	NB 93m
Y 90	Y 90	PB 210	TC 99
CS 134	TC 99	PO 210	SN 126
CS 137	RH 106	RA 225	SN 126
SM 151	CS 134	AC 225	SB 126m
EU 154	CS 137	RA 226	PO 210
PU 238	BA 137m	TH 229	AC 225
PU 239	SM 151	TH 230	RA 225
NP 239	EU 154	U 233	RA 226
PU 240	PU 238	NP 237	TH 229
AM 241	NP 239	PU 239	TH 230
AM 243	PU 238	NP 239	U 233
CM 244	PU 240	PU 240	PA 233
CM 245	AM 241	AM 241	U 234
	AM 243	AM 243	U 236
	CM 244	CM 245	NP 237
	CM 245	CM 246	NP 239
			PU 239
			PU 240
			AM 241
			PU 242
			AM 243
			CM 245
			CM 246

TABLE 1.4.3

Important Isotopes in Cladding Waste

$0 - 10^3$ Years	$10^3 - 10^6$ Years
Ingestion Toxicity	Ingestion Toxicity
FE 55	NI 59
NI 59	NI 63
CO 60	ZR 93
NI 63	NB 93m
SR 90	I 129
Y 90	PB 210
SB 125	RA 226
TE 125m	TH 229
CS 134	TH 230
CS 137	NP 237
PU 238	PU 239
PU 239	PU 240
PU 240	AM 241
AM 241	PU 242
AM 243	AM 243
CM 244	CM 245

TABLE 1.4.4

Important Isotopes in Intermediate-Level Waste

$0 - 10^3$ Years	$10^3 - 10^6$ Years
Ingestion Toxicity	Ingestion Toxicity
SR 90	I 129
Y 90	PB 210
CS 137	AC 225
PU 238	RA 225
PU 239	RA 226
PU 240	TH 229
AM 241	TH 230
AM 243	NP 237
	PU 239
	PU 240
	AM 241
	PU 242

TABLE 1.4.5

Important Isotopes in Low-Level Waste

$0 - 10^3$ Years	$10^3 - 10^6$ Years
Ingestion Toxicity	Ingestion Toxicity
NP 237	PB 210
PU 238	PO 210
PU 239	AC 225
PU 240	RA 225
PU 241	RA 226
AM 241	TH 229
PU 242	TH 230
	U 233
	NP 237
	PU 239
	PU 240
	AM 241
	PU 242

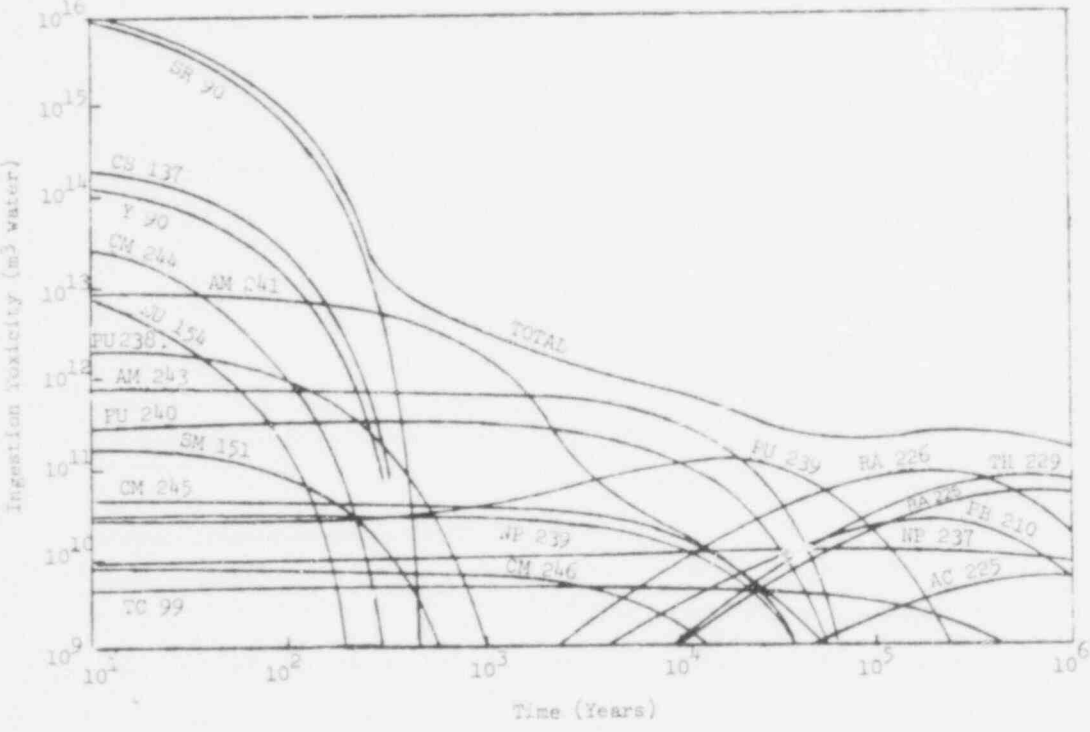

Figure 1.4.1 Ingestion Toxicity for High-Level Waste

403 027

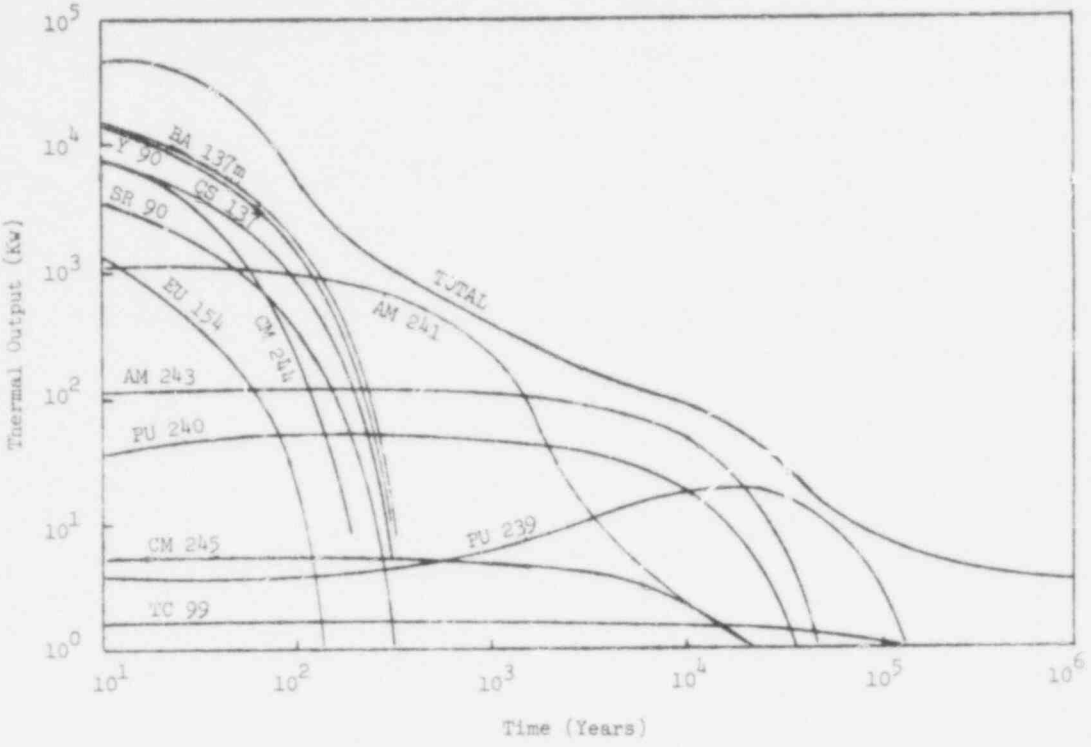

Figure 1.4.2 Thermal Output of High-Level Waste

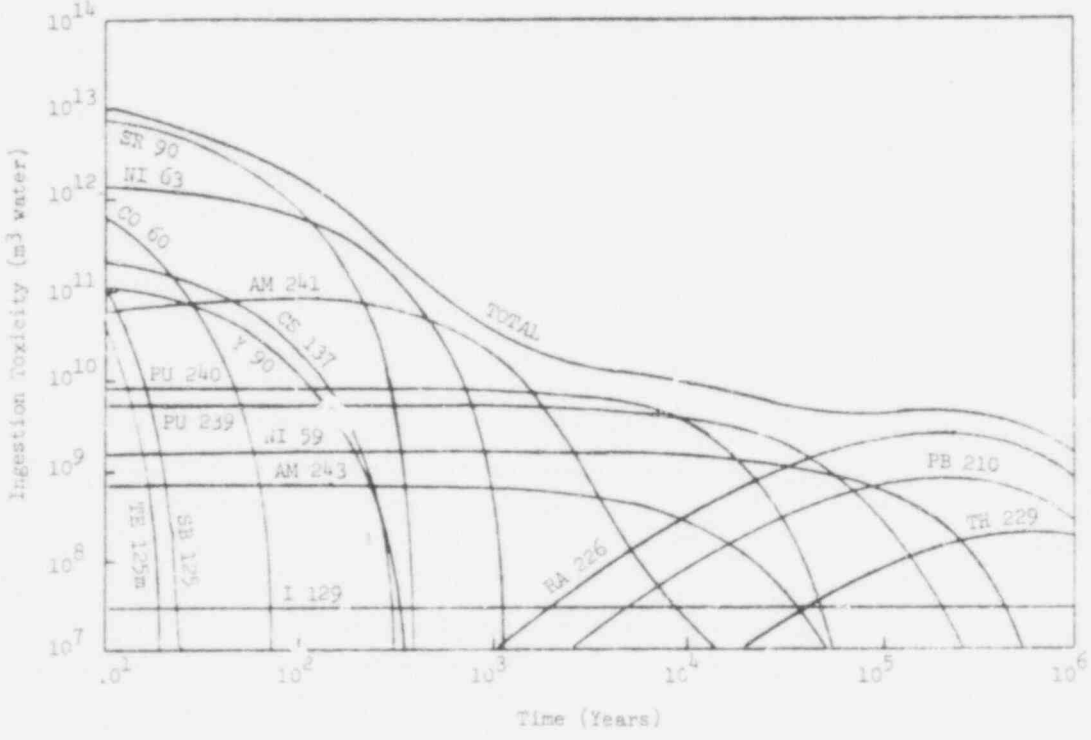

Figure 1.4.3 Ingestion Toxicity for Cladding Wastes

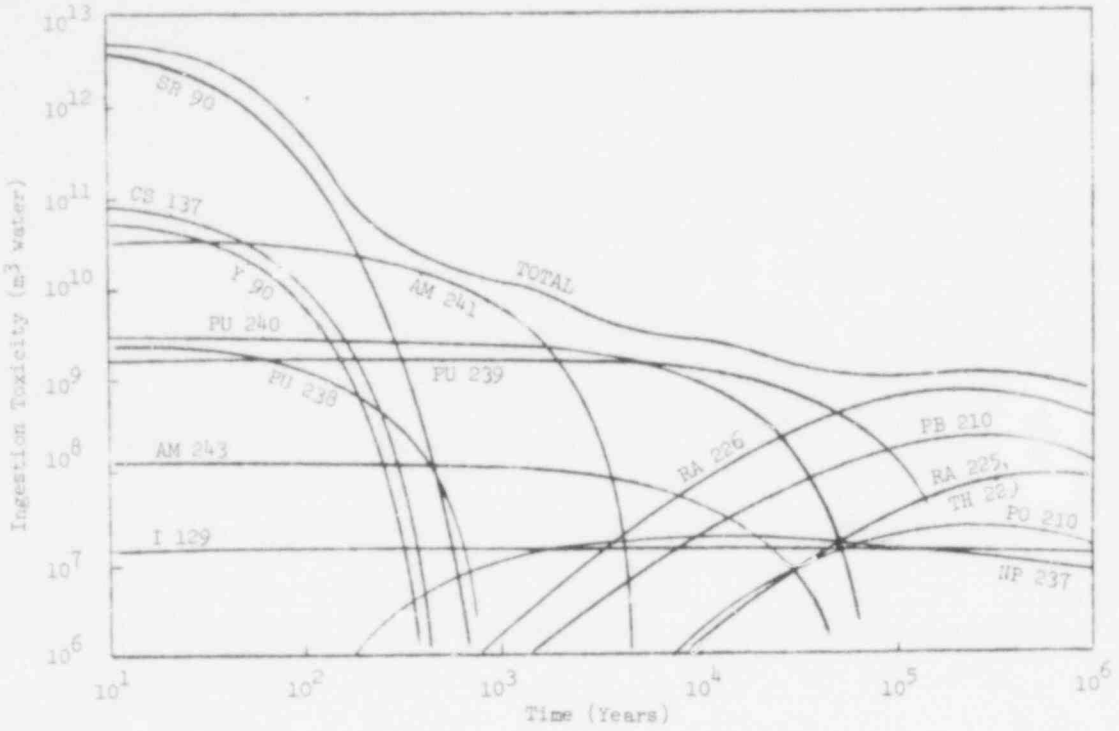

Figure 1.4.4 Ingestion Toxicity for Intermediate-Level Waste

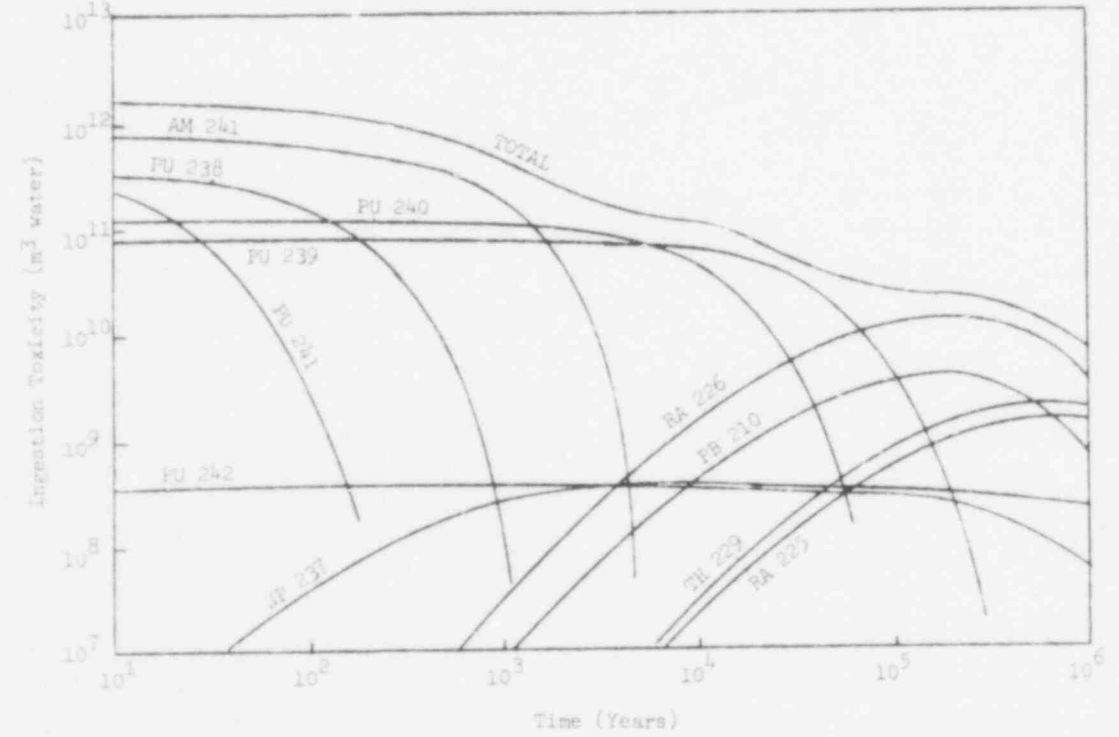

Figure 1.4.5 Ingestion Toxicity for Low-Level TRU Wastes

403 029

Ingestion toxicity as used here does not take into account dynamic phenomena such as different relative rates of migration of various nuclides through soils and different biosphere pathways which can affect actual risks. Thus, the lists of isotopes in Tables 1.4.2 through 1.4.5 may be subject to further additions or deletions as this study progresses.

References - Chapter 1

1.1. "Waste Isolation Facility Description - Bedded Salt" prepared by Parsons, Brinckerhoff, Quade & Douglas, Inc., for Office of Waste Isolation, Union Carbide Corporation, Oak Ridge, TN, Y10WI/SUB-76/16506, Sept. 1976.

1.2. "National Waste Terminal Storage Program Progress Report" for period April 1, 1975, to Sept. 30, 1976. Office of Waste Isolation, Union Carbide Corporation - Nuclear Div., Oak Ridge, TN, YIOWI-8, Nov. 30, 1976, Section 3.2.5, pp. 103-107.

1.3. Blomeke, J. O. and C. W. Kee, Projections of Wastes to be Generated, International Symposium on the Management of Wastes from the LWR Fuel Cycle, Denver, CO, July 11-16, 1976.

1.4. Bell, M. J., ORIGEN - The ORNL Isotope Generation and Depletion Code, ORNL-4628, Oak Ridge, TN (1973).

1.5. Lee, C. W., Private communication (1976).

1.6. 10 CFR 20

CHAPTER 2. CHANCES OF A RELEASE OF RADIOACTIVE WASTE FROM THE REFERENCE REPOSITORY

2.1 Introduction

This chapter is concerned with the possibility that radioactive waste may be released from the confines of the reference repository at some time in the future. The subject matter is restricted to those processes and events that lead to a release of radioactivity in the immediate neighborhood of the repository. The processes and events that contribute to the dispersal of waste and its distribution on a regional or worldwide scale are treated in later chapters of this report.

The definitions of release are stated in Section 2.2 and several scenarios are provided to give meaning to these definitions and to indicate their relative importance in any assessment of the hazards posed by a repository in deep, geologic media. The presently identifiable natural processes and events that contribute to conditions favoring release are listed in Section 2.3 and are then subjectively organized in Section 2.4. This subjective organization leads to a tentative choice of nine release sequences, or failure modes, one of which is complex and involves any adverse effects of the placement of the repository upon the repository's capacity to contain the waste. This latter failure mode is called the self-induced failure, and is studied by simulation in Appendix 2A of this chapter. In Section 2.5, mathematical models are constructed to provide estimates of the probability that release occurs at a given time through any one of the identified release modes. The mathematical formalism that is used to combine these models is described in Subsection 2.5.1. That formalism is based on the notion of system failure in the presence of several competing but statistically independent causes of failure. The formalism requires that failure rates be prescribed for the nine release modes; these failure rates are constructed in Subsections 2.5.4.1 through 2.5.4.9, using plausible models of the sequence of events occurring in each release mode. The failure rates depend upon a set of parameters that--though they are themselves "random variables"--have a more operational, or measurable, quality than the release mode probabilities possess. In this interim report, only nominal values of the parameters are quoted. Results of a sample calculation with the simple competing risk model are presented in Section 2.6, using most of the failure rates for the release mechanisms discussed in Subsections 2.5.4.1 through 2.5.4.9.

The reader of this chapter will note that modeling efforts described in the chapter are incomplete. The authors acknowledge that they are indeed incomplete; but they believe that enough material has been included to illustrate ways in which a truly effective treatment of release from a radioactive waste repository could be implemented.

2.4 Events That Define System Failure

By sealing potentially harmful radioactive wastes in stable, deeply buried rock strata, it is expected that these wastes will be kept out of the biosphere until their activity is reduced to harmless levels. The biosphere--those parts of the earth and its atmosphere that support life--consists of the lower atmosphere (below the troposphere), the uppermost few meters of the earth's crust, all surface waters on the continents, and the oceans and seas to great depths. If radioactive waste somehow reaches any of the elements of the biosphere during the term when it is hazardous, one can say that the disposal system has failed (although the consequences of such a failure are uncertain and remain to be explored). Conversely, if the radioactive wastes are kept away from the elements of the biosphere during their hazardous term, the disposal system may be regarded as having been successful from the standpoint of waste isolation.

Such a distinction makes easy the definition of the events that define system failure. Any one of the following four broadly defined events will thus imply failure of the disposal system:

1. Release to Deep Groundwater -- Radionuclides from the disposal chamber become dissolved in circulating groundwaters (phreatic zone).
2. Release to Soil -- Radionuclides from the disposal chamber become dissolved in groundwaters percolating through the soil (vadose zone), or become chemically fixed to the soil.
3. Release to Surface Water -- Radionuclides from the disposal chamber become dissolved in surface waters, or become fixed in sediments within the basins of surface waters.
4. Release to the Atmosphere -- Radionuclides from the disposal chamber are dispersed and suspended in the earth's atmosphere.

Though deep groundwaters are not normally considered part of the biosphere, event 1 is included because deep groundwater is a pathway to the biosphere by way of the hydrologic cycle. Similarly, event 4 is not confined to the lower atmosphere, per se, because of the known connection between the stratosphere and the lower atmosphere.

In addition, the existence of regional hydrologic cycles and global atmospheric circulation imply that the occurrence of any one of the four events above leads to the eventual occurrence (to some degree) of the other three. The net effect is an obvious one: once the radionuclides escape containment in the vicinity of the waste disposal site, there is a gradual dispersal away from the site by means of groundwater transport, sediment transport, and aerosolization followed by transport by winds. These processes are diagrammed in Figure 2.1.1 for the case of a release to the deep groundwaters near the disposal chamber. However, the present chapter is concerned only with the mechanisms of release and the assessment of probabilities for those mechanisms. Figure 2.1.1 has been included here mainly to show the logic behind the choice of emphasis upon failure by release to deep groundwater.

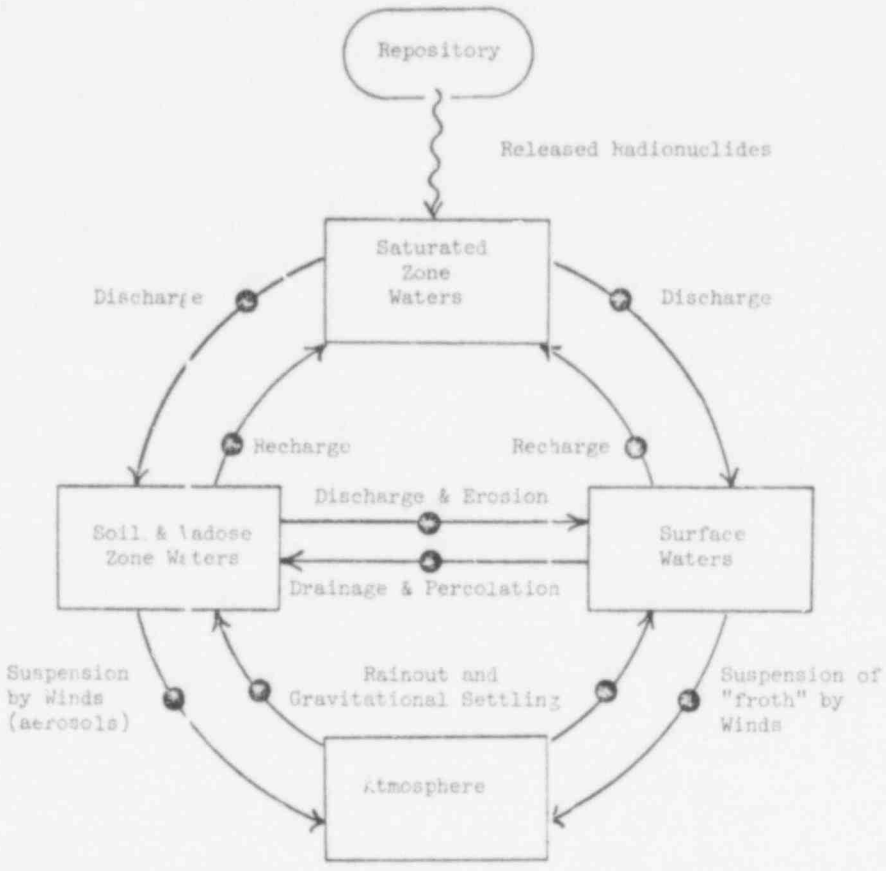

Figure 2.1.1. Processes of Radionuclide Dispersal After Release

The analysis of the hazards of waste disposal must address the question: in what ways may the radionuclides (RN's) be injected into those elements of the biosphere mentioned in the definitions of events 1 through 4? Whatever those mechanisms may be, it is clear that, with the possible exception of volcanism and exhumation, they must first have a local effect, and that they must operate prior to the dispersive mechanisms shown in Figure 2.1.1. The requirement that release mechanisms act locally already orders the importance (likelihood) of the four failure events, and justifies emphasis on the release to deep groundwater. Further qualitative justification is supplied in the next four subsections that supply examples of the ways each failure event might be realized. Before studying these examples, the reader should gain a mental picture of the features of a waste disposal site by studying Chapter 1, which describes the reference site, or "type site", used as a focus for the analysis in this study.

2.2.1 Event 1 - Releases to Deep Groundwater

Example: The access shafts to the waste vaults are possible points of vulnerability in the design of a waste repository. These shafts must necessarily pass through all layers of rock above the waste disposal level including any layers that contain flowing groundwater. Although the shafts are to be sealed or filled with some impermeable material after the repository is decommissioned, the technology for sealing such large-diameter holes is still imperfect, and it is reasonable to suppose that the seal between native rock and shaft fill may eventually deteriorate

in such a way that pathways for water are created. Once these pathways are fully developed, water conceivably could begin dissolution of the salt backfill and, in time, reach the waste vaults. Provided that the waste canisters have degraded at the time of infiltration by water, the leaching of the RN's into the brine could begin and some of the concentrate could, by diffusion, find its way back into the flowing groundwater above the vaults. The process of diffusion proceeds slowly; but if two or more shaft seals fail, the possibility exists that convective flow would be established between the opened pathways, leading to accelerated dissolution of the salt backfill, and eventually to enhanced transport of the dissolved RN's out of the dissolution cavity and into the aquifer.

Example: Even if the access shaft seals remain intact, the thermal stresses induced in the surrounding rock strata by the flow of heat away from the hot waste in the vaults may produce fractures in the barrier rocks that separate the vaults from the aquifers. If the thermal stress is severe, it is plausible that connected fractures could provide pathways for water and initiate a sequence of events similar to that just described in the example of shaft seal failure. Note that thermal stress cracking is not necessarily restricted to only the overlying rocks but could conceivably also affect the underlying units such that water could ultimately reach the vaults from water-bearing strata below, as well as from those above.

Example: A different kind of potential release mechanism is posed in the example of undiscovered pathways for water infiltration. These pathways might be: undiscovered, unsealed boreholes; voids adjacent to the waste vaults (perhaps the so-called breccia pipes); or extensive fractures in the barrier layers separating host rocks from the water-bearing layers. Numerous possibilities exist and the presence of any one of these pathways could initiate (or could already have initiated, at the time of decommissioning) a sequence of events leading to a release to ground water in a manner similar to that quoted for the shaft failure example.

These few examples should suffice to make the point that a relatively small rate of energy input is required to eventually effect a release of the radionuclides to deep groundwater. Energy required to grow cracks in the shaft seals might be supplied by seismic activity acting over a long period of time. Existing gravitational potentials supply energy for water convection, and the free energy required to establish the density gradients that drive diffusion is supplied by the salt/water system. The potential for energy release through undiscovered structures seems large, depending upon the likelihood of the existence of such structures. For these reasons, it is believed that releases to deep groundwater are the most likely of the four failure events and warrant the most attention. However, circumstances of direct release to the biosphere elements (events 2, 3, and 4) need also to be examined.

2.2.2 Event 2 - Direct Releases to the Vadose Zone

If waste is deeply buried below the vadose zone and layers of rock, perhaps 100 m thick, are interposed between the waste and surface soil, it is obvious that rather special circumstances would be required to drive the waste RN's directly to the soil without making substantial contact with deep groundwaters. Some examples of singular circumstances are given below.

Example: Suppose that several boreholes are inadvertently drilled in the exclusion area to depths sufficient to reach the waste vaults. With very small probability, one or more of the waste containers could be damaged and some radioactive fragments could be brought up into contact with the soil. If the local containment of the waste RN's has failed by the time of penetration and the RN's are dispersed into the immediate volumes surrounding their vaults, the chances of bringing radioactivity up to contaminate the soil would be higher, particularly if dispersion is first accomplished by a release to the groundwater.

A much more probable consequence of inadvertent exploration would be the creation of new pathways for water infiltration, thus initiating a sequence of events leading to a deep groundwater release and, perhaps, depending on the hydraulic head, transport of contaminated water directly to the surface.

It is possible to bring RN's directly into contact with the soil through a borehole if the radionuclides are gaseous or volatile, and if the canisters are ineffective as containers long enough before penetration time to permit the diffusion of the RN's into the surrounding rock. The only gaseous or volatile RN's present in the reference repository are ^{129}I, ^{220}Rn, and ^{222}Rn. Only the last of these has a substantial inventory in the reference site.

Example: Consider a rapid excavation of the waste vaults produced by the detonation of a high-yield nuclear weapon over the site, or the impact of a large meteorite. Such an agent would certainly bring part of the waste directly into contact with the soil (and simultaneously into contact with the local surface waters and atmosphere). Claiborne and Gera[2.1] have studied such events and conclude they are unlikely, though their consequences could be significant, depending upon the depth of the repository.

It is reasonable to expect that smaller explosions over and around the site are much more probable than the explosions or impacts of the magnitude required for excavation. Such lower-intensity events would most likely contribute to local fracturing of the rocks. It is doubtful that this could lead to new pathways for water infiltration.

These two examples of direct release to the vadose zone (and it is hard to think of other examples) indicate that the direct failure event is unlikely. Either persistent and deep penetrations of the exclusion area or huge releases of energy on or within the site are required. Both can be largely discounted by placing the repository at sufficient depth.

2.2.3 Events 3 and 4 - Direct Releases to Surface Water and Direct Releases to the Atmosphere

The examples and comments in the previous subsection apply even more forcefully to direct releases to local surface waters and to the atmosphere.

In fact, all of the examples quoted so far in this section are intended to show informally that failure of the disposal system is most likely to occur by slow releases of energy over long times by natural processes. All such "slow" processes that have been conceived so far lead first to infiltration of the waste vaults by water.

2.3 Events and Processes That Influence System Stability

If the waste disposal site were entirely an engineered system and if all the potential hazards could be realized on time scales small compared with the facility lifetime, then the appropriate methods for identifying factors that influence stability would be the event tree and fault tree formalisms.[2.2] But it has already been noted in Chapter 1 that engineered features of a waste disposal site in deep geologic media are only a part of the total system, the rest being natural and largely unpredictable to a degree that presently exceeds engineering design capabilities. It was also noted in Chapter 1 that potential hazards could be realized over time scales extremely long in comparison with the lifetime of a facility. We are dealing with a very poorly understood system at the present time in contrast with the admonition that:

> "Before the construction of a fault tree can proceed, the analyst must acquire a thorough understanding of the system."[2.3]

One purpose of the material in this chapter is to begin building an understanding of the system in question. The approach taken will, therefore, of necessity be one based on the plausibility of assertions that certain factors might influence system stability.

A list of events and processes that might influence stability of a waste disposal site is given in Table 2.3.1. The list is a composite of those items considered important by workers concerned with site selection criteria[2.4, 2.5] and by analysts who have attempted the fault tree or logic diagram methods.[2.6, 2.7]

Most items contained in Table 2.3.1 were reviewed by a panel of experts who were assembled to provide input on the importance of these factors.[2.8] The following paragraphs describe some of these phenomena and are intended to indicate the relative importance as seen by individual members of the group. The remarks apply to the generic concepts of waste disposal in deep geologic media and are in response to the question: How important is the factor under consideration for the long-term stability of a waste disposal site?

TABLE 2.3.1

Events or Processes that May Influence the Stability of a Waste Disposal Site in Deep Geologic Media

I. SUDDEN DISRUPTIVE EVENTS AND PROCESSES

1. Meteorite Impact
2. Hurricanes
3. Earthquakes, Seiches, Tsunamis
4. Landslides
5. Volcanic Activity
6. Faulting

II. SLOW DISRUPTIVE EVENTS AND PROCESSES

A. Subsurface Processes

7. Dissolution
8. Rock Deformation
9. Rock Permeability Change
10. Thermal Expansion and Related Effects

B. Surficial Processes

11. Erosion and Sedimentation
12. Regional Subsidence and Uplift (applies also to subsurface)
13. Glaciation, Pluvial Periods, and Sea Level Variations

III. EVENTS AND PROCESSES INITIATED BY MAN (LONG-TERM PHASE)

A. Effects of Engineered Repository

14. Subsidence and Caving
15. Shaft and Borehole Seal Failures
16. Thermally or Excavation Induced Stress in Host Rocks
17. Radiation Effects (radiolysis and energy storage)
18. Chemical Effects
19. Other Physical Effects (e.g., migration of brine bubbles)

B. External Events Independent of Repository

20. Inadvertent Intrusion (by drilling, mining, or hydrofracture)
21. Hydrologic Stresses (irrigation, dams)
22. Explosions (including nuclear warfare)

IV. UNDETECTED FEATURES AND PROCESSES

A. Geologic Features

23. Voids or Hydraulically Interconnected Fracture Systems Near Site
24. Undiscovered Perched Water Table Near Site
25. Undiscovered Potentially Valuable Mineral Resources Near Site

B. Man-Made Features

26. Undiscovered Boreholes and Mines (sealed or unsealed) Near the Site
27. Location of Site Near Strategic Industrial Centers

2.3.1 Meteorite Impact

Because the frequency of impacts or meteorites large enough to cause direct damage is extremely low, meteorite impact events are not important in relation to certain other events that could lead to damage.

2.3.2 Hurricanes

Hurricanes may be important to the safety of disposal sites located on the margins of the Gulf of Mexico, the State of Florida, and on the east coast of the United States during the operational phase. In the postoperational phase, adverse effects might conceivably arise from alteration of groundwater flow patterns and from imposed hydrostatic loading on the site; however, such effects are likely to be transient and of no long-term consequence. The effects of seiches and tsunamis would likely be similar to that of hurricanes.

2.3.3 Earthquakes (seiche/tsunami)

The phenomenon of earthquakes, their frequency of occurrence in a region (seismicity), and the magnitude of induced acceleration might be important to site stability but mainly because of the relationship of seismicity to other geologic events (e.g., faulting, rock deformation, and other changes in rock properties). Small induced accelerations might, if prolonged, alter rock permeability, thermal conductivity, and enhance fracturing along joints between native rock and the fill material of mined cavities. The effects of large seismic accelerations on buried site structures need to be further studied. Large accelerations have a positive probability of occurrence, even in seismically quiet regions. The effects of seiches and tsunamis induced by earthquakes are considered with those of hurricanes (see previous paragraph).

2.3.4 Landslides

Landslides, in the sense of abrupt flows of rock and earth in terrain of high relief, are probably not important for considerations of site stability because a site probably would not be located in terrain of high relief. Regional scale "sliding" of rock structures, on the other hand, might be important. This class of "landslide" is related to regional tectonics (see section 2.3.11).

2.3.5 Volcanic Activity

Volcanism is obviously important, but in a site-specific context. For instance, it might be important in considerations of formations at NTS, Nevada, as a candidate site, but not very important for Pierre shale, bedded salt, or salt domes. The distinction between surficial manifestations of igneous activity (volcanism) and subsurface phenomena (magmatic intrusion) should be maintained. The former are associated with the so-called volcanic provinces, whose time-history is becoming better known (e.g., the Hawaiian Island chain) and, thus, somewhat predictable. Subsurface manifestations are less well known.

2.3.6 Faulting

Faulting is a potential hazard for waste repositories in that it could affect pathways for the movement of groundwater. The distribution and ages of active faults in the several geologic provinces of the USA have been mapped to some extent, and these maps are currently being updated.

2.3.7 Dissolution

Dissolution, the dissolving of rock by water, is obviously very important on a site-specific basis. Salt, gypsum, and limestone formations have the potential for dissolution. The rate of dissolution depends, in a large part, upon the availability of the water and its flow pattern. Consequently, strong connections exist with other items in the list: rock permeability, climate (glaciation, pluvial periods, and sea level variations) and many of the events and processes initiated by man (see Table 2.3.1, III).

2.3.8 Rock Deformation and Permeability Change

The elastic and anelastic responses of the host rocks to applied stress are obviously important and are closely related to faulting, earthquakes, and diapirism in salt. Important related problems concern the response of the mined cavity to static loading over the designed load. Each problem is likely to be specific to the hazard item and site under consideration and should be considered individually (evaluation research).

2.3.9 Thermal Changes (Time-Dependent)

Naturally occurring, time-dependent thermal changes might be important as indicators of more hazardous items (e.g., subsurface igneous activity). Changes in the temperature profile might possibly change permeability. Thermal changes related to the emplacement of waste in the host rocks can be more important than naturally occurring changes in causing the hazards (see Sections 2.3.15 and 2.3.17).

2.3.10 Erosion and Sedimentation

Erosion and sedimentation are important primarily through their connection with regional tectonics. Erosion alone, at a worldwide average of ~ 1 mm/year, is unlikely to be a hazard for an emplacement 800 m under the surface; however, rates of erosion could be higher in uplifting regions. Sedimentation may influence the distribution of surface waters and increase the static loading over a site. It is also a factor in diapirism.

2.3.11 Regional Subsidence and Uplift

This item refers to the tectonics (deformation and structure) of the earth's crust and its local manifestations of regional uplift and subsidence. Such regional manifestations are directly important only if they occur rapidly (as in the "Palmdale bulge", uplifted 1 m in 10 years). Indirectly, they might be important as indicators of the potential for more hazardous phenomena, such as faulting and accelerated erosion. In general, coastal and shield regions are rising while certain interior basins are subsiding.

2.3.12 Glacial-Pluvial Period, Sea-Level Variations

These items can be particularly important for disposal schemes in the unsaturated zone (arid lands) and in rock structures showing evidence of dissolution. In other instances, the effects of a glacial-pluvial period or of a sea-level variation must be assessed on a site-specific basis.

Data on the distribution of the Pleistocene lakes in the continental United States have been compiled and the approximate margins of recent glaciers have been mapped. But, in spite of advances in the understanding of past climates, arising out of the CLIMAP program, certain information about continental climate in pluvial periods is missing, such as rainfall and stream flow. Some inferences can be made from indirect geological and biological evidence.

2.3.13 Subsidence and Caving

Subsidence and caving in and around the waste emplacement following backfill are potentially important factors, mainly because of the possibility of opening pathways for water flow. These factors are obviously site specific and are partly under the control of site design and current technology.

2.3.14 Shaft and Borehole Seal Failures

The consequences of deterioration of the joints between native rock and sealing material would be important in connection with other modes of failure. Possible mechanical failure modes are associated with earthquakes, subsidence, and thermally induced stress (see Section 2.3.15). There might also be failure modes associated with chemical reactions at the shaft fill and host rock interface.

2.3.15 Thermally Induced Stress in Host Rocks

Thermal loading from emplaced waste was deemed to be important in the initiation of more hazardous events (shaft seal failure, fracture of barrier rocks). Its connection with other factors could be highly complex. The role of thermal loading might be determined by calculations of the degree of thermal cracking induced in host rocks or by actual in-situ measurements of near-field stress change during a pilot plant phase of the facility.

2.3.16 Radiation Effects (Radiolysis and Energy Storage)

The principal effect considered here is the change in mineral stability caused by the absorption of gamma radiation from radionuclide decay. A certain amount of hydrolysis of water is also to be expected. The effect is not important in salt and probably not important in other rock types although some further research might be warranted.

2.3.17 Chemical Effects, Other Physical Effects

Further research is needed before the importance of these items is known. Naturally occurring chemical changes of the host rocks are probably not important, but chemical changes induced by the mined emplacement might be. Such induced interactions seem to be least significant in granites and more important for salt and shales.

Chemical effects could influence radionuclide transport by fluids; and, although transport is not a factor, per se, in considering site stability, the role of chemistry in enhancing radionuclide leaching and transport requires further study. The introduction of organics and chelating agents in a waste emplacement could accelerate the local transport of radionuclides. However, the "far-field" transport properties of the host rocks are probably the most important items in the consideration of the time to reach the biosphere, given waste release.

2.3.18 Inadvertent Intrusion (by Drilling, Mining, or Hydrofracture)

The possibility of intrusion of the repository at some time in the future was not seen as a question for geoscientists. Although the chances of intrusion might be influenced by the presence of valuable natural resources under or near the disposal site, the attitudes towards resources in the distant future were regarded as being beyond speculation.

2.3.19 Hydrologic Stresses (Irrigation, Dams)

Hydrologic stresses produced by human diversion and impoundment of water have about the same hazard potential as the stresses produced by natural confinement. Comments on the glacial-pluvial period item also apply here. Determining the likelihood of future, man-made changes in the hydrologic system is not the responsibility of earth scientists. However, there are many case histories of such man-made changes of which geologists and hydrologists may be aware.

2.3.20 Explosions (Including Nuclear Warfare)

The probability of spontaneous explosion in a waste emplacement is virtually nonexistent during the post-operational phase, given proper site design technology and an understanding of the chemical interactions between waste materials and host rocks. Explosions at the surface might be very hazardous for emplacements in the unsaturated zone, but could be accounted for emplacement at considerable depth (e.g., 500 m).

2.3.21 Undetected Features and Processes

The importance of undetected features and processes was not considered by the panel. However, undetected voids, fracture systems, boreholes, and mines located near the site might be important factors in assessing risk from waste emplacement. The potential for causing harm to the site integrity through each of these natural or man-made features needs to be investigated on a site-specific basis. Item 25, Table 2.3.1 (undiscovered valuable mineral resources) is

connected with the possibility of intrusion of the site by man. Item 26, Table 2.3.1 (the future location of a strategic or industrial complex over or near the site) has intuitive connections with inadvertent intrusion and nuclear warfare. But it seems unlikely that these connections can ever be reliably identified and quantified.

The preceding paragraphs should reveal the need for further study and organization of the phenomena that influence the long-term stability of a disposal system. In the next section, subjective judgment and physical reasoning are applied to the organization of some of the phenomena cited in Table 2.3.1, in preparation for making models of waste release mechanisms and site stability.

2.4 Identifying Some Waste Release Modes

The 27 events, processes, or features listed in Table 2.3.1 are already organized into four broad categories:

I. Sudden Disruptive Events and Processes

II. Slow Disruptive Events and Processes

III. Events and Processes Initiated by Man

IV. Undetected Features and Processes

An identification of some of the more obvious release mechanisms and their associated release modes can be made by examining the items in each of these four categories.

Of the items in Category I, only (1) meteorite impact and (5) volcanic activity could lead to instantaneous release of radionuclides to the biosphere; (6) faulting could also be a direct cause of release, although a long period of time would likely be required for this to be effected. Items (2) and (4) could not lead directly to a release of waste from the reference site, since they are surficial phenomena.

Of the items in Category II, only (7) dissolution and (11) erosion could initiate a direct release of waste when acting alone in the context of the reference site. All other items in this category can only contribute indirectly to release. A possible exception is glacial erosion (13). But glaciers are not known to erode rock layers to the depths considered here for waste burial.

Two different classes of Events and Processes Initiated by Man (Category III) are worth considering for the long-term phase of the repository: a class pertaining to the effects of the engineered repository (Class A) and a class of events that occur external to and may be independent of the presence of the repository (Class B). Of the items listed under Class A, only (14) subsidence and caving, (15) shaft seal and borehole failures, and) thermal or excavation induced stress of host rocks can lead to water intruding the repository, perhaps in concert with solutioning. A consideration of the remaining Class A effects, items (17) through (19), suggests that their role in

causing release is presently uncertain: they are energetically weak phenomena in the context of the reference site, but they may contribute indirectly to conditions favoring release. Events listed under Class B are quite different: only items (20) and (22), inadvertent intrusion (by drilling, mining, or hydrofracture) and explosions, respectively, would be capable of initiating release. In the latter event, a nuclear explosion of extremely large yield would be required and to exhume the waste would require a direct hit over a repository located at depths less than those currently being considered. Hydraulic stresses caused by man's activity (21) may only accelerate (or inhibit) other conditions that would directly lead to release of radionuclides from the repository.

Finally, the only features among the Category IV list that are associated directly with a release are items (23) and (26): undiscovered voids and hydraulically interconnected fracture systems and undiscovered, man-made penetrations. The other features (24), (25), and (27) are only factors to be considered in assessing conditions that favor release.

Thus, there appear to be 12 potential causes of failure (underlined in preceding paragraphs) and 15 events, processes, or features that may influence or catalyze the potential causes of release, but may not initiate release when acting alone.

The 12 potential causes of release can be further organized into two groups:

1. Those events and processes that are initiated by the excavation of the repository and the placing of heat-producing radioactive waste within it.
2. Those events, processes, or features that could initiate or contribute to release of radionuclides (by excavation or solution) in ways that are independent of the presence of the repository.

Only solutioning (7) and subsidence/caving (14) are common to the two groups. Group 1 can reasonably be called a self-induced release because the processes within it are initiated by the creation of the facility and because they also contribute to a failure of the facility. On the other hand, the processes and events in group 2 are potential release modes that are, in first approximation, indifferent to the presence of the repository.

An appeal to physical and geological causality gives the most obvious release mechanisms in groups 1 and 2. A summary of the processes that contribute to self-induced release are shown in Table 2.4.1; release mechanisms that are roughly independent of the repository are listed in Table 2.4.2.

TABLE 2.4.1

Interacting Events or Processes that Determine Self-Induced Release

- THERMAL OR EXCAVATION STRESS OF HOST ROCKS (16); followed by fracture formation and solutioning (7); interacting with other factors.
- SUBSIDENCE AND CAVING (14); accelerated by: Earthquakes (3), Landslides (4), Solutioning (7), Regional Subsidence (12), Pluvial Periods (13), Explosions (22), Hydrologic Stresses (21). Interaction with other factors.
- SHAFT SEAL FAILURE (15); accelerated by: Earthquakes (3), Landslides (4), Solutioning (7), Regional Subsidence (12), Pluvial Periods (13), Explosions (22), Hydrologic Stresses (21). Interaction with other factors.
- RADIOLYSIS AND ENERGY STORAGE (17); interacting with other factors.
- CHEMICAL EFFECTS (18); interacting with other factors.
- OTHER PHYSICAL EFFECTS (19); interacting with other factors.

TABLE 2.4.2

Some Causes of Release Independent of Presence of the Repository

- UNDISCOVERED BOREHOLES AND MINES (26); followed by: Solutioning (7) and Subsidence (14) if unsealed. If initially sealed: Solutioning and Subsidence are preceded by shaft seal failure (15).
- UNDISCOVERED VOIDS AND FRACTURE SYSTEMS (23); followed by: Solutioning (7) and Subsidence (14) if initially inactive, some of the processes in Shaft Seal Failure (15), Figure 1, apply to activation.
- EROSION AND SEDIMENTATION (11); influenced by the processes: Landslides (4), Regional Subsidence and Uplift (12), Glaciation and Pluvial Periods (generally, climate) (13).
- FAULTING ON OR NEAR SITE (6); followed by: Solutioning (7) and Subsidence (14).
- EXPLOSIONS ON OR NEAR SITE (22), influenced by: Location near Strategic or Industrial Centers (27), followed by Solutioning (7) and Subsidence (14).
- VOLCANIC ACTIVITY (5); highly correlated with Faulting (6).
- METEORITE IMPACT ON OR NEAR SITE (1)
- INADVERTENT INTRUSION (20); followed by: Solutioning (7) and Subsidence (14); influenced by: Existence of Mineral Resources near Site (25), and Location of Site near Strategic or Industrial Centers (27).

403 044

In the mathematical modeling of these release mechanisms, it has proved convenient and insightful to separate the two groups identified above into two distinct kinds of models. We first treat the release mechanisms of group (2) in terms of a probabilistic model of competing risks (of release) by the eight modes listed in Table 2.4.2. This is done in the following sections 2.5 and 2.6, where the eight causes of release shown in Table 2.4.2 will be treated as though they are statistically independent modes in the analysis presented in later sections. However, it should be emphasized that the assumption of independent modes is made only to simplify a first analysis of the phenomena and to establish their ordering of priority for further investigations. It is easy to find examples where one or more of the eight causes of release shown in Table 2.4.2 interact with one another, or with the self-induced release mode. Whether the interactions are significant remains to be determined.

The self-induced release mechanisms require a different kind of modeling effort, to be described in Appendix 2A of this chapter. Briefly, the model of the combined self-induced release mechanisms is a deterministic, lumped-parameter simulation of the geological stability of the repository when it is stressed by heat-producing waste and subsidence of the overburden. Since the repository simulation is deterministic, the outputs of the model (e.g., times required for solutioning to progress to the repository level) are incompatible with the probabilistic model of competing risk used for the eight mechanisms deemed to be independent of the repository (Table 2.4.2). One way to get around this incompatability - and thus be able to uniformly compare the importance of all identified release modes - is suggested but not implemented in Section 2.5 (Subsection 2.5.4.1).

2.5 Estimating Probabilities of Release--External Modes

In this section, we construct models that provide estimates of the probabilities of release of waste through most of the release modes described in Section 2.4. Emphasis is placed upon the causes of release that were judged to be essentially independent of the presence of the repository (Table 2.4.2). However, an attempt is made to cast the results of the simulations of self-induced release (Appendix 2A, this chapter) in a form that is compatible with the mathematical formalism used to analyze the other release modes. This attempt should be regarded as a temporary measure, since it is clear that the self-induced mode of release is not entirely independent of the so-called "external" modes.

The formalism of the probabilistic models is first presented in the following Subsection 2.5.1, without discussion of the supporting logical and physical assumptions. The justification for the formalism is briefly treated in Subsection 2.5.2. Physical principles that are common to certain of the models of release mechanisms are explained in Subsection 2.5.3; the models are then derived and explained in Subsection 2.5.4.

2.5.1 Formalism of the Probabilistic Models

It is assumed that N independent release mechanisms have been identified for the system in question; and that probability distribution functions, P_i, for the waiting times, T_i, until release occurs by the ith mechanism have been prescribed for each of the N modes:

$$P_i(t) = \Pr\left\{T_i \leq t\right\}, \quad i = 1, 2, \ldots, N .$$

Each waiting time is a positive random variable and the origin of time is chosen at the point when the system is placed in operation (for a waste disposal facility, this is the time at which the facility is sealed).

If it is assumed that the probability of initial release equals zero, it can be shown that the P_i's are all of the form:

$$P_i(t) = 1 - \exp\left[-\int_0^t \phi_i(s)\, ds\right] . \tag{2.5.1}$$

The function ϕ_i defined here is called the failure rate[2.9] for the ith mode. It must be an integrable, non-negative function on the interval $(0, \infty)$. The failure rate is usually interpreted as a probability density conditioned on the event: no failure occurs up to time t. The probability density function associated with each P_i is obtained by formally differentiating Eq (2.5.1):

$$p_i(t) = \phi_i(t) \exp\left\{-\int_0^t \phi_i(s)\, ds\right\} . \tag{2.5.2}$$

Note that, by Eq (2.5.2):

$$\phi_i(t) = \frac{p_i(t)}{1 - P_i(t)} . \tag{2.5.3}$$

The system under study is now assumed to be set in operation and, henceforth, subject to failure through the action of any one of the N release mechanisms. The probability that the system survives to a time $t > 0$ is then

$$P_S = \prod_{i=1}^{N} (1 - P_i) , \tag{2.5.4}$$

(where the implied dependence on t is dropped for brevity).

The consequences of release* may be quite different for each mode and one needs the probability of a release by time t for each of the N, competing release mechanisms. These probabilities can be calculated from the failure rates, defined by Eq (2.5.3), in the following way.

Define $\pi_o(t)$ and $\pi_i(t)$, i = 1, 2, ... N, as respectively the probabilities of: no release prior to time t, and release by the ith mechanism prior to time t. Then, using Eqs (2.5.1 and 2.5.4):

$$\pi_o(t) = P_s = \exp\left[- \sum_{i=1}^{N} \int_o^t \phi_i(s)\, ds \right] , \tag{2.5.5}$$

and

$$\pi_i(t) = \int_o^t p_i(s) \prod_{\substack{j=1 \\ j \neq i}}^{N} \left[1 - P_j(s)\right] ds = \int_o^t \frac{p_i(s)}{1 - P_i(s)} \prod_{j=1}^{N} \left[1 - P_j(s)\right] ds ,$$

or

$$\pi_i(t) = \int_o^t \phi_i(s)\, \pi_o(s)\, ds , \tag{2.5.6}$$

by use of Eq (2.5.3).

It is seen that the probabilities of release by the ith mechanism prior to time t can be computed by performing the integration over functions involving the ϕ_i's, as indicated in Eq (2.5.6) If the ϕ_i's are constants (exponentially distributed failure times), then the integration may be performed analytically.

When the modes of "release" are statistically independent, the formalism just described is called a model of competing risks from independent causes. For a survey of competing risk methodologies, some of which are more general than the present one, see References 2.10 and 2.11.

The basic ingredients of the formalism just described are the failure rates: $\phi_i(t)$, $t > 0$, i = 1, 2, ... N. Failure rate functions for most of the N = 9 modes of release described in Figure 2.4.2 are constructed in later subsections, using physical reasoning and certain assumptions concerning the statistical occurrence of natural and anthropogenic features in the vicinity of the reference repository.

403 047

*The consequences of release in the present chapter are the rates of release of the radionuclides to the several biosphere elements.

2.5.2 Justification of the Formalism

The formalism described in the preceding section provides a means for estimating the *a priori* probabilities of release of waste from the repository, provided that either the probability distribution functions for the times until release or the associated failure rates are given for each of the N, identified release modes. Three ways to construct probability distributions, failure rates, or any other measures of likelihood are:

1. Use of physical data obtained by making repeated trials of system performance, combined with statistical theory.

2. Use of data obtained by making repeated trials (simulations) with a suitable mathematical model of the system, or parts of it. A variant of this approach bypasses the trials by simulations, and attempts to construct the mathematical forms of the distributions from simple assumptions, leaving their numerical scale to be determined by a small number of parameters that have physical meaning and are measurable.

3. Use of professional judgment (the guess of an expert, or the consensus of a group of experts).

These three techniques are listed in order of decreasing objectivity. Item (1) is, of course, the mainstay of quality control and epidemiology. For complex but well understood systems, a combination of items (1) and (2) might be brought to bear on the problem when performance statistics are available for the system components: a mathematical model is constructed that logically connects the system components, and the rules for combining probabilities are then used to estimate the overall probability of certain system performance events. A combination of techniques (1) and (2) has been used in the Reactor Safety Study[2.12] to assess the probabilities of various kinds of "accidents" that a nuclear reactor may experience.

However, in most problems of risk assessment, the system being considered is complex and there is a poor understanding of the function and interconnections of its subcomponents, and/or the type of performance statistics that characterize the subcomponents. In such problems, a combination of the methods outlined under (1) and professional judgment, (3), are used as a last recourse in order to gain insight into the order-of-magnitude of the risks. The attendant loss of objectivity is accepted in the bargain that returns increased insight in a timely fashion. Most of the complex and poorly understood systems faced by the analyst fall into the categories of purely natural systems, or engineered systems that strongly involve some natural phenomena. We have already stressed the point (Section 2.3) that a waste disposal site in deep geologic media is in the latter category.

2.5.3 Physical Content of the Probabilistic Models

The a priori failure rates to be constructed in the following subsection require estimates of the rate of growth of solution cavities in bedded salt. This subsection provides some rough formulae to estimate such growth in a context that is appropriate to the probability models. Much of the material presented here overlaps the treatment of solutioning in Appendix 2A of this chapter.

Natural salt, or Halite, has a very low permeability--about 10^{-13} cm^2--according to laboratory measurements;[2.13] but, because of inclusions of other minerals, the bulk permeability of bedded salt could be four orders of magnitude greater than that of pure Halite.[2.14] In any case, the speed of flow of brine through salt at the reference site is small, about 10^{-7} to 10^{-3} m/yr. The more likely mechanism for bringing large volumes of water (or brine) into contact with the radioactive waste is the mechanism of solutioning in which columns of fresh water gain access to the salt beds through fissures or cracks in the relatively impermeable shale. The small amounts of fresh water that first reach the salt layer would dissolve some of the layer and become saturated; then, in principle, no further dissolution would occur unless certain processes operate to reduce the salt concentration in the brine columns (one such process is ordinary molecular diffusion of salt ions through water). If the salt concentration is reduced, further dissolution of the layer becomes possible, and a cavity may begin to grow in the salt bed at the junction of the salt layer and the water conduit. The situation is shown in the following highly idealized diagram.

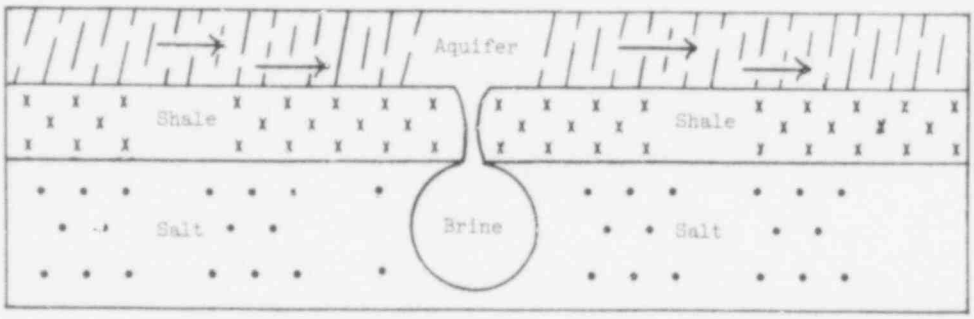

The shape of the developing brine cavity is uncertain, owing to possible inhomogeneities in the salt layer and, in cases of convective brine transport, to the location of inlet and outlet openings through the shale layers. The cavity is likely to be convex, however, and its volume can be approximated by the volume of an ellipsoid = $(4\pi/3)$ abc; where a, b, and c are the three semi-major dimensions of the ellipsoid. To further simplify matters, a geometric mean of the cavity dimensions,

$$R \equiv \left(\frac{4\pi}{3}\ abc\right)^{1/3} ,$$

will be used as a measure of the cavity size. The rate of growth of the cavity is then given by

$$\frac{d}{dt} R^3 = V(t) , \qquad (2.5.7)$$

where V(t) is the volumetric rate of flow of salt (say, in $m^3\ yr^{-1}$) out of the cavity (by, for example, the processes of diffusion or convective brine transport). The rate of flow of salt out of the cavity changes in time, mainly because of changes in the effective areas of the inlet/outlet channels connecting the aquifers to the salt layer. This time variation of V will not be considered here. Instead, we replace V(t) with its constant, "average" value, $\dot{V}$, and integrate Eq (2.5.7) to get

$$R^3(t) = \dot{V}t \quad , \tag{2.5.8}$$

where time, t, is measured from the time of cavity initiation. In other words, a typical cavity dimension increases as the cube root of time elapsed since the formation of a channel for water flow.

Some of the processes for salt removal from brine cavity are discussed below. These examples show how to make crude numerical estimates of the magnitude of $\dot{V}$ for the possible brine removal mechanisms.

2.5.3.1 Diffusion -- If the water in the channel is static, the only means for salt removal is by diffusion. One can show that, approximately,

$$\dot{V} = A\, V_{aq}\, \frac{v^*}{v^* + V_{aq}} \qquad m^3 \cdot yr^{-1} \quad , \tag{2.5.9}$$

where

v^* = D/ℓ, the diffusive flux velocity ($m\ yr^{-1}$)

A = effective opening area of channels (m^2)

V_{aq} = pore velocity of fresh water in aquifer ($m\ yr^{-1}$)

D = effective diffusion coefficient of salt in water ($m^2\ yr^{-1}$)

ℓ = effective length of channel or fissure (m).

For true molecular diffusion, it is almost always true that $v^* << V_{aq}$; in which case:

$$\dot{V} \approx A\, v^* \qquad m^3 \cdot yr^{-1} \quad . \tag{2.5.10}$$

One numerical example will show why molecular diffusion alone cannot be important in the formation of solution cavities. Consider the case of solutioning through an open 60-m channel, 0.1 m in diameter. The diffusion constant for salt ions (Na^+, Cl^{-1}) in water at 20°C is about $3.6 \times 10^{-2}\ m^2\ yr^{-1}$. Then, $\dot{V} \approx 4.7 \times 10^{-6}\ m^3\ yr^{-1}$, and it would take 10^6 years to solution less than $5\ m^3$ of salt.

403 050

However, there are very special circumstances in which the effective diffusion coefficient can be many orders of magnitude larger than the coefficient of simple molecular diffusion. The circumstances are those in which the mechanical equilibrium of the water column is first made unstable through an adverse thermal or concentration gradient. Turbulent convection then proceeds in order to return the system towards equilibrium and in the process, a rapid mixing of materials in adjacent layers of the water ensues. The net mass transport of salt may then be calculated in terms of Fick's law for diffusive mass transport, but with an anomalous diffusion constant, D_a, sometimes called the eddy diffusivity or turbulent diffusivity.[2.15] The anomalous diffusivity may be of the order of 1 $cm^2\ s^{-1}$ (or about $\pi \times 10^3\ m^2\ yr^{-1}$).[2.16]

Using the example of a 60 m-long channel, one finds that the effective mass transport velocity in this instance, D_a/ℓ, is of the order of 50 m yr^{-1}. This is on the order of the pore velocity of fresh water in the aquifers bounding the reference repository: $V_{aq} \approx 185$ m yr^{-1}. From (2.10), and for the 10 cm diameter channel, $V \approx 0.3\ m^3\ yr^{-1}$. In other words, about $3 \times 10^5\ m^3$ of salt would then be removed from the cavity produced by the channel in 10^6 years.

Note that the aquifer pore velocities always define the upper limit for the diffusive flux velocity at which salt can be removed from a solutioning cavity. This limit holds for convective processes of removal as well as the diffusive ones.

2.5.3.2 Convection -- Removal of salt from a solution cavity by brine convection is also possible under special conditions, two of which are sketched below.

(1) Channels connecting cavity to one aquifer.

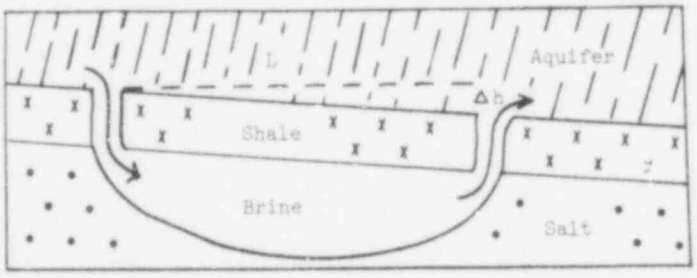

(2) Channel connects both aquifers through salt.

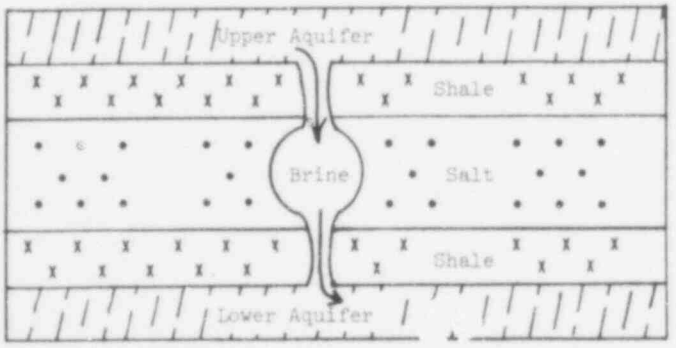

In the case (1) diagrammed above, fresh water flows in the inlet (left); mixes in the cavity, and becomes saturated brine. The difference in head, $\Delta h/L$, allows some of the brine to be convected through the outlet (right) and into the fresh water aquifer. The mechanics of this "siphoning" effect are described in Appendix 2A of this chapter.

The convective flow of water in case (2), diagrammed above, would require a hydrologic model for a complete analysis since the normal flow of water in the aquifers could be significantly changed--not merely perturbed as in case (1). But conservation of mass suggests that the limiting speed of transport of salt would be dictated by the specific discharge times unit area allowed in the aquifer with the highest hydraulic conductivity.

The foregoing examples suggest that one take $v^{\ddagger}$ to be the larger of the normal aquifer flow velocities near the repository and therefore set

$$\dot{V} = A v_{aq}^{\ddagger}, \tag{2.5.11}$$

where A is the effective area of the open channels through the shale, connecting the aquifer to the salt bed. Although this assumption contributes a conservative element, other factors might also affect the degree of conservatism. For example:

1. The potential for cavity collapse is ignored. The neglect of collapse of rock over the growing solution cavity leads to an underestimate of the growth rate. In general, it is believed that collapse would increase the effective area, A_c, for infiltration of fresh water thus increasing the volumetric removal rate of salt according to Eq (2.5.11).

2. The effects of salt flow in retarding (or altogether precluding) cavity growth are ignored. Hamstra[2.17] has suggested that, below a certain depth, the salt would creep and tend to fill the cavity faster than solutioning could keep it open. Neglect of this effect in the present formulae tends to be conservative; i.e., gives an overestimate of the rate of solutioning.

3. The model cavity geometry is highly idealized. The idealization of the cavity shape makes uncertain the effective cavity dimension by a factor that could be as much as 5 or 6. An overestimate of cavity size is as likely as an underestimate of it.

For the present work, the rules for solutioning will be taken from Eqs (2.5.8) and (2.5.11), though modifications will certainly have to be made in any future assessments of the effects of solutioning. The most crucial modification needed is some way of taking into account the potential time-dependence of A (the effective area of the open channels through shale).

2.5.4 Construction of Failure Rates for External Modes of Release

In the following paragraphs, we attempt the construction of a priori probability distributions and associated failure rates for most of the release modes described in Section 2.4. The release modes are considered in no special order, except that the release through undiscovered boreholes is outlined first because we believe it best illustrates the approach to modeling that is used.

2.5.4.1 Failure Rate From Undiscovered Boreholes -- Because of exploration or mineral extraction activities in times prior to the siting of the waste disposal facility, there may be numerous boreholes penetrating the rock strata that border and contain the waste. The location and mapping of such man-made penetrations has a high priority in the final site selection process, and normally the waste emplacement would not be located in a region that has known extensive drilling and mining in the past.

However, there can never be total assurance that all boreholes are located. The possibility that one or more undetected boreholes remain, even after a thorough search, must be taken into account in assessing the hazards of water intrusion.

It is assumed that the only potentially hazardous boreholes are the ones that penetrate at least to the level of the salt beds enclosing the vaults, so only this population of undetected penetrations will be considered. Such holes may be sealed (perhaps imperfectly) or unsealed. If they are unsealed, the process of salt solutioning may already have begun at the time of shutdown of the facility.

It is here assumed that the area surrounding the disposal site is punctured with undetected boreholes with mean density β holes per square kilometer. Though the pattern of previous exploratory drilling may have dictated a nonrandom placement of the holes, it will be assumed that the ones remaining undetected occur randomly over the area surrounding the site: hence, β is the parameter of a Poisson distribution.

Let f denote the fraction of the undiscovered holes that are unsealed. Then the mean density of unsealed holes is $f\beta$ and the mean density of sealed holes is $(1 - f)\beta$. The seals on a borehole cannot last forever, and at some random time after sealing the plug will no longer be effective in blocking the flow of water. Without being too specific about its meaning, let $\psi(t)$ be the failure rate of the seals; i.e., $\psi(t)$ is the probability per unit time that a plug has ceased to block the flow of water. It is assumed that the plugs fail independently, and in that case, the expected number of sealed boreholes that have failed in the time interval (O, t) is given by:

$$B(t) = (1 - f)\,\beta \left\{ 1 - \exp\left[- \int_0^t \psi(s)\, ds \right] \right\} \text{km}^{-2} \quad . \qquad (2.5.12)$$

In deriving a failure rate, one must consider separately the cases of the initially unsealed boreholes, and the sealed but failed boreholes. It is reasonably assumed that a failed borehole will conduct less water than an open one, owing to the nonsoluble material that remains in the shaft.

1. Unsealed, Undetected Boreholes -- Since the boreholes are randomly distributed, the probability that exactly n unsealed boreholes penetrate within the area, A, of the working level is

$$p(n) = \frac{(f\beta A)^n}{n!} e^{-\beta A f} \qquad n = 0, 1, 2 \ldots \ . \tag{2, 5, 13}$$

Now, for any borehole that penetrates the salt layer, there is a shortest distance from the axis of the hole to the nearest waste drift. If boreholes are randomly located in the region surrounding the site, this minimum distance, S, is a random variable. The distribution of S (under these assumptions) is site-specific but unknown: it could be estimated by a numerical simulation that explicitly takes account of the geometry of the mined cavities. For purposes of illustration, we will assume a general distribution of S:

$$\Pr\{S \leq s\} = G(s) \ , \qquad s_0 \leq s \leq \infty \ ,$$

and specialize later.

As a final ingredient, one needs to connect the time at which any waste drift is overrun by a solution cavity from a borehole, to the initial, shortest distance to the borehole. Suppose s is the shortest distance and T is the random time at which water from the cavity reaches a waste drift, then:

$$\Pr\{T \leq t \mid S = s\} = u\left[t - \sigma(s)\right] \ ,$$

where

$$u(x) = \begin{cases} 0 & \text{if } x < 0 \\ 1 & \text{if } x \geq 0 \end{cases} \ , \text{ the unit step function,}$$

and $\sigma(s)$ is the solutioning time required to open a cavity of radius $\simeq s$. In the simple solutioning model of Section 2.5.3,

$$\sigma(s) = \frac{s^3}{\dot{V}} \ .$$

A derivation of a cumulative distribution function (cdf) for the waiting time until a drift is overrun by solutioning cavities initiated at any unsealed boreholes now follows.

403 054

For any one unsealed borehole in the region surrounding the repository, the random variable, T, has cdf:

$$\Pr\left\{T \le t\right\} = \int_0^\infty \Pr\left\{T \le t \mid S = s\right\} d\left(G(s)\right)$$

$$= \int_0^\infty u\left[t - \sigma(s)\right] d\left(G(s)\right) = G\left[\sigma^{-1}(t)\right] \quad ; \qquad (2.5.14)$$

where $\sigma^{-1}(t)$ is the inverse function to $\sigma(s)$ and it is assumed that:

$$\sigma^{-1}(t) \to \infty \quad \text{as} \quad t \to \infty \ ,$$

$$G(s) \to 1 \quad \text{as} \quad s \to \infty \ .$$

If there are $n > 1$ unsealed boreholes in the region surrounding the site, and if each such borehole is randomly placed, then there will be times $T_1, T_2, \ldots, T_n$, at which the solution cavities from each borehole, 1, 2, 3, ... n, will overrun a waste drift. According to the assumptions, these times are independent and identically distributed. The time of first overrun of a waste drift from any of n unsealed boreholes is then:

$$T(n) = \min\left(T_1, T_2, \ldots, T_n\right) \ ,$$

and from (2.5.14),

$$\Pr\left\{T(n) \le t\right\} = 1 - \left\{1 - G\left[\sigma^{-1}(t)\right]\right\}^n \ , \quad n = 0, 1, 2, \ldots \ . \qquad (2.5.15)$$

The cdf for the first time, T_u, of overrun, from any unsealed borehole is obtained by using (2.5.13) to remove the conditioning on n boreholes:

$$\Pr\left\{T_u \le t\right\} = \sum_{n=0}^{\infty} \Pr\left\{T(n) \le t\right\} p(n)$$

$$= 1 - \sum_{n=0}^{\infty} \left\{1 - G\left[\sigma^{-1}(t)\right]\right\}^n \frac{(f\beta A)^n}{n!} e^{-f\beta A}$$

or

$$F_u(t) = \Pr\left\{T_u \le t\right\} = 1 - \exp\left\{-f\beta A\, G\left[\sigma^{-1}(t)\right]\right\} \ . \qquad (2.5.16)$$

NOTES:

It is worth noting that, by Eq (2.5.16), there is a positive probability that waste drifts will never be overrun by solutioning cavities initiated at unsealed boreholes:

$$\lim_{t \to \infty} F_u(t) = 1 - e^{-f\beta A} < 1 \ .$$

(The term, $e^{-f\beta A}$, is the probability that there are no unsealed boreholes penetrating area A.)

The function $F_u(t)$ is not what is usually referred to as a cumulative distribution function since $\lim_{t\to\infty} F_u(t) < 1$. Feller [2.34] refers to such a function as a defective distribution function.

To illustrate further, take the hypothetical case where:

$$\beta = 10^{-2}\ \text{km}^{-2}, \qquad f = 0.5 \ ,$$

and let A be equal to four times the area of the site ($32.3\ \text{km}^2$). Then

$$1 - e^{-f\beta A} \approx f\beta A = 1.23 \times 10^{-2} \ .$$

In other words, using these hypothetical parameter values, there is only a 3 percent chance that water will intrude a waste drift from solutioning cavities initiated at unsealed boreholes.

2. Sealed but Failed Boreholes -- The waiting time distribution for T_f, the random time at which water reaches a waste drift owing to solutioning through a sealed but failed borehole, is derived in a manner identical to the one used to derive Eq (2.5.16). In fact, one can simply make the replacements:[2.18]

$$\beta \to B(t) \ ,$$

where B(t) is given by (2.5.12), and

$$\dot{V} \to \dot{W} \ ,$$

where $\dot{W}$ is the rate of salt removal from a cavity in $\text{m}^3 \cdot \text{yr}^{-1}$ when the cavity is formed from the failure of a sealed borehole. It is reasonable to expect that the rate of salt removal is less for a sealed borehole than for an unsealed borehole ($\dot{W} \ll \dot{V}$).

With the replacements indicated above, the cdf for the first time, T_f, of overrun from any sealed but failed borehole follows from Eq (2.5.16):

$$F_f(t) = \Pr\left\{T_f \le t\right\} = 1 - \exp\left\{-AB(t)\, G\left[\sigma^{-1}(t)\right]\right\} \qquad (2.5.17)$$

3. The Total Failure Rate -- The failure rate from undiscovered boreholes (unsealed, or sealed but failed) follows from the distribution of:

$$T = \min (T_u, T_f) \ ,$$

which is

$$\Pr\{T \le t\} = 1 - \left[1 - F_u(t)\right]\left[1 - F_f(t)\right] \ .$$

From the definition of failure rate, Eq (2.5.3)

$$\phi(t) = \frac{F_u'(t)}{1 - F_u(t)} + \frac{F_f'(t)}{1 - F_f(t)} \ , \qquad (2.5.18)$$

where the primes, ($'$), denote the time derivative. Note that $\phi(t)$ is just the sum of the respective failure rates from: (a) undiscovered, unsealed boreholes, and (b) undiscovered, sealed but failed boreholes.

NOTES:

(i) The derivation of the failure rate, Eq (2.5.18), used two as-yet unspecified functions, G(s) and $\sigma(s)$, that were defined respectively as: the cdf for the minimum distance between a randomly placed borehole and a waste drift, and the solutioning time required to enlarge a cavity to a characteristic size equal to s. In the sample calculations (Section 2.6), we will use the solutioning law derived in Section 2.5.3 and set

$$\sigma(s) = \frac{s^3}{\dot{V}} \ , \quad \text{or} \ \frac{s^3}{\dot{W}} \ .$$

Thus,

$$\sigma^{-1}(t) = (\dot{V}t)^{1/3} \ , \quad \text{or} \ (\dot{W}t)^{1/3} \ .$$

Furthermore, it will be assumed that G(s) is a uniform distribution on an interval $[s_0, s_1]$, with density

$$g(s) = \begin{cases} 0 \ , & \text{if} \quad s < s_0 \ , \\ \dfrac{1}{s_1 - s_0} \ , & \text{if} \quad s_0 \le s \le s_1 \ , \\ 0 \ , & \text{if} \quad s > s_1 \ . \end{cases} \qquad (2.5.19)$$

403 057

The assumption of a uniform distribution should be conservative and is convenient: the empirical distribution of the minimum distance could be determined by solving the implied problem in geometric probability,* using a map of the mined facility. But that problem has not been solved in this study. The empirical distribution of minimum distance would be more heavily weighted towards large values of s than the uniform distribution assumed here; hence, the uniform distribution is probably conservative. Whatever distribution is chosen, the assumption of a finite support $[s_0, s_1]$, for it is a natural one. The undetected boreholes that occur within the site's perimeter either terminate just below the salt-shale interface, in which case the nearest waste chamber is at most 113 meters away; or, at the other extreme, the boreholes can pass entirely through the working level and remain undetected in supporting pillars or dividers between the chambers, in which case a minimum distance would be about 1/2 the pillar dimension plus drift dimension. The chances of a very close pass-through at the working level seem small, because such a feature would be easily detected during the operational phase of the facility (via the appearance of wet salt or even caving of drifts).

(ii) Though the results will not be used in the present study, it is interesting (and perhaps even useful) to present the failure rate of water intrusion from sealed boreholes whose positions are known, in contrast to the randomly placed, undetected boreholes.

Suppose that there are N of these, located at known minimum distances, x_n, $n = 0, 1, 2, \ldots N$, from waste drifts. It is assumed that the plug failure rates are identical and equal to $\psi(t)$. Then one can show that the failure rate of water intrusion from any one or more of these mapped boreholes is:

$$\phi(t) = \sum_{n=1}^{N} \frac{F'(t - x_n^3/W)}{1 - F(t - x_n^3/W)} \quad , \tag{2.5.20}$$

where

$$F(t) = \begin{cases} 1 - \exp\left\{ - \int_0^t \gamma(s)\, ds \right\}, & t \geq 0 \\ 0 \qquad\qquad\qquad\qquad , & t < 0 \end{cases} .$$

---

*i.e., find the empirical distribution of the minimum distances between random lines that normally penetrate and terminate in a layered medium, and a set of regular voids (here, the backfilled waste drifts) imbedded in a layer. The solution to this problem might require a direct simulation such as Monte Carlo.

403 058

If the plug failure rate is constant, $\psi(t) = \tau^{-1}$, and Eq (2.5.20) reduces to a particularly simple form:

$$\varphi(t) = \tau^{-1} \sum_{n=1}^{N} u(t - x_n^3/\dot{W}) \quad ,$$

where u(t) is the unit step function defined earlier. The failure rate increases in "jumps" of magnitude τ^{-1} occurring at the times, $x_n^3/\dot{W}$, n = 1, 2, 3, ... N. It becomes constant and equal to $N\tau^{-1}$ for

$$t > \max_n \left(\frac{x_n^3}{\dot{W}} \right) .$$

Discussion of Parameters

1. β = mean density of undiscovered boreholes (km^{-2}).

For the reference site, it might be reasonable to assume a value of 10^{-2} km^{-2}. In practice, the mapping of the detectable penetrations in the region surrounding the site and the detection (or nondetection) of penetrations in the working level openings during operational phase should provide data that could be used to place a high-confidence upper bound on β.

2. f = fraction of undiscovered boreholes that are unsealed.

It is assumed that this parameter at the reference site is $f \simeq 0.1$. Again, the mapping of detectable penetrations would give information on the range of f.

3. $\psi(t)$ = failure rate for the plugs or seals of boreholes (yr^{-1}).

There is no quantitative basis at present for assigning a reliable mean time-to-failure of a borehole plug. "Failure" can also mean different things. Here, it is suggested that failure be defined as the creation of a continuous channel along the perimeter of the borehole, having a cross-sectional area equal to 10 percent of the open borehole area. It is also suggested that the failure rate be assumed a constant, τ^{-1}, with τ = 200 years.

4. A = area of working level = 8.088 km^2.

5. $\dot{V}$, $\dot{W}$ = the removal rate of salt in $m^3 \cdot yr^{-1}$ from a solution cavity by, respectively, transmission through an unsealed and a sealed but failed borehole.

For an open, 10 cm diameter borehole, a conservative value at the reference site is, $\dot{V} = 1.5\ m^3 \cdot yr^{-1}$.

For a sealed but failed borehole of the same size, $\dot{W} = 0.15\ m^3 \cdot yr^{-1}$.

6. s_1 = maximum possible distance in meters, between the waste drifts and the shaft of a borehole that penetrates at least to the salt level within facility perimeter.

   For the reference site, $s_1 = 113$ meters.

7. s_0 = a subjectively determined minimum distance in meters, between a waste drift and the shaft of a borehole that penetrates through the salt layer within facility perimeter.

   For the reference site, $s_0 = 27$ meters.

2.5.4.2 Failure Rate From Undiscovered Voids and Fracture Systems -- In addition to the pathways for water provided by man-made boreholes (treated in 2.5.4.1), there are naturally occurring penetrations that connect either upper or lower aquifers with the salt bed through the shale layers that bound the salt. These voids, or fracture systems in the shale, will here be called simply "features" to avoid specialization to any one of their geologic causes, most of which are poorly understood. Existing features (e.g., breccia pipes) may be associated with active solutioning, or they may be dry; in the latter case it is prudent and conservative to presume that their intrusion by water is inherent. The largest features may have surficial manifestations (subsidence troughs or collapse structures) and, subject to a proper geological interpretation, can be mapped. The very small or very young features are probably not detectable, so their density must be inferred from indirect geologic evidence.

For the purpose of this model, it is simply assumed that all classes of existing features occur in the vicinity of the site with a mean density, λ_0 per square kilometer. The fracture systems are not necessarily points in two dimensions whose projections to the surface may be linear and interconnected. However, their true geometry is not too important at this point* in model development, and one may regard λ_0 as the two-dimensional point density of the centroids of such features.

---

*Note, however, that the uncertainty in feature dimensions, such as lengths and opening sizes, introduces a wide uncertainty in the $\dot{V}$ parameter defined in this subsection.

403 060

The rate of creation of such features in the future, after site closure, is almost beyond speculation. Here it will be allowed that features are created randomly in the shale formation near the facility at a mean rate, λ_1 $km^{-2} \cdot yr^{-1}$. If the processes that lead to feature formation are stationary in time, then an estimate of λ_1 may be found by dividing λ_0 by the youngest age of the shale formation. The geologic interpretations of these features at a given site may require a time-dependent rate of formation, in which case the assumption of a constant rate could be changed without complicating the present model much.

With constant λ_0 and λ_1, it follows that:

$$\lambda(t) = \lambda_0 + \lambda_1 t \ km^{-2} \tag{2.5.21}$$

can be interpreted as the mean density of features in the region surrounding the site at some time $t > 0$, following site closure at time zero. The features are assumed to occur randomly, so that the probability of exactly n of them occurring in an area A, by time t, is

$$p(n,t) = \frac{[A\lambda(t)]^n}{n!} \exp\left[-A\lambda(t)\right] \qquad n = 0, 1, 2, \ldots . \tag{2.5.22}$$

Given relations in Eqs (2.5.21) and (2.5.22), the derivation of a failure rate from water intrusion via a feature can proceed in the same way that was used to derive the failure rate from undiscovered boreholes. The details need not be repeated again; one finds that

$$\phi(t) = \frac{F'(t)}{1 - F(t)} , \tag{2.5.23}$$

where

$$F(t) = 1 - \exp\left\{-A\lambda(t)\, G\left[\sigma^{-1}(t)\right]\right\} , \tag{2.5.24}$$

and the functions $G(s)$ and $\sigma(s)$ have the same forms as were given in Subsection 2.5.4.1. In particular, it is again assumed that $G(s)$ is a uniform distribution on $[s_0, s_1]$, see Eq (2.5.19). However, the minimum distance s_0 requires a different interpretation. As in the case of undetected boreholes, it again seems necessary to assume that the presence of a void or fracture system near the working level excavations would become evident during the operational period of the facility--particularly if the feature carried water. But here, the minimum distance should be dictated by considerations of remote sensing of such features. The minimum distance, s_0, should be set equal to that thickness of salt which is capable of shielding from detection (by any means) the presence of a typical (say) breccia pipe during the ten to twenty-year operational lifetime.

Discussion of Parameters

1. λ_0 = mean density (in km^{-2}) of centers of voids or centroids of fracture systems that connect either the upper or lower aquifers with the salt bed.

This parameter can obviously be measured only indirectly. For the sake of illustration, suppose that two sink holes have been observed in the reference site basin (covering an area of 1.86×10^4 km^2). It is determined that these sink holes are the result of local dissolution of the salt layer at 629-meter depths. Based on the extent of coverage of the basin by Pleistocene sediments, geologists estimate that there could be about ten times the number of sink holes visible if the sediments were removed. A good guess of λ_0 in this case would be:

$$\lambda_0 = \frac{20}{1.86 \times 10^4} \cong 1 \times 10^{-3} \text{ km}^{-2} \quad .$$

2. λ_1 = rate of creation, per unit area, of voids or fracture systems that connect either the upper or lower aquifers with the salt bed (units: $km^{-2} \cdot yr^{-1}$).

Given λ_0 and the youngest age of the shales, $\tau = 1.9 \times 10^8$ yrs (Triassic),

$$\lambda_1 \approx \frac{\lambda_0}{\tau} = 5.6 \times 10^{-12} \text{ km}^{-2} \cdot \text{yr}^{-1} \quad .$$

3. A = area of mined emplacement - 8.088 km^2.

4. $\dot{V}$ = volume rate of solutioning in $m^3 \cdot yr^{-1}$.

This parameter is highly variable, since even a conservative estimate of it requires a knowledge of the average dimensions and opening size of the relevant fractures. Here, it will be assumed that the fracture has an effective length of 1 km and an opening size of 1 mm. The effective area is then ~ 1 m^2. Accordingly, a conservative rate of solutioning at the reference site is

$$\dot{V} = 185 \text{ m}^3 \cdot \text{yr}^{-1} \quad .$$

5. s_0 = minimum thickness of natural salt capable of shielding from detection the presence of a void in the salt with characteristic dimension ~ 1 m, during the operational phase.

A guess: $s_0 \simeq 50$ meters.

6. s_1 (see 2.5.4.1).

$s_1 \simeq 113$ meters.

2.5.4.3 Failure Rate of Excavation by Erosion -- Though the probability of excavation by erosion per se can always be reduced to virtually zero by choosing a depth of burial well below global base level, it is worthwhile to estimate that probability for arbitrary depths of burial, just to provide perspective. The following model of the erosion/sedimentation processes acting over the site will be used.

Let X_i be the net thickness of overburden removed by erosion (or deposited as sediment) in the ith year after closing the waste vaults. Count distance downwards as being positive so that X_i is positive for net erosion, and negative for net deposition. Each X_i is assumed to be normally distributed with mean = m, and variance equal to σ^2. Then the total thickness of material removed (or deposited) in n years is

$$S(n) = X_1 + X_2 + X_3 + \ldots + X_n \ .$$

Going over to "continuous" time, one can set

$$t \approx nt_0, \qquad t_0 \equiv 1 \text{ yr}$$

so that the continuous analogue of S(n) is S(t), a Brownian motion process[2.19] with a mean = μt and a variance = at.

$$\mu = \frac{m}{t_0} \text{ meters/yr} \ ,$$

$$a = \frac{\sigma^2}{t_0} \text{ meters}^2\text{/yr} \ , \qquad a > 0 \ .$$

A representation of this random process is sketched below.

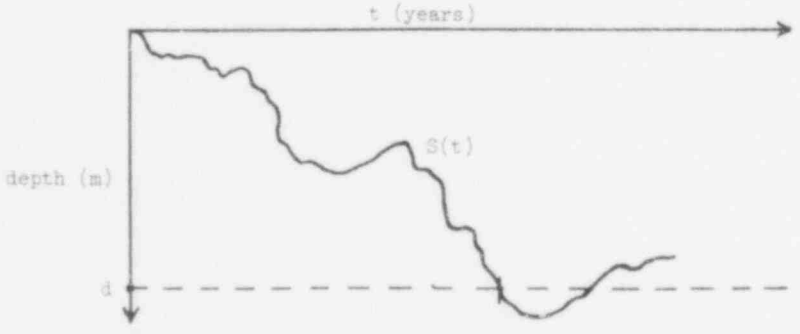

One is interested in the probability distribution of the time of first passage through a layer originally at a depth d, say, below the surface. This distribution corresponds to the distribution of waiting times, T, until first excavation by erosion, given that none of the other failure mechanisms operate. For $\mu \geq 0$, the cdf is:[2.20]

$$F(t) = \int_0^t \frac{d}{\sqrt{2\pi a \tau}} \exp\left\{-\frac{(d - \mu\tau)^2}{2a\tau}\right\} d\tau \qquad (2.5.25)$$

and the associated failure rate is found from Eq (2.5.25) by the usual formula:

$$\phi(t) = \frac{F'(t)}{1 - F(t)} .$$

Note that the integral in Eq (2.5.25) can be evaluated in terms of the tabulated error function, or the complimentary error function.[2.21]

Parameters

The parameter, μ, can be interpreted as the regional erosion/deposition rate. The world-wide, continental average of this rate is of the order of 10^{-3} m/yr. The parameters σ^2 and a have less direct meanings, and might be connected with terrain relief, geomorphic forces, and climate. Some guesses of the nominal values for these parameters in context of the reference site follow.

$\mu = 0 \pm 10^{-3}$ meters yr^{-1} ,

$a = 2 \times 10^{-3}$ meters^2 yr^{-1} ,

$d = 629$ meters (depth to emplacement) .

2.5.4.4 Failure Rate From Faulting -- The possibility that one or more large faults pass through the repository is considered here. This problem was considered by Claiborne and Gera,[2.22] who also estimated the chances of faulting through a repository (similar to the reference repository) located in southeastern New Mexico. They claim that the probability per year of a fault intersection is about 4×10^{-11} per year, for their particular hypothetical site. The model for a failure rate to be presented in this subsection is similar to that of Claiborne and Gera, but certain different assumptions will be made in order to make it more widely applicable. The assumptions are listed and discussed below.

1. It is assumed that there are no detectable faults near the site at closure time. The possibility that one or more undetected faults exist is treated in the failure rate calculation for Undiscovered Voids and Fracture Systems (Subsection 2.5.2.2). In a more realistic treatment of the problem than is possible here, there would be no distinction made between the small-scale fractures considered in Subsection 2.5.2.2 and the larger faults considered in the present section.

403 064

2. It is assumed that the reference site lies within a specific fault zone. For purposes of this study, a fault zone is a geographical region in which the observed faulting is predominantly of one type. Because of errors and biases which arise in the process of fault detection, the boundaries between fault zones are only roughly defined. The reference site's fault zone is assumed to have area A, with faults occurring in this area with a frequency ν faults per year. It is possible to assign a rough faulting frequency within a particular zone, though the values obtained are highly uncertain owing to ambiguities in the measured ages of mapped faults. The frequency of appearance of faults of detectable size (generally 1 km or greater in length) within the continental USA ranges from 10^{-7} yr^{-1} to 10^{-3} yr^{-1}.[2,23]

It is impossible, at present, to tell whether the faulting frequency characterizing a zone is changing in time. The parameter ν postulated above is a constant--but a time-dependent frequency could easily be incorporated into the present model if the geologic evidence provides the justification.

3. The lengths of all faults are exponentially distributed with a mean length, $\lambda \simeq 3$ km.

There is ample empirical evidence for this hypothesis if one considers the statistics for the observable faults that are usually of length > 1 km.[2,23] It is then natural to suppose the observed fall-off in frequency of faults with lengths < 500 m is simply a consequence of observational errors, and to extend the size spectrum downwards to features of arbitrarily small length.

However, because of analytical difficulties, only the fact that the mean fault length is ~ 3 km will be used in the present model.*

4. It is assumed that the faults grow so slowly that their intersections with the salt bed remain closed, i.e., the salt has time to flow and reconsolidate. Thus the openings presented by faults are such that no paths of high permeability are maintained for very long through the salt beds. This point is a controversial one, though the evidence pertaining to the reference site's assumed fault zone indicates that salt healing will predominate.

---

*It is possible, but analytically messy, to compute a failure rate that takes into account the fact that faults intersecting the repository may have a distribution of lengths--hence a distribution of effective openings for water infiltration of salt beds.

5. Finally, the probability, q, that a single fault of length ℓ intersects the repository (given that the fault occurs randomly within the fault zone) is taken from Claiborne and Gera's work.[2.24] This probability is given approximately by:

$$q = p_1 + p_2 + p_3 \quad , \tag{2.5.26}$$

where

$$p_1 = (r/R)^2, \quad \alpha = \ell/R \quad ,$$

$$p_2 = p_1 \left[\frac{\alpha^2 + 1}{\pi \alpha^2} \sin^{-1}\left(\frac{\alpha}{\sqrt{1+\alpha^2}} \right) + \frac{1}{\alpha\pi} - \frac{1}{2} \right] \quad .$$

$$p_3 = \frac{2}{\pi\alpha} \left(p_1\right)^2 \cos^{-1}\left(\frac{\bar{y}^2 + 1 - \alpha^2}{2\bar{y}} \right) \quad ,$$

and

$$\bar{y} = \frac{1}{2} \left[1 + \alpha + \sqrt{1+\alpha^2} \right] \quad .$$

In the above, r is the effective radius (in km) of the reference site; and R is the effective radius in kilometers of the fault zone ($\pi R^2 = A$).

The probability of intersection, q, is a function of r, R and the fault length, ℓ. For analytic simplicity, it is assumed that $\ell = \lambda$, the mean fault length.

From assumptions (1), (2), and (5), it follows that the probability that the repository is intersected by exactly N faults in the time interval (0, t) is

$$p(N, t) = \frac{(q\nu t)^N}{N!} e^{-q\nu t} \qquad N = 0, 1, 2, \ldots \tag{2.5.27}$$

and a constant failure rate, $q\nu$, follows from Eq (2.5.27), provided that one ignores the implications of assumption (4) and the time interval required to solution the salt lying above the waste drifts. The required time interval is taken to be

$$\Delta t = s^3/\dot{V} \text{ yr}$$

(see Subsection 2.5.3), where $s = 113$ meters at the reference site, and $\dot{V}$ is the volume rate of salt removal through the fault opening. Here, $\dot{V}$ is clearly proportional to the total length of the faulting that intersects the site, and this fact should be taken into account. The total length of faulting intersecting the repository is random, but an upper limit of its mean value, $\bar{\ell}$, is $\bar{N}(t)\lambda$, where $\bar{N}$ is the expected number of faults that intersect the site in the time interval (0, t). From (Eq 2.5.27), $\bar{N}(t) = q\nu t$. Thus,

$$\dot{V} = w\bar{\ell} = w\lambda q\nu t \quad , \tag{2.5.28}$$

where w is the effective volume removal rate for salt per unit length of fault (units: $m^2 \cdot yr^{-1}$). Thus, the condition that $t > \Delta t$ before water may infiltrate the waste drifts implies that

$$t \geq s^3/(w\lambda q\nu t)$$

or that

$$t \geq \left(\frac{s^3}{w\lambda q\nu}\right)^{1/2} .$$

The failure rate for water infiltration, owing to massive faulting is therefore:

$$\phi(t) = \begin{cases} 0 & \text{if } t < \left(s^3/w\lambda q\nu\right)^{1/2} \\ \\ q\nu & \text{if } t \geq \left(s^3/w\lambda q\nu\right)^{1/2} \end{cases} . \tag{2.5.29}$$

In the above, λ should be expressed in meters.

Discussion of Parameters

1. ν = faulting frequency that characterizes the fault zone in which site is located.

The hypothetical reference site is located in a zone that contains very few faults relative to its size. However, the site also lies very near the boundaries of a rift zone similar to the one in the Rio Grande Valley of New Mexico. Given the uncertainty in the boundaries of fault zones, it seems prudent to assign the faulting frequency according to the site's nearness to the more active zone. Accordingly, one sets

$$\nu = 1.3 \times 10^{-4}\ yr^{-1} .$$

As mentioned, a possible range for ν is 10^{-7} to $10^{-3}\ yr^{-1}$.

2. A, R = respectively, the area and the effective radius of the fault zone.

The rift zone mentioned in (1) has a roughly defined area of 2×10^5 km^2. The effective radius would be about 252 kilometers. The effective radius of the repository is 1.6 km.

3. λ = mean linear length of faults in kilometers. Here, λ = 3 km. Note that the value of q, the probability of intersection of the repository, is about 10^{-3} for a 3 km long fault and the values of R, r assigned in (2).

4. s = the vertical distance from the waste drifts to the boundary of the salt layer. s = 113 meters.

5. w = the effective volume removal rate of salt per unit length of fault (units: $m^2 \cdot yr^{-1}$).

From the considerations of Section 2.4,

$$w = dv^*$$

where d is here the effective opening thickness of a fault and v^* is the maximum velocity of brine in the fault opening. It is assumed that $d \sim 1$ mm $= 10^{-3}$ meters, and for hydraulic conditions at the reference site, assume that $v^* \approx v_{aq}$, or 185 m yr^{-1}. Thus w is 0.185 $m^2 \cdot yr^{-1}$.

2.5.4.5 Failure Rate From Igneous Intrusions -- The chances of intrusion of magma upon the waste repository appear to be proportional to the rate of faulting in the zone containing the site: almost all forms of igneous intrusion are associated with faulting (or vents and fissures) whereas many faults are not associated with magma flows. Thus, one may tentatively take the frequency of intrusion by magma to be

$$kq\nu$$

where q, ν are as defined in Subsection 2.5.4.4, and k is a dimensionless parameter that is positive but ≤ 1. The parameter k can have various physical interpretations, depending upon the type of igneous intrusions being referenced.

The types of intrusions to be considered are important because only the consequences of an intrusion and the time delays associated with those consequences matter in an assessment of the failure rate (as defined in this section). Many scenarios for magmatic intrusion upon the site can be imagined; and for most of these, the immediate consequences are uncertain but probably negligible. Two examples will suffice.

403 068

1. Suppose that a fault intersects the lower aquifer and shale layer and magma flows into it, forming a dike or sill. The "immediate" effects would be a change in the local permeability of the lower aquifer. The deep groundwater flow might be redirected and some solutioning of the salt layer could be initiated. However, the time delays and release rates for the scenario would not be radically different from the postulated effects of faulting alone.

2. The same dike or sill (above) now penetrates the salt layer through the repository and also the upper shale layer. In the process of formation, a small amount of the waste could become dissolved in the magma, but the major effect would still be the change in local permeability, leading to a redirection of ground water flow with perhaps a small amount of contamination of the groundwater that contacts the dissolved waste on the magma. In this example, it still seems that the bulk of the waste would be isolated from water until solutioning developed. Again, the effects would not be substantially different from the postulated effects of faulting on the repository.

On the other hand, if the magma vents at the surface, there is the possibility of a hazard different from the one posed by faulting, since some of the waste could be entrained in the flow, carried upwards and distributed over the surface near the vents. The venting of lava may proceed rapidly in comparison with the slow process of salt solutioning, so that time delays between initiation and completion of the release event could be small. The extreme examples of venting are volcanoes: the scale of these makes it easy to believe that a significant amount of waste could be intercepted by the flow and widely dispersed. Once it is dispersed, there is the possibility of direct contact with soil and surface water, though much of the ejected waste would be fixed in the solidified lave or ash. The degree of exposure of the waste radionuclides in ejected lava is hard to quantify, but the possibility of making direct contact with the elements of the biosphere is real enough.

These examples illustrate the plausibility of the following assignment of a failure rate:

$$\phi = kq\nu, \qquad t \geq 0 \tag{2.5.30}$$

where k is estimated by the ratio: (the number of observed faults in the site's fault zone that are associated with coeval vented igneous material)/(the total number of observed faults in the site's fault zone). For the reference site context, a rough estimate of k is $\sim 10^{-2}$. The parameters q, ν are those defined in Subsection 2.5.4.4.

2.5.4.6 Failure Rate From Explosions -- The derivation of a failure rate of water intrusion, or excavation of the site, owing to the effects of an explosion is a highly speculative exercise. Much of this subject--like the subject of inadvertent intrusion--requires subjective judgments concerning the actions of humans in the future. One begins by considering the energy that is necessary to substantially change the rock formations bounding the salt and then makes rational assumptions about the usefulness of energy releases of such magnitudes. The following discussion is conducted within the context of the reference site.

Useful empirical relations between crater dimensions and explosive yield are given for surface nuclear bursts in Effects of Nuclear Weapons.[2.25] According to these relations, a surface explosion of 635 megaton (MT)* yield would be required to excavate a crater 629 meters deep. To excavate through the shale layer (510 m depths) requires a 356 MT yield. Nuclear explosions of such yield are unknown, though it is perhaps possible to build such a device. More typically, a thermonuclear weapon of the kind that might be deployed against strategically important targets would have a yield of 200 kilotons (KT) to 10 MT. Such a weapon would most likely be delivered by a ballistic missile or released from a satellite; and there seems to be no incentive for the use of larger-yield weapons in warfare. Thus, one must rationally reject the possibility of explosions in the 100 MT range over the site, and inquire of the potential effects of a surface burst in the 10 MT range.

If it is assumed that the fracture zone surrounding a burst crater in hard rock extends to a radius that is 1.5 times the apparent crater radius, as for smaller yield weapons, one finds that a 10.5 MT burst is barely sufficient to fracture the upper shale layer and perhaps provide pathways for water infiltration of the salt. In this case, the fracture zone lies mostly in the sandstone aquifer and covers an area of ~ 0.8 km^2; the apparent crater depth is 160 meters.

What is the effect of small yield explosions? Perhaps it is now obvious why explosions of the type used for construction or seismic exploration--a few hundred pounds of TNT at most--are not seriously considered here: their effects may be indistinguishable from seismic "noise." In general, "For very low-yield weapons, it is difficult to produce significant damage to a buried structure unless it is within the rupture zone around the crater."[2.25]

The most plausible scenario for failure by explosions is therefore the following one.

One or more nuclear weapons in the 10 MT yield range are, by accident or in the event of war, detonated on or near the surface of the reference site. The explosions cause some fracturing in the upper shale layer; water infiltrates the salt layer, and a solution cavity is formed that may in some time reach the waste drifts.

---

*1 MT = 4.2×10^{15} Joules.

403 070

The probabilities of the events that build the scenario described above a highly uncertain. Some speculation on these probabilities follows.

1. Probability of War

The appeal is to the historic incidence of war, although there is evidence that the advent of nuclear weapons may have invalidated the use of historic statistics for estimating the future probabilities of war. At any rate, using the data of Quincy Wright,[2.26] "L. F. Richardson[2.27] found that the number of wars which begin in each year from 1500 to 1931 fit a Poisson distribution with mean number of outbreaks" equal to 0.692 per year.[2.28] Thus, the "failure rate" for war is relatively large, and probably represents an upper limit in modern (and future?) times. The small sample, apparent frequency for modern world conflicts (two in past 77 years is 0.026 per year).

2. Probability of Accidental Release

One would have to examine the statistics on armaments inventories, preparedness exercises and the incidence of "accidents" during those exercises, to infer a realistic number. But it is reasonable to suppose that the frequency of accidental release is proportional to the frequency of war, the proportionality constant being a number $<< 1$. The frequency of any release, accidental or intentional, is therefore nearly the apparent frequency of war.

3. Probability of Impact on Site, Given Release

There is no rational reason for targeting the waste disposal site directly; rather, the impact of a vehicle carrying a weapon would be accidental or could occur as a result of missing an intended target. The likely intended targets for a large-yield weapon would be: large industrial centers, missile silos, strategic bomber bases and large naval bases. Assuming that one or more of these intended targets are near the waste disposal site, the probability of impact on the site can be estimated. The estimate is made for one target that is assumed to be at a ground distance $= r\sigma$ from the center of the waste disposal site.* The variable r is the distance between target and site measured in units of σ, the standard deviation of the weapon delivery vehicle's miss distance, assuming that the miss distance is distributed with a circular normal distribution with mean equal to target coordinates and variance equal to σ^2. For convenience, the waste disposal site is here assumed to be a circular area of radius $= R\sigma$. With these definitions, the probability of impact on the site, given an attack against the nearby target is, to a good approximation,[2.29]

*If there is more than one potential target of the indicated class near to the site, a probability for each one should be calculated by Eq (2.5.30) and the result summed to give the overall estimate.

$$q = \begin{cases} \dfrac{2R^2}{4+R^2} \exp\left\{-\dfrac{2r^2}{4+R^2}\right\} & \text{if } R < 1 \ , \\ P(x_1) & \text{if } R > 1 \ , \\ P(x_2) & \text{if } R > 5 \ , \end{cases} \qquad (2.5.31)$$

where $P(x) \equiv 1/2\left[1 + \operatorname{erf}(x/\sqrt{2})\right]$, and

$$x_1 = \frac{\left[R^2/(2+r^2)\right]^{1/3} - \left[1 - \frac{2}{9}\cdot\frac{2+2r^2}{(2+r^2)^2}\right]}{\left[\frac{2}{9}\,\frac{2+2r^2}{(2+r^2)^2}\right]^{1/2}}$$

$$x_2 = r - \sqrt{R^2 - 1} \ .$$

The probability that the given target is attacked with a weapon of yield > 10 MT, given the advent of war, is assumed to be one for conservatism.

4. Fracturing of Shale and Water Infiltration

Given some fracturing of the shale and the attendant water infiltration, solutioning is assumed to proceed according to the rule given in 2.5.3. The time interval required to infiltrate waste drifts following shale fracture is

$$\Delta t = s_1^3/\dot{V} \ , \qquad (2.5.32)$$

where s_1 is the distance from the drifts to the top of the salt layer, and $\dot{V}$ is a volume removal rate for salt ($m^3 \cdot yr^{-1}$) through the fractured shale.

The discussions in paragraphs 1 - 4, above, lead immediately to a failure rate of water intrusion, owing to explosions initiated on the site surface.

403 072

If λ_w is the mean frequency of war, and q, Δt are given in Eqs (2.5.31 and 2.5.32) then

$$\phi(t) = \begin{cases} 0 & \text{if } t < s_1^3 / \dot{V} \\ q\lambda_w & \text{if } t \geq s_1^3 / \dot{V} \end{cases} \qquad (2.5.33)$$

Discussion of Parameters

1. λ_w = the mean frequency of war (yr^{-1}), assuming the occurrence of war is a stationary process.

A guess: $\lambda_w = 0.026\ yr^{-1}$ (see text, para. (1)).

2. σ = standard deviation of weapon delivery system miss distance (km). Unclassified σ's are of the order of 1 km.

3. r = distance between nearest potential target center and center of waste disposal site, measured in units of σ.

For illustration, it will be assumed that a strategic center lies 145 km to the northwest of the reference site. Thus r = 145.

4. R = effective radius of reference site, measured in units of σ.

For the present reference site, $\pi(R\sigma)^2 = 8.08\ km^2$ gives R = 1.6.

5. Note that with σ = 1 km, r = 145, and R = 1.6, the formula for q gives a value $\ll 10^{-14}$. Hence the calculated q is vanishingly small. Accordingly, it seems prudent to always set q equal to

$$\max(\text{calculated } q,\ 1.568 \times 10^{-8}) .$$

The second number, $\sim 10^{-8}$ in the parentheses, is simply the ratio:

$$\frac{\text{site area}}{\text{area of earth's surface}} .$$

This ratio is the probability of impact on the site for a completely random impact point distribution over the earth's surface. A random impact point distribution would be appropriate if missile guidance failed entirely.

6. s_1 = 113 meters for the reference site.

7. $\dot{V}$ = the volume removal rate of salt in $m^3 \cdot yr^{-1}$ through the fractured shale produced by a 10 MT surface burst.

The area presented for infiltration by water is probably much less than the total area estimated for the fracture zone (0.8 km^2). A guess is that about 10^{-4} of the fracture zone area represents the effective opening area. Accordingly, $\dot{V}$ for the reference site is about 1.5×10^4 m^3/yr.

2.5.4.7 Failure Rate From Meteorite Impact -- Claiborne and Gera have thoroughly reviewed the possibility that a waste disposal facility in deep, geologic media might be excavated by the impact of a large meteorite. For a facility having an area of 8 km^2, and burial at 600 meter depths, they estimate the changes of excavation to be 2×10^{-7} in a one-million year period.[2.30] This probability is based on estimates of the frequency of impacts of meteorites capable of producing craters with diameters greater than 2 km (it is assumed that crater depth is one-half crater diameter). The physical basis for estimates of impact frequency, i.e., the frequency versus mass and diameter versus impact speed relationships, are adequately reviewed in papers by Brown;[2.31] Shoemaker, Hackman and Eggleston;[2.32] and Hartmann.[2.33]

The present model for the failure rate from meteorite impact will adopt the estimate of Claiborne and Gera, with scaling to a facility of arbitrary area, A km^2:

$$\phi = 2(A/8) \times 10^{-13} \text{ yr}^{-1} . \qquad (2.5.34)$$

No attempt is made to scale the result to arbitrary depths of burial, although the relationships provided in References 2.20 and 2.22 are easily applied if it proves necessary. For the reference site, A = 8.088 km^2 and the depth of burial is 629 meters.

2.5.4.8 Speculations on Inadvertent Intrusion -- The potential failure of disposal owing to inadvertent intrusion of the waste repository is the most poorly defined issue among the ones that have so far been considered. A quantitative treatment of the problem seems impossible so none will be made in this study, though models of failure by intrusion based on definite assumptions about future scenarios for society could easily be constructed. Thus, the following remarks are intended only to present one subjective view of the subject.

The standard, general scenario for accidental intrusion is the following.

At some time in the future, there is a loss of administrative control of the exclusion area surrounding the site; and after loss of control there is ultimately a loss of social "memory" regarding the site's location and purpose. It is then assumed that, once location and purpose are forgotten, the surface features above the site would become indistinguishable from the neighboring terrain and would thereby become equally vulnerable to intrusion by some future society that is searching for mineral resources or scientific knowledge. In fact, one might add curiosity to the list of motives for intrusion and claim that some kind of exploration would occur with high probability, since the surface temperature over the reference site would be slightly higher than ambient: the 8 km^2 area would probably be visible on infrared photographs taken from an aircraft.

The hazards attending an intrusion according to the scenario are alleged to be small. Some radioactive material might be accidentally raised to the surface and cause local contamination. But, more likely, the purpose of the site would be recognized, decontamination measures would be taken, and the exploratory holes would be sealed. The area would, in effect, be placed again under some form of administrative control. The first exploratory drilling would thus add only a long-term hazard very similar to that postulated for undetected boreholes in Subsection 2.5.4.1.

A failure rate model for the long-term hazard from future exploratory drilling would require two modifications of the treatment in 2.5.4.1.

1. The introduction of a delay in time to represent the sum of the lifetimes of administrative control and social memory concerning the site. The time delay is a random variable whose distribution is beyond speculation. That part of it representing the waiting time until loss of control might be related to the frequency of large wars (see 2.5.4.6); but there are no suggestions forthcoming for the lifetime of social memory.

2. The exploratory drilling from the surface would in principle allow a borehole to pass arbitrarily close to a waste drift, in contrast to the non-zero lower limit placed on the drift-shaft distance in the treatment of boreholes created contemporaneously with the repository.

One expects that these two modifications would have an opposing effect in their contribution to a failure rate. The delay time until exploratory penetration would be compensated by the possibly shorter solutioning times required to bring water in contact with the waste. But since the delay time required by modification (1) is highly uncertain, the model of a failure from future exploratory drilling has not been followed up in the present work.

2.5.4.9 Incorporating Self-Induced Release Modes in the Competing Risk Model -- The ways by which the reference repository could adversely affect the long-term stability of its own surroundings have been called the "self-induced" release modes (Section 2.4). Study of this class of complex and ill-defined mechanisms for release of waste has been deferred to Appendix 2A of this chapter, where methods for sorting out the more important modes are proposed and some simulation tools for quantitative studies of identified modes are developed.

It will be seen that the simulation models developed in Appendix 2A are deterministic in nature: the model results express a unique, physical state of the system (repository + host rocks) as functions of time. This deterministic nature of the present simulation contrasts with the models of the so-called external release modes (treated in Subsections 2.5.4.1 through 2.5.4.7) which provide estimates of the probability that the system is in a given physical state during a given interval of time. Granting the need for a uniform, probabilistic treatment of all identified release modes, the question that arises is: how does one incorporate deterministic results into a probabilistic formalism, such as the Competing Risk Model proposed in Subsection 2.5.1? One way of forcing an incorporation is described below.

We first anticipate the developments given in Appendix 2A and briefly describe the essential features of the simulation model. The latter consists of a system of non-linear, ordinary differential equations whose independent variables describe the time-dependent state of a highly idealized (lumped-parameter) repository and its surroundings. During a simulation run, the equations are numerically integrated to obtain the values assumed by the dependent variables over prescribed intervals of time. The results of a run are usually plotted or printed to allow for their subsequent study and interpretation.

Among the many variables that are output by the simulator, the more relevant to the present discussion are ones that specify the thickness of salt layer removed by solutioning mechanisms. There are several of these variables because there are several assumed mechanisms in the model: however, for purpose of illustration, we will assume that there is only one such variable and will call it $D(t)$ in this subsection. The first time of waste drift overrun through the mechanism that generates $D(t)$ will be called T. Then it is clear that

$$T = \min \{t:\ D(t) \geq 113\ m\}\ , \tag{2.5.35}$$

where 113 m is the approximate thickness of salt separating the waste drifts from the layers of shale. Though T is not a random variable, a formal cumulative distribution function (cdf) can still be defined for it. If $D(t)$ is nondecreasing,

$$F(t) \equiv Pr\{T \leq t\} = \begin{cases} 0 & \text{if } D(t) < 113\ m \\ 1 & \text{if } D(t) \geq 113\ m\ . \end{cases}$$

403 076

In other words, the formal cdf is just the unit step function (defined in 2.5.4.1) centered on 113 m.

Once could use the formal cdf given above to derive a formal "failure rate," though the result is numerically inconvenient. Instead, we modify the unit step function slightly by introducing a slope on its front edge and defining a new function:

$$w(x) = \begin{cases} 0 & \text{if } x < 0 \\ \frac{x}{\epsilon} & \text{if } 0 \leq x < \epsilon \\ 1 & \text{if } x \geq \epsilon \end{cases} \qquad (2.5.36)$$

where ϵ is a small number with the same units as x. If ϵ is small (in this case: if $\epsilon \ll 113$ m), then the modification is inessential and one has the numerically tractable, formal cdf,

$$F(t) = w[D(t) - 113\ \text{m}] \ , \qquad (2.5.37)$$

and an associated failure rate, which is explicitly given by

$$Q(t) = \begin{cases} \frac{D'(t)}{\epsilon + 113\ \text{m} - D(t)} & \text{if } 113\ \text{m} \leq D(t) < 113\ \text{m} + \epsilon \\ 0 & \text{otherwise} \end{cases} \ . \qquad (2.5.38)$$

The failure rate, Eq (2.5.38), could be used in the competing risk model of 2.5.1 along with the failure rates for the external release modes to place all release modes on an equal footing, so to speak. This would of course require that the two codes for implementing the two different models be combined. The derivative of D(t) indicated in Eq (2.5.38) is easily computed in the process of evaluating the derivatives in the differential equations that describe the waste/host rock simulation scheme. A choice of ϵ should be made that reflects the uncertainty in the distance of overrun by solutioning but is not too small: for the reference repository we suggest that $\epsilon = 6$ m (or about the vertical dimension of a waste drift).

The method indicated above for incorporating deterministic simulation results into the competing risk model would permit the parallel exercise of both types of models in an integrated computer code. This possibility is important for several reasons, but mainly for reasons that bear upon the needs of model sensitivity analyses. We note that many of the uncertain parameters appearing in the failure rates for the external release modes (Subsections 2.5.4.1 through 2.5.4.7) also appear in the models of waste/host rock interactions of Appendix 2A: for example, the specific discharge rate of the aquifers, the mean density of boreholes and the mean density of fractures. When there are so many statistically dependent parameters common to the models, a separate sensitivity analysis for each model would be difficult to implement, and might lead to incorrect conclusions if parameter dependence were ignored.

2.6 Sample Calculations of External Mode Probabilities

A computer code has been written to implement the competing risk formalism and the failure rate models described in Section 2.5. The purpose of the code is simply to illustrate the feasibility of numerical calculations with the formalism at this stage of development.

Results of a sample calculation with the code are plotted in Figure 2.5.4, which gives the logarithms (base 10) of the probabilities of release by way of the external release modes versus the logarithm of elapsed time since site closure. The failure rates derived in Subsections 2.5.4.1 through 2.5.4.7 were used in the sample calculation: the values used for the appropriate parameters in the sample calculation are also the nominal parameter values quoted in the subsection treating each failure rate. A cut-off probability of 10^{-6} was used to delimit the ordinate of Figure 2.5.4. Thus any mode that does not achieve a computed probability greater than 10^{-6} within $10^{6.2}$ years is not represented on the plot. This was the case for erosion and meteorite impact.

No particular conclusions concerning long-term repository stability should be drawn from the results that appear in Figure 2.5.4. Note that these estimates of probability are highly sensitive to changes in certain of the parameter values. In turn, the ranges of the parameter values are uncertain and may be large. These example calculations do, however, point out certain inconsistencies between the geological assumptions made about the reference site and our choice of parameters used to illustrate the models. The relatively high probabilities achieved for modes (1), (2) and (4) (respectively: boreholes, voids and fractures, faulting) after 10^4 years are consequences of a high rate of salt solutioning that is implicit in our choice of aquifer discharge rate and areas for the several kinds of penetrations of the shale barriers. If such a high rate of solutioning had prevailed at the reference site in the past, then the hypothetical salt lens in which the repository is placed would probably not be present. The inconsistency serves to emphasize the point that we are dealing with models that require real data to test their validity.

The most sensitive parameters in the present model appear to be the ones specifying a volumetric removal rate of salt from solution cavities initiated through undiscovered boreholes, undiscovered voids, explosions and faulting. The rates of salt removal were thought to be conservative (overestimates) when assigned. However, this presumption may be wrong. In addition, the conceptual assumptions made in the models of salt solutioning may be incorrect (see Section 2.5.3 for a discussion of the salt solution models).

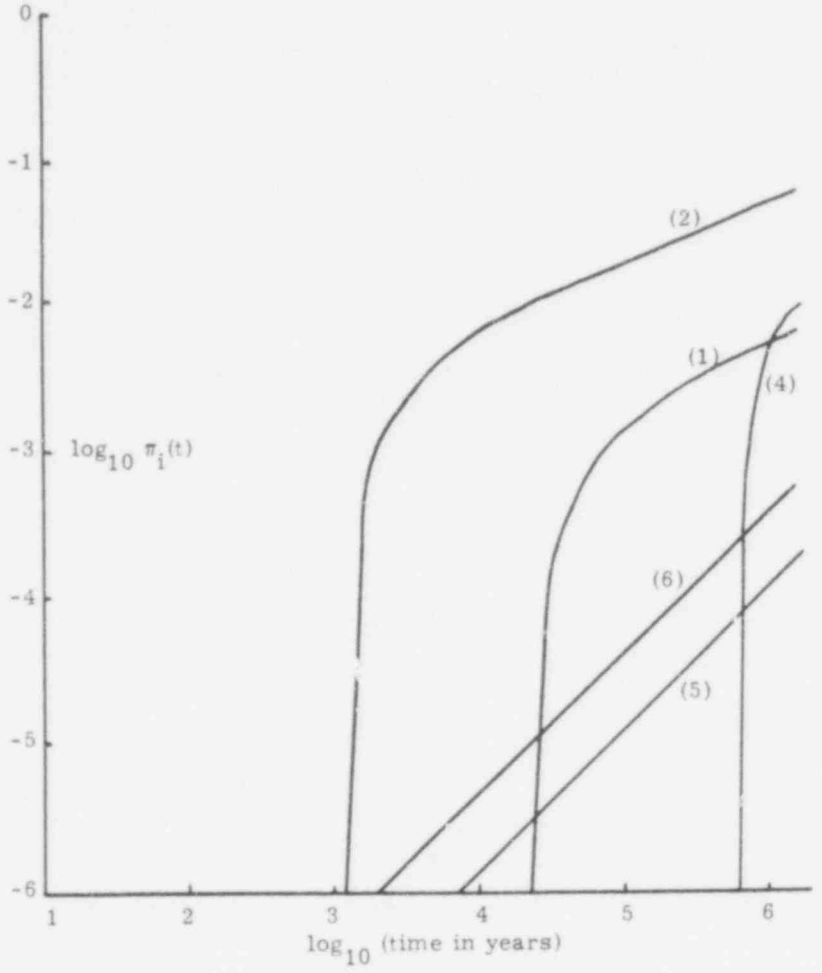

Sample Calculation Results

(1) - undetected boreholes

(2) - undetected voids and fractures

(4) - faulting

(5) - magmatic intrusions

(6) - nuclear explosions

Figure 2.5.4

References - Chapter 2

2.1 H. C. Claiborne and Ferrucio Gera, Potential Containment Failure Mechanisms and Their Consequences at a Radioactive Waste Repository in Bedded Salt in New Mexico, ORNL-TM-4639, Oak Ridge National Laboratory, Oak Ridge, TN, pp 13-29, October 1974.

2.2 For examples, see Chapter 3 in: G. E. Apostalakis, Mathematical Methods of Probabilistic Safety Analysis, UCLA-ENG-7464, UCLA-School of Engineering and Applied Science, September 1974.

2.3 R. E. Barlow and H. E. Lambert, "Introduction to Fault Tree Analysis," in Reliability and Fault Tree Analysis - Theoretical and Applied Aspects of System Reliability and Safety Assessment, SIAM, Philadelphia, PA, pp 7-35, 1975.

2.4 Stanley E. Logan, (editor), Workshop on Geologic Data Requirements for Radioactive Waste Management Assessment Models, UNM Report No. NE-27(76), Union Carbide 297-1, The University of New Mexico, Albuquerque, NM, p 32, September 1976.

2.5 Alternatives for Managing Wastes from Reactors and Part-Fission Operations in the LWR Fuel Cycle, ERDA-76-43, Vol. 4, UC-70, Sections 23 and Subsection 2.5.1, May 1976.

2.6 K. J. Schneider and A. M. Platt (editors), High Level Radioactive Waste Management Alternatives, BNWL-1900, Battelle-Northwest, Richland, WA, 1974.

2.7 G. Bertozzi, M. D'Alessandro, F. Girardi, and M. Vanossi, "Evaluation de la Surete du Stockage de Dechets Radioactifs en Formations Geologiques: Une Application Preliminaire de la Fault Tree Analysis a des Formations Salines," in proceedings of the Workshop on Risk Analysis and Geologic Modelling, OECD Nuclear Energy Agency/CEC Joint Research Center, Ispra, Italy, 1977.

2.8 The panel members and their affiliations are: William S. Twenhofel, USGS, Denver, CO; William W. Dudley, USGS, Denver, CO; Randolph Stone, LLL, Livermore, CA; Frederick J. Pearson, USGS, Reston, VA; Herbert R. Shaw, USGS, Menlo Park, CA; Donald Caldwell, USNRC, Washington, DC; Ben Ross, The Analytical Sciences Corp., Reading, MA; Edward Hawkins, USNRC, Washington, DC; and Martin Tierney, Sandia Laboratories, Albuquerque, NM. Working sessions of this panel were held on December 7-8, 1976, at Grand Canyon, Arizona; and again on April 13, 1977, in Carlsbad, New Mexico.

2.9 Richard E. Barlow and Frank Proschan, Statistical Theory of Reliability and Life Testing - Probability Models, Holt, Rinehart and Winston, Inc., New York, 1975.

2.10 H. N. Sather, Biostatistical Aspects of Risk - Benefit: The Use of Competing Risk Analysis, UCLA-ENG-7477, UCLA, School of Engineering and Applied Science, 1974.

2.11 H. N. Sather, Statistical Models for Competing Risk Analysis, UCLA-ENG-7676, UCLA-School of Engineering and Applied Science, August 1976.

2.12 United States Nuclear Regulatory Commission, "Reactor Safety Study" WASH-1400 (NUREG-75/014), October 1975.

2.13 E. F. Gloyna and T. D. Reynolds, "Permeability Measurements of Rock Salt," JGR, 11, pp 3913-3921, 1961.

2.14 F. J. Pearson, USGS (Sandia Laboratories), Albuquerque, NM, personal communication, June 1977.

403 080

2.15 Byron Bird, Warren Stewart, and Edwin Lightfoot, Transport Phenomena, John Wiley & Sons, Inc., New York, Ch. 20, p 629, 1960.

2.16 Herbert Shaw, USGS (Sandia Laboratories), Albuquerque, NM, personal communication, May 1977.

2.17 J. Hamstra, "The Waterproof Geometry of Salt Domes: etc." in IAEA-SM-207/42, pp 295-302, 1976.

2.18 G. E. Apostalakis has criticized the derivation of a failure rate for sealed but failed boreholes given in the text. He has provided an alternative, rigorous derivation of the failure rate (Apostalakis, personal communication, April 1978) that is computationally more difficult to implement. Trial calculations with this rigorous formulation have shown that it gives a numerical result that is not significantly different from results obtained by the model described in the text.

2.19 Samuel Karlin, A First Course in Stochastic Processes, Academic Press, New York, p 270, 1966.

2.20 D. R. Cox and H. D. Miller, The Theory of Stochastic Processes, John Wiley and Sons, Inc., New York, pp 220-21, 1965.

2.21 Handbook of Mathematical Functions, Milton Abramovitz and Irene A. Stegun, editors, U. S. Department of Commerce, National Bureau of Standards, Applied Mathematics Series - 55, 1964. Formula No. 7.4.33, p 304.

2.22 Reference 2.1, pp 31-43.

2.23 Herbert Shaw, USGS, Menlo Park, CA, personal communication, April 1977.

2.24 Reference 2.1, Appendix, pp 73-77.

2.25 Samuel Glasstone, ed., Effects of Nuclear Weapons, Revised edition, United States Atomic Energy Commission, pp 289-293, April 1962.

2.26 Quincy Wright, A Study of War, Chicago, IL, 1942.

2.27 L. F. Richardson, "Statistics of Deadly Quarrels," reprinted in The World of Mathematics, by James Newman, Simon and Schuster, p. 1254, 1956.

2.28 Elliott W. Montroll and Wade W. Badger, Introduction to Quantitative Aspects of Social Phenomena, Gordon and Breach Science Publishers, New York, p. 99, 1974.

2.29 Reference 2.21: See formulae No. 26.3.13, p 936; 26.3.24 through 26.3.27, p 940.

2.30 Reference 2.1, pp 13-16.

2.31 Harrison Brown, "The Density and Mass Distribution of Meteoric Bodies in the Neighborhood of the Earth's Orbit," JGR, Vol. 65, pp 1679-1683, 1960.

2.32 E. M. Shoemaker, et al., "Interplanetary Correlation of Geologic Time," Advan. Astronaut. Sci., 8, pp 70-89, 1962.

2.33 W. K. Hartmann, "Terrestrial and Lunar Flux of Large Meteorites in the Last Two Billion Years," Icarus, 4, pp 157-165, 1965.

2.34 W. Feller, An Introduction to Probability Theory and Its Applications, John Wiley and Sons, Inc., New York, p. 129, 1971.

APPENDIX 2A

Methods of Simulation Analysis Applied to Questions of Geological Stability of the Reference System

2A.1 Introduction

At the present stage of development there is relatively little cohesion between the model types described earlier in this chapter. Need exists to integrate the several modeling efforts to: (a) quantify their implications in a comprehensible format, and (b) test for interactions between different models and for feedback loops connecting two or more process models.

Toward this goal several integrating methodologies are available, in principle to define the scope of such relationships. One of these consists of various forms of fault tree analysis, in the broad sense discussed by Barlow and Lambert[2A.1]; another is simulation analysis using some form of the many computer simulation languages available today.* The analysis in previous parts of this chapter explores some of the difficulties in trying to describe a geologic system in probabilistic terms. These difficulties include: (a) problems of scale-- i.e., what are the physical and temporal bounds of the system which must be analyzed? (b) problems of knowledge -- there is a lack of rigorous numerical constitutive relations for geologic behavior and a lack of geophysical data and time series to generate probabilities, (c) problems of coupling and feedback- there is usually no simple way to take account of complicated interactions using probabilistic methods, and (d) probabilistic methods often obscure some of the common sense physical relationships in the system. Point (b) is analogous to problems of weather predictions, except that we have the additional problem of analyzing both the geological system (the geological "weather" system) and an engineered structure that interacts with and affects geological "weather" changes. With respect to probability analysis, we also have the problem of generating the geological analog of the performance characteristics normally supplied for the analysis of engineered structures. Simulation methods seem necessary to make any substantial progress toward that goal in the foreseeable future. Geological data collection is notoriously slow and difficult by comparison with engineered systems because of the limited accessibility and long times involved.

---

* We have chosen in this report to use the language, DYNAMO, distributed and maintained by Pugh-Roberts Associates, Inc., Five Lee Street, Cambridge, Mass., 02139; see references 2A.4 and 2A.11.

2A.1.1 Simulation Models and Geological Perspectives

The method of simulation used in this report was chosen because it is highly developed in many fields of systems analysis[2A.4] and is particularly useful in problems where boundary conditions and system variables are poorly known - e.g., as in applications to economic models.[2A.5][2A.9] Application to natural systems is not known to us, but the method is promising in that context because of the ability to simplify system behavior both conceptually and mathematically. To us, this approach to geological simulation has the following advantages:

1. It does not obscure common sense relations or mask the identity of simplified functions,
2. It is very easily modified or completely rearranged as experience accrues on boundary conditions or as other research modifies various constitutive relations,
3. It provides a united framework against which to view total system behavior,
4. It allows for feedback loops of conceptually any length or complexity,
5. By its physical simplicity it keeps the analyst aware of model limitations that are sometimes lost in a more mathematical format.

This last point cannot be overemphasized. We are dealing with idealogical models that simply reproduce relationships that are either known or reasonably suspected and are permitted to interact in ways that suggest, but do not predict, how the real world may behave. We repeat this for emphasis.

Simulation calculations of the sort described remind us by their very simplicity that they are just idealized models. They only reproduce phenomena already known or reasonably suspected and suggest, but do not predict, how the real world may behave.

2A.1.1.1 Questions of Geological Stability -- Three types of questions challenge our ability to evaluate the containment potential of a repository site: (1) How accurately can we describe the natural changes that affect the integrity of a given volume of rock over specified intervals of time from tens of years to a million years? (2) With what confidence can we state how these natural changes will be modified by the disturbances invoked by a radioactive waste repository? (3) How comprehensively can we describe and analyze the behavior of the waste repository facility -- an engineered structure which presents problems somewhat analogous in difficulty to those of nuclear reactor safety studies.

403 083

2A.1.1.2 Strategies of Systems Analysis -- We view the methodology development as an evolving process dependent on interaction of many analytical methods. The examples cited above indicate that geological analysis is a key phase without which others may be meaningless exercises. There may be stages at which analytical progress will be directly contingent on the laborious process of geological data collection. In the meantime, however, the array of problems that may have to be addressed geologically can be sorted and organized by the artificial creation of system structures involving simulation analyses. These may take the form of detailed geochemical transport modeling, thermochemical-mechanical interaction simulation, simulations of multiple dynamic feedback processes, or possibly even some forms of fault-tree/event-tree analyses when there develops a sufficient understanding of processes to warrant them. Though feedback simulation is addressed in this part of the chapter, there is no recommendation that it supersede any other, except in the sense of exploring new terrain for study and in the possibility of providing a communications medium for coordinating other techniques.

2A.1.1.3 Role of Approximations in Systems Analysis -- Approximations are implicit, though often hidden, in all analytical efforts however sophisticated the final product may appear. To address analytical goals of system behavior, the system must be defined in terms of consistent relationships between the dimensional scales of the phenomena involved. For instance, in petrography we do not go directly to the oil immersion lens or scanning electron microscope. First we examine the rock in the field setting, in hand specimen, in rough cut, in binocular field, petrographic microscope, etc., sometimes winding up with highly focused and sophisticated x-ray structure analysis of one of the mineral grains. There are many levels of meaning and information at all stages of this process which interact and potentially form part of what we call our knowledge of that rock. Even this multistage process is a small part of the total effort. There are chemistry, geochronology, physical property measurements, other field surveys (such as provided by mapping, paleontological and geophysical techniques), and so forth.

The point is that numerical simulation analysis consists of similar hierarchies of effort. The reconnaissance survey is often of crucial importance in either the actual or simulation cases to the value of any highly sophisticated analysis.

Taken together, these questions pose a problem of incredible intricacy. No unequivocal statement seems possible concerning the precise nature of future system states. With respect to question (1) alone, our understanding of the composite history of any given geological site on this dynamic planet is insufficient to give evaluations other than by educated opinion or assertion. Entire continents are postulated to move distances commensurate with their half-widths on time scales of the order of 100 million years. To be sure, old rocks of relatively undisturbed character exist, but the rocks that are now of entirely different character or have been chemically broken down, dispersed and reconstituted in various ways were once represented by states resembling these so-called stable rock types. The problem is that usually we are not able to say exactly where and when these changes have taken place or will take place. An example pertinent to this

report is shown by 200 million-year-old salt beds that still exist today, except for those beds that have been partly or totally dissolved away. This would be a conundrum but for the traces derived from indirect geological deductions based on local and regional studies of structural, geochemical, stratigraphic, and geochronological continuity.

Another case in point is the phenomenon of the 1.8 billion-year-old "fossil nuclear reactor" Oklo in the Republic of Gabon.[2A.3] This natural situation demonstrates the potential retention capacity of some geological settings. Oklo, however, also illustrates some of the above questions. With what assurance can we state that another site has exactly the same characteristics? Although "most" of the fission products generated at Oklo have been retained, what precisely is that amount and what is the geometric scale of dispersal of the percentage lost? Is it possible to say what percentage of the radionuclides reached surface waters? Is there any major distinction between 10 percent, 1 percent, etc., from the standpoint of potential pathways to humans? An event of major chemical alteration apparently affected some of the Oklo rocks about 10 million years ago (Ref. 2A.3, p. 257). Could that have been predicted at a million years or less before its occurrence?

The point concerning Oklo is that evidence of radionuclide retention does not necessarily answer the more relevant questions concerning conditions and mechanisms of fractional loss. It does demonstrate, however, that geological data, if extensive enough, can delimit a time-space framework against which evaluations of dispersal mechanisms can be tested.

Another aspect of geological stability is that macroscopic chemical integrity is possible even though there has been extensive chemical exchange at the levels of trace element concentrations (e.g., less than parts per thousand; see Ref. 2A.15). The fact that a rock has existed with mineralogical and textural integrity for a long time is not in itself admissable testimony to its chemical integrity. Documentation of the sort partially compiled for Oklo is essential to such claims. The opportunity to document analogous cases for other geological media exists at the sites of past underground nuclear explosions (e.g., the Gnome Site near Carlsbad, N.M., which is in rocks similar to those of another site in that vicinity which is being considered for a possible radioactive waste facility).

In our view the most important, and seemingly contradictory, value of approximate ("lumped parameter") analyses, is that the very nature of the simplifications used for numerical relationships enforces the reminder that numerical simulation under any circumstance is an approximation technique. We are continuously warned against believing the result simply because

we know that the primary relationships themselves are incomplete approximations. "Belief" is often a subtle and powerful tendency when great effort and intricacy has gone into building a sophisticated model.*

It is usually easier to change or abandon parts of a DYNAMO simulation, for example, than it is to change or abandon results of sophisticated finite difference or finite element modeling. Reconnaissance calculations also are many times faster and much cheaper. A hundred DYNAMO runs involving many coupled phenomena can be made probably with less expenditure of time and money than one relatively refined (but still incomplete) three-dimensional heat conduction calculation (presupposing similar levels of prior analytical experience and insight in the two cases). In either case the greatest time, effort, and importance goes into "setting up the problem" or formulating the ideas and numerical content of the system structure. Once a question can be addressed hypothetically or approximately, however, simulation languages like DYNAMO can give conditional answers very quickly.

2A.1.1.4 Conceptual Importance of Feedback Phenomena -- There are three general categories of functional relationships important to system behavior: (a) independent phenomena, (b) directly coupled phenomena, and (c) phenomena that are part of feedback cycles. These categories are artificial in the sense that (b) may partly imply (a), and (c) usually involves aspects of both (a) and (b).

Independence was assumed, for example, in the probabilistic discussion of this report (Section 2.5) and requires no further explanation here. However, one qualification is offered. Events or processes that can be treated in isolation from other events or processes in one time-space framework may be influenced by feedback mechanisms on other scales of behavior. A patently distorted, but graphic, example of this sort of effect can be imagined relative to meteorite impact. Suppose that the current incidence of impacts were sufficient to effect changes in the earth's orbital parameters so as to bring it into more direct intersection with asteroid orbits which resulted in much higher incidences of meteorite impacts? The independence of the event is no longer defined only by external conditions. In this case the energy and time scales indicate that the effect is inappropriate to the scale of our problem, but the existence of this type of behavior requires diligent searching for analogous cases that may be relevant. Other large-scale examples can be found in relationships between atmospheric circulation, climate, and vegetation zones.

---

*There is a major distinction between building an isolated sophisticated model and a sophisticated numerical scheme that is capable of rigorous calculations involving many variables. The latter is used in conjunction with reconnaissance techniques and field observations to force part of the analysis to its logically rigorous conclusion if justification exists. This capability (like the transport modeling capability described in the main report) will be of crucial importance to any future abilities to make more specific statements. The rougher structural framework, however, remains as a check on tendencies to follow this special path to the exclusion of others.

Coupled phenomena represent the class of problems most often encountered in engineered systems. For example, flow of the working fluid in some sort of chemical reactor may influence the behavior of other parts of the system by heat and/or chemical transfers, but the resulting changes in behavior may have no reciprocal influence on the thermal or chemical sources. Evaluation of the consequences is in practice often difficult and intricate, but it is relatively straightforward.

Feedback phenomena exist in a variety of forms. There are types involving phenomena that are also highly coupled and types involving remote and circuitous paths. We can never say that we have discovered all of the latter, but we must continue to look for their existence if we are to operate by other than blind faith in functional independence. Feedback may be positive (or regenerative) leading to unstable system states, or negative tending toward steady or equilibrium states.

An example of a highly coupled feedback phenomenon that is easily grasped and documented, and is of potentially major concern to the behavior of mechanical systems, consists of the relation between mechanical work, dissipation as heat, and thermal effects on system properties. In many cases a feedback loop is established in which the mechanical work rate itself becomes influenced by this chain of events, thereby perpetuating the cycle. The situation is easily visualized in the flow of viscous liquids, particularly as it has been placed in dimensional perspective by Gruntfest.[2A,6,7] Here the heat generated by frictional resistances in viscous flow decreases the viscosity and thereby increases the flow rate, the local heat generation rate, and the rate of decrease of viscosity for a given driving potential. This sort of positive feedback cycle is highly unstable.

Positive thermal feedback phenomena have been shown to be important to the flow behavior of rocks at high temperatures and pressures by several workers (see Ref. 2A,12 for relationships between melting and deformation phenomena). Since we are concerned with rock deformation in connection with repository stability, a simple test of this sort of feedback was performed relative to possible stresses and deformation rates that could be encountered in a repository in a bedded salt deposit. At shallow depths, low stress differences and temperatures in the neighborhood of 100°C (±10°C), energy balance calculations indicate that the time scale of a possible thermal feedback instability is much greater than the time scale of interest (i.e., >>1 million years). Hence we conclude that the laboratory and the in situ field measurements concerning behavior of salt deformation are applicable to salt deposits at shallow depths and low stress concentrations to the extent that other sorts of phenomena are not involved.*

*Thermal feedback effects become enhanced at higher pressures and temperatures, hence further analyses are indicated relative to behavior of large-scale salt diapirism.

Several other phenomena in salt deposits appear to call for feedback analyses which we have not performed. Important among these are the behavior of fluid inclusions and possible interactions between the chemical stability of mineral hydrous phases and the mechanical properties of the rocks.

The migration of fluid inclusions in salt caused by thermal gradients is known to represent a form of feedback (Ref. 2A.2, p. 164). Without going into details, the temperature dependence of the solubility of salt in liquid water leads to inclusion migration up the thermal gradient. This effect is countered by an inverse solubility relation if temperatures become high enough to form a vapor phase. In that case the migration tendency is reversed and inclusion distributions in principle would become stabilized. This would seem to represent a form of negative feedback tending toward dynamic equilibrium and quasisteady inclusion distributions. In our opinion, however, the reality of this conclusion is not completely established, and further work is needed from the standpoint of mechanical interactions and relation to temperature histories. This report has given attention only to some questions of potentially greater wholesale consequences.

2A.1.2 Numerical Simulation Methods

2A.1.2.1 Choice of Simulation Language -- Several simulation languages are in widespread use. We have chosen DYNAMO as the initial vehicle because of immediate availability, simplicity, and convenience of operation. We plan to explore the possibility of using GASP IV[2A.10] or other such languages, that offer greater options for handling discrete and discontinuous phenomena.

2A.1.2.2 Characteristics of DYNAMO -- DYNAMO is a computer technique for the ordering and approximate solution of sets of ordinary differential equations. Its advantages stem from many years of widespread use and consequently many built-in conveniences involving automatic equation ordering, internal tests for consistency and redundancy, automatic or specified plotting limits, relatively complete and convenient error messages, speed, and flexibility. The equations are essentially statements concerning quantities (Level Equations), their rates of change (Rate Equations), and statements concerning any other relationships required to define the Rate and Level Equations (Auxiliary Equations).

The calculation consists of evaluation of all Auxiliary Equations at a given time based on previous statements for the Levels (obtained either from specified initial values or previous calculations) followed by calculations of the Rate Equations and their inputs to the Level quantities over some specified time change. The output is in a form displaying the continuous

functions (ten functions at a time can be plotted).* Depending on purpose, it may be desired to compare different functions on the same plot or the same function with several choices of parameter variations. In the latter case one need only be sure that the equations are uniquely specified for the different choices. Equation listings for examples of the two modes are given in the section on results.

Although time is plotted linearly, the effect of logarithmic variation can be examined by means of repeated calculations with lengths and plotting periods progressively increasing, for example, by factors of ten. A time sequence can thereby be pieced together which simultaneously illustrates on the same plot contrasts of short-term and long-term variations of the prescribed sets of quantities.

More complete descriptions and instructions for DYNAMO are given in Refs. 2A.4 and 2A.11. With these guides in hand, the more specific characteristics of DYNAMO are quickly picked up by making test runs of functional behavior using test problems with real or invented equations.

2A.2 Reference System for DYNAMO Simulation

The reference system used for DYNAMO calculations is similar to that described in Chapter 1. Any differences reflect approximations assumed for the sake of illustrating numerical capability. All numerical quantities and relationships in this report are subject to review, correction, or revision.

2A.2.1 Rudimentary Geometric Structure

The simplified reference system is shown in Figure 2A.1. The approach is to portray as many physically meaningful relationships as possible with the fewest possible geometric constraints. In other words, as many parameters as possible are lumped into relationships that approximate general behavior as though describing a one-cell model. For example, heat distributions are treated only in terms of conservative input-output balances for a single volume element. As will be shown, considerable information is obtained from such a simplistic "model" even though little spatial detail is available. The latter sort of information is independently available from the multi-cell modeling techniques (thermal-elastic modeling and transport modeling). Comparison with DYNAMO results shown later illustrates the degree of approximation available from the one-cell approach and reinforces our position that several different integrated techniques are needed to build understanding of system performance.

*The fact that the functions are continuous is sometimes an apparent drawback. It is possible, however, by judicious consideration of system structure to simulate discontinuities by continuous but rapidly changing functions. Many kinds of variation can be considered so long as care is used in choices of time steps and in checks for physical plausibility, etc.

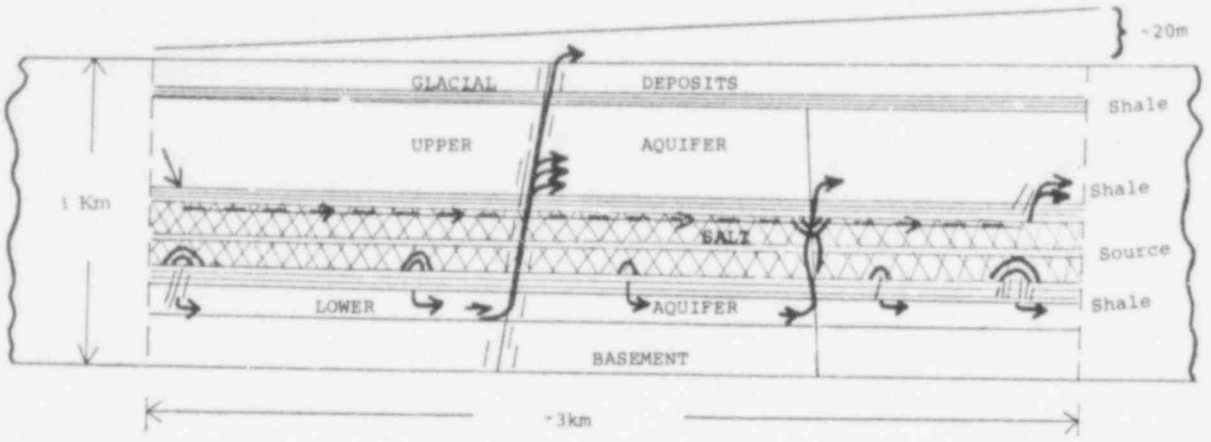

Figure 2A.1. Simulation Reference Volume for DYNAMO

Other relationships such as thermal expansion uplift, compaction, subsidence, cracking and so forth are also lumped or averaged over the same volume element. The form of these approximations will be evident when the system equations are defined.

The several groundwater pathways schematically portrayed in Figure 2A.1 are used only to guide the form of potential access of water to the salt horizons. Mass transport mechanisms appropriate to a given path are then examined for their potential magnitude limits. The potential reality of these conditions are subject to other considerations (further modeling, geological data synthesis, etc.). Our general aim will be revealed more clearly when we describe flow diagrams of functional system structure.

2A.2.2 Capabilities of Increased Geometric Complexity Using DYNAMO

There is no theoretical restriction on the number of cells that might be defined for feedback calculations. We feel that such refinements should only be attempted, however, when the system interactions of interest are well known in the lumped parameter mode so that deviations originating in geometric factors (including variations of physical properties, etc.) can be meaningfully isolated. Therefore, we restrain our calculations to aspects that are, or may be, generically meaningful in the absence of spatial detail, recognizing that greater detail is obtainable at a price. The price is not primarily computer time and money, but the potential distraction of analysis from pursuit of unexplored causal relationships for the sake of numerical precision in relationships that are only partially understood.

There are times, however, when detail may be very important to other aspects of feedback approximation if system responses are sensitive to, or triggered by, small fluctuations in some specific variable (e.g., temperature). Recognition of such situations inevitably depends on the insight of the analyst. Again, this emphasizes the need for parallel and simultaneous analytical tools.

2A.3 Systems Diagrams

The beginning of any numerical simulation consists of organizing the active functional relationships. For consistency with DYNAMO and previous practice, we have used the form of systems diagram and symbols described by Forrester.[2A.4]

2A.3.1 Descriptive System

An attempt is made to verbally describe the nature of the reference system structure as it is viewed from the standpoint of potential feedback relationships. The terms described in Section 2A.3.1.1 are given no quantitative values. Explicit terms for numerical work are defined in Section 2A.3.2.

2A.3.1.1 System Structure -- Figure 2A.2 shows a schematic diagram of system structure as it pertains to questions addressed to the reference system shown in Figure 2A.1. Minimum complexity is again emphasized. An effort is made to involve the fewest possible level and Rate Equations that still might be capable of identifying processes in the schematic system affecting geological stability and radionuclide dispersal. Actual mechanisms of dispersal, however, have not been addressed in the numerical demonstrations subsequently described, because considerably more effort is desirable in probing the kinds of behavior symbolized in the lower portions of the diagram. Currently, we have only studied some questions relevant to possible access of groundwater to the salt horizons of Figure 2A.1.

The Levels of Figure 2A.2 (rectangles) are mostly self-explanatory and simply represent conservation statements concerning the respective quantities. Most of the Levels are composite. For example, the mechanical work (MW) Level represents several effects such as thermal expansion (TE), compaction (C), work of earthquakes and faulting (EF), and other mechanical work terms (OMW).

The ways in which the levels are organized depends on the aim of the analysis. Our idea in this particular scheme is to explore various effects on potential groundwater access to the repository. Levels labeled FRACTURES and OPENINGS are separated because, in principle, fracturing does not necessarily create porosity (in fact, it could create barriers to flow with consequent major changes in flow paths).

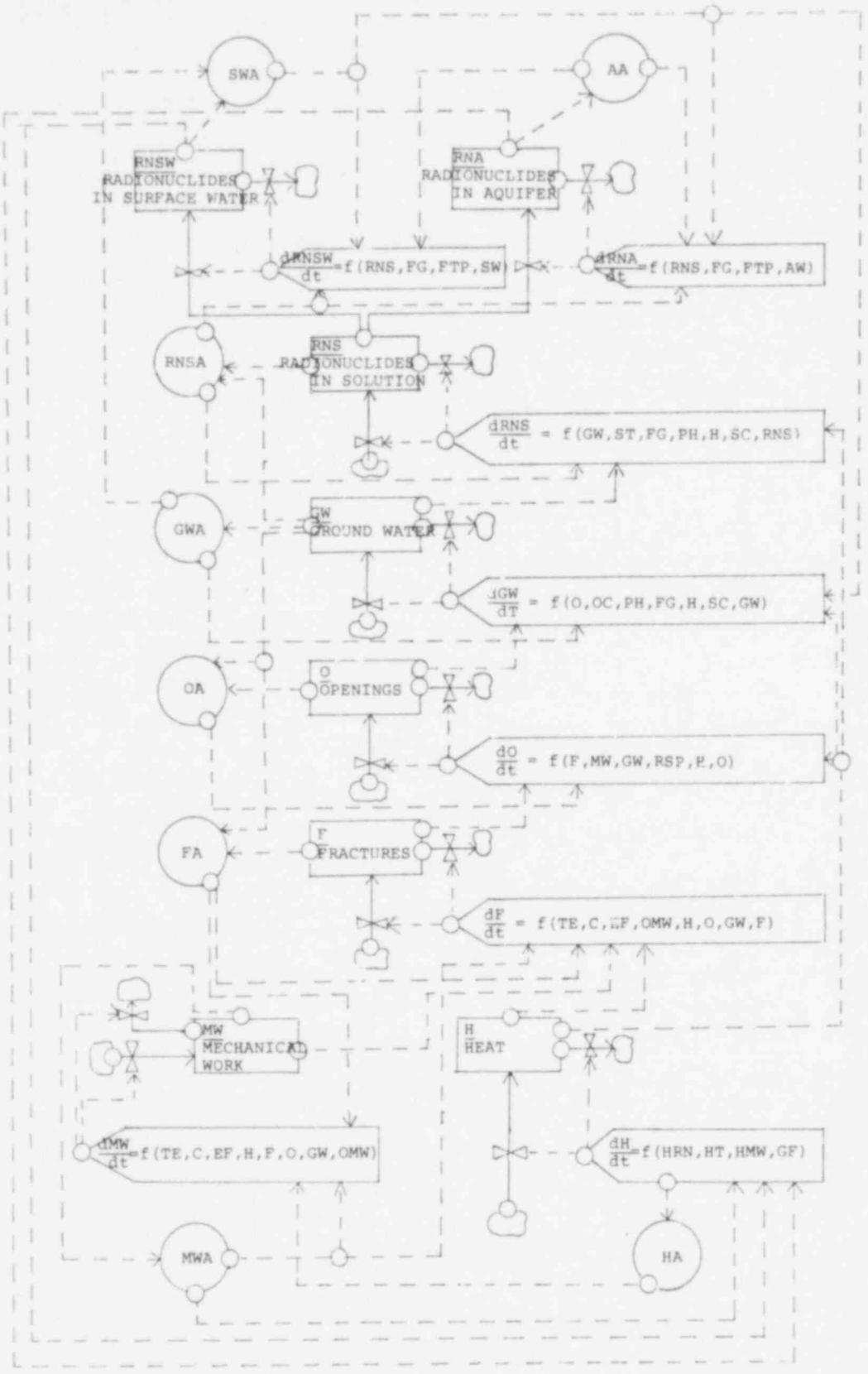

Figure 2A.2. System Structure Diagram

The interactions portrayed in Figure 2A.2 involve effects of the following general kinds: (1) effects of radionuclide decay on thermal mechanical and chemical states, (2) effects of mining and backfill properties on lithologic integrity, porosity and compaction, (3) effects of these work mechanisms and faulting mechanisms on fracturing, (4) the above composite effects on rock openings, (5) composite effects on groundwater quantities and flow states, (6) effects of groundwater on rock openings via influences on mechanical and chemical properties (particularly salt solubility in the context of the reference system), (7) effects of all processes on the potential access of groundwater to radionuclides and rates of their incorporation in the groundwater system, and (8) net effects on dispersal of radionuclides out of the system via either aquifer or surface water pathways.

Changes in the above relations are schematically described by a series of rate equations that govern input-output balances via the schematic valve symbols. The source-sink "cloud" symbols simply indicate that the quantity may relate to mass and energy reservoirs of different kinds that are defined outside the system; physically, they remind us of various possible initial conditions, boundary conditions, and time dependent influences of external origins (changes in geothermal flux, tectonic effects, and so on). Some types of point events (e.g., meteorite impact) and intermittent or pulse events (e.g., earthquakes) might be crudely approximated as to very simplified consequences using DYNAMO, but this is an area of simulation technique that needs innovative research attention.

Level and Rate Equations are related by sets of Auxiliary Equations. In a completed diagram the interrelationships are displayed by a network of dashed Information Lines. In Figure 2A.2, the Auxiliary Equations are completely lumped in one general symbol for each Level; many different kinds of functions are implied by each symbol. Here the Information Lines are shown only to indicate their purpose; i.e., the Information Lines of Figure 2A.2 are not complete and are not necessarily even rigorously correct. We have included some improbable connections to emphasize that fact. It is suggested that other persons involved in the analysis of radioactive waste management study this diagram or reconstruct others of their own in terms of attempts to identify functional dependencies.*

*The Information Line between RNSW and SWA, for example, may be misleading in the present physical context. The amount of radionuclides in surface waters is not expected to have an effect on the hydrology, unless there is a bizarre effect like influence on growth of massive algae deposits that influence stream flow. Effects of radionuclide interactions on aquifer properties are possibly less farfetched (e.g., as regards heat).

The symbols for the Auxiliaries in Figure 2A.2 are simply the Level symbols followed by A. Later on, the terms included in the various equations will be assigned specific descriptive name symbols. Symbols in the schematic Rate Equations are also the same as the Level symbols, with the following additions:

HRN - Heat produced by RadioNuclides as originally placed in the repository.

HT - Heat Transfer by conduction and convection.

GF - Geothermal Flux balances.

HMW - Heat produced by dissipation of Mechanical Work.
Note: Dissipation is included as an example of an input that might be overlooked; as discussed in the text, this term probably is not significant in the context of the general balances relative to the conditions of the reference system.

TE - Thermal Expansion (in context of reference system, this takes the form of uplift).

C - Compaction of pore space (such as produced by residual porosity of mining activities, salt dissolution, etc.).

EF - Tectonic energy induced by Earthquakes and/or Faulting.

OMW - Other Mechanical Work (e.g., induced by buoyancy forces of various origins).

RSP - Rock Solubility Parameters (mineralogical phases present, their stabilities, solution properties, etc.).

OC - Openings Connectivity (in part overlaps with FG).

PH - Pressure Head (in present context defined externally by reference to hydrologic modeling; see discussion in Chapter 3).

FG - Flow Guides (in present context, identified by geometric structure and specified assumptions relative to Figure 2A.1: repetitive modeling of hydrologic options is essential to sorting the relative importances of artificially imposed flow conditions).

SC - Solute Concentration (as it affects solubility, hydraulic properties of water, thermodynamic stabilities of minerals and so on).

ST - Source Terms (local conditions of water access to canisters, canister stability, leaching, etc.).

403 094

FTP - Fluid Transport Properties (relative to hydrology, radionuclide distributions influenced by distribution coefficients, etc.).

AW - Aquifer Water (hydrologic factors in aquifer flows).

SW - Surface Water (hydrologic factors in surface flows).

Inspection will show that this is not a comprehensive list of the Rate Equations and variables. It is given to indicate the general idea and to stimulate searches for the relevant variables and their interdependencies.

Closer inspection of Figure 2A.2 will disclose various types of potential Feedback Loops. Possibly, the most conspicuous type of feedback is of the sort already described (e.g., mechanical work-heat cycles). Another fundamental kind is the effect of a Level quantity on the rate of change of that quantity. In one way or another this form of feedback affects every Level. For example, the amount of heat stored in the reference system affects the rate of heat loss and hence the subsequent heat quantity. The amount of mechanical deformation (relative to some initial reference configuration) performed on a system influences the mechanical states and properties of the rocks of the system, hence the future mechanical work rates. Similar statements are true of fracturing and production of rock openings. Groundwater quantities influence future Level states via consequent hydrologic flow rates. Radionuclide quantities in solution influence future rates of incorporation by depletion of the finite source, and so on.

Many types of indirect Feedback Loops can be found by careful study of diagrams like Figure 2A.2. Formally, all closed circuits in the directions of Information Arrows represent Feedback Loops. There is virtually an infinity of involutions and convolutions of these possible connections. The problem forced on us by questions of radioactive waste containment in geological media is to find the dominant loops and to understand their magnitude-time relations as regards geological stability. Diligent and repetitive construction of such Systems Diagrams, Information Lines, and Feedback Loops assists these hierarchical sorting processes.

Only two indirect Feedback Loops will be mentioned as typical examples. The first of these is very simple to understand, but it is the most indirect and is quantitatively contingent on some form of numerical solution of all system variables which has not been accomplished to this date. Starting with the Heat Level on the lower right of the diagram, Information Lines can be traced through the entire diagram and back to the Heat Level. That is, the amount and distribution of heat generation by radioactivity simply depends on what happens to the radionuclides other than simple decay in their original configurations. From the standpoint of the overall system this represents a Negative Feedback Loop tending toward thermal equilibrium. This conclusion, however, should not encourage complacency concerning other forms of potential thermal feedback.

Local Positive Feedback Loops of thermal origins are conceivable within this system-wide negative feedback cycle (a simple case being thermally induced chemical reactions triggered by transport of hot solutions).

The second specific example considers feedback between Mechanical Work, Fracturing, Openings and Groundwater. The Heat Level is an input via Thermal Expansion (TE) and via the temperature dependence of mechanical properties. Hydrologic parameters, in particular the Pressure Head (PH), can be defined outside this particular subsystem, but it should be possible to incorporate the hydrology as part of the Feedback Loop by judicious iterations in sequence with the Hydrologic Transport Model of this Report (Chapter 3).

The main feedback of this artificial subsystem, which will be referred to as the H-MW-F-O-GW Sector, is a consequence of salt solubility and brine transport. The feedback is strongly positive. The rest of this appendix, other than the section on Recommendations, deals with numerical approximations for this Sector.

2A.3.2 Specific Diagram and Equations for the H-MW-F-O-GW Sector

The bottom half of the system diagram of Figure 2A.? is redrawn more explicitly in Figure 2A.3. For practical reasons, some Levels, particularly Mechanical Work, were subdivided into several Levels. The remainder of Section 2A.3 identifies the respective equations within a DYNAMO format, without going into their physical content. Section 2A.4 discusses the physical approximations and dimensional content of the equations and attempts to identify their limitations. Section 2A.5 gives the computer results.

2A.3.2.1 Heat Level -- Letter symbols at the left margin for each equation shown in the following paragraphs indicate its type: Level (L), Rate (R), Auxiliary (A), Constant (C), Initial Value (N), Table (T), Supplementary (S), Continuation (X).

```
L     H.K = H.J + DT*(HINR.JK - HOUTR.JK)        HEAT
```

The indices J, K, L refer, respectively to an immediately preceding time (J), the current time (K) and immediate future time (L). The time step of the calculations is DT and corresponds in length to the past interval (JK) and future interval (KL). Algebraic symbols are standard, except that the asterisk indicates multiplication. For algebraic conventions and other elaborations of equation writing for DYNAMO, see Pugh[2A.11] and Forrester.[2A.4]

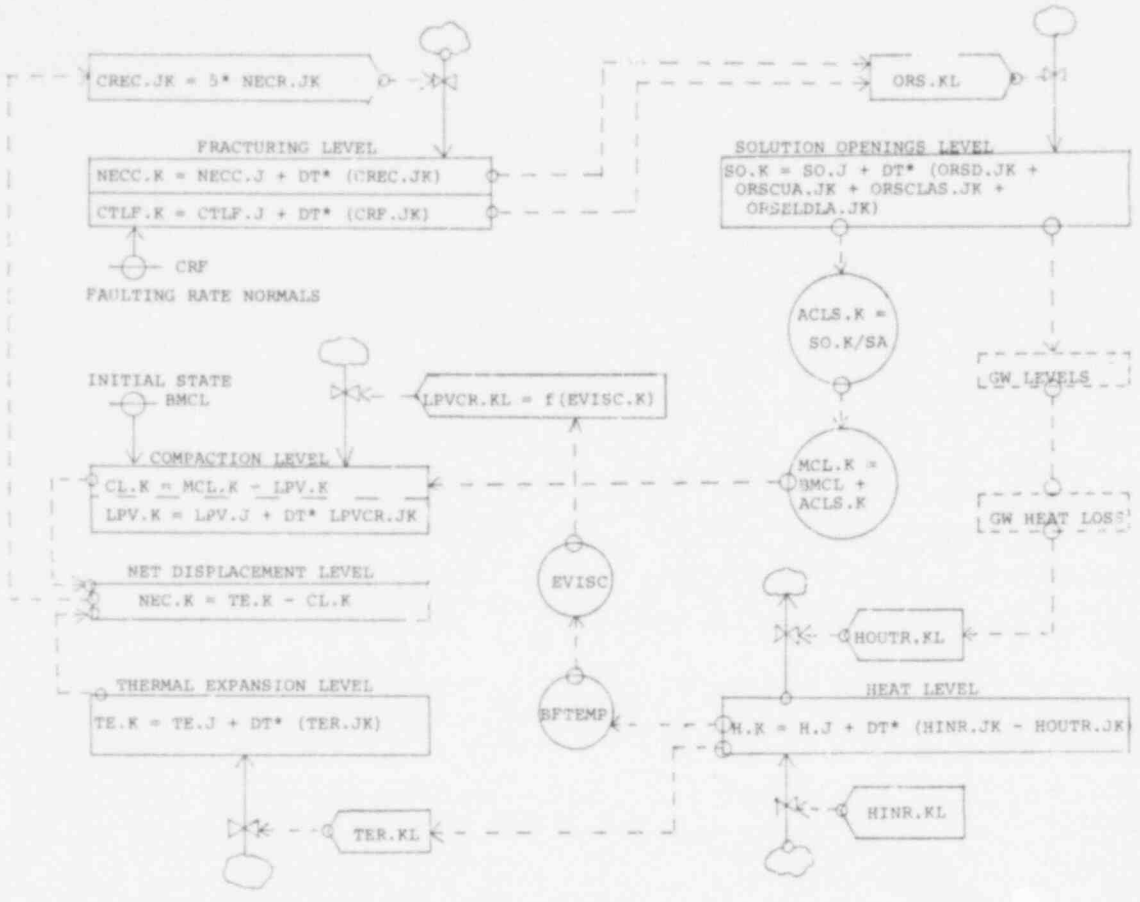

Figure 2A.3. System Diagram for H-MW-F-O-GW Sector

The active equations for the Heat Level are as follows (in this section equations are simply named without derivations or dimensional quantities; where equations could not be completed without discussion of physical principles, their types are indicated parenthetically - see Sec. 4):

R HINR.KL = DCP*FD.K HEAT INPUT RATE

A FD.K = (Table function) FRACTIONAL DECAY

C DCP = (Constant) DIMENSIONAL CONSTANT FOR THERMAL POWER

R HOUTR.KL = DELAY (SHLR.JK, DSHF) HEAT OUTPUT RATE
(Note: "DELAY" refers to built-in DYNAMO functions that introduce delayed responses of output to input functions; see Ref. 9.4, Chapter 9)

R SHLR.KL = (Analytic function) STEADY HEAT LOSS RATE

C DSHF = (Time Constant) DELAY OF SURFACE HEAT FLUX

403 097

2A.3.2.2 Thermal Expansion Level -- Thermal expansion is, of course, directly coupled with the Heat Level via equations of the following type:

L TE.K = TE.J + DT*(TER.JK) THERMAL EXPANSION UPLIFT

R TER.KL = UEC*(HINR.JK - HOUTR.JK)*HC THERMAL EXPANSION RATE

C UEC = (Constant) UNIT EXPANSION COEFFICIENT

C HC = (Constant) HEAT CAPACITY (AVERAGE)

2A.3.2.3 Compaction Level -- Compaction refers primarily to average vertical displacements caused by collapse of pore space in the salt horizons due to the weight of the overburden strata; the pore space arises from both mining activities and imagined salt solutioning mechanisms. The equations are written for the one-dimensional case as follows:

L CL.K = MCL.J - LPV.J COMPACTION LENGTH

A MCL.K = (Constant + Output of Solution Openings Level)
MAXIMUM COMPACTION LENGTH

L LPV.K = LPV.J + DT* (LPVCR.JK) LINEAR PORE VOLUME

R LPVCR.KL = (Analytic + Table Functions) LINEAR PORE VOLUME
COMPACTION RATE

2A.3.2.4 Net Displacement Level -- This Level represents simple algebraic summation of the Thermal Expansion and Compaction Levels:

L NEC.K = TE.K - CL.K NET EXPANSION MINUS COMPACTION

2A.3.2.5 Fracturing Levels -- In any rigorous analysis, this composite Level involves many intricate and complex phenomena which in themselves depend on other forms of interaction and feedback not explicitly represented in the simplistic system structures of Figures 2A.2 and 2A.3. In order to carry through with the demonstration, these relations have been given conditional roles. For the purposes of the feedback demonstration, the dominant relation appears to be the connection between net vertical displacements (NEC) and fracturing:

L NECC.K = NECC.J + DT*(CREC.JK) NET EXPANSION COMPACTION
CRACKING

403 098

R CREC.KL = (Analytic function of NEC.K) CRACKING RATE FROM EXPANSION AND COMPACTION

L CTLF.K = CTLF.J + DT*(CRF.JK) CRACK TRACE LENGTH FROM FAULTING

R CRF.KL = (Analytic function of external sources) CRACKING RATE FROM FAULTING

2A.3.2.6 Solution Openings Level -- The production of openings by salt dissolution is explored artificially by means of assumed pathways like those shown in Figure 2A.1 using externally defined hydrologic parameters. Each of these modes requires internally consistent modeling to ascertain pressure-velocity relations and pathways resulting from special permeability distributions such as are caused by fracture networks and solution cavities. Solutioning, however, depends on some of the following specialized forms of transport:

L SO.K = SO.J + DT*(ORSD.JK + ORSCUA.JK + ORSCLAS.JK + ORSEDLA.JK) SOLUTION OPENINGS

R ORSD.KL = (Analytic function of fracture openings) OPENING RATE FROM SOLUTIONING BY DIFFUSION

R ORSCUA.KL = (Analytic function of fracture openings) OPENING RATE FROM SOLUTIONING BY CONVECTION TO UPPER AQUIFER

R ORSCLAS.KL = (Analytic function of fracture openings) OPENING RATE FROM SOLUTIONING BY CONVECTION FROM LOWER AQUIFER TO SURFACE

R ORSEDLA.KL = (Analytic function of fracture openings) OPENING RATE FROM SOLUTIONING BY EDDY DIFFUSION TO LOWER AQUIFER

L ACLS.K = SO.K/SA AVERAGE COMPACTION LENGTH FROM SOLUTIONING

C SA = (Constant) SURFACE AREA (REPOSITORY)

L MCL.K = BMCL + ACLS.K MAXIMUM COMPACTION LENGTH

C BMCL = (Constant) BACKFILL MAXIMUM COMPACTION LENGTH

403 099

2A.3.2.7 Dominant Feedback Loops Investigated in the H-MW-F-O-GW Sector -- Two loops are considered. In the first loop, Heat affects Thermal Expansion (TE) directly and Compaction (C) indirectly via influence on the effective viscous response of a porous salt medium (EVISC) to loading. The Net Displacement (NEC) affects Fracturing (F) by directly coupled responses; Fracturing is additionally affected by externally defined inputs from Faulting (CRF). The amount of Fracturing affects Solutioning (SO) which affects the amount of pore space (LPV) available for renewed Compaction (C). At this stage a Positive Feedback Loop is established and the solutioning effects progressively increase.

The second loop considers the effect of the transport cycle on the cooling history (HOUTR) and hence on the TE-NEC-F-SO-C loop. This coupling has not been examined in detail to date, however, because the solutioning feedback is so strong that small perturbations are sufficient to set it in motion. This latter point is explored quantitatively in Section 5 on Computer Calculations. Groundwater effects on cooling have been studied using the Hydrologic Transport Model of Chapter 3. Heat transfer by groundwater is very important to the long term cooling history but does not significantly influence early thermal effects relative to the feedback processes discussed in this section.

2A.4 Physical Content of System Equations

2A.4.1 The Basic Assumption

The working principle adopted for the trial calculations was to keep them simple enough that the roles of the individual effects could be detected when the composite system was permitted to interact. Thus, heat transfer functions mechanical equations of state, etc., are simplistic without being totally hypothetical. Rock properties are essentially those of the reference site: for convenience, rock properties are listed in Table 2A.1.

2A.4.2 Simplified Physical Relationships

The equation forms are described in words and then in DYNAMO format (i.e., as typed on computer input cards); quantities usually are in c.g.s. (centimeter, gram, second) units which are then scaled to dimensions more suitable to the scope of the problem (meters, kilometers, years, etc). DYNAMO equations are normally labeled with their numerical units.

2A.4.2.1 Heat Inpu - Heat input (HINR) is determined from the waste load specifications given in Chapter 1. It is expressed as a Table Function of decay fraction versus time which is multiplied by a dimensional constant representing the assumed initial thermal power:

$$\text{HINR} = \frac{(\text{sec/yr})(\text{Initial Power; watts/acre})(\text{Fractional Decay Table})}{(\text{joules/cal})(\text{sq.cm/acre})(\text{Depth to Source;cm})(\text{Density;gm/cu.cm.})}$$

cal/gm/yr.

TABLE 2A.1

Physical Properties Assumed for Roclas of the Reference Site

Property	Upper Sand and Gravel	Upper Shale	Middle Sand	Repository (Salt)	Salt (Ambient)	Lower Shale	Lower Sand	Bedrock
Density ($gm \cdot cm^{-3}$) of saturated rock at 30% porosity	2.3	2.1	2.3	1.7	2.2	2.2	2.3	2.6
Thermal Conductivity ($cal \cdot cm^{-1} \cdot sec^{-1} \cdot °C^{-1}$)	"Dry" 5.0×10^{-3} @ 0°C 1.1×10^{-3} @ 400°C	"Wet" 10^{-2} @ 0°C 4×10^{-3} @ 400°C	v: 10^{-2} @ 0°C 4×10^{-3} @ 400°C	(same as Upper Sand)	(isotropic) 11.7×10^{-3} @ 0°C +0 5.9×10^{-3} @ 200°C	(isotropic) 14.6×10^{-3} @ 0°C +0 7.4×10^{-3} @ 200°C	(same as Upper Sand)	(same as Upper Sand)	7.0×10^{-3} (constant)
Horizontal:	(vertical the same)	h: 5×10^{-3} @ 0°C 1.1×10^{-3} @ 400°C							
Vertical:									
Heat Capacity ($cal \cdot gm^{-1} \cdot °C^{-1}$) Rock + Water	0.50 @ 0°C 0.54 @ 400°C	0.50 @ 0°C 0.54 @ 400°C	0.50 @ 0°C 0.54 @ 400°C	0.16 @ 0°C 0.19 @ 400°C	0.21 @ 0°C 0.24 @ 400°C	(same as Upper Shale)	(same as Upper Sand)	(same as Upper Sand)	0.2 (constant)
Thermal Expansion ($°C^{-1}$)				(isotropic)	(isotropic)	(same as Upper Shale)	(same as Upper Sand)	(same as Upper Sand)	(isotropic) 10^{-5}
Horizontal:	10^{-5}	10^{-5}	10^{-5}	1.4×10^{-5}	4.2×10^{-5}				
Vertical:	10^{-5}	2.0×10^{-5}	10^{-5}						
Young's Modulus ($dyne \cdot cm^{-2}$)				(isotropic)	(isotropic)	(same as Upper Shale)	(same as Upper Sand)	(same as Upper Sand)	(isotropic) 5×10^{11}
Horizontal:	10^{11}	10^{11}	10^{11}	6.7×10^{10}	2×10^{11}				
Vertical:	6.7×10^{10}	6.7×10^{10}	6.7×10^{10}						
Modulus of Rigidity ($dyne \cdot cm^{-2}$)	5×10^{10}	5×10^{10}	5×10^{10}	2.7×10^{10}	8×10^{10}	(same as Upper Shale)	(same as Upper Sand)	(same as Upper Sand)	2.3×10^{11}

For an Initial Power of 61 kw/acre, this function in DYNAMO

is written:

```
R    HINR.KL = 0.094*FD.K          RN POWER (CAL/GM/YR)
```

The Dimensional Coefficient of Power (DCP = 0.094 cal/gm/yr) is an amount that would produce an initial average thermal rise in overlying rock of roughly 1/2°C per year, a rate which rapdily decreases with time because of radionuclide decay. This decay is described by the nondimensional ratio:

$$FD = \frac{\text{Thermal Power at TIME}}{\text{Initial Thermal Power}}$$

Note: TIME is the built-in DYNAMO name for the value of time starting from a specified zero, or from a specified initial value.

For the numerical work, a TABLE Function was generated in DYNAMO Language making use of Auxiliary relations for logarithmic transformation (see the DYNAMO User's Manual; Ref. 2A.11), where N at the left margin indicates an Initial Value Equation and T indicates the values of the TABLE Function; X indicates a Continuation Card when more than one card is needed to list the values.

```
A    FD.K = EXP(2.303*LOGFD.K)      RN DECAY FRACTION
N    FD = 1.0
A    LOGFD.K = TABLE(FDTAB,LOGT.K,0, 6, 0.5)     LOGTEN DECAY FRACTION
```

Note: The values of FDTAB are LOG_{10} values of FD at values of LOG_{10} TIME ranging from 1 to 10^6 years at intervals of LOG_{10} TIME = 0.5.

```
T    FDTAB = 0/-0.03/-0.11/-0.38/-1.00/-1.80/-2.17/-2.51/-2.80/
X    -3.84/-4.0/-4.0          LOGTEN DECAY FRACTION TABLE
```

Note: Any date identifies a particular set of data when more than one set is used in the same context.

```
A    LOGT.K = LOGN(TIME.K)/2.303          LOGTEN TIME (YEARS)
```

Note: The built-in Log function in DYNAMO, LOGN, is to the Base e.

```
N    LOGT = 0
```

Note: The starting time for DYNAMO runs as displayed here is at 1 year; initializing the TIME depends on the problem scale of interest.

2A.4.2.2 Heat Output -- If a constant heat source were turned on at TIME = 0 at a specified depth in the earth, a steady-state heat flow from source to surface would be approached in a time given roughly by the ratio (depth;cm)^2/(Avg. Thermal Diffusivity Rock; cm^2/sec). The source depth of roughly 600 m (see Chapter 1) indicates that this characteristic time would be of the order 10,000 years, although detectable surface loss would begin at a time of the order of 1000 years.

This simple test gives an idea of the time delay involved in the average thermal response, though the actual heat source decreases with time. The response near the repository level is, of course, much faster and requires detailed calculations of transient heat transfer mechanisms. The point is that a range of delay functions is indicated by this kind of relation that will give an idea of thermal responses over different length scales. Some of these choices are displayed later and are compared with the more complete calculations.

For an initial estimate, we let the output be defined as proportional to twice the mean temperature (e.g., as though the steady gradient were linear between a surface at 20°C and the repository source). We also imposed an initial geothermal gradient of 20°C/km and assumed that all radioactive heat is eventually lost to the surface. This means that the initial temperature at the repository depth is 32°C, for a surface temperature of 20°C, and the initial mean temperature is 26°C.

The mean temperature is given by the mean heat content divided by the mean heat capacity. This defines the initial value for the Heat Level:

H = (Mean Temperature;°C)(Mean Heat Capacity;cal/gm/°C)

N H = 5.2 CAL/GM INITIAL HEAT (MTEMP = 26°C)

Thus, the Heat output in the steady state can be written as Steady Heat Loss Rate (SHLR) (note that the geothermal flux is both input and output and therefore cancels out):

$$SHLR = \frac{(2)\,(\text{Mean Heat Content; cal/gm})\,(\text{Thermal Conductivity; cal/cm/sec/°C})\,(\text{sec/yr})}{(\text{Heat Capacity; cal/gm/°C})(\text{Depth to Source; cm})^2(\text{Density; gm/cu cm})}$$

$$- \frac{(\text{Steady Geothermal Flux; cal/sq cm/sec})\,(\text{sec/yr})}{(\text{Depth to Source; cm})\,(\text{Density; gm/cu cm})} \quad , \text{ cal/gm/yr}$$

403 103

which in DYNAMO becomes the approximate equation (using averages of physical properties from Table 2A,1):

```
R   SHLR.KL = 25.0*(H.K-4.0)/1.32E5-2.273 E-4
          STEADY HEAT LOSS RATE (CAL/GM/YR)
N   SHLR = 0
```

The Heat Output Rate is then related to SHLR by means of a Delay function. The sharpness of the output wave can be determined by the order of the Delay. For these preliminary purposes a third-order Delay illustrates the general form of the thermal history (The mathematical structure of the Delay function in terms of Levels and Rates is described graphically and numerically by Forrester, Ref. 2A,4, Chapter 9):

```
R   HOUTR.KL = DELAY3 (SHLR.JK,DSHF)        HEAT LOSS RATE (CAL/GM/YR)
N   HOUTR = 0
    Note: The expected initial value is often written only as a reminder to check the
          numerical printout for internal consistency; DYNAMO automatically
          initializes if equations are complete.
C   DSHF = 1000 YRS          DELAY SURFACE HEAT FLUX
    Note: We experimented with delays of various lengths and order. The values
          used are indicated in the equation listings for particular calculations
          cited later. The terms in parentheses on the right of HOUTR represent
          the input and delay intervals in three cascaded first-order delays, each
          with intervals DSHF/3.
```

The above equations define the Heat Level at subsequent time intervals, from which the updated values of mean temperature are calculated;

```
A   MTEMP.K = (H.K-4.0)/0.2 +20      MEAN TEMP FOR STEMP = 20°C
N   MTEMP = 26   DEG C
```

Although the implied surface heat flux is already computed by the above equations, it is sometimes convenient to write it (or other output variables) in other forms. For this purpose Supplementary Equations can be written for printing and plotting purposes which otherwise play no active role in the computations. For example, the Surface Heat Flux in units of geological heat flow units (microcalories per square cm per sec) is written as follows:

```
S   SURFLX.K = 1.0 + 1.32E5*(HOUTR.JK/30)
          SURFACE FLUX (MICROCAL/SQ CM/SEC)
N   SURFLX = 1.0 MICROCAL/SQ CM/SEC
```

403 104

2A.4.2.3 Thermal Expansion -- Expansion of the planar slab is simply given by the change of mean temperature times the thermal expansion coefficient times the thickness. The latter two terms are combined as the Unit Expansion Coefficient (UEC). Details of expansion near the repository margins require detailed study by means of two-dimensional thermal stress calculations. The Thermal Expansion Rate (TER) is directly obtained from the Heat Rate equations as follows:

$$TER = \frac{\text{(Unit Expansion Coefficient;cm/°C)}}{\text{(Heat Capacity;}} \quad \frac{\text{(Heat Input Rate-Heat Output Rate; cal/gm/yr)}}{\text{cal/gm/°C)}}$$

or,

```
R   TER.KL = UEC*(HINR.JK -HOUTR.JK)/0.2
          LINEAR THERMAL EXPANSION RATE (CM/YR)
```

Note: The Heat Capacity and Thermal Expansion coefficients are averages for relatively dry rock. Effects of the more realistic variations of these coefficients as shown in Table 2A.1, are quite significant and are discussed following presentation of computer results.

```
N   TER = 0.423    CM/YR
C   UEC = 0.9      CM/DEGC UNIT EXPANSION CONSTANT
```

The cumulative expansion is computed from the Level Equation:

```
L   TE.K = TE.J + DT*(TER.JK)    LINEAR THERMAL EXPANSION (CM)
N   TE = 0       INITIAL THERMAL REFERENCE STATE
```

2A.4.2.4 Compaction -- Two principal effects are considered. One is the quantitative settling and compaction of unfilled pore space in the backfill material which is assumed to be salt. We also assume a uniform distribution of voids with bulk porosities ranging from 3 to 30 percent. Since the backfill layer is designed to be about 6 m thick, we assume maximum possible compaction lengths ranging from 20 cm to 180 cm.

The second effect is compaction of porosity caused by solutioning. In order to make the calculation similar to the above mechanism, we assume that solutioning was uniformly distributed. Local compaction or collapse rates (e.g., as occurs in the formation of at least some breccia zones in salt) have not been explicitly simulated, though some estimate of the possible growth rate of a localized cavity is made later in the solutioning calculation.

The simplistic assumption from the mechanical standpoint is that the response to loading is approximately similar to the collapse of cavities in a viscous material. We emphasize that the rheology of salt is highly complex and incompletely known. An assumption such as ours gives, at best, an estimate of gross displacements averaged over long times. The averaging is based on comparisons with effective times for viscous deformation obtained from data given by Heard[2A.8] and from the in situ measurements made during Project Salt Vault.[2A.2] The validity of the assumption depends on the phenomenon being simulated. Average subsidence rates in a widespread planar layer may be approximated on this basis, whereas it may have no validity at all for the deformation around a single waste canister.

The relationship used is based on some experiments by one of the authors on collapse of cavities in a viscous material simulating molten rock.[2A.14] It was found that the approximate compaction rate was exponentially dependent on the time interval multiplied by the ratio of effective pressure acting on the voids to the effective viscosity of the matrix. This relationship was checked against average convergence rates in the Salt Vault experiments using an estimate of viscosity for salt from Ref. 2A.8. The comparison agreed within a factor of about three; this agreement is considered good in terms of the assumptions and the fact that we are dealing with effective viscosities of the order of 10^{18} to 10^{19} dyne/sec/cm^2 (poise). The compaction function was roughly adjusted to the Salt Vault data and a TABLE Function was derived for the effective viscosity. It is emphasized, however, that this "calibration" cannot be considered general, because every site is to a degree structurally and compositionally distinct. We therefore tested variations differing by a factor of ten.

The Compaction Equations involve relations between the three lengths (one-dimensional case): Compaction Length (CL), Maximum Compaction Length (MCL) and Linear Pore Volume (LPV). The latter represents the uncollapsed void space at a given time:

```
L   CL.K = MCL.K-LPV.K    COMPACTION LENGTH (CM)
L   LPV.K = LPV.J + DT*LPVCR.JK      LINEAR PORE VOLUME (CM)
N   LPV = BMCL
N   CL = 0        INITIAL COMPACTION REFERENCE STATE
C   BMCL = 60 CM      BACKFILL MAX COMPACTION LENGTH (CM)
```

Note: A value of about 10 percent initial porosity was assumed in most calculations as an estimate of the best possible backfill procedures; values two or three times larger are considered likely by many observers.

403 106

The Linear Pore Volume Compaction Rate (LPVCR) is based on the function given in Reference 2A.14.

$$\text{LOG}_{10}\frac{\text{Linear Pore Volume at TIME K}}{\text{Linear Pore Volume at TIME J}}$$

$$= \frac{-(\text{Effective Load Pressure; dyne/sq cm})}{(\text{Effective Viscosity; dyne sec/sq cm})} \text{ (TIME JK; sec)}$$

Rewritten in DYNAMO format this becomes:

```
R   LPVCR.KL = LPV.K*EXP(-2      ELP*3E7*DT/EVISC.K)/DT-LPV.K/DT
          LINEAR PORE VOLUME COMPACTION RATE (CM/YR)

C   ELP = 1.3E8 DYNE/SQ CM          EFFECTIVE LOAD PRESSURE

A   EVISC.K = TABLE (EVTAB,BFTEMP.K,0,250,25)          EFFECTIVE
          VISCOSITY (POISE)

T   EVTAB = 1.15E19/7.08E18/4.47E18/2.81E18/1.78E18
X   1.26E18/8.91E17/6.61E17/5.01E17/3.80E17/3.02E17
```

Note: The effective Viscosity is tabulated at intervals of 25°C from 0 to 250°C. The temperature dependence was estimated from Ref. 2A.8.

```
A   BFTEMP.K = 32 + 2*(MTEMP.K-26)      APPROX BACKFILL
          TEMPERATURE (DEGC)

N   BFTEMP = 32          (DEGC)
```

Note: The temperature near the Repository depth is assumed to dominate the compaction rate. It is taken to be the initial steady state temperature plus twice the change in mean temperature of the overburden.

The Maximum Compaction Length (MCL) is introduced above as a variable because later it is related to the amount of solutioning. We also reiterate that the above equations are of the most simplistic form for the mechanics of compaction. We could, for example, have written a stress-strain-time-temperature function from results like those given by Bradshaw and McClain[2A.2], but the complexity would only add confusion to the demonstration calculations at this stage. When the simulation results are better understood, however, it may well become critically important to simulate the rheology in great detail.

403 107

2A.4.2.5 Cracking -- Relationships describing fracturing phenomena are based largely on intuitive guesses constrained by some simple observations of limits. These guesses are required to carry through a numerical example of how such generic functions can be coupled together. It is hoped that they will also serve to encourage more realistic assessment.

The potential multiplicity of cracking phenomena is reduced to two kinds of input functions: (1) cracking caused by bending and layer extensions as consequences of vertical motions, (2) cracking related to existing and created fracture zones produced by any faulting phenomena.

Figure 2A.4 schematically illustrates the reasoning applied to cracking caused by vertical motions of layers. Here, the distributions and orientations of cracks are drawn only in the intuitive sense that some distributed cracking will occur and there are likely to be zones of more concentrated cracking related to regions of greatest flexure. The only quantitative tests made to date are from numerical modeling of maximum elastic stresses caused by thermal expansion. As shown in Figure 2A.5 the loci of maximum tensile stresses are near the repository margins and are concentrated in the shale layers.* Although some incompetent rocks fail at these stress levels in laboratory tests, most rocks have higher apparent strengths. The view expressed here, however, is that whereas this is true for short-term experiments, most rocks will fail in one way or another under such sustained stresses if the stresses are maintained for periods exceeding 100 years.

The limiting condition for the amount of extension cracking was estimated on the assumption that if the layer is assumed to be "clamped" at some lateral distance from the repository site, then any vertical motion implies a change in length which is compensated by fracture porosity. This does not allow for ductility and a compensating attenuation of thickness, which is one point, among many, that will require detailed analysis of all relevant rheological parameters (stress, strain, time, temperature, mineralogical state, textural state and anisotropy, pore fluid pressure, etc.).

403 108

*The calculations behind Figure 2A.5 will be discussed in 2A.4.2.5.1.

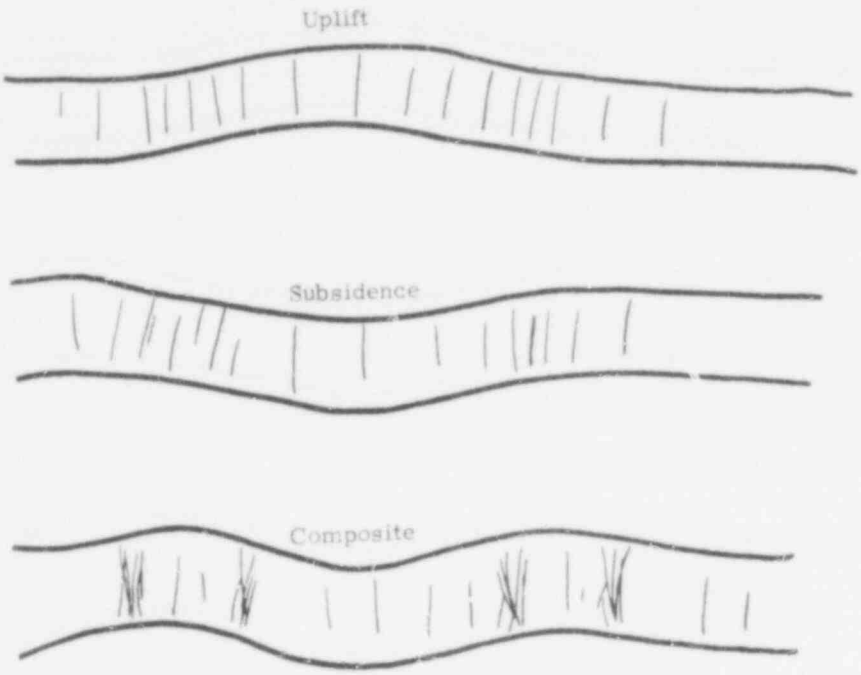

Figure 2A,4. Combined Effects of Uplift and Subsidence

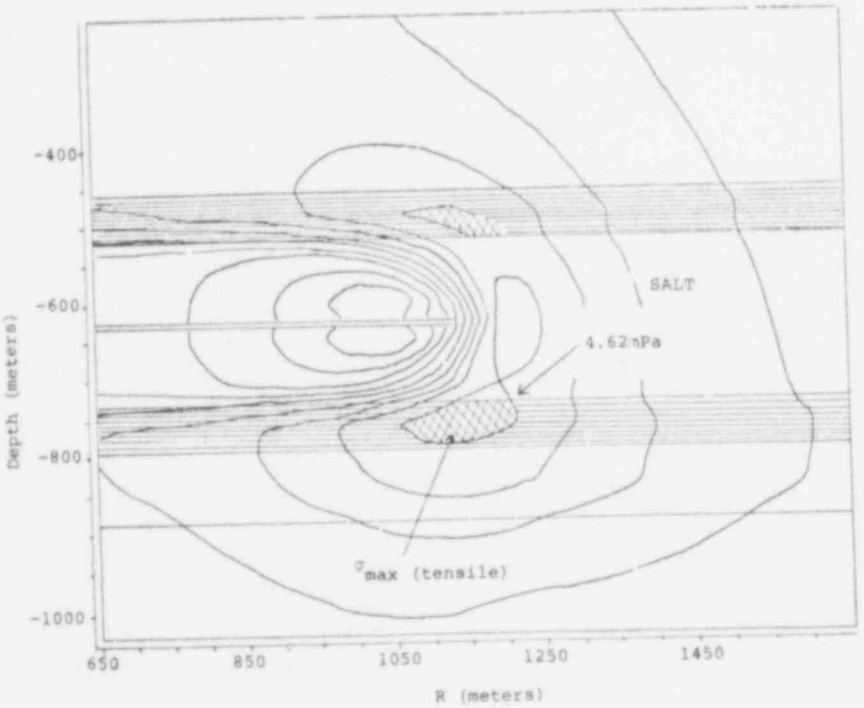

Figure 2A,5. Contours of Maximum Normal Stress Near Repository at t = 50 years

403 109

The magnitude of the extensional fracturing can be expressed in terms of numbers of Reference Cracks of trace dimensions 1 millimeter width by about 3 km in length (roughly the diameter of the repository). The volume of fractures depends on the number and depth range of such cracks. During uplift or subsidence, imaginary horizontal lines will be stretched by amounts depending on flexural form and any compensating ductile flow. For example, a simple conical uplift of a meter would produce a change in surface area of a stratigraphic horizon (e.g., change from the area of a plane circular disc to the surface area of a right circular cone) of the order of 2×10^4 cm^2. This would correspond to the trace area of roughly one Reference Crack. Convex, concave, or even more abrupt punch-like forms of uplift or subsidence create greater and more localized forms of extension near the margins of the deformation. A change of surface area of a punch-like uplift or depression (which seems likely for such a tabular source horizon, either from thermal expansion or compaction) could produce an areal stretching of some horizontal reference plane by something like 1×10^8 cm^2 per meter of vertical motion. The volume of cracks formed is impossible to estimate, and their distributions would be complex, but in terms of areal ratios of extension to trace area of a Reference Crack one can estimate about 5000 cracks.

Another way of looking at limits is to consider the displaced volume of one meter vertical displacement over the repository area (a meter is used as a comparison length because of the backfill maximum compaction lengths, BMCL, discussed in the preceding section). This would amount to about 10^{13} cm^3 volumetric displacement. If even one percent of this volume is not totally compensated by displacements at the ground surface, an internal fracture space amounting to some hundreds of cracks of Reference Volume 50 meters x 3 kilometers x 1 millimeter ($= 1.5 \times 10^8$ cm^3) could be formed. Cracks of this dimension are chosen for comparison because they dimensionally represent the scale of cracking that could significantly breach the shale layers above and below the salt horizons of the Reference Site.

These general bounds suggest that cracking may be roughly proportional to vertical displacement with a proportionality constant ranging from about 1 to 1000 Reference Cracks per meter displacement. In later calculations we have usually used the factor 5*h Reference Cracks, where h is vertical displacement in centimeters. Intuitively, this factor is probably near the upper bounds of estimate, so we have also made calculations over several decades of decreasing magnitudes.

The corresponding DYNAMO equations are written as follows:

```
L   NECC.K = NECC.J + DT*(CREC.JK)      NUMBER OF REFERENCE CRACKS
                FROM NEC
N   NECC = 0        INITIAL STATE OF CRACKING
```

403 110

R CREC,KL = 5*SQRT(NECR,JK*NECR,JK) CRACKING RATE
FROM NEC RATE (REF CRACK/YR FOR CM/YR)

Note: The square root function is used because NECR may be either positive or negative. One Reference Crack corresponds to 2 x 10^8 cm^3 fracture pore space. The coefficient 5 is probably a high estimate, though under special circumstances the value conceivably could be several times larger.

Estimates of cracking produced by fault motions are even more tenuous than the above estimates. Toward this goal we made compilations of fault measurements based on U. S. Geological Survey maps, and also made some preliminary statistical analyses of the results. The results were used to guide our initial assumptions, but they are highly tentative and must be studied in much greater detail. We have chosen high and low estimates of both the initial amount of fracturing related to fault zones and the rate of production of new cracking. In these cases the fracture trace lengths at the ground surface are assumed to represent planes that cut all strata of the Reference Site.

One of the initial states assumes that there are no fault-related fractures at the beginning of the simulation period but that they are created at rates ranging from a millimeter to a tenth of a kilometer trace length per year. Geologically, this might represent the situation in a stable tectonic region adjacent to an actively evolving tectonic province that is encroaching with time on the stable region. The low rate of 1 mm/year is probably imperceptible either by mapping or seismology unless it has been operating for some time. The high rate represents a region of major faulting and earthquakes during a period of very intense activity. The value of 0.1 km/yr, however, does not correspond to single fault plane slips of that magnitude, but represents the integrated trace lengths of fault-related cracks in a complex fault zone. For this purpose we assume that there are roughly 100 times the fracture trace lengths as fault zone length, meaning that the zone itself is growing at a rate of about 1 m/yr (this is many times faster than mean crustal plate motions and therefore represents an episode of abnormally high strain release).

Although the high rate represents a very active fault region that would be seismically conspicuous, it is included to give some insight on solutioning consequences of high faulting rates that are either undetected because of poor historical records or represent unexpected rejuvenation or initiation of major faulting.

The statistical data base for these assumptions is very sensitive to data selection, age biasing and so on. It may be proven in time that the growth rate estimates are partly artifacts of sampling and age criteria. It is important to notice, however, that even if the lowest rate that might be estimated were permitted to proceed very long, there would be a great deal of fracturing already in existence. Anyone who has spent any time in man-made underground openings of various

kinds cannot help but be impressed by this fact. Therefore, whereas our estimates may be incorrect in space-time distributions, there is no doubt that fracture pathways are important even in relatively stable geologic domains. These older fractures may have an important role in that even if the vertical displacement of the previous section caused by combined thermal expansion and compaction are insufficient to cause failure of intact rock, they still may induce extensional opening of existing fractures. Therefore, partly as a reminder of the above importance, we write the following tentative equations including an option for an initial value of 100 km cracking trace length that has accumulated within the repository area over geologic time:

L CTLF.K = CRLF.J + DT*(CRF.JK) CRACK TRACE LENGTH FROM FAULTING (CM)

N CTLF = 0 ASSUMED MIN INITIAL REFERENCE STATE (CM)

N CTLF = 1.0E7 AVERAGE INITIAL REFERENCE STATE (CM)

Note: This last figure is based on an areal averaging of measurements of all mapped faults younger than about 15 million years in the conterminous U. S. normalized to trace length per 100 sq. km. It also assumes 100 fracture lengths per unit fault length (i.e., for the zone of influence).

R CRF.KL = 1.0E-1 MIN CRACK RATE FROM FAULTING (CM/YR)

R CRF.KL = 1.0E4 MAX CRACK RATE FROM FAULTING (CM/YR)

Note: It is assumed that fracturing of given trace length penetrates all strata vertically. The crack volume associated with above faulting depends on faulting style. We have assumed that all cracks have a mean width of 1 millimeter.

2A.4.2.5.1 Digression on Two-Dimensional Stress Analysis Calculations -- Figure 2A.5 shows a representation of the loci of maximum tensile stress near the repository margins. We digress momentarily to explain the source of that figure.

To check some of the results obtained with the present DYNAMO simulation, a two-dimensional transient thermal stress analysis of the reference repository was performed using a finite element computer code. The goals of these calculations were to (1) determine the thermal, stress and displacement response of a reference geological salt formation to a reference nuclear waste decay function, and (2) evaluate the effect of selected unknown variables in order to identify important parameters for future analytical modeling.

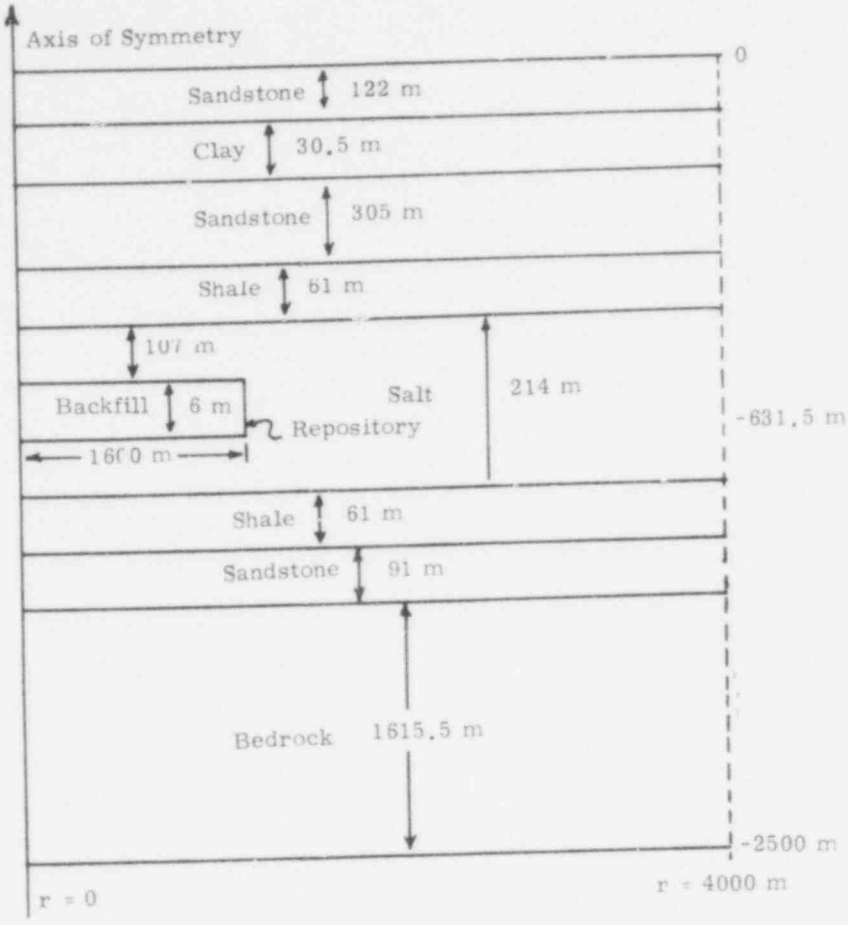

Figure 2A.6. Idealized Site Geometry for Thermal and Structural Calculation

A schematic of the reference geological salt formation used in the calculations is shown in Figure 2A.6. The model of the formation was assumed to be axisymmetric about the z-axis, extending 4000 m in the radial direction and 2500 m in depth. In addition, the waste repository was located at a depth of 631.5 m and had a radius of 1600 m. Of considerable importance are the overall dimensions of the model, which must be large so that the boundary conditions do not affect the thermal and stress states of interest near the repository. This distance can be determined from the thermal diffusion constant of the material and the time of the problem.

A close-up view of the model and the zoning used in the vicinity of the repository is shown in Figure 2A.7.

403 113

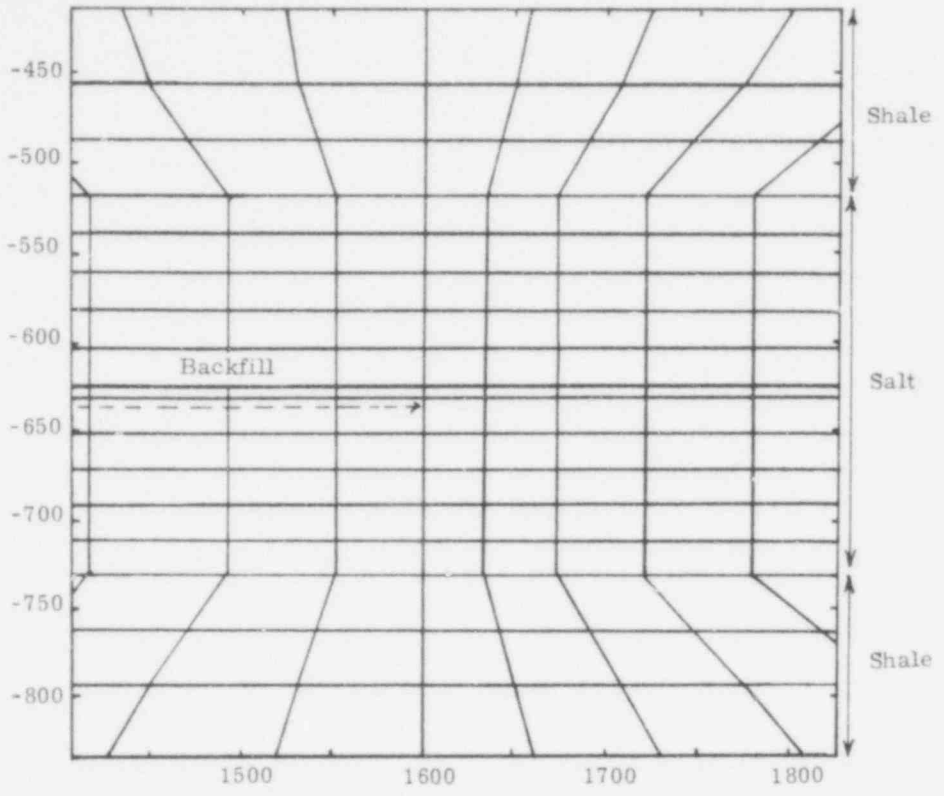

Figure 2A.7. Close-up View of Finite Element Zoning at Edge of Nuclear Waste Repository

For the thermal problem, the boundary conditons are:

1. Prescribed heat flux as a function of time from nuclear waste.
2. Constant temperature at 20°C at top surface and 70°C at bottom surface.
3. Zero heat flux across outer circumferential surface.

The tempera'ure difference between top and bottom surfaces reflects a geothermal gradient of 20°C/km. The initial condition to the thermal problem is the steady state solution with the geothermal gradient.

The boundary conditions for the stress problem are:

1. Stress-free top surface.
2. Zero normal displacement at bottom surface and outer circumferential surface.

403 114

Initially, at t = 0 years, the entire region is considered to be stress-free. Because of the initial thermal gradient and the fixed displacement boundaries, the thermal stresses were not everywhere zero at t = 0. The stress-free condition was determined by first calculating the initial stresses and displacements and then subtracting these from the same quantities calculated at all subsequent times.

Physical and mechanical properties of the various geological layers are given in Table 2A.1. The effects of temperature and anisotropy have been included; however, all materials were assumed to be linear elastic.

The reference waste heat decay function is given in Table 2A.2. Upon closing the repository, it is required to have an initial heat generation rate of 61.3 kw/acre based upon a 1000-acre site.

TABLE 2A.2

Assumed Thermal Power, W(t), of Waste in Repository as a Function of Time

$\log_{10}$ (time in years)	$\log_{10}$ [W(t)/W(1)]
0	0
1	-0.3
2	-0.6
3	-1.45
4	-2.2
5	-3.2
6	-3.2

Some of the results of the calculations on the reference geological formation are summarized in Figure 2A.8. From these plots, and other calculations in which selected variables were changed, the following conclusions can be drawn:

1. With regard to the far-field thermal calculations, the maximum temperature occurs at the center of the repository (r = 0, z = -631.5 m). This temperature peaks at 94°C at 35 years. Local temperatures near the canisters in the plane of the repository may be higher but were not considered.

403 115

2. The largest positive normal stress (σ_{max}) occurs in the lower shale layer radially outward from the repository. Stress contours for t = 50 years are shown in Figure 2A.5. The maximum shear stress (τ_{max}) occurs in the salt layer directly above and below the repository. This is also the location of the maximum compressive stress (σ_{min}). The largest value for σ_{max} is 4.6 MPa, for τ_{max} is 22.5 MPa and for (σ_{min}) is -45 MPa. All are a maximum at approximately the same time. Superimposed upon these thermal stresses, however, is a hydrostatic compression stress of 14 MPa. Hence, there are no resultant tensile stresses.

3. The shape of the waste heat decay function, especially for t = 100 years, has considerable effect on the temperature distributions.

4. The maximum ground uplift occurs directly over the center of the repository. Its magnitude and distribution with time is strongly affected by the thermal expansion coefficient of the salt layer, since this is where the largest temperature differences occur.

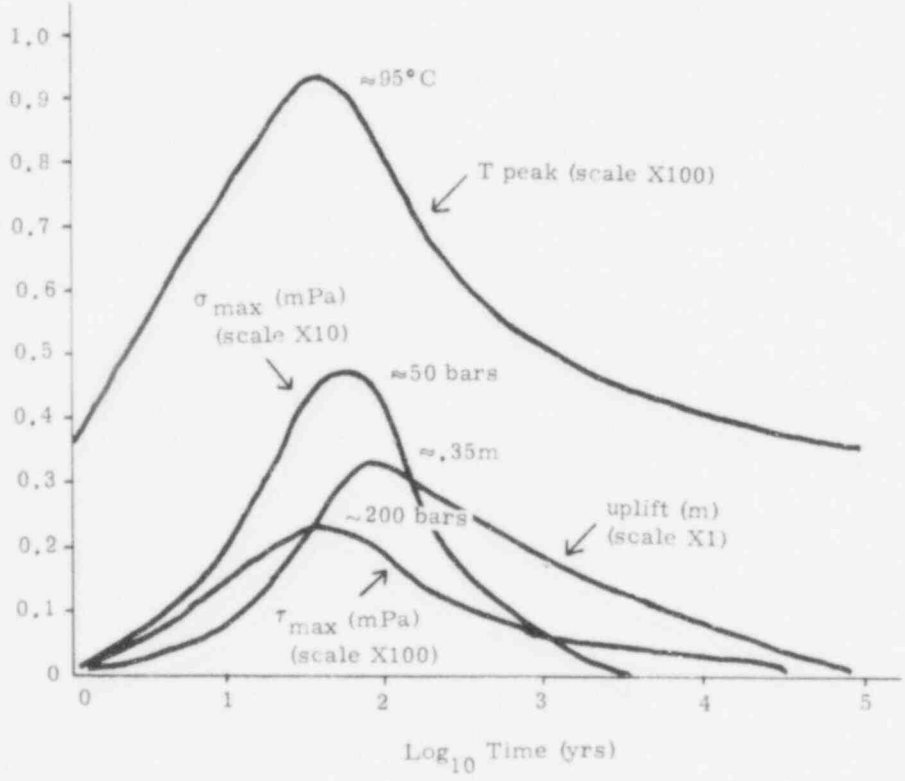

Figure 2A.8. Summary of Results of 2-D Calculation for Reference Repository and Waste Heat Function

403 116

2A.4.2.6 Openings From Solutioning Effects -- Only the openings related to the fracturing effects discussed in 2A.4.2.5 are considered numerically. Other openings, such as dilations caused by uplift, subsidence, and deformations of other origins (geothermal effect of igneous phenomena, tectonic block sliding, vertical tectonic motions such as the "Palmdale Bulge" in California, and so on) are not evaluated, though all of such phenomena are candidates for feedback analyses.

First, we write an expression for the volume of solutioning related to various mechanisms and then discuss the assumed limits of the respective rate equations, as follows:

```
L   SO,K = SO,J + DT*(ORSD,JK + ORSCUA,JK + ORSCLAS,JK + ORSEDLA,JK)
          SOLUTION OPENINGS (CU CM)

N   SO = 1 CU CM      MIN INITIAL REFERENCE STATE
```

Note: This latter value is assigned as the minimum limit in case logarithmic transformations or inverse ratios become involved in the calculations (i.e., functions often need checking to see that they do not involve the Log of zero or zero in a denominator). Other initial values are implied by the assumptions on initial fracture states.

The rate equations were previously named and are discussed below.

2A.4.2.6.1 Opening Rate From Solutioning by Diffusion (ORSD) -- This rate is assumed to depend primarily on pathways between the salt horizons and groundwater in aquifers, which depend, according to our assumptions, on intersecting crack volumes.

The calculation supposes that all cracks defined above intersect the aquifers and provide a diffusion path of brine from the salt horizons (we are not considering radionuclide diffusion at this stage).

The mass transfer depends on the following approximate relation:

(Mass Diffusion Flux;gm/cm^2/sec) = -(Diffusivity;cm^2/sec)
*(Gradient of Concentration; gm/cm^4)

Assuming an average gradient between pure water and saturated brine over a path length of about 50 meters shale thickness, we obtain an order of magnitude estimate of 10^{-4} g/cm^4, which for a diffusivity of 10^{-5} cm^2/sec (typical of aqueous solutions at room temperature) gives a mean flux of 3×10^{-2} gm/cm^2/yr.

403 117

There are, of course, factors like concentration and temperature dependence of solubility and diffusion, tortuosity of paths, and so on, but these refinements are masked by the coarseness of the assumptions on fracturing. We note this but also try not to forget that whereas our assumptions may be reasonable for gross transport, the details of diffusion would be important in any situation where a chemical species might act as a catalytic trigger to some other form of instability (e.g., access of even small amounts of water can be of crucial importance to the mechanical stability of glass).

There are three contributions to the integrated mass flux or mean mass transport rate: (a) crack trace lengths from NEC, (b) crack trace lengths from faulting rates, and (c) initial fracture trace lengths. The combined effect leads to the combined proportions:

```
R   ORSD.KL = 1.0E4*SQRT(NEC.K*NEC.K) + 1.0E2*TIME.K + 1.0E5
          OPENING RATE FROM SOL BY DIFFUSION (CU CM/YR)
```

Note: We have rounded to the nearest factors of ten and have ignored corrections for the density of brine.

The first term on the right depends on the non-linear history of compaction and expansion, the second term represents the high estimate of constant fault fracturing rate, and the last term represents the high estimate of initial fractures. These terms illustrate that if NEC is of the order of 1 meter, then the second term only becomes more significant than the first term for solutioning after about 10^4 years. The last term on the right initially dominates the other two but is exceeded by the first term when NEC exceeds 10 cm. With feedback, however, even if NEC caused by thermal expansion and backfill porosity were initially negligible, the porosity from solutioning by the latter two terms eventually will allow the first term to dominate. It is also noted, and displayed later, that the volumetric magnitudes for diffusion transport are not large (e.g., of the order of one cubic meter per year per meter of NEC for the first term. This value occurs after 10^4 years for the second term).

2A.4.2.6.2 Opening Rate From Solutioning by Convective Transfer to Upper Aquifer (ORSCUA)--Figure 2A.9 shows the assumed pathway. This is a U-tube siphoning effect dependent on the hydraulic gradient of the upper aquifer, the cracking distribution in the shale horizon above the salt, the permeability of the shale-salt interface, and the salt content of interbeds in the shale.

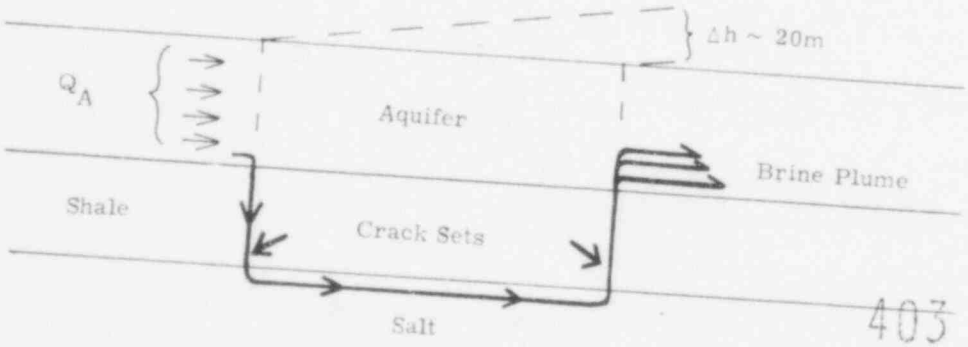

403 118

Figure 2A.9. Assumed Water Pathway for Solutioning by Convection to Upper Aquifer

Initially, we assume that the crack sets are localized near the repository margins, that the permeability of the salt-shale interface is not rate determining, and that there is enough salt in the shale sequence to saturate water in fractures. The second assumption is consistent with the existence of fragmented and structurally chaotic zones between shale and salt in at least some evaporite sequences; the last assumption is consistent with the existence of both salt interbeds and salt admixtures in shales of evaporite sequences. The hydraulic gradient is roughly the same as that of the Reference Site (see Chapter 3).

With these conditions outlined, we simply estimated laminar flow in narrow slot-like conduits corresponding to 1 millimeter wide fractures. We did not allow for growth of crack width or for the much higher transport rates of wider cracks. These effects and various forms of channel focussing represent other types of feedback that remain to be included in more detailed calculations.

With these boundary conditions, we applied a relation given in Reference 2A.13 for viscous flow in narrow tabular slots:

$$\text{(Volume rate; cm}^3\text{/sec)} = \frac{\text{(Pressure Difference; dyne/cm}^2\text{)(Width;cm)}^3\text{(Trace Length, cm)}}{\text{(12)(Viscosity of Fluid; poise)(Transport Length; cm)}}$$

Taken literally, this equation gives very high transport rates (water that encounters salt is assumed to be instantly saturated relative to the time scales of interest). Limiting factors, however, are the flow rates of the aquifer and changes of the pressure head. For example, when the effluent of the fracture U-tube is injected into the aquifer at a given rate it will tend to "pile up" to an extent determined by how fast it is swept away by the mean flow. This pile-up occurs to a maximum value equivalent to a factor that compensates the pressure head by the brine density. If the water in the shale is saturated and the aquifer contains pure water, the effluent brine column could grow to about 2/3 the head difference (Δh). This would be the case if the conduit flow is large for small pressure differences, as it is in the assumed situation.

That is, the brine plume quickly builds up until it approaches hydrostatic equilibrium and thereafter it is replenished at a rate determined by how fast it is carried away by the aquifer flow. Thus, for the hydrology of Chapter 3, the total discharge rate across the width of the repository is of the order of 0.3(300 m)(100 m/yr)(3000 m) = 3×10^7 m^3/yr (= 3×10^{13} cm^3/yr). From the head balances, the height of the brine plume would be about 4 percent of the aquifer thickness, giving a maximum brine discharge of the order of 10^{12} cm^3/yr.

403 119

On the basis of this limit, we estimated the transport rate as follows (the maximum possible rate is not reached until NEC $\simeq$ 100 m, i.e., when the salt above the repository layer is nearly all removed):

R ORSCUA.KL = 1.0E8*SQRT(NEC.K*NEC.K) OPENING RATE FROM SOL BY CONVECT TO UP AQUIF. (CU CM/YR)

Note that we have included only the cracking from vertical motions, because as mentioned in the last section, it is assumed to dominate. If for some reason, however, there is assumed to be negligible thermal expansion or backfill porosity, then additional terms like those included in ORS[illegible] must be added. Those terms then provide potential feedback inputs to NEC in ORSCUA as written above.

Note: Numerical calculations with terms of this type have not been carried out as yet in as many combinations as would be desirable. They should be included in future work.

2A.4.2.6.3 Opening Rate From Solutioning by Convective Transfer from Lower Aquifer to Surface (ORSCLAS) -- This solutioning rate depends principally on the number of throughgoing cracks and the pressure head in the aquifer below the salt horizons. Since the minimum rate is zero, we have written a relation only for the maximum rate, in the form

R ORSCLAS.KL = 6.0E10*TIME MAX OPEN RATE BY CONVECT L. AQUIF TO SURFACE PER ATM HEAD (CU CM/YR)

These rates are potentially very high and are limited only by the potential total discharge rate of the aquifer (e.g., for the above equation this could be achieved in less than 1000 years). They are, however, subject to the difficult question of pressure distributions in fractures relative to the lower aquifer, which may have zero or negative values. The latter implies downward flow. Such a flow regime may be analogous to ORSCUA but with potentially higher rates because they are not limited by the salinity plume effect. Even without the forced convection term, however, there could be a substantial mass transfer to the lower aquifer by free convection. This is examined in the next section.

2A.4.2.6.4 Opening Rate From Solutioning by Eddy Diffusion to Lower Aquifer (ORSEDLA) -- An important reservation and admonition concerning either forced or free convection transport to horizons below the salt is that gravitational forces favor instabilities of various types that may have quite different forms from those associated with strata above the salt. One of these effects relative to brine flow is considered below. A potential major effect, however, that has not been studied in adequate dimensional perspective is the mechanical instability that will occur in the salt strata when solutioning from below occurs. We expect that certain conditions could lead to rapid propagation of breccia zones. These involve

forms of localized fracturing that are not accounted for by any of the equations for fracturing we have discussed so far. Some perspective is given by the time required to form large single cavities. This is shown later in the numerical results. However, feedback leading to even faster local penetration seems possible, because gravity favors higher fracturing potentials, larger fracture spacings and higher local brine transport rates by either free or forced convection. Understanding this problem from the feedback standpoint is an important future goal and should be high on the list of demonstration calculations for all projects related to waste repositories in salt media.

A start on this problem has been made by evaluating the transport in terms of a one-dimensional diffusion analogy. This form is suggested by work in progress by several investigators elsewhere relative to the Solution Mining industry. The assumption also simplifies the calculation in that the discharge rate can be estimated in a manner parallel to that for ORSD, except that because the fracture pathways are below the repository we can't assume the same proportionality to NEC. That is, at present we have no intuitive feel for where the fracture permeability will occur below the repository even though extensional stress concentrations are indicated by Figure 2A.5 in the underlying shale layer. It seems possible, for example, that part of the compaction displacement could be taken up by upward displacements of the floor of the repository by virture of isostatic and thermally buoyant adjustments in rock immediately around and below this depth.

Our interpretation of this form of transport is that turbulent brine eddies can propagate downward with mean diffusivities at least as great as 0.1 cm^2/sec. At present this must be considered an unsupported assumption until the relevant investigations have been described in detail. On this assumption, transport occurs at a rate 10^4 times faster than with the coefficient in ORSD. If there is a relation for NEC analogous to that in the equation for ORSD, the new coefficient is 1.0E8 in the first term of the ORSD equation, which gives a transport rate of the same magnitude as ORSCUA. Though we are not able to document that assumption, the consequence of it is indicated by the ORSCUA output (except for the brecciation mechanisms mentioned above). Therefore, at present we write ORSEDLA only in terms of fractures produced by the faulting equations, as follows:

R ORSEDLA,KL = 1.0E6*TIME + 1.0E9 OPENING RATE SOL EDDY DIFF TO L AQUIF (CU CM/YR)

Note: This equation does not account for all potentially important mechanical feedback mechanisms. The transport rate assumes constant rates of fracture creation from faulting sources only. See discussion in text.

403 121

In concluding the section on salt transport it is appropriate to comment again on the relationships of simulation models and more detailed transport modeling of Chapter 3. The hydrologic model is capable of giving very good estimates of transport rates and geometric distributions of species when the permeability regimes are known. It cannot, however, handle variable rock properties and boundary conditions during a calculation. Therefore, we envisage a coupled mode of calculation in which DYNAMO (or other languages) simulates the time changes of these variable conditions, the transport model then computes the amounts and distributions of chemical transport (salt removal, etc.) for some specified time interval, DYNAMO recomputes changes in system properties, fracture pathways, etc., and the transport model performs another iteration in that mode, and so on. In practice, a set of permeability regimes could be defined by reconnaissance DYNAMO calculations (or prescribed by other modeling or geological constraints). From this set the transport model can generate tables of transport data which then become table functions to be used by DYNAMO whenever a calculation encounters the appropriate conditions. In this way, a large catalog of transport functions could be accumulated and used interactively with a variety of different simulation sequences.

2A.5 Computer Runs: H-TE-C-F-O-GW Sector

It is evident from the repeated warnings in the foregoing text that numerical calculations reported here are strictly test cases designed to provide the flavor of this approach to geological simulation without implying any rigid substantive conclusions. We have made over two hundred computer calculations during the report period in learning by trial and error some of the combinations possible using DYNAMO. The total costs in computer time are trivial (only a few dollars per calculation). We mention this to illustrate that: (a) the present report of work represents a bare beginning on problems of Geological Feedback Simulation using a very simple form of Simulation Language, and (b) rapid progress can be made, however, with inexpensive simulation techniques once a problem is defined.

We cannot display many of the calculations in this report. Therefore we give equation listings and examples of time plots in the form of direct computer outputs for two types of calculations: (1) a composite plot of simultaneous parameter variations, as an example of solutioning feedback, and (2) a series of plots showing results of single parameter variations (we refer to these later as "multiplots"). Because of their length, the time plots representing items (1) and (2) are supplied at the end of Appendix 2A.

The multiplots, shown in Figure 2A.11 (a-l) are computed in the same way as the plot of simultaneous parameter variation shown in Figure 2A.10. However, the multiplots demonstrate the effects of varying some of the parameters individually; these effects are shown sequentially on a series of plots each of which contains outputs for a single type of variable computed from several different choices of input assumptions.

2A.5.1 Equation Listings

In order to compile the equations discussed in Section 2A.4 in one concise format, we show a typical listing from one of the solutioning calculations in Table 2A.3. (The equation list for each plot displayed in Figures 2A.7 and 2A.8 is given in a key that precedes the Tables and Figures at the end of Appendix 2A.

Parallel, but somewhat abbreviated, listings are given for the actual calculations displayed. The names of functions were necessarily modified for multiplots of single variables. The general scheme for the multiplots was to write the same equations repeatedly with similar but unique equation variables. We chose this approach in order to be explicit about data and equation sets, although there are automatic rerun options that can make use of sets of redefined Equation Constants (see Ref. 2A.11).

2A.5.2 Computed Time Series

Examples of computer plots are shown in Figure 2A.10* and 2A.11(a-l) for the Equation Listings in Table 2A.4 and Table 2A.5. These calculations are shown on a time scale of 10,000 years as a compromise that gives some idea of both short term and long term behavior. Other calculations have been made on time scales ranging from a thousand to a million years.

Generally a short title and other I.D. are shown at the top (or at the left margin if the TIME axis runs from left to right) followed by the correspondence of Equation Variables and Plot Symbols (HINR = P, etc.). The plotting scale is next identified for each plotting symbol for the chosen chart divisions (either by assignment or automatically by DYNAMO); the letter symbol immediately following the number scale represents the order of magnitude: A represents 10^{-3}, T represents 10^{3}, etc. (see Ref. 2A.11). Symbols that happen to plot at the same point on the chart are listed together at the margin (e.g., E and N plot together at the upper limit of the variable at 1000 years in Figure 2A.10, and P, C and M plot together at the lower limit of the variable at the same value of TIME).

The equation list and function plots for the multiplots (Table 2A.5 and Figures 2A.11) may seem confusing, but a complete explanation would be excessively long. The idea in generating these plots was to pick a set of functions for display and perform the calculations with several different choices of input parameters. The following tables give the choices of functions whose input parameters were varied in Figure 2A.11:

---

*At end of Appendix 2A.

403 123

Function Name	Figure 2A.11
MTEMP	a
HOUTR	b
TE	c
HINR	d
SURFLX	e
EVISC	f
CL	g
NEC	h
NECSD (NEC with solutioning by diffusion)	i
SCDD (SCDIAM with solutioning by diffusion)	j
NECSC (NEC with solutioning by convection)	k
SCDC (SCDIAM with solutioning by convection)	l

The functions related to Heat content (Figures 2A.11 a-f) were varied by choosing three different values of thermal loading (roughly 30, 60, and 120 kw/acre) with various Delay times.

The compaction calculations of Figure 2A.11g were included to show comparisons of results using constant viscosities ranging from 10^{18} poise (curve A) to 10^{19} poise (curve C), and using variable viscosities from table functions (curves D, E, F). Curve D in 2A.11g represents a different compaction function from the other curves and has a somewhat lower final value of CL.

The multiplots in Figures 2A.11 i-l show the range of solutioning effects for the range of physical property variations in the preceding multiplots. Particularly, note the small range of times in Figure 2A.11k where NEC goes off scale (exceeds 100 meters of solutioning and compaction) despite the fairly wide range of variations in the input parameters.

Table 2A.6 and Figure 2A.12(a-b) give results for a time scale of one million years to show the long-term behavior of temperature and of solutioning compaction when the solutioning rate is decreased progressively by four orders of magnitude.

2A.5.3 Discussion of Computer Calculations

2A.5.3.1 General Summary -- As a guide to examination of the charts, some of the general points are summarized as follows: (1) the thermal steady state is achieved between 10,000 and 100,000 years, at which time temperatures and heat flux are indistinguishable from the normal geothermal gradient at a resolution of $1^{\circ}C$, (2) mean temperatures (MTEMP) quickly rise to maxima, generally less than $100^{\circ}C$, on a time scale of 1000 years or less and fall to below $50^{\circ}C$ in the first 10,000 years; the position of the maximum is sensitive to assumed values of heat loss delays and distributions of thermal properties, (3) backfill temperatures (BFTEMP) are shown as roughly twice the mean temperature in order to represent the approximate average temperatures near the repository level ignoring short-term variations relative to canister distributions; the true values and their time distributions are very sensitive to the depth regions of averaging and to differences of thermal properties of the rock strata, (4) thermal expansion is equivalent to uplifts measured in tens of centimeters when compaction is not taken into account; the maximum follows soon after the thermal peak, (5) simple compaction of backfill porosity occurs rapidly in the first few hundred years and has nearly reached equilibrium in times of the order of 1000 years, (6) disturbance of the surface geothermal flux may be detectable within the first 10,000 years or so in dry environments, but convective heat transfer by groundwater probably will obliterate this effect in most systems (see Chapter 3), (7) solutioning effects related to the assumed fracture paths are very large relative to the scales of thermal expansion and backfill compaction because of feedback and may be commensurate with the thickness of the entire sale formation on a time scale of 10,000 years.

These general results are important for comparison with the calculations provided by the multicell model discussed in 2A.4.2.5.1. Figure 2A.8 shows some results of the finite-element thermal stress calculation. The differences emphasize the inaccuracies of the lumped parameter nature of the DYNAMO calculations but confirm the general magnitudes. The sharp contrast of the larger thermal expansion coefficient of halite relative to the rock average (see Table 2A.1) partly explains why the thermal expansion peak occurs much sooner in Figure 2A.8 than in the DYNAMO runs. This contrast combines with the more accurate representation of peak temperature in salt at the repository level (rather than a value based on the mean of average rock properties) to greatly shorten the peak response time. Factors of this type must be watched for continually in thinking about the results of simplified calculations. It is important, however, to have a feel for both this sort of response scale and the average response on the larger scale as represented by the DYNAMO calculations. Apparently, the very simple DYNAMO calculations categorically reproduce the kinds of responses found in much more sophisticated thermal calculations.

The most important general result, however, is that DYNAMO simulation is able to anticipate phenomena, such as item (7) above, that could not be predicted with the more specialized models and which are not intuitively obvious. This conceptual conclusion supports our introductory defense of simulation modeling as the simplest and quickest basis for discovering hidden effects that arise from feedback mechanisms.

2A.5.3.2 Conclusions on Salt Solutioning-Compaction Feedback -- The results of simulation calculations indicate the possibility for removal of a 100-meter layer of salt in less than 5000 years (Figure 2A.10, curve C; Figure 2A.11k) and the local penetration of the entire salt formation in less than 1500 years (Figure 2A.10, curve D; Figure 2A.11f). These are drastic consequences, at face value, and need some explanation.

The reason for this rather dramatic solutioning behavior is two-fold: (1) any mechanism at all that initiates cracking and establishes a convective siphon of the type postulated in Figure 2A.9 catalyzes the rapid acceleration of solutioning rates via the Feedback Loop of Figure 2A.3, and (2) the maximum rate of solutioning is large because of the large capacity and discharge rate of the Upper Aquifer of the Reference System in Figure 2A.1.

This simulation conclusion is made more severe by the fact that liberal variations in thermal loading (Figure 2A.11 a-d), effective viscosities (Figure 2A.11f) and backfill porosity (Figure 2A.13*) have only minor effects on the solutioning time (Figure 2A.11k and l; Figure 2A.13*). Figure 2A.13 is the result of a calculation in which the backfill maximum compaction length, BMCL, was reduced to 20 cm (about 4 percent initial porosity) and the thermal load was halved. As shown by curves C, N, and D of that figure, the solutioning times cited above are increased only by 20 to 30 percent. In fact, other calculations were made with zero initial backfill porosity and a low value of thermal load, and the solutioning times were still less than 10,000 years. The main conclusion is that if the conditions permit any cracking of the sort postulated, and if the hydrologic conditions are sufficiently dynamic, solutioning instabilities of layered salt media could occur on short time scales and hence represent major hypothetical threats to release of radionuclides to aquifers.

In order to test these phenomena for less active hydrologic environments, we made several runs on a million year time scale with solutioning rate coefficients (constants in functions like ORSCUA) progressively smaller by factors of ten. One example is shown in Figure 2A.12 (a-b).* Two main conclusions are indicated: (a) the "incubation time" before the solutioning instability becomes conspicuous increases more or less in inverse proportion to the coefficient (the correspondence is not exact because of the nonlinearities of the various responses; this point needs additional "sorting"), and (b) by the same token, the system may appear stable to solutioning effects for long times (say on the 10,000 or 100,000 year scales), and still it may be susceptible to wholesale solutioning on the million-year time scale.

---

* At end of Appendix 2A.

Geologically, it is clear even in other kinds of rock (e.g., limestone), that any process that initiates chemical transport along fracture pathways may act as a catalyst to increased transport. This general form of solutioning cycle is consistent with geological phenomena like Carlsbad Caverns of similar volumetric scale to the repository that occurred on a time scale roughly a hundred times longer in less soluble rock. There are, however, major scale differences in depth, deformation rate phenomena, chemistry, and presumably in hydrology so that only qualitative comparisons may be meaninful.

The reality of the higher solutioning rates will require much more careful analysis. The rates depend critically on the criteria of fracturing, which are very difficult to specify with rigor. The ranges of possibilities, however, can be narrowed by making calculations based on other forms of fracturing criteria than the simplistic assumptions used for the sake of demonstrating the simulation method. These refinements combined with a more appropriate rheological equation of state for salt may greatly modify the results.

Much geological evidence exists that can be brought to bear on these apparent conclusions. Unfortunately, geological knowledge of solutioning mechanisms has not been adequately systematized in a form that permits very great restrictions on maximum rates. Also, conditions of the sort artificially catalyzed by the local and rapid thermal loading are not presently known in the geologic record (to our knowledge). It is very difficult to state, however, from the existing statistically small sampling of the vast areas of salt deposits, that such phenomena as described in this report have not taken place at similar rates in some circumstances.

2A.6 Recommendations

There is a major and sometimes confusing distinction between the use of numerical results of simulation analysis and belief in those results. We do not believe the foregoing consequence curves in a context much stronger than confirmation of existing geological knowledge and intuition that such instabilities can happen. We suggest that the results be used to continue building on these combined experiences until some confidence is gained on how likely is the possibility. Here again we need be careful on subjective probabilities versus empirical probabilities, though to some degree they will have to be combined (e.g., as occurs in weather "prediction").

We conclude that simulation analysis adds an important new dimension to methodology development that can be expanded and can add new perspectives to other analytical schemes. However, conclusions drawn from feedback calculations simply mirror and potentially amplify the insight (or lack thereof) of the analyst. Hence, progressive incorporation of greater geological insight is also desired. Feedback systems analysis can in itself provide a form of communications medium if it is used within common sense geological perspectives.

403 127

Though we have not tried to do so in the time available for preparation of this report, it is recommended that problems be classified by means of System Diagrams and Feedback Loops of the sorts we have discussed. Several have been mentioned in addition to solutioning processes. In these efforts we particularly recommend emphasis on searches for hidden effects that may have significant consequences on specified time scales (e.g., time scales that may be specified as important from the standpoint of exposure of the biosphere to radiation). One example of a hidden effect is the time scale for the "incubation period" of solutioning feedback.

As examples of application of simulation techniques to other forms of analysis, we recommend exploration as a tool for generating statistical populations of undersirable consequences with associated time scales. This might be approached from the standpoint of Monte Carlo series calculated from fairly unrestricted sets of input parameters, contrasted with other calculations from specified ranges and weighted interdependence of parameters (e.g., as might be specified for ranges of mechanical behavior limited according to deformation functions such as those described by Heard).[2A, 8] These methods could provide one basis for "quick and dirty" Sensitivity Analysis; the main value of this would be to explore the relevant numerical techniques within a context that has some specific physical meaning from the standpoint of a hypothetical simulation model. It would still be understood that the results have no other specific import than possibly identifying most likely outcomes among a set that are already known in the simulation mode. For example, families of results for solutioning feedback might be illustrated this way, but the results would say nothing about triggering mechanisms not recognized in the simulation.

Another application implied by our discussions, and one we also recommend, is the use of DYNAMO and other Simulation Languages to provide the footwork to map out problems, boundary conditions, and specific questions to be more rigorously "solved" by multicell modeling techniques. The example highlighted is the relation of fracture permeability to chemical transport in the variety of regimes postulated. That is, are the paths, pressure heads, discharge rates, etc., realistic or are they artifacts of geometrical assumptions?

The statements of this report are not intended to represent alarmist or defeatist viewpoints. In fact, we feel that this sort of approach suggests some optimism for an eventual ability to characterize a repository sufficiently to greatly reduce fears that have grown from doubts raised concerning partial analysis.

Statements concerning the ultimate aims of assessing risks to the health and genetic future of mankind have been avoided in this report. For example, no position has been taken on the undesirability of release of radionuclides to active groundwater systems. Questions of dilution factors, absorption factors and path lengths are also relevant to the criteria of radiation hazards. More comprehensive systems analysis is required before geologic instabilities of the sort described can be considered categorically bad. It is suggested, however, that Systems Diagrams and Simulation Plots like those presented can also be helpful in this broader context.

Tables of DYNAMO Program Listings
and Plots of Simulation Runs

Tables	Figures
2A.3	None relevant
2A.4	2A.10
2A.5	2A.11(a-l)
2A.6	2A.12(a & b)
2A.7	2A.13

403 129

TABLE 2A.3

Typical Listing from a Solutioning Calculation

```
DYNAMO IIF, VERSION 3.02


*     SIMPLE HEAT,THERMAL EXPANSION,COMPACTION AND SOLUTION SECTORS
N     TIME=1.    YEAR
L     H.K=H.J+DT*(HINR.JK-HOUTR.JK)      HEAT ABOVE ZERO TEMP CAL/GM
N     H=5.2  CAL/GM                      INITIAL HEAT HTEMP=26C
R     HINR.KL=0.047*FD.K       RN POWER  CAL/GM/YR  1/2 ORIGINAL
N     HINR=0
A     FD.K=EXP(2.303*LOGFD.K)            RN DECAY FRACTION
N     FD=1.0
A     LOGFD.K=TABLE(FDTAB,LOGT.K,0,6,0.5)  LOGTEN DECAY FRACTION
N     LOGFD=0
T     FDTAB=0/-0.03/-0.11/-0.34/-1.00/-1.8/-2.17/-2.51/-2.85/-3.28/
X     -3.84/-4.0/-4.0   LOGTEN DECAY FRACTION TABLE   REVISED 6/20/77
A     LOGT.K=LOGN(TIME.K)/2.303          LOGTEN TIME (YEARS)
N     LOGT=0
R     SHLR.KL=25.0*(H.K-4.1)/1.32E5-2.373E-4   STEADY HEAT LOSS RATE CAL/GM/YR
N     SHLR=0
R     HOUTR.KL=DELAY3(SHLR.JK,DSHF)      HEAT LOSS RATE CAL/GM/YR
N     HOUTR=0
C     DSHF=1000 YRS    DELAY SURFACE HEAT FLUX
A     HTEMP.K=(H.K-4.0)/3.2+25.          MEAN TEMP FOR STEMP=20C
N     HTEMP=26
S     SURFLX.K=1.0+1.32E5*(HOUTR.JK/30)    SURFACE FLUX MICROCAL/SQCM/SEC
N     SURFLX=1.0
L     TE.K=TE.J+DT*(TER.JK)              LINEAR THERMAL EXPANSION (CM)
N     TE=0                    INITIAL THERMAL REFERENCE STATE
R     TER.KL=UEC*(HINR.JK-HOUTR.JK)/0.2    LINEAR TE RATE (CM/YR)
N     TER=0.423
C     UEC=0.9 CM/DEGC          UNIT EXPANSION CONSTANT
S     DTEMP.K=DT*(HINR.JK-HOUTR.JK)/0.2      DELTA TEMP JK DEGC
N     DTEMP=0
A     NEC.K=TE.K-CL.K   NET EXPANSION MINUS COMPACTION (CM)
N     NEC=0
A     BFTEMP.K=32+2*(HTEMP.K-26)    APPROX BACKFILL TEMP DEGC
N     BFTEMP=32
L     CL.K=MCL.J-LPV.J  COMPACTION LENGTH (CM)
N     CL=0
L     LPV.K=LPV.J+DT*LPVCR.JK   LINEAR PORE VOLUME (CM)
N     LPV=60
R     LPVCR.KL=LPV.K*EXP(-2.303*ELP*3.3E7*UT/EVISC.K)/DT-LPV.K/DT
NOTE          LINEAR PORE VOLUME COMPACTION RATE (CM/YR)
A     MCL.K=BMCL+ACLS.K  MAX COMPACT LENGTH AT TIME (CM)
C     BMCL=60 CM  BACKFILL MAX COMPACT LENGTH
A     ACLS.K=SO.K/SA.K  AVG COMPACT LENGTH FROM SOL (CM)
A     SA.K=RA  SOLUTIONING AREA (SQ.CM)
C     RA=7.9E10  REPOSITORY AREA (SQ.CM.)
C     ELP=1.3E8  DYNE/SQCM  EFFECTIVE LOAD PRESSURE
A     NECR.K=TER.JK-LPVCR.JK  NET EXPANSION MINUS COMPACT RATE(CM/YR)
A     EVISC.K=TABLE(EVTAB,BFTEMP.K,0,250,25)  EFFECTIVE VISC (POISE)
T     EVTAB=1.15E19,7.03E18,4.47E18,2.81E18,1.78E18,1.26E18,
X     8.91E17,6.61E17,5.01E17,3.80E17,3.02E17
L     SO.K=SO.J+DT*(ORSO.JK+ORSCUA.JK+ORSCLAS.JK+ORSEDLA.JK)  SOLUT.OPEN.(CUCM
N     SO=1 CU.CM.  MINIMUM SOLUTION OPENINGS
R     ORSO.KL=0
R     ORSCUA.KL=1.3E8*MAX(NEC.K,-NEC.K)  OPEN RATE FROM SOLUTION BY CONVECTION
NOTE                                     UP AQUIFER (CU.CM./YR)
R     ORSCLAS.KL=0
R     ORSEDLA.KL=0
A     SCDIAM.K=2.0*EXP(LNVFUNC.K)  SINGLE CAVITY DIAM(CM)
A     LNVFUNC.K=0.33*LOGN(SO.K)-0.46
NOTE
PRINT CL,NEC,SO,SCDIAM,ORSCUA,ACLS,MCL,LPV,BFTEMP,TE,HINR,HOUTR
PLOT  ACLS=A(0,1.0E4)/SCDIAM=D(0,7.0E4)/SO=S(0,0.8E5)/CL=C(0,1.0E4)/
X     NEC=N(-1.0E4,0)/BFTEMP=B/TE=E/HINR=P/HOUTR=O
SPEC  DT=10/LENGTH=1.0E5/PLTPER=1.0E4/PRTPER=100
RUN   10 YR DT TO 1.0EE  NEW HINR,FDTABLE,ORSCUA  DSHF=1000
SCR *
FLX
HP
R


    1347  OF   2472  DATA LIST WORDS
     127  OF   200   SYMBOL TABLE VARIABLES
       0  OF    10   MACRO DEFINITIONS
      11  OF    15   OUTPUT RECORDS (PLOT CARDS/PRINT LINES)
```

403 150

TABLE 2A.4

Equation Listing for Plots in Figure 2A.10

```
DYNAMO IIF, VERSION 3.02


*     BMCL=60, SO MIN AND ORSCUA=1.0E8...
N     TIME=1.    YEAR
L     H.K=H.J+DT*(HINR.JK-HOUTR.JK)        HEAT ABOVE ZERO TEMP CAL/GM
N     H=5.2  CAL/GM                        INITIAL HEAT HTEMP=26C
R     HINR.KL=0.094*FD.K                   RN POWER  CAL/GM/YR
N     HINR=0
A     FD.K=EXP(2.303*LOGFD.K)              RN DECAY FRACTION
N      FD=1.0
A     LOGFD.K=TABLE(FDTAB,LOGT.K,0,6,0.5)  LOGTEN DECAY FRACTION
N      LOGFD=0
T     FDTAB=0/-0.03/-0.11/-0.36/-1.30/-1.80/-2.17/-2.51/-2.80/-3.28/
X     -3.54/-4.0/-4.0   LOGTEN DECAY FRACTION TABLE   REVISED 6/20/77
A     LOGT.K=LOGN(TIME.K)/2.303            LOGTEN TIME (YEARS)
N      LOGT=0
R     SHLR.KL=25.0*(H.K-4.1)/1.32E5-2.273E-4  STEADY HEAT LOSS RATE CAL/GM/YR
N      SHLR=0
R     HOUTR.KL=DELAY3(SHLR.JK,DSHF)        HEAT LOSS RATE CAL/GM/YR
N      HOUTR=0
C     DSHF=100
A     HTEMP.K=(H.K-4.0)/0.2+20.            MEAN TEMP FOR STEMP=20C
N      HTEMP=26
S     SURFLX.K=1.0+1.32E5*(HOUTR.JK/30)    SURFACE FLUX MICROCAL/SQCM/SEC
N      SURFLX=1.0
L     TE.K=TE.J+DT*(TER.JK)                LINEAR THERMAL EXPANSION (CM)
N     TE=0                          INITIAL THERMAL REFERENCE STATE
R     TER.KL=UEC*(HINR.JK-HOUTR.JK)/0.2    LINEAR TE RATE (CM/YR)
N      TER=0.423
C     UEC=0.9 CM/DEGC              UNIT EXPANSION CONSTANT
S      DTEMP.K=DT*(HINR.JK-HOUTR.JK)/0.2    DELTA TEMP JK DEGC
N     DTEMP=0
A     BFTEMP.K=32+2*(HTEMP.K-20)    APPROX BACKFILL TEMP DEGC
N     BFTEMP=32
C     BMCL=60 CM  BACKFILL MAX COMPACT LENGTH
A     SA.K=RA  SOLUTIONING AREA (SQ.CM)
C     RA=7.9E10  REPOSITORY AREA (SQ.CM.)
C     ELP=1.3E8  DYNE/SQCM  EFFECTIVE LOAD PRESSURE
A     EVISC.K=TABLE(EVTAB,BFTEMP.K,0,250,25)  EFFECTIVE VISC (POISE)
T     EVTAB=1.15E19,7.08E18,4.47E18,2.81E18,1.78E18,1.26E18,
X     8.91E17,6.61E17,5.01E17,3.85E17,3.02E17
R     ORSCU1.KL=1.0E8*MAX(NEC1.K,-NEC1.K)
A     NEC1.K=TE.K-CL1.K
N     NEC1=0
L     CL1.K=MCL1.J-LPV1.J
N     CL1=0
L     LPV1.K=LPV1.J+DT*(LPVCR1.JK)
N     LPV1=60
R     LPVCR1.KL=LPV1.K*EXP(-2.303*ELP*3.0E7*DT/EVISC.K)/DT-LPV1.K/DT
A     MCL1.K=BMCL+ACLS1.K
A     ACLS1.K=SO1.K/SA.K
N     SO1=1  CU.CM.
L      SO1.K=SO1.J+DT*PIECE(0,ORSCU1.JK,ACLS1.JK,1.0E4)
A     SCOI41.K=2.0*EXP(LNVFU1.K)
A     LNVFU1.K=0.33*LOGN(SO1.K)-0.46
NOTE
PRINT HINR,HOUTR,SURFLX,TE,NEC1,BFTEMP,CL1,MCL1,SCOI41,SO1,ORSCU1,ACLS1
PLOT  HINR=P/HOUTR=O/SURFLX=F/TE=E/NEC1=N/(-1.0E4,0)/BFTEMP=B
X     CL1=C,MCL1=M(0,1.0E4)/SCOI41=D(0,2.0E4)
SPEC  DT=1/LENGTH=1.0E4/PLTPER=100/PRTPER=100
RUN   ORSCUA CONSTANT BUT NOTHING ELSE
)SED -
)P


     1030  OF   2472  DATA LIST WORDS
      123  OF    200  SYMBOL TABLE VARIABLES
        9  OF     15  MACRO DEFINITIONS
       11  OF     15  OUTPUT RECORDS (PLOT CARDS/PRINT LINES)
```

TABLE 2A.5

Equation Listing for Plots in Figure 2A.11 (a - 1)

```
DYNAMO IIF. VERSION 3.02

*     SIMPLE HEAT AND COMPACTIO  SECTORS
*     SOLUTIONING BY DIFFUSION
*     SOLUTIONING BY CONVECTION
N     TIME=1.  YEAR
A     FD.K=EXP(2.303*LOGFD.K)              RN DECAY FRACTION
N      FD=1.0
A     LOGFD.K=TABLE(FDTAB,LOGT.K,0,6,0.5)  LOGTEN DECAY FRACTION
N      LOGFD=0
T     FDTAB=0/-0.03/-0.11/-0.33/-1.00/-1.80/-2.17/-2.51/-2.80/-3.28/
X     -3.84/-4.0/-4.0   LOGTEN DECAY FRACTION TABLE   REVISED 6/28/77
A     LOGT.K=LOGN(TIME.K)/2.303            LOGTEN TIME (YEARS)
N      LOGT=0
A     FDX.K=EXP(2.303*LOGFDX.K)              RN DECAY FRACTION
N      FDX=1.0
A     LOGFDX.K=TABLE(FDXTAB,LOGT.K,0,6,0.5)  LOGTEN DECAY FRACTION
N      LOGFDX=0
T     FDXTAB=0/-0.12/-0.29/-0.91/-0.80/-1.12/
X    -1.48/-1.83/-2.18/-2.56/-3.22/-3.22/-3.22 LOGTEN DECAY FRACTION TABLE
C     ELP=1.3E8  DYNE/SQCM  EFFECTIVE LOAD PRESSURE
T     EWTAB=1.15E19,7.04E18,4.47E18,2.81E18,1.78E18,1.26E18,
X     8.91E17,6.61E17,5.31E17,3.80E17,3.02E17
*     SIMPLE HEAT SECTOR
R     HINR1.KL=0.094*FD.K
N     HINR1=0
R     HINR2.KL=0.188*FD.K
N     HINR2=0
R     HINR3.KL=0.047*FD.K
N     HINR3=0
R     HINRX.KL=0.094*FDX.K
N     HINRX=0
R     SHLR1.KL=12.8*(HZ.K-4.0)/1.32E5*2.273E-4
N     SHLR1=0
R     SHLR2.KL=25.0*(H8.K-4.0)/1.32E5*2.273E-4
N     SHLR2=0
C     DSHF1=5000
C     DSHF2=1000
C     DSHF3=200
L     H1.K=H1.J+DT*(HINR1.JK-HOUTR1.JK)
N     H1=5.2
R     HOUTR1.KL=DELAY3(HINR1.JK,DSHF1)
N     HOUTR1=0
A     HTEMP1.K=(H1.K-4.0)/0.2+20
S     SURFL1.K=1.0+1.32E5*(HOUTR1.JK/30)
L     H2.K=H2.J+DT*(HINR1.JK-HOUTR2.JK)
N     H2=5.2
R     HOUTR2.KL=DELAY3(HINR1.JK,DSHF2)
N     HOUTR2=0
A     HTEMP2.K=(H2.K-4.0)/0.2+20
S     SURFL2.K=1.0+1.32E5*(HOUTR2.JK/30)
L     H3.K=H3.J+DT*(HINR1.JK-HOUTR3.JK)
N     H3=5.2
R     HOUTR3.KL=DELAY3(HINR1.JK,DSHF3)
N     HOUTR3=0
A     HTEMP3.K=(H3.K-4.0)/0.2+20
S     SURFL3.K=1.0+1.32E5*(HOUTR3.JK/30)
L     H4.K=H4.J+DT*(HINR2.JK-HOUTR4.JK)
N     H4=5.2
R     HOUTR4.KL=DELAY3(HINR2.JK,DSHF1)
N     HOUTR4=0
A     HTEMP4.K=(H4.K-4.0)/0.2+20
S     SURFL4.K=1.0+1.32E5*(HOUTR4.JK/30)
L     H5.K=H5.J+DT*(HINR3.JK-HOUTR5.JK)
N     H5=5.2
R     HOUTR5.KL=DELAY3(HINR3.JK,DSHF1)
N     HOUTR5=0
A     HTEMP5.K=(H5.K-4.0)/0.2+20
S     SURFL5.K=1.0+1.32E5*(HOUTR5.JK/30)
L     H6.K=H6.J+DT*(HINR1.JK-HOUTR6.JK)
N     H6=5.2
R     HOUTR6.KL=DELAY1(HINR1.JK,DSHF1)
N     HOUTR6=0
A     HTEMP6.K=(H6.K-4.0)/0.2+20
S     SURFL6.K=1.0+1.32E5*(HOUTR6.JK/30)
L     H7.K=H7.J+DT*(HINR1.JK-HOUTR7.JK)
N     H7=5.2
R     HOUTR7.KL=DELAY3(SHLR1.JK,DSHF1)
N     HOUTR7=0
A     HTEMP7.K=(H7.K-4.0)/0.2+20
S     SURFL7.K=1.0+1.32E5*(HOUTR7.JK/30)
```

TABLE 2A.5 (Cont)

```
R     HOUTR5.KL=DELAY3(HINR3.JK,DSHF1)
N     HOUTR5=0
A     MTEMP5.K=(H5.K-4.0)/0.2+20
S     SURFL5.K=1.0+1.32ES*(HOUTR5.JK/30)
L     H6.K=H6.J+DT*(HINR1.JK-HOUTR6.JK)
N     H6=5.2
R     HOUTR6.KL=DELAY1(HINR1.JK,DSHF1)
N     HOUTR6=0
A     MTEMP6.K=(H6.K-4.0)/0.2+20
S     SURFL6.K=1.0+1.32ES*(HOUTR6.JK/30)
L     H7.K=H7.J+DT*(HINR1.JK-HOUTR7.JK)
N     H7=5.2
R     HOUTR7.KL=DELAY3(SHLR1.JK,DSHF1)
N     HOUTR7=0
A     MTEMP7.K=(H7.K-4.0)/0.2+20
S     SURFL7.K=1.0+1.32ES*(HOUTR7.JK/30)
L     H8.K=H8.J+DT*(HINR1.JK-HOUTR8.JK)
N     H8=5.2
R     HOUTR8.KL=DELAY3(SHLR2.JK,DSHF1)
N     HOUTR8=0
A     MTEMP8.K=(H8.K-4.0)/0.2+20
S     SURFL8.K=1.0+1.32ES*(HOUTR8.JK/30)
L     H9.K=H9.J+DT*(HINR1.JK-HOUTR9.JK)
N     H9=5.2
R     HOUTR9.KL=DELAY1(SHLR1.JK,DSHF3)
N     HOUTR9=0
A     MTEMP9.K=(H9.K-4.0)/0.2+20
S     SURFL9.K=1.0+1.32ES*(HOUTR9.JK/30)
C     UEC=0.9
L     TE1.K=TE1.J+DT*(TER1.JK)
N     TE1=0
R     TER1.KL=UEC*(HINR1.JK-HOUTR1.JK)/0.2
L     TE2.K=TE2.J+DT*(TER2.JK)
N     TE2=0
R     TER2.KL=UEC*(HINR1.JK-HOUTR2.JK)/0.2
L     TE3.K=TE3.J+DT*(TER3.JK)
N     TE3=0
R     TER3.KL=UEC*(HINR1.JK-HOUTR3.JK)/0.2
L     TE4.K=TE4.J+DT*(TER4.JK)
N     TE4=0
R     TER4.KL=UEC*(HINR2.JK-HOUTR4.JK)/0.2
L     TE5.K=TE5.J+DT*(TER5.JK)
N     TE5=0
R     TER5.KL=UEC*(HINR3.JK-HOUTR5.JK)/0.2
L     TE6.K=TE6.J+DT*(TER6.JK)
N     TE6=0
R     TER6.KL=UEC*(HINR1.JK-HOUTR6.JK)/0.2
L     TE7.K=TE7.J+DT*(TER7.JK)
N     TE7=0
R     TER7.KL=UEC*(HINR1.JK-HOUTR7.JK)/0.2
L     TE8.K=TE8.J+DT*(TER8.JK)
N     TE8=0
R     TER8.KL=UEC*(HINR1.JK-HOUTR8.JK)/0.2
L     TE9.K=TE9.J+DT*(TER9.JK)
N     TE9=0
R     TER9.KL=UEC*(HINR1.JK-HOUTR9.JK)/0.2
A     EVISC1.K=TABLE(EVTAB,BFT1.K,0,250,25)
A     BFT1.K=32+2*(MTEMP1.K-26)
A     EVISC2.K=TABLE(EVTAB,BFT2.K,0,250,25)
A     BFT2.K=32+2*(MTEMP2.K-26)
A     EVISC3.K=TABLE(EVTAB,BFT3.K,0,250,25)
A     BFT3.K=32+2*(MTEMP3.K-26)
A     EVISC4.K=TABLE(EVTAB,BFT4.K,0,250,25)
A     BFT4.K=32+2*(MTEMP4.K-26)
A     EVISC5.K=TABLE(EVTAB,BFT5.K,0,250,25)
A     BFT5.K=32+2*(MTEMP5.K-26)
A     EVISC6.K=TABLE(EVTAB,BFT6.K,0,250,25)
A     BFT6.K=32+2*(MTEMP6.K-26)
A     EVISC7.K=TABLE(EVTAB,BFT7.K,0,250,25)
A     BFT7.K=32+2*(MTEMP7.K-26)
A     EVISC8.K=TABLE(EVTAB,BFT8.K,0,250,25)
A     BFT8.K=32+2*(MTEMP8.K-26)
A     EVISC9.K=TABLE(EVTAB,BFT9.K,0,250,25)
A     BFT9.K=32+2*(MTEMP9.K-26)
C     SIMPLE HEAT AND COMPACTION SECTORS WITH SOLUTIONING CONNECTION
A     NECSC1.K=TE1.K-CLSC1.K
N     NECSC1=0
L     CLSC1.K=CLSC1.J-LPVSC1.J
N     CLSC1=0
L     LPVSC1.K=LPVSC1.J+DT*LPVRC1.JK
N     LPVSC1=60
R     LPVRC1.KL=LPVSC1.K*EXP(-2.303*ELP*3.3E7*DT/EVISC1.K)/DT-LPVSC1.K/DT
A     HCLSC1.K=60+ACLSC1.K
```

TABLE 2A.5 (Cont)

```
A      BFT9.K=1/2*(HILHP9.K-20)
NOTE   SIMPLE HEAT AND COMPACTION SECTORS WITH SOLUTIONING BY CONNECTION
A      NECSC1.K=TE1.K-CLSC1.K
N      NECSC1=0
L      CLSC1.K=MCLSC1.J-LPVSC1.J
N      CLSC1=0
L      LPVSC1.K=LPVSC1.J+DT*LPVRC1.JK
N      LPVSC1=60
R      LPVRC1.KL=LPVSC1.K*EXP(-2.303*ELP*3.0E7*DT/EVISC1.K)/DT-LPVSC1.K/DT
A      MCLSC1.K=60+ACLSC1.K
A      ACLSC1.K=SOC1.K/7.9E10
L      SOC1.K=SOC1.J+DT*(ORSC1.JK)   SOL OPEN BY CONV
N      SOC1=1
R      ORSC1.KL=1.0E8*MAX(NECSC1.K,-NECSC1.K)
A      SCOC1.K=2.0*EXP(LNVFC1.K)
A      LNVFC1.K=0.33*LOGN(SOC1.K)-0.46
A      NECSC2.K=TE2.K-CLSC2.K
N      NECSC2=0
L      CLSC2.K=MCLSC2.J-LPVSC2.J
N      CLSC2=0
L      LPVSC2.K=LPVSC2.J+DT*LPVRC2.JK
N      LPVSC2=60
R      LPVRC2.KL=LPVSC2.K*EXP(-2.303*ELP*3.0E7*DT/EVISC2.K)/DT-LPVSC2.K/DT
A      MCLSC2.K=60+ACLSC2.K
A      ACLSC2.K=SOC2.K/7.9E10
L      SOC2.K=SOC2.J+DT*(ORSC2.JK)   SOL OPEN BY CONV
N      SOC2=1
R      ORSC2.KL=1.0E8*MAX(NECSC2.K,-NECSC2.K)
A      SCOC2.K=2.0*EXP(LNVFC2.K)
A      LNVFC2.K=0.33*LOGN(SOC2.K)-0.46
A      NECSC3.K=TE3.K-CLSC3.K
N      NECSC3=0
L      CLSC3.K=MCLSC3.J-LPVSC3.J
N      CLSC3=0
L      LPVSC3.K=LPVSC3.J+DT*LPVRC3.JK
N      LPVSC3=60
R      LPVRC3.KL=LPVSC3.K*EXP(-2.303*ELP*3.0E7*DT/EVISC3.K)/DT-LPVSC3.K/DT
A      MCLSC3.K=60+ACLSC3.K
A      ACLSC3.K=SOC3.K/7.9E10
L      SOC3.K=SOC3.J+DT*(ORSC3.JK)   SOL OPEN BY CONV
N      SOC3=1
R      ORSC3.KL=1.0E8*MAX(NECSC3.K,-NECSC3.K)
A      SCOC3.K=2.0*EXP(LNVFC3.K)
A      LNVFC3.K=0.33*LOGN(SOC3.K)-0.46
A      NECSC4.K=TE4.K-CLSC4.K
N      NECSC4=0
L      CLSC4.K=MCLSC4.J-LPVSC4.J
N      CLSC4=0
L      LPVSC4.K=LPVSC4.J+DT*LPVRC4.JK
N      LPVSC4=60
R      LPVRC4.KL=LPVSC4.K*EXP(-2.303*ELP*3.0E7*DT/EVISC4.K)/DT-LPVSC4.K/DT
A      MCLSC4.K=60+ACLSC4.K
A      ACLSC4.K=SOC4.K/7.9E10
L      SOC4.K=SOC4.J+DT*(ORSC4.JK)   SOL OPEN BY CONV
N      SOC4=1
R      ORSC4.KL=1.0E8*MAX(NECSC4.K,-NECSC4.K)
A      SCOC4.K=2.0*EXP(LNVFC4.K)
A      LNVFC4.K=0.33*LOGN(SOC4.K)-0.46
A      NECSC5.K=TE5.K-CLSC5.K
N      NECSC5=0
L      CLSC5.K=MCLSC5.J-LPVSC5.J
N      CLSC5=0
L      LPVSC5.K=LPVSC5.J+DT*LPVRC5.JK
N      LPVSC5=60
R      LPVRC5.KL=LPVSC5.K*EXP(-2.303*ELP*3.0E7*DT/EVISC5.K)/DT-LPVSC5.K/DT
A      MCLSC5.K=60+ACLSC5.K
A      ACLSC5.K=SOC5.K/7.9E10
L      SOC5.K=SOC5.J+DT*(ORSC5.JK)   SOL OPEN BY CONV
N      SOC5=1
R      ORSC5.KL=1.0E8*MAX(NECSC5.K,-NECSC5.K)
A      SCOC5.K=2.0*EXP(LNVFC5.K)
A      LNVFC5.K=0.33*LOGN(SOC5.K)-0.46
A      NECSC6.K=TE6.K-CLSC6.K
N      NECSC6=0
L      CLSC6.K=MCLSC6.J-LPVSC6.J
N      CLSC6=0
L      LPVSC6.K=LPVSC6.J+DT*LPVRC6.JK
N      LPVSC6=60
R      LPVRC6.KL=LPVSC6.K*EXP(-2.303*ELP*3.0E7*DT/EVISC6.K)/DT-LPVSC6.K/DT
A      MCLSC6.K=60+ACLSC6.K
A      ACLSC6.K=SOC6.K/7.9E10
L      SOC6.K=SOC6.J+DT*(ORSC6.JK)   SOL OPEN BY CONV
N      SOC6=1
R      ORSC6.KL=1.0E8*MAX(NECSC6.K,-NECSC6.K)
```

POOR ORIGINAL

TABLE 2A.5 (Cont)

```
A       MCLSC6.K=60+ACLSC6.K
A       ACLSC6.K=SOC6.K/7.9E10
L       SOC6.K=SOC6.J+DT*(ORSC6.JK)  SOL OPEN BY CONV
N       SOC6=1
R       ORSC6.KL=1.0E8*MAX(NECSC6.K,-NECSC6.K)
A       SCOC6.K=2.0*EXP(LNVFC6.K)
A       LNVFC6.K=0.33*LOGN(SOC6.K)-0.46
A       NECSC7.K=TE7.K-CLSC7.K
N       NECSC7=0
L       CLSC7.K=MCLSC7.J-LPVSC7.J
N       CLSC7=0
L       LPVSC7.K=LPVSC7.J+DT*LPVRC7.JK
N       LPVSC7=60
R       LPVRC7.KL=LPVSC7.K*EXP(-2.303*ELP*3.0E7*DT/EVISC7.K)/DT-LPVSC7.K/DT
A       MCLSC7.K=60+ACLSC7.K
A       ACLSC7.K=SOC7.K/7.9E10
L       SOC7.K=SOC7.J+DT*(ORSC7.JK)  SOL OPEN BY CONV
N       SOC7=1
R       ORSC7.KL=1.0E8*MAX(NECSC7.K,-NECSC7.K)
A       SCOC7.K=2.0*EXP(LNVFC7.K)
A       LNVFC7.K=0.33*LOGN(SOC7.K)-0.46
A       NECSC8.K=TE8.K-CLSC8.K
N       NECSC8=0
L       CLSC8.K=MCLSC8.J-LPVSC8.J
N       CLSC8=0
L       LPVSC8.K=LPVSC8.J+DT*LPVRC8.JK
N       LPVSC8=60
R       LPVRC8.KL=LPVSC8.K*EXP(-2.303*ELP*3.0E7*DT/EVISC8.K)/DT-LPVSC8.K/DT
A       MCLSC8.K=60+ACLSC8.K
A       ACLSC8.K=SOC8.K/7.9E10
L       SOC8.K=SOC8.J+DT*(ORSC8.JK)  SOL OPEN BY CONV
N       SOC8=1
R       ORSC8.KL=1.0E8*MAX(NECSC8.K,-NECSC8.K)
A       SCOC8.K=2.0*EXP(LNVFC8.K)
A       LNVFC8.K=0.33*LOGN(SOC8.K)-0.46
A       NECSC9.K=TE9.K-CLSC9.K
N       NECSC9=0
L       CLSC9.K=MCLSC9.J-LPVSC9.J
N       CLSC9=0
L       LPVSC9.K=LPVSC9.J+DT*LPVRC9.JK
N       LPVSC9=60
R       LPVRC9.KL=LPVSC9.K*EXP(-2.303*ELP*3.0E7*DT/EVISC9.K)/DT-LPVSC9.K/DT
A       MCLSC9.K=60+ACLSC9.K
A       ACLSC9.K=SOC9.K/7.9E10
L       SOC9.K=SOC9.J+DT*(ORSC9.JK)  SOL OPEN BY CONV
N       SOC9=1
R       ORSC9.KL=1.0E8*MAX(NECSC9.K,-NECSC9.K)
A       SCOC9.K=2.0*EXP(LNVFC9.K)
A       LNVFC9.K=0.33*LOGN(SOC9.K)-0.46
NOTE
PLOT    NECSC1=1,NECSC2=2,NECSC3=3,NECSC4=4,NECSC5=5,NECSC6=6,
X       NECSC7=7,NECSC8=8,NECSC9=9(-1.0E4,0)
PLOT    SCOC1=1,SCOC2=2,SCOC3=3,SCOC4=4,SCOC5=5,SCOC6=6,
X       SCOC7=7,SCOC8=8,SCOC9=9(0,2.0E4)
PRINT NECSC1,NECSC2,NECSC3,NECSC4,NECSC5,NECSC6,NECSC7,NECSC8,NECSC9
PRINT CLSC1,CLSC2,CLSC3,CLSC4,CLSC5,CLSC6,CLSC7,CLSC8,CLSC9
PRINT LPVSC1,LPVSC2,LPVSC3,LPVSC4,LPVSC5,LPVSC6,LPVSC7,LPVSC8,LPVSC9
PRINT LPVRC1,LPVRC2,LPVRC3,LPVRC4,LPVRC5,LPVRC6,LPVRC7,LPVRC8,LPVRC9
PRINT ACLSC1,ACLSC2,ACLSC3,ACLSC4,ACLSC5,ACLSC6,ACLSC7,ACLSC8,ACLSC9
PRINT SOC1,SOC2,SOC3,SOC4,SOC5,SOC6,SOC7,SOC8,SOC9
PRINT ORSC1,ORSC2,ORSC3,ORSC4,ORSC5,ORSC6,ORSC7,ORSC8,ORSC9
PRINT SCOC1,SCOC2,SCOC3,SCOC4,SCOC5,SCOC6,SCOC7,SCOC8,SCOC9
SPEC    DT=10/LENGTH=1.0E4/PLTPER=100/PRTPER=100
RUN     SOLUTION ING BY CONVECTION
END
X
L1
L2
L3
```

TABLE 2A.6

Equation Listing for Plots in Figure 2A.12 (a - b)

```
DYNAMO IIF, VERSION 3.C2


*     TEST OF CHANGE IN ORSCUA CONSTANT
N     TIME=1.   YEAR
L     H.K=H.J+DT*(HINR.JK-HOUTR.JK)      HEAT ABOVE ZERO TEMP CAL/GM
N     H=5.2  CAL/GM                      INITIAL HEAT HTEMP=26C
R     HINR.KL=0.094*FD.K                 RN POWER  CAL/GM/YR
N     HINR=0
A     FD.K=EXP(2.303*LOGFD.K)            RN DECAY FRACTION
N      FD=1.0
A     LOGFD.K=TABLE(FDTAB,LOGT.K,0,6,0.5)  LOGTEN DECAY FRACTION
N      LOGFD=0
T     FDTAB=(/-0.03/-0.11/-0.33/-1.00/-1.90/-2.17/-2.51/-2.80/-3.29/
X     -3.94/-4.0/-4.0   LOGTEN DECAY FRACTION TABLE   REVISED 6/20/77
A     LOGT.K=LOGN(TIME.K)/2.303          LOGTEN TIME (YEARS)
N      LOGT=C
R     SHLR.KL=25.0*(H.K-4.)/1.32E5-2.273E-4  STEADY HEAT LOSS RATE CAL/GM/YR
N      SHLR=C
R     HOUTR.KL=DELAY3(SHLR.JK,DSHF)      HEAT LOSS RATE CAL/GM/YR
N      HOUTR=0
C     DSHF=1000 YRS    DELAY SURFACE HEAT FLUX
A     HTEMP.K=(H.K-4.0)/5.2+26.          MEAN TEMP FOR STEMP=26C
N      HTEMP=26
S     SURFLX.K=1.0+1.32E5*(HOUTR.JK/30)   SURFACE FLUX MICROCAL/SQCM/SEC
N      SURFL)=1.0
L     TE.K=TE.J+DT*(TER.JK)              LINEAR THERMAL EXPANSION (CM)
N     TE=0                        INITIAL THERMAL REFERENCE STATE
R     TER.KL=UEC*(HINR.JK-HOUTR.JK)/0.2    LINEAR TE RATE (CM/YR)
N      TER=0.423
C     UEC=0.0 CM/DEGC          UNIT EXPANSION CONSTANT
S      DTEMP.K=DT*(HINR.JK-HOUTR.JK)/0.2     DELTA TEMP JK DEGC
N     DTEMP=0
A     BFTEMP.K=32+2*(HTEMP.K-26)   APPROX BACKFILL TEMP DEGC
N     BFTEMP=32
C     BMCL=60 CM  BACKFILL MAX COMPACT LENGTH
A     SA.K=RA  SOLUTIONING AREA (SQ.CM)
C     RA=7.9E10  REPOSITORY AREA (SQ.CM.)
C     ELP=1.7E8  DYNE/SQCM  EFFECTIVE LOAD PRESSURE
A     EVISC.K=TABLE(EVTAB,BFTEMP.K,0,250,25)  EFFECTIVE VISC (POISE)
T     EVTAB=1.15E19,7.08E18,4.47E18,2.81E18,1.78E18,1.26E18,
X     8.91E17,6.61E17,5.01E17,3.80E17,3.02E17
R     ORSCU1.KL=1.0E8*MAX(NEC1.K,-NEC1.K)
A     NEC1.K=TE.K-CL1.K
N     NEC1=0
L     CL1.K=BCL1.J-LPV1.J
N     CL1=C
L     LPV1.K=LPV1.J+DT*(LPVCR1.JK)
N     LPV1=60
R     LPVCR1.KL=LPV1.K*EXP(-2.303*ELP*3.0E7*DT/EVISC.K)/DT-LPV1.K/DT
A     BCL1.K=BMCL*ACLS1.K
A     ACLS1.K=SO1.K/SA.K
N     SO1=1  CL.CM.
L      SO1.K=SO1.J+DT*(IFGE(0,ORSCU1.JK,ACLS1.JK,1.0E4)
A     SCCIA1.K=2.0*EXP(LNVFU1.K)
A     LNVFU1.K=0.33*LOGN(SO1.K)-0.46
R     ORSCU2.KL=1.0E7*MAX(NEC2.K,-NEC2.K)
A     NEC2.K=TE.K-CL2.K
N     NEC2=0
L     CL2.K=BCL2.J-LPV2.J
N     CL2=0
L     LPV2.K=LPV2.J+DT*(LPVCR2.JK)
N     LPV2=60
R     LPVCR2.KL=LPV2.K*EXP(-2.303*ELP*3.0E7*DT/EVISC.K)/DT-LPV2.K/DT
A     BCL2.K=BMCL+ACLS2.K
A     ACLS2.K=SO2.K/SA.K
N     SO2=1  CL.CM.
L      SO2.K=SO2.J+DT*(IFGE(0,ORSCU2.JK,ACLS2.JK,1.0E4)
A     SCCIA2.K=2.0*EXP(LNVFU2.K)
A     LNVFU2.K=0.33*LOGN(SO2.K)-0.46
R     ORSCU3.KL=1.0E8*MAX(NEC3.K,-NEC3.K)
A     NEC3.K=TE.K-CL3.K
N     NEC3=0
L     CL3.K=BCL3.J-LPV3.J
N     CL3=C
L     LPV3.K=LPV3.J+DT*(LPVCR3.JK)
N     LPV3=60
R     LPVCR3.KL=LPV3.K*EXP(-2.303*ELP*3.0E7*DT/EVISC.K)/DT-LPV3.K/DT
A     BCL3.K=BMCL+ACLS3.K
A     ACLS3.K=SO3.K/SA.K
N     SO3=1  CL.CM
```

TABLE 2A.6 (Cont)

```
N     NEC1=0
L     CL1.K=PCL1.J-LPV1.J
N     CL1=0
L     LPV1.K=LPV1.J+DT*(LPVCR1.JK)
N     LPV1=60
R     LPVCR1.KL=LPV1.K*EXP(-2.303*ELP*3.0E7*DT/EVISC.K)/DT-LPV1.K/DT
A     PCL1.K=BMCL+ACLS1.K
A     ACLS1.K=SO1.K/SA.K
N     SO1=1  CU.CM.
L      SO1.K=SO1.J+DT*(IFGE(0.,ORSCU1.JK,ACLS1.JK,1.0E4)
A     SCCIA1.K=2.0*EXP(LNVFU1.K)
A     LNVFU1.K=0.33*LOGN(SO1.K)-0.46
R     ORSCU2.KL=1.0E7*MAX(NEC2.K,-NEC2.K)
A     NEC2.K=TE.K-CL2.K
N     NEC2=0
L     CL2.K=PCL2.J-LPV2.J
N     CL2=0
L     LPV2.K=LPV2.J+DT*(LPVCR2.JK)
N     LPV2=60
R     LPVCR2.KL=LPV2.K*EXP(-2.303*ELP*3.0E7*DT/EVISC.K)/DT-LPV2.K/DT
A     PCL2.K=BMCL+ACLS2.K
A     ACLS2.K=SO2.K/SA.K
N     SO2=1  CU.CM.
L      SO2.K=SO2.J+DT*(IFGE(0.,ORSCU2.JK,ACLS2.JK,1.0E4)
A     SCCIA2.K=2.0*EXP(LNVFU2.K)
A     LNVFU2.K=0.33*LOGN(SO2.K)-0.46
R     ORSCU3.KL=1.0E6*MAX(NEC3.K,-NEC3.K)
A     NEC3.K=TE.K-CL3.K
N     NEC3=0
L     CL3.K=PCL3.J-LPV3.J
N     CL3=0
L     LPV3.K=LPV3.J+DT*(LPVCR3.JK)
N     LPV3=60
R     LPVCR3.KL=LPV3.K*EXP(-2.303*ELP*3.0E7*DT/EVISC.K)/DT-LPV3.K/DT
A     PCL3.K=BMCL+ACLS3.K
A     ACLS3.K=SO3.K/SA.K
N     SO3=1  CU.CM
L      SO3.K=SO3.J+DT*(IFGE(0.,ORSCU3.JK,ACLS3.JK,1.0E4)
A     SCCIA3.K=2.0*EXP(LNVFU3.K)
A     LNVFU3.K=0.33*LOGN(SO3.K)-0.46
R     ORSCU4.KL=1.0E5*MAX(NEC4.K,-NEC4.K)
A     NEC4.K=TE.K-CL4.K
N     NEC4=0
L     CL4.K=PCL4.J-LPV4.J
N     CL4=0
L     LPV4.K=LPV4.J+DT*(LPVCR4.JK)
N     LPV4=60
R     LPVCR4.KL=LPV4.K*EXP(-2.303*ELP*3.0E7*DT/EVISC.K)/DT-LPV4.K/DT
A     PCL4.K=BMCL+ACLS4.K
A     ACLS4.K=SO4.K/SA.K
N     SO4=1  CU.CM
L     SO4.K=SO4.J+DT*(ORSCU4.JK)
A     SCCIA4.K=2.0*EXP(LNVFU4.K)
A     LNVFU4.K=0.33*LOGN(SO4.K)-0.46
R     ORSCU5.KL=1.0E4*MAX(NEC5.K,-NEC5.K)
A     NEC5.K=TE.K-CL5.K
N     NEC5=0
L     CL5.K=PCL5.J-LPV5.J
N     CL5=0
L     LPV5.K=LPV5.J+DT*(LPVCR5.JK)
N     LPV5=60
R     LPVCR5.KL=LPV5.K*EXP(-2.303*ELP*3.0E7*DT/EVISC.K)/DT-LPV5.K/DT
A     PCL5.K=BMCL+ACLS5.K
A     ACLS5.K=SO5.K/SA.K
N     SO5=1  CU.CM
L     SO5.K=SO5.J+DT*(ORSCU5.JK)
A     SCCIA5.K=2.0*EXP(LNVFU5.K)
A     LNVFU5.K=0.33*LOGN(SO5.K)-0.46
NOTE
PRINT ACLS1,ACLS2,ACLS3,ACLS4,ACLS5,SCCIA1,SCCIA2,SCCIA3,SCCIA4,SCCIA5,
X     HTEMP,SURFLX
PLOT  ACLS1=1,ACLS2=2,ACLS3=3(0,1.0E4)/ACLS4=4/ACLS5=5/
X     HTEMP=H/SURFLX=F
PLOT  SCCIA1=6,SCCIA2=7,SCCIA3=8,SCCIA4=9,SCCIA5=0(0,2.0E4)/
X     HTEMP=H/SURFLX=F
SPEC  DT=100/LENGTH=1.0E6/PLTPER=1.0E3/PRTPER=1.0E3
RUN   VARYING THE ORSCUA CONSTANT
SEC -
HP
```

```
     1625  OF  2672  DATA LIST WORDS
      153  OF   200  SYMBOL TABLE VARIABLES
```

403 137

TABLE 2A.7

Equation Listing for Plots in Figure 2A.13

```
DYNAMO IIF, VERSION 3.02


*     BMCL=20, SO MIN AND ORSCU1=1.0E9...
N     TIME=1.   YEAR
L     H.K=H.J+DT*(HINR.JK-HOUTR.JK)        HEAT ABOVE ZERO TEMP CAL/GM
N     H=F.2  CAL/GM                        INITIAL HEAT HTEMP=260
R     HINR.KL=0.047*FD.K          1/4 POWER  CAL/GM/YR  1/2 ORIGINAL
N     HINR=0
A     FD.K=EXP(2.303*LOGFD.K)              RN DECAY FRACTION
N     FD=1.0
A     LOGFD.K=TABLE(FDTAB,LOGT.K,0,6,0.5)  LOGTEN DECAY FRACTION
N     LOGFD=0
T     FDTAB=0/-0.03/-0.11/-0.33/-1.00/-1.80/-2.17/-2.51/-2.80/-3.28/
X     -3.94/-4.0/-4.3   LOGTEN DECAY FRACTION TABLE   REVISED 6/20/77
A     LOGT.K=LOGN(TIME.K)/2.303            LOGTEN TIME (YEARS)
N     LOGT=0
R     SHLR.KL=25.0*(H.K-4.)/1.32E5-2.273E-4  STEADY HEAT LOSS RATE CAL/GM/YR
N     SHLR=0
R     HOUTR.KL=DELAY3(SHLR.JK,DSHF)        HEAT LOSS RATE CAL/GM/YR
N     HOUTR=0
C     DSHF=1000 YRS    DELAY SURFACE HEAT FLUX
A     MTEMP.K=(H.K-4.0)/3.2+25.            MEAN TEMP FOR STEMP=200
N     MTEMP=25
S     SURFLX.K=1.0+1.32E5*(HOUTR.JK/30)    SURFACE FLUX MICROCAL/SQCM/SEC
N     SURFLX=1.0
L     TE.K=TE.J+DT*(TER.JK)                LINEAR THERMAL EXPANSION (CM)
N     TE=0                        INITIAL THERMAL REFERENCE STATE
R     TER.KL=LEC*(HINR.JK-HOUTR.JK)/0.2    LINEAR TE RATE (CM/YR)
N     LEC=0.423
C     UEC=0.9 CM/DEGC              UNIT EXPANSION CONSTANT
S     DTEMP.K=DT*(HINR.JK-HOUTR.JK)/0.2    DELTA TEMP JK DEGC
N     DTEMP=0
A     DFTEMP.K=32+2*(MTEMP.K-25)   APPROX BACKFILL TEMP DEGC
N     DFTEMP=32
C     BMCL=20
A     SA.K=RR  SOLUTIONING AREA (SQ.CM)
C     RA=7.9E10  REPOSITORY AREA (SQ.CM.)
C     ELP=1.3E3  DYNE/SQCM  EFFECTIVE LOAD PRESSURE
A     EVISC.K=TABLE(EVTAB,DFTEMP.K,0,250,25)  EFFECTIVE VISC (POISE)
T     EVTAB=1.15E19,7.38E18,4.47E18,2.71E18,1.78E18,1.25E18,
X     8.81E17,6.61E17,5.01E17,3.80E17,3.02E17
R     ORSCU1.KL=1.0E9*MAX(NEC1.K,-NEC1.K)
A     NEC1.K=TF.K-CL1.K
N     NEC1=0
L     CL1.K=MCL1.J-LPV1.J
N     CL1=0
L     LPV1.K=LPV1.J+DT*(LPVCR1.JK)
N     LPV1=20
R     LPVCR1.KL=LPV1.K*EXP(-2.303*ELP*3.0E7*DT/EVISC.K)/DT-LPV1.K/DT
A     MCL1.K=BMCL+ACLS1.K
A     ACLS1.K=SO1.K/SA.K
N     SO1=1  CL.CM.
L     SO1.K=SO1.J+DT*(FIFGE(),ORSCU1.JK,ACLS1*JK,1.0E+4)
A     SCDIA1.K=2.0*EXP(LNVFU1.K)
A     LNVFU1.K=0.33*LOGN(SO1.K)-0.46
NOTE
PRINT HINR,HOUTR,SURFLX,TE,NEC1,DFTEMP,CL1,MCL1,SCDIA1,SO1,ORSCU1,ACLS1
PLOT  HINR=P/HOUTR=O/SURFLX=F/TE=E/NEC1=N/-1.0E+4,0/DFTEMP=T
X     CL1=C,MCL1=M(0,1.0E+4)/SCDIA1=D(0,2.0E+4)
SPEC  DT=1/LENGTH=1.0E+4/PLTPER=100/PRTPER=100
RUN   ORSCU1 CONSTANT BUT NOTHING ELSE
USER -
END
```

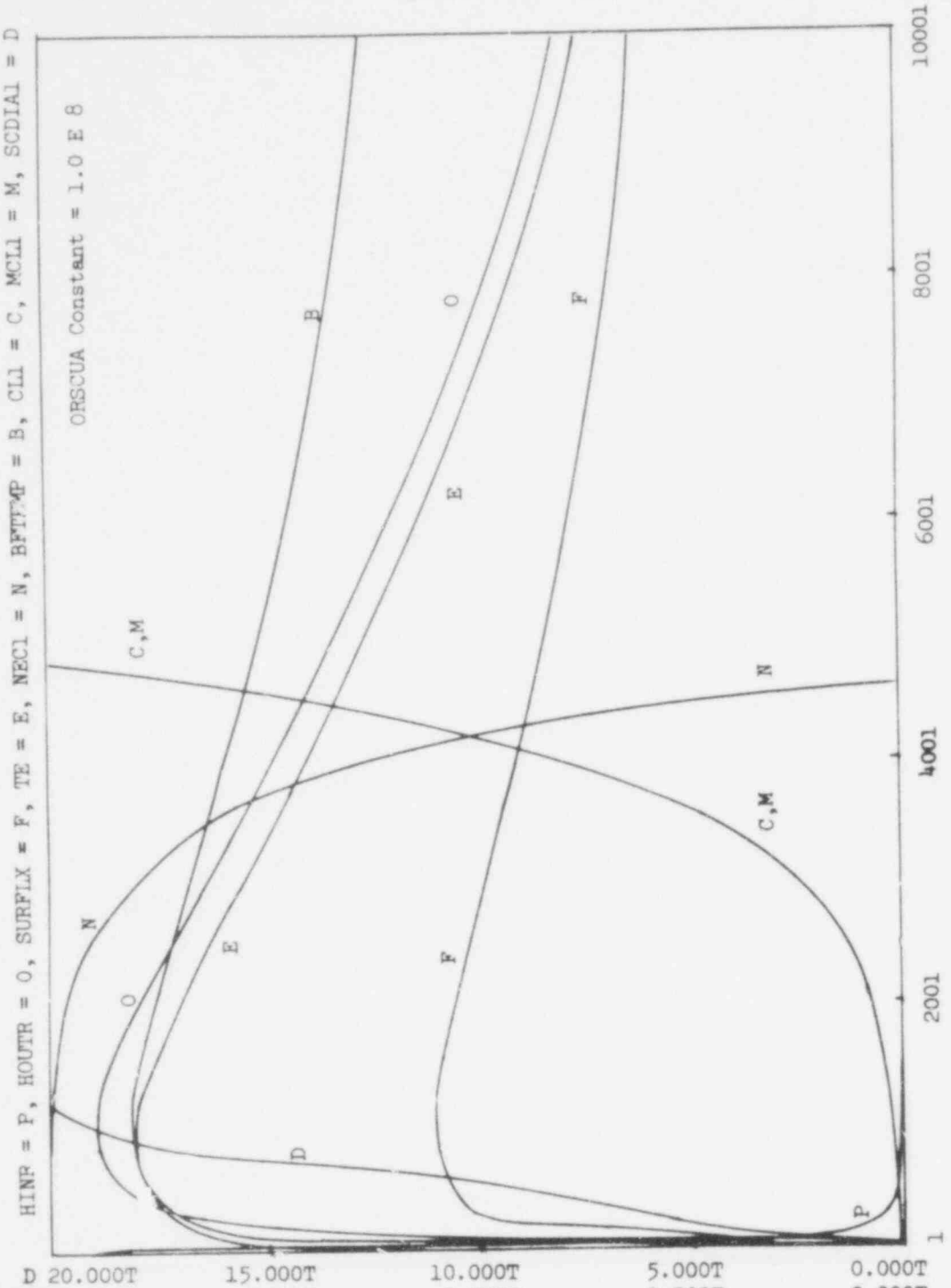

D	20.000T	15.000T	10.000T	5.000T	0.000T
CM	10.000T	7.500T	5.000T	2.500T	0.000T
B	80.000	60.000	40.000	20.000	0.000
N	0.000T	-2.500T	-5.000T	-7.500T	-10.000T
E	20.000	15.000	10.000	5.000	0.000
F	8.000	6.000	4.000	2.000	0.000
O	.800A	.600A	.400A	.200A	0.000A
P	100.000A	75.000A	50.000A	25.000A	0.000A

Units: See Table
T = 1.0 E 3, A = 1.0 E-3

Figure 2A.10. Simple Heat, Thermal Expansion, Compaction and Solution Sectors

403 139

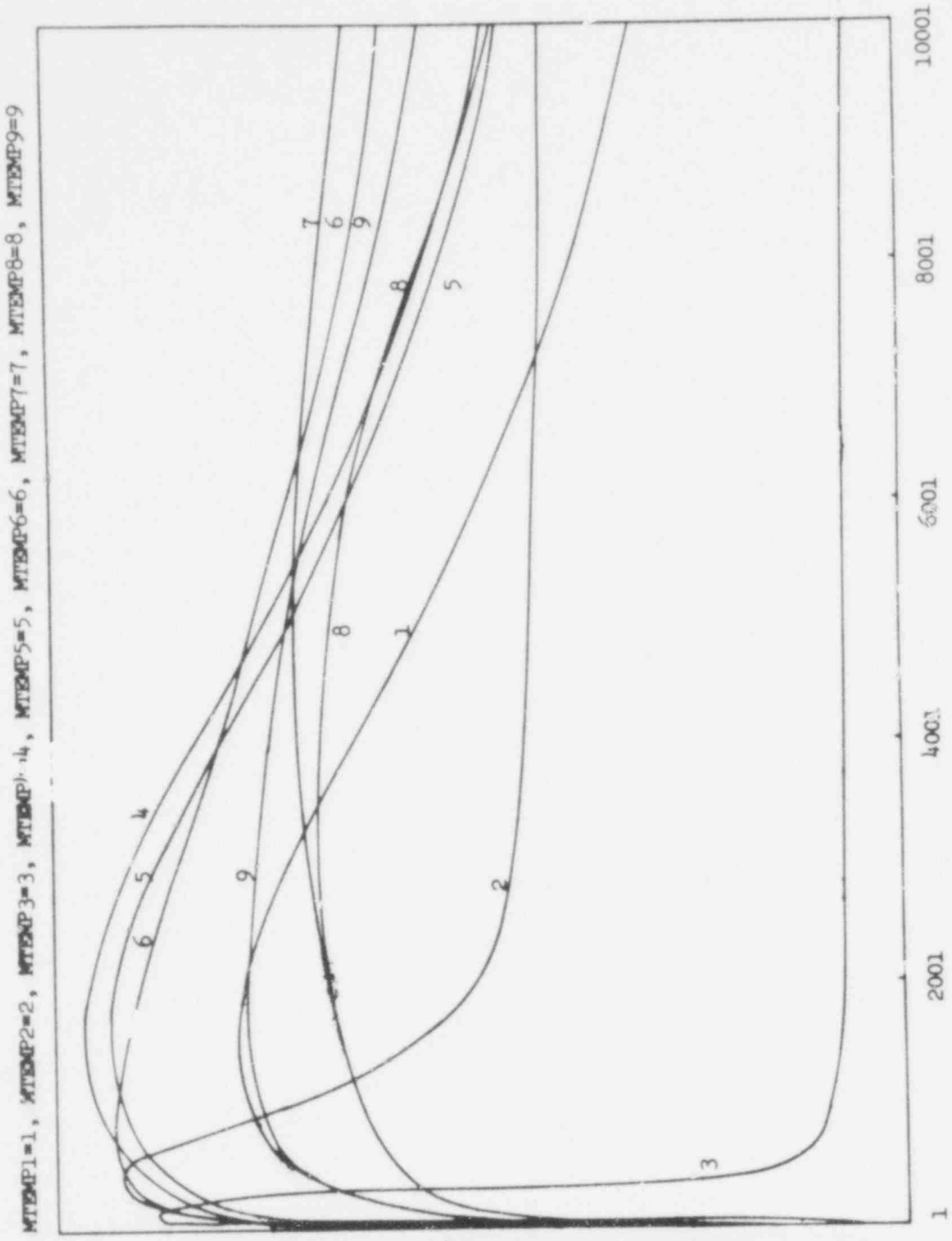

9	60.000	50.000	40.000	30.000	20.000
7,8	80.000	60.000	40.000	20.000	0.000
6	50.000	40.000	30.000	20.000	10.000
5	40.000	35.000	30.000	25.000	20.000
4	80.000	60.000	40.000	20.000	0.000
3	45.000	40.000	35.000	30.000	25.000
2	50.000	40.000	30.000	20.000	10.000
1	60.000	50.000	40.000	30.000	20.000

Units: Degrees Centigrade

Figure 2A.11a. Examples of Heat and Compaction Sectors

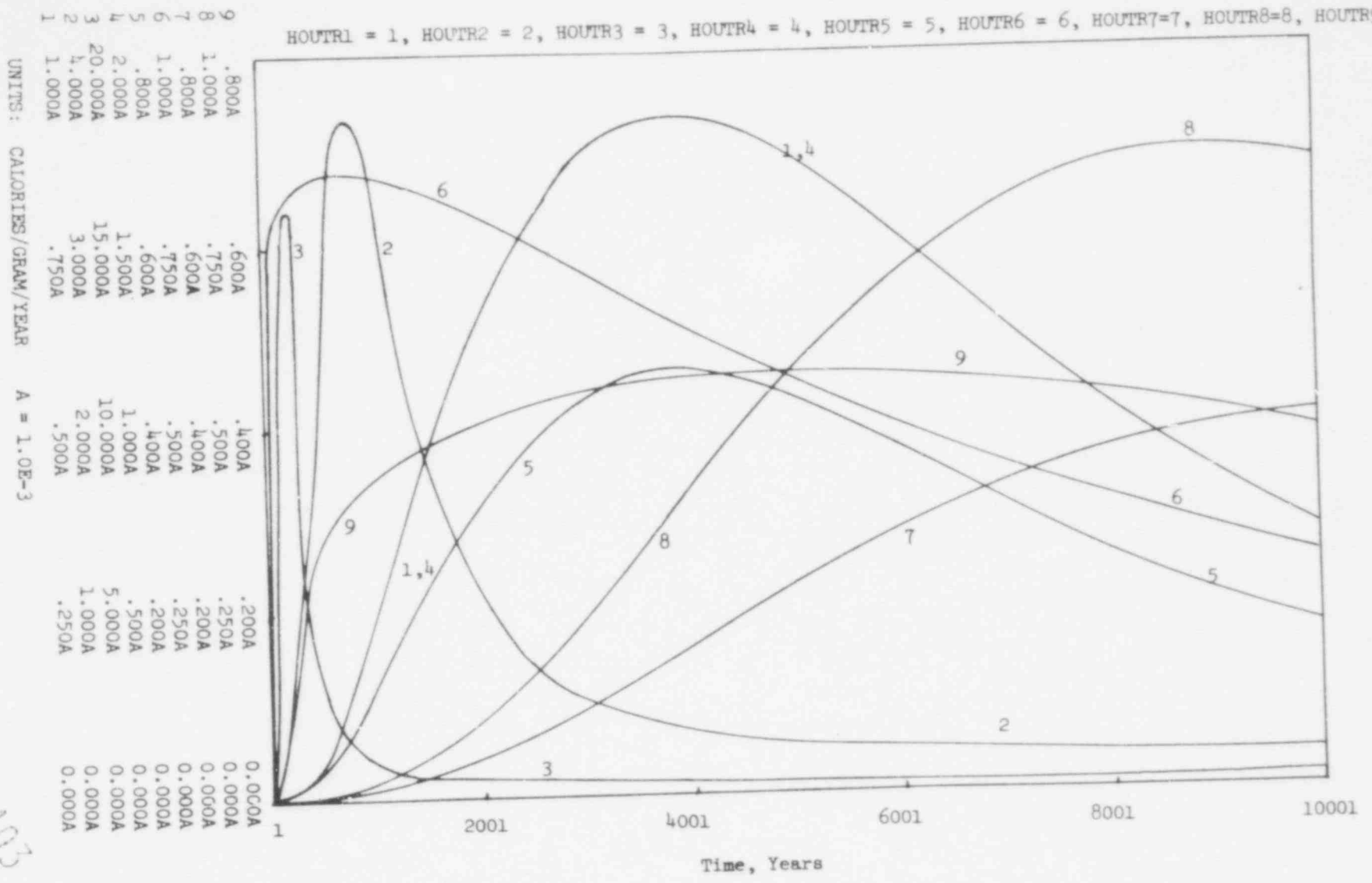

Figure 2A.11b. Examples of Heat and Compaction Sectors

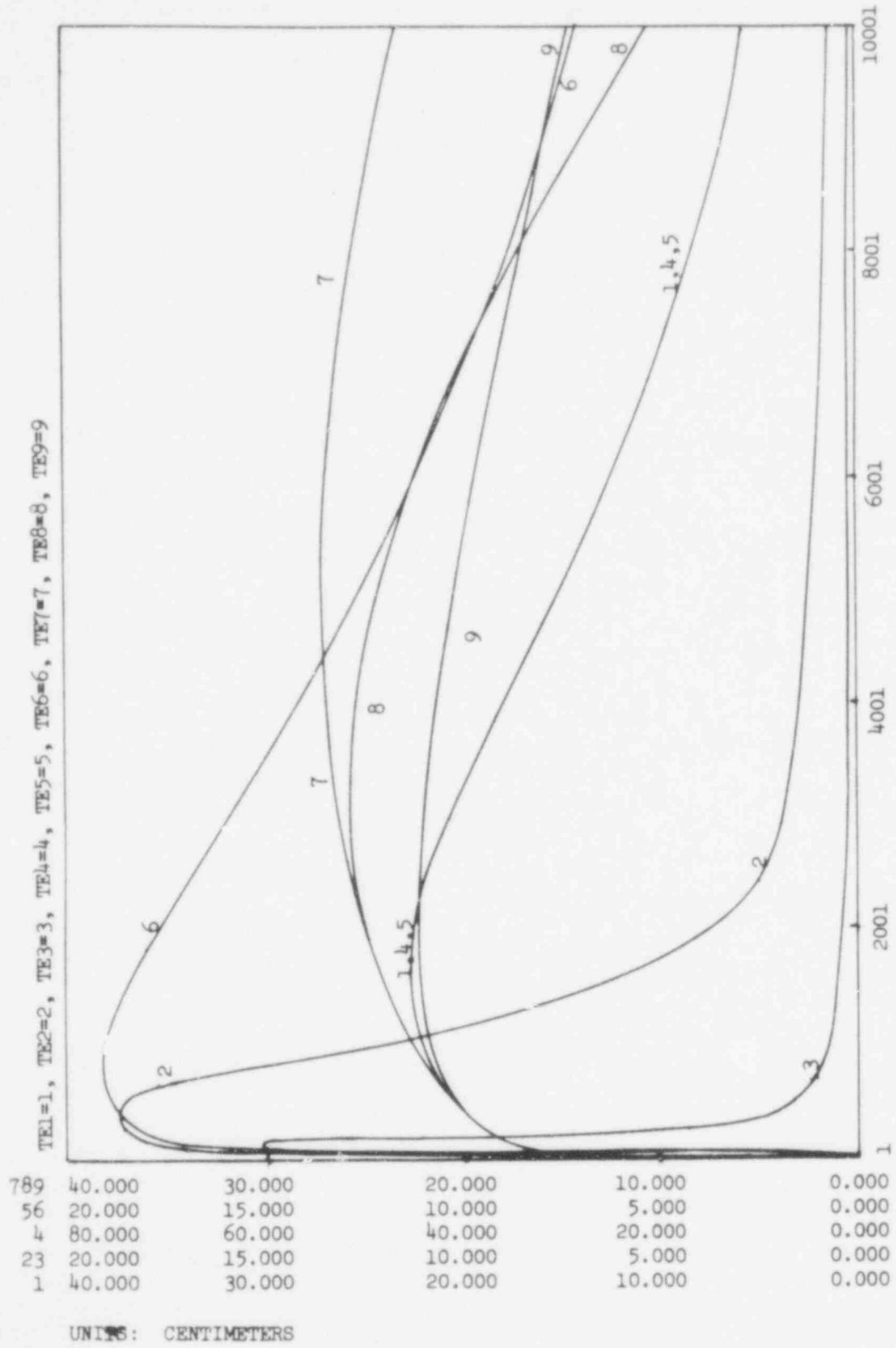

Figure 2A.11c. Examples of Heat and Compaction Sectors

403 142

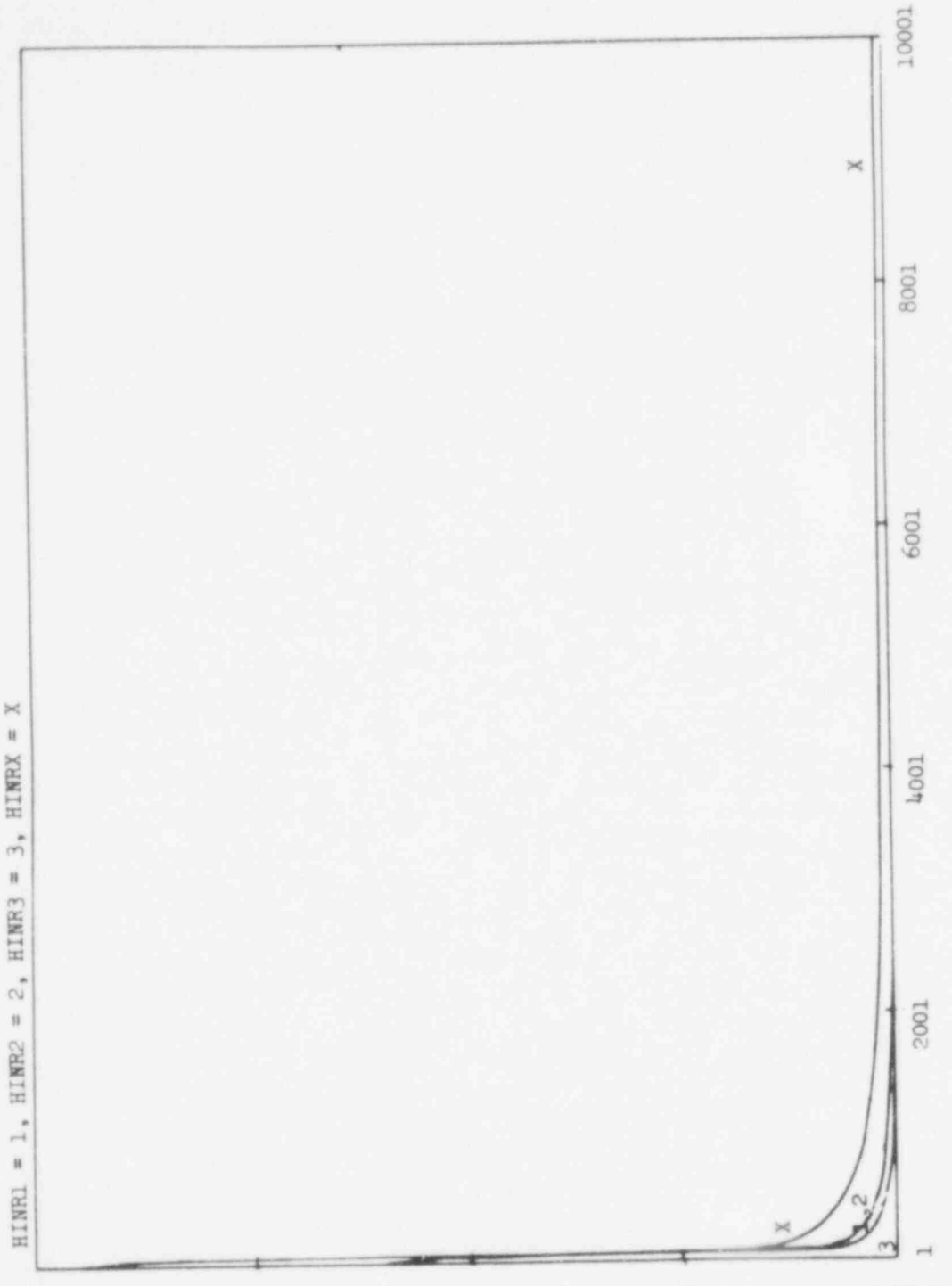

X	100.000A	75.000A	50.000A	25.000A	0.000A
3	80.000A	60.000A	40.000A	20.000A	0.000A
2	.200	.150	.100	.050	0.000
1	100.000A	75.000A	50.000A	25.000A	0.000A

UNITS: CALORIES/GRAM/YEAR
A = 1.0E-3

Figure 2A.11d. Examples of Heat and Compaction Sectors

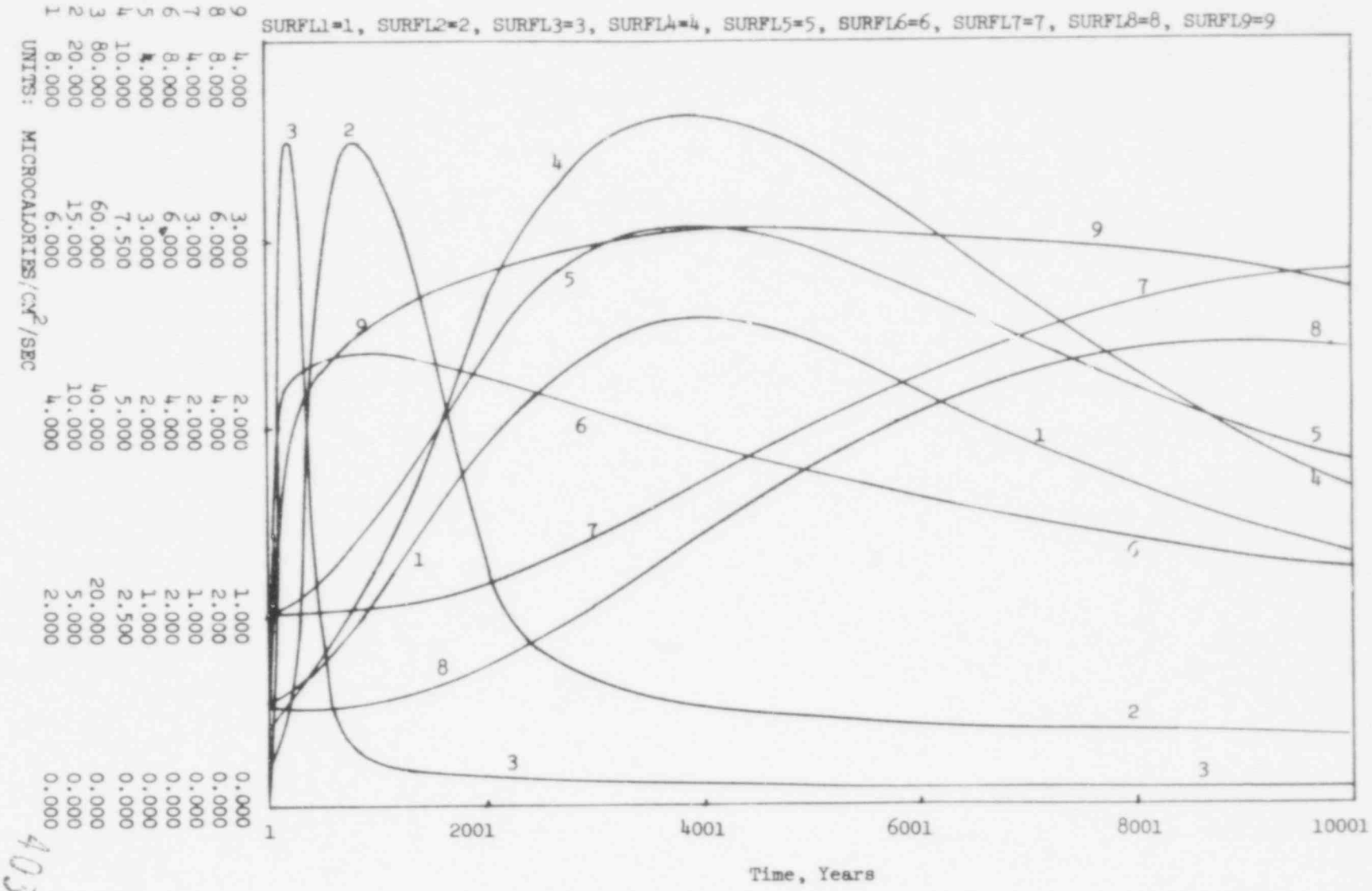

Figure 2A.11e. Examples of Heat and Compaction Sectors

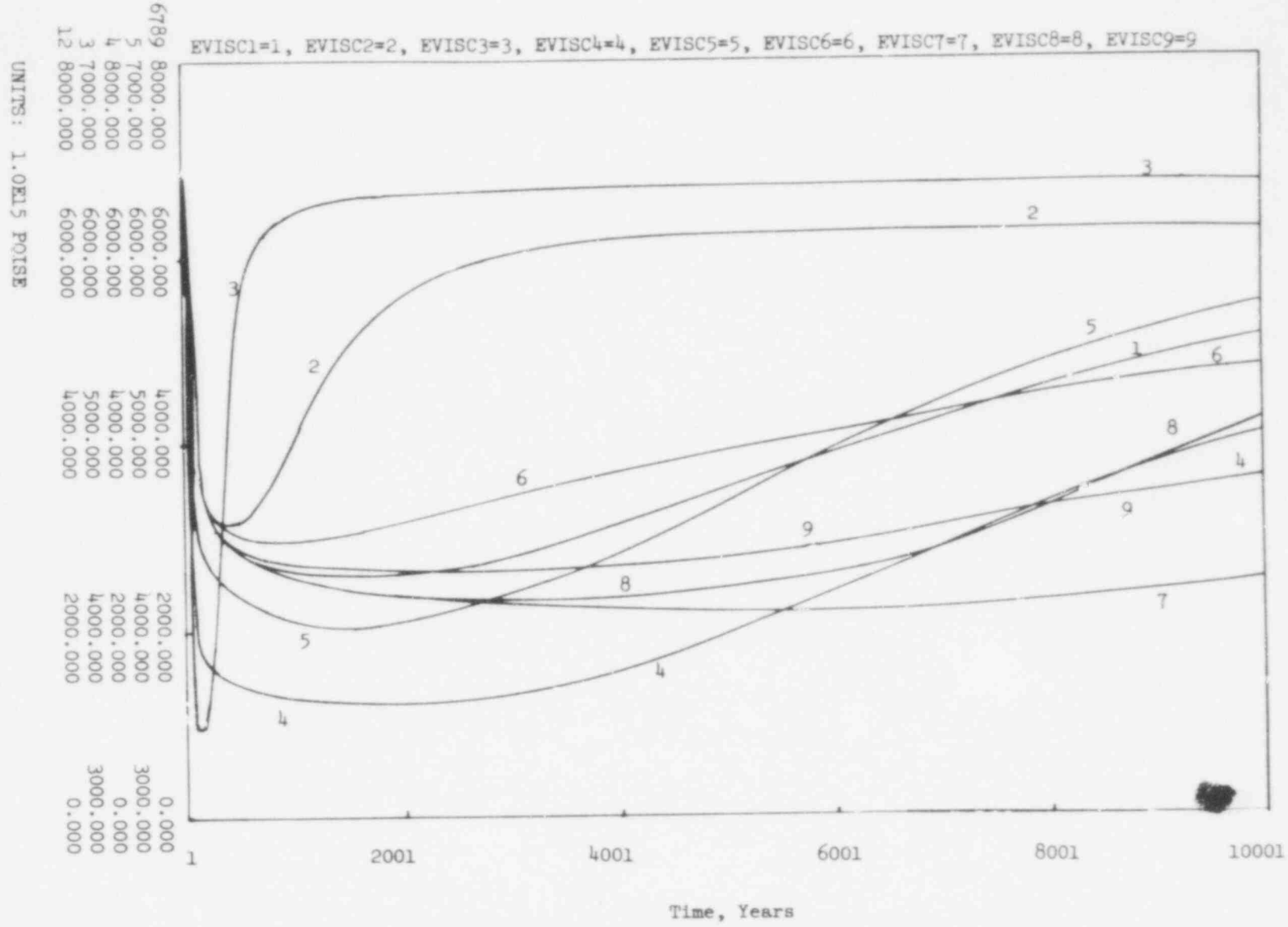

Figure 2A.11f. Examples of Heat and Compaction Sectors

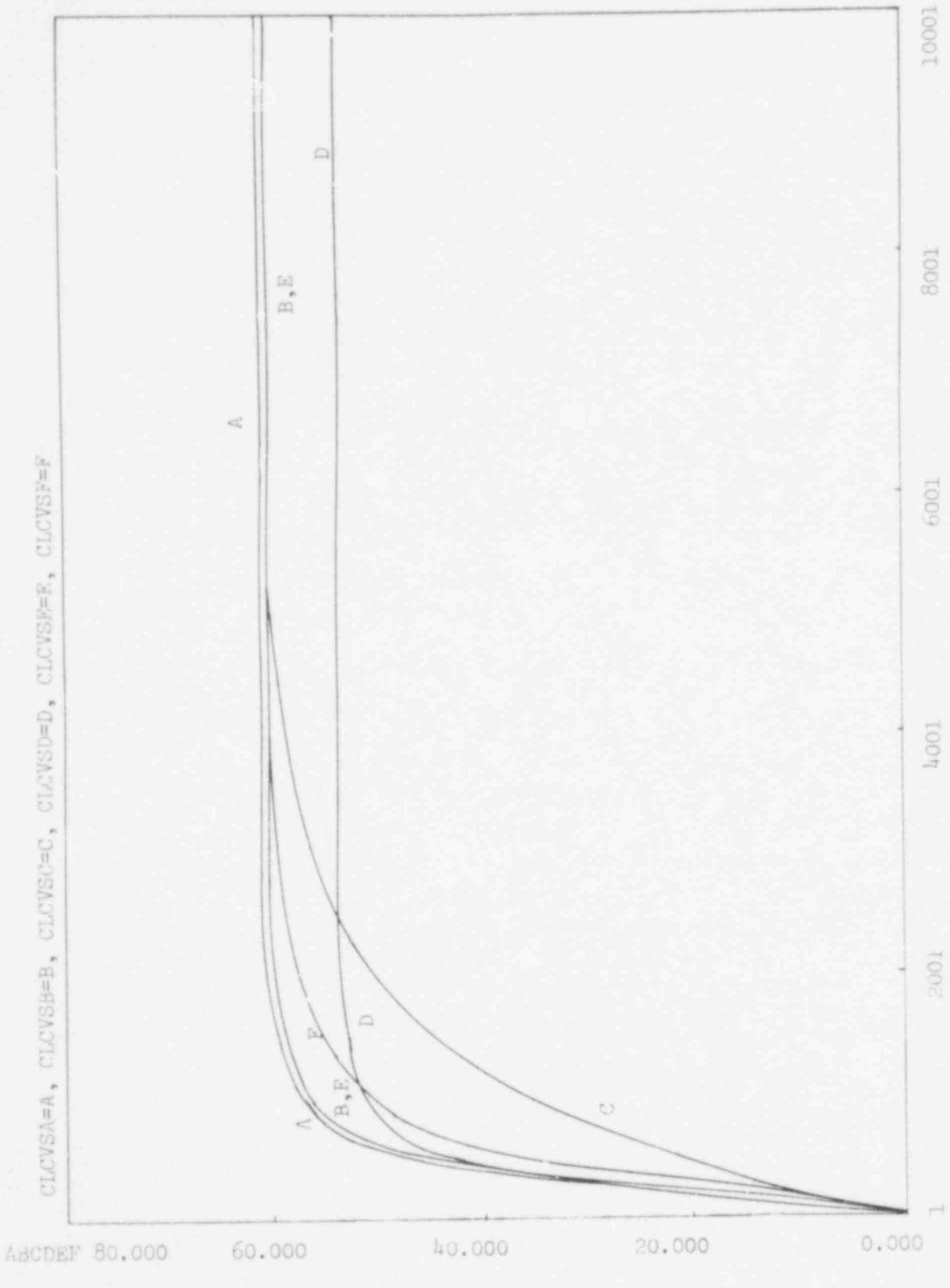

Figure 2A.11g. Examples of Heat and Compaction Sectors

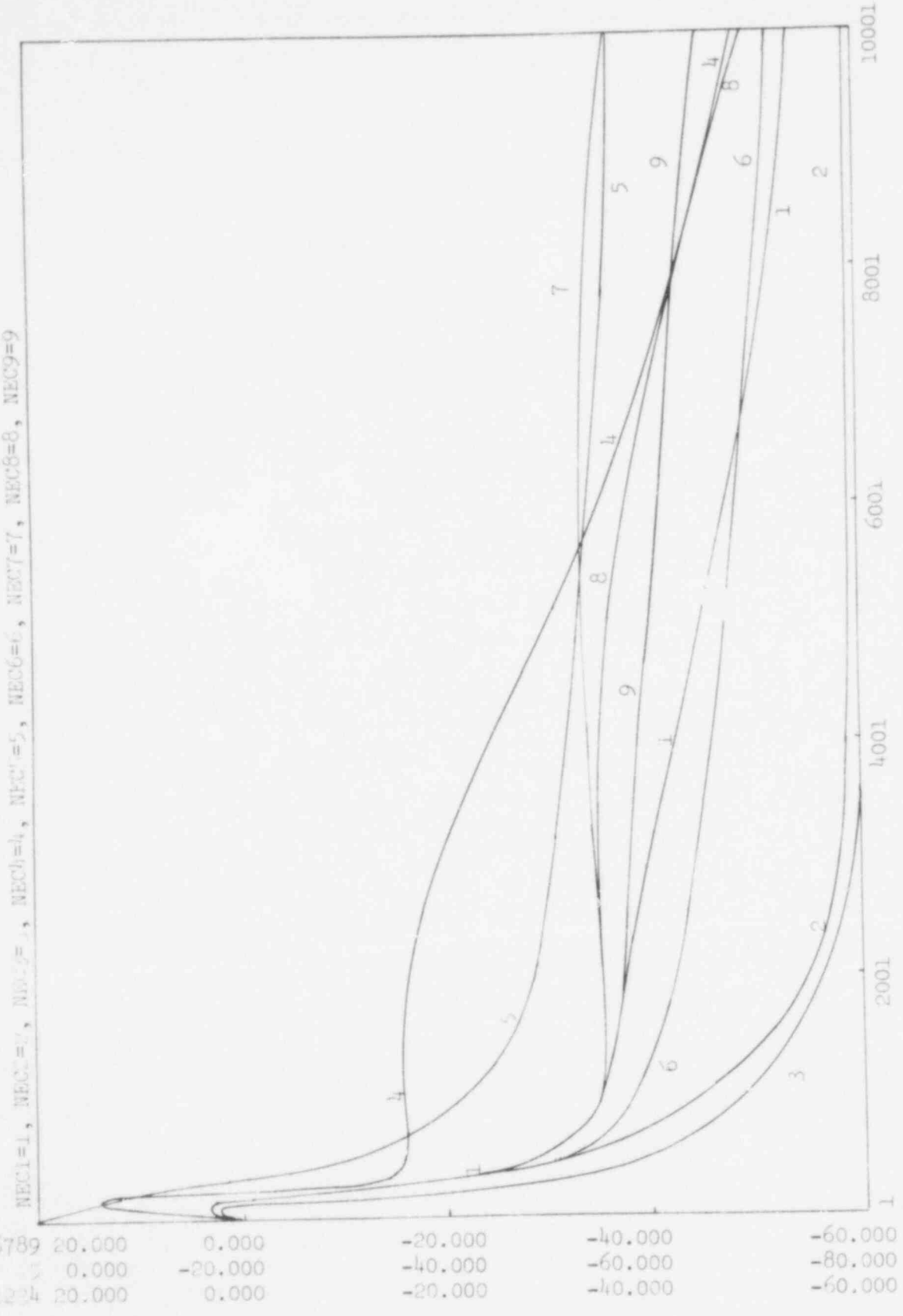

Figure 2A.11h. Examples of Heat and Compaction Sectors

403 147

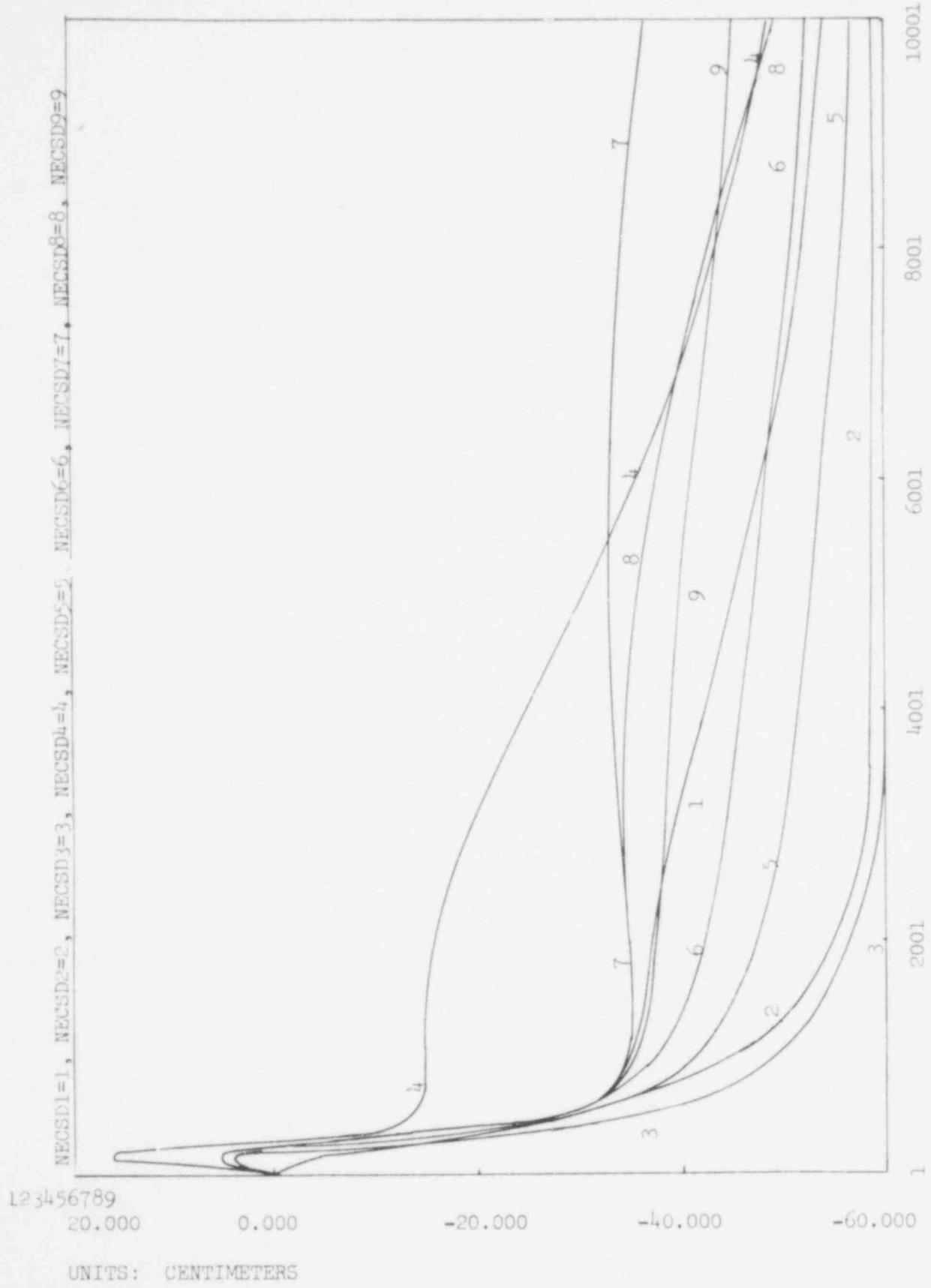

Figure 2A.11i. Solutioning by Diffusion

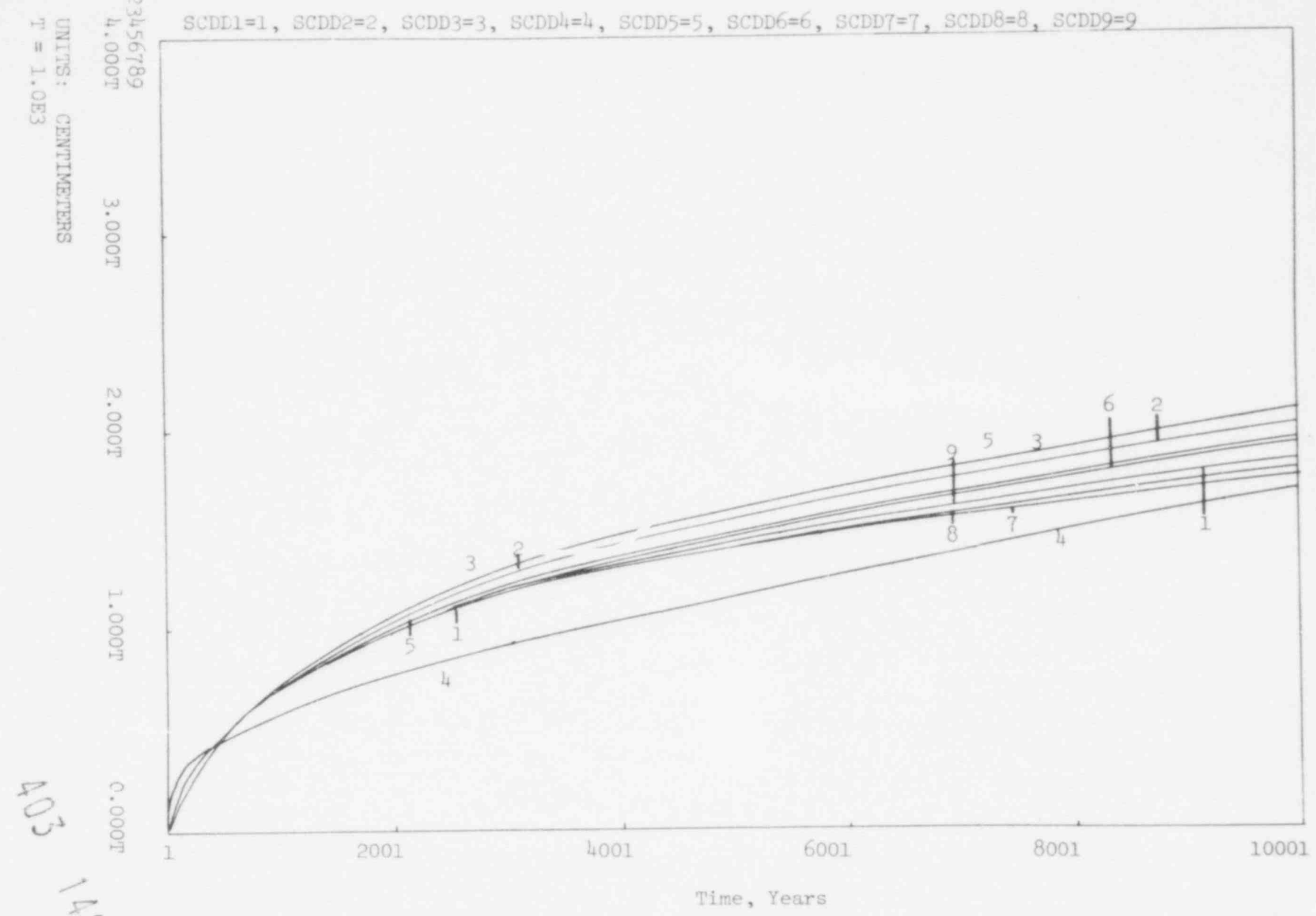

Figure 2A.11j. Solutioning by Diffusion

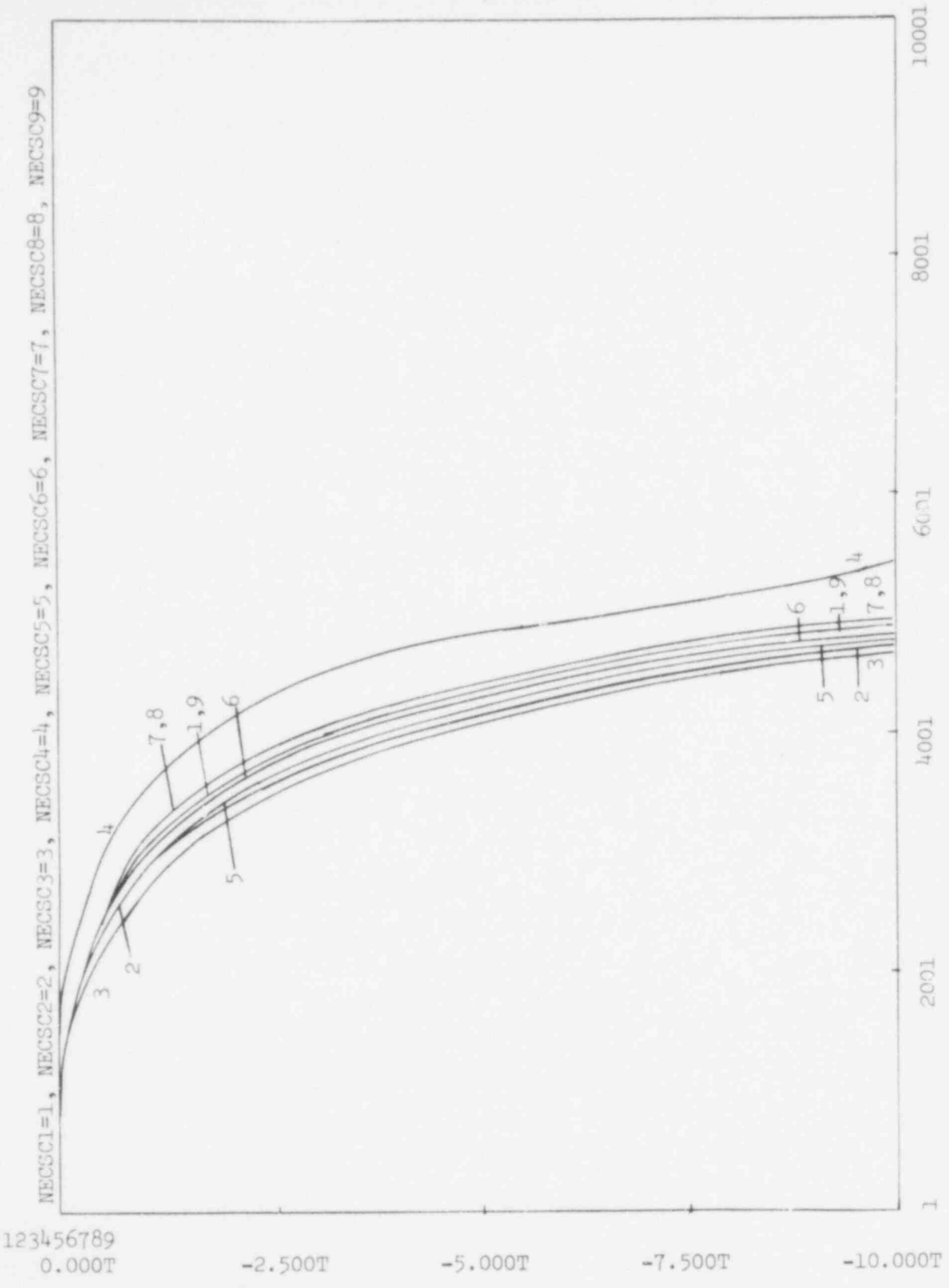

Figure 2A,11k. Solutioning by Convection

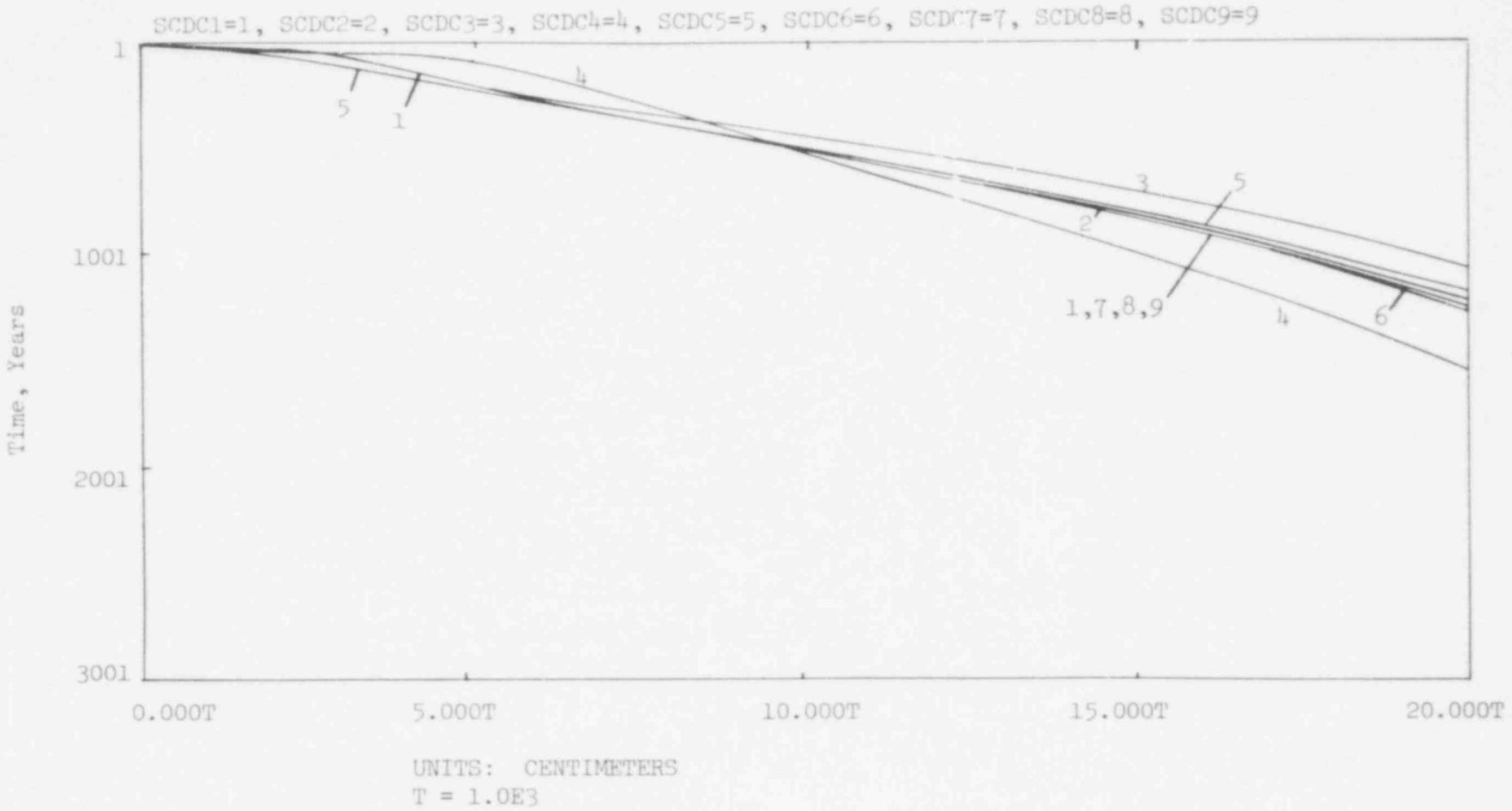

Figure 2A.11ℓ. Solutioning by Convection

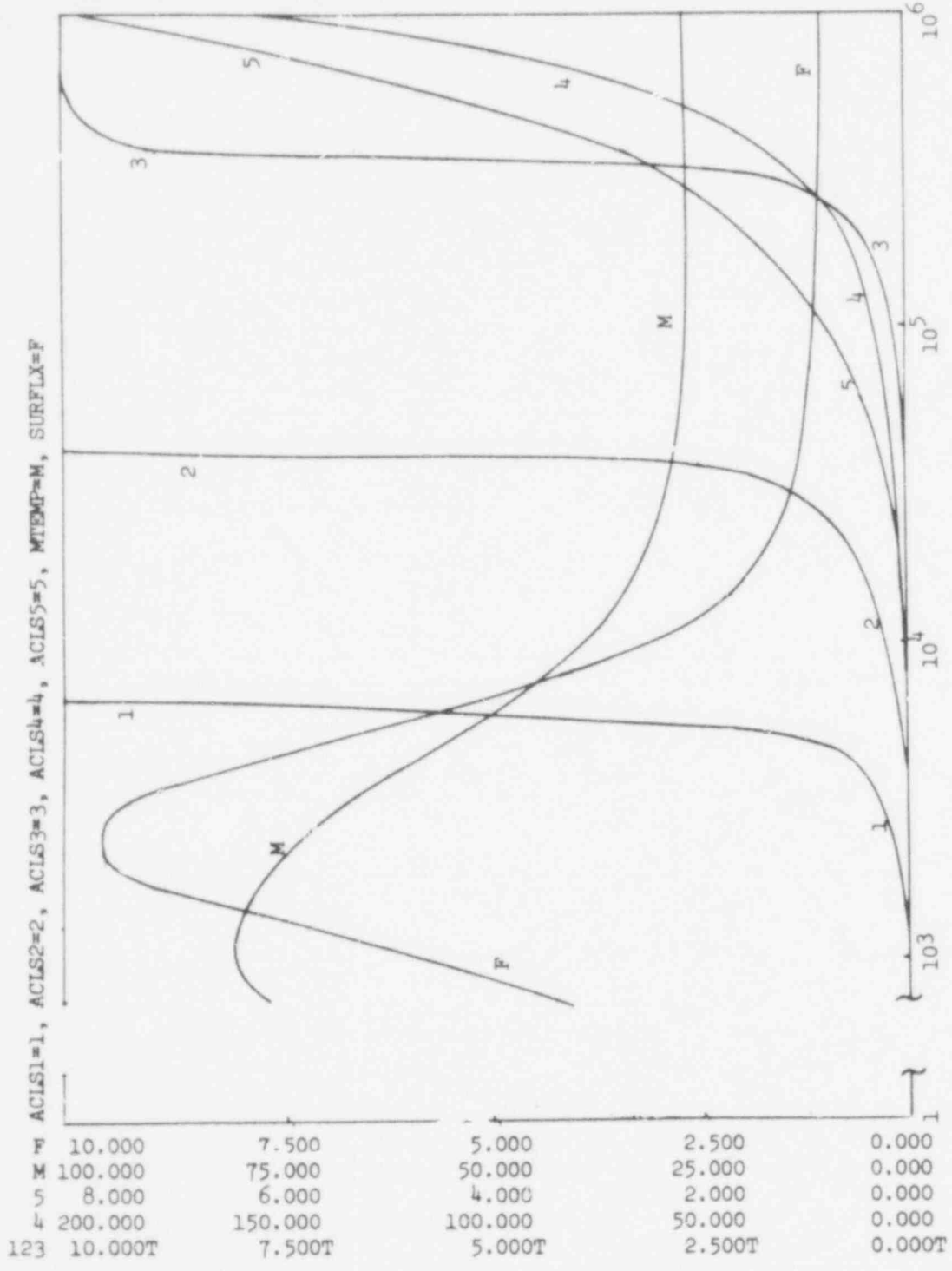

F	10.000	7.500	5.000	2.500	0.000
M	100.000	75.000	50.000	25.000	0.000
5	8.000	6.000	4.000	2.000	0.000
4	200.000	150.000	100.000	50.000	0.000
123	10.000T	7.500T	5.000T	2.500T	0.000T

UNITS: SEE TABLE 5.2.3
T = 1.0E3

Figure 2A.12a. Varying the ORSCUA Constant

403 152

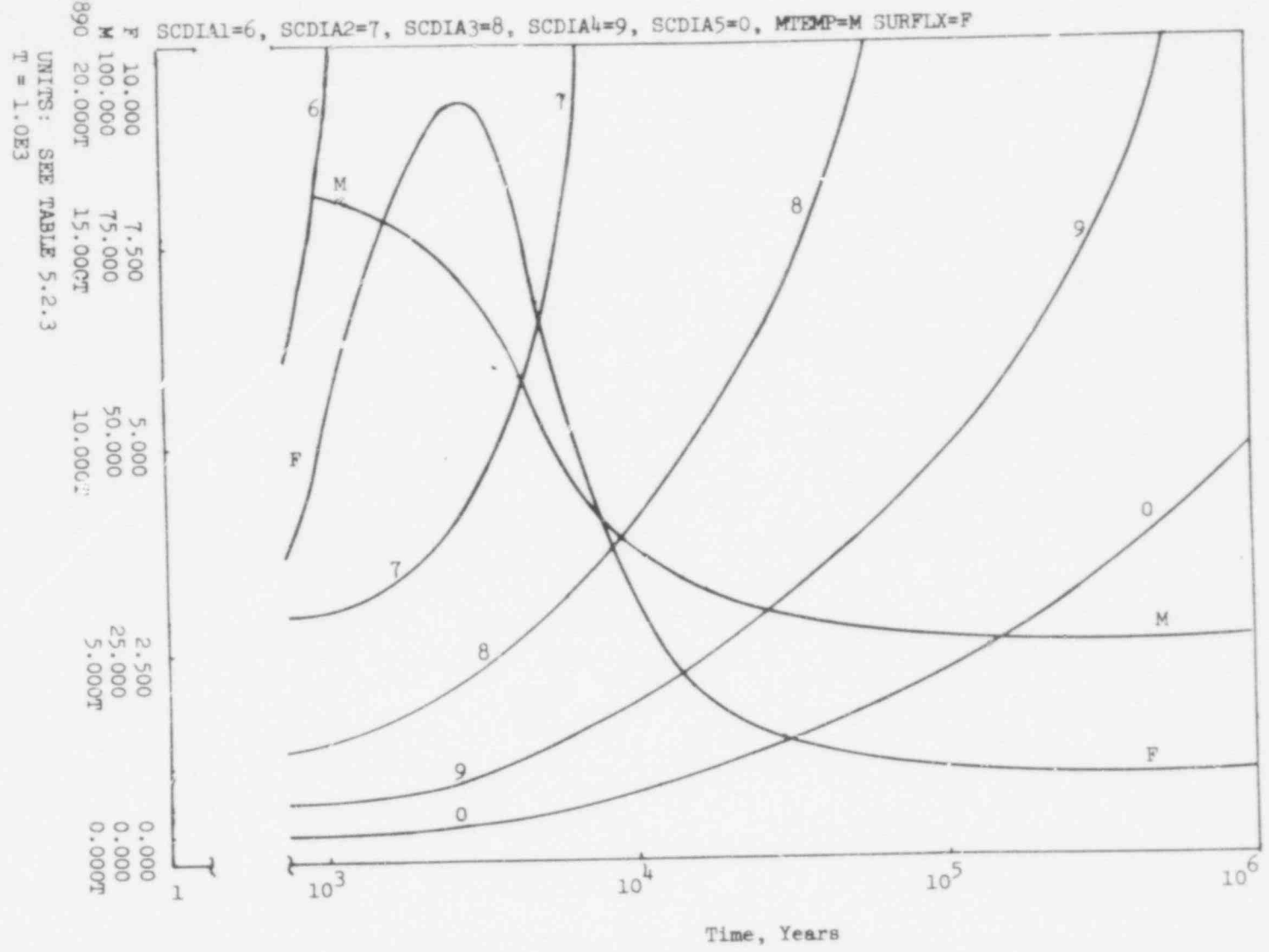

Figure 2A.12b. Varying the ORSCUA Constant

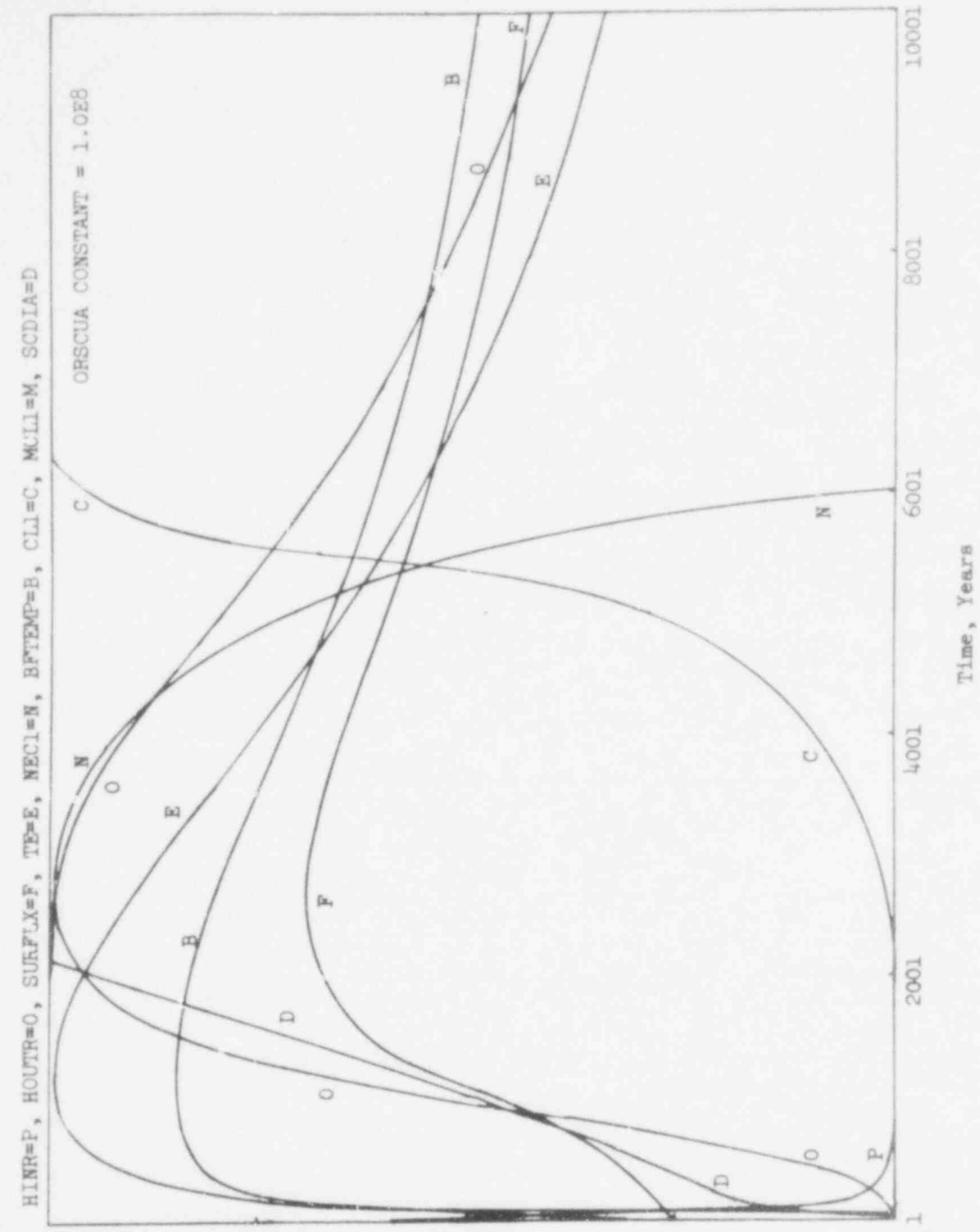

D	20.000T	15.000T	10.000T	5.000T	0.000T
CM	10.000T	7.500T	5.000T	2.500T	0.000T
B	60.000	50.000	40.000	30.000	20.000
N	0.000T	-2.500T	-5.000T	-7.500T	-10.000T
E	10.000	7.500	5.000	2.500	0.000
F	4.000	3.000	2.000	1.000	0.000
O	.400A	.300A	.200A	.100A	0.000A
P	80.000A	60.000A	40.000A	20.000A	0.000A

UNITS: SEE TABLE 5.3.2
T = 1.0E3
A = 1.0E-3

Figure 2A.13. Solutioning Feedback with Half of Original Thermal Load

References

Appendix 2A

2A.1 R. E. Barlow and H. E. Lambert, 1975, "Introduction to Fault Tree Analysis: in Reliability and Fault Tree Analysis; Theoretical and Applied Aspects of System Reliability and Safety Assessment," SIAM, Philadelphia, PA, p. 7-35.

2A.2 R. L. Bradshaw and W. E. McClain (eds.), 1971, Project Salt Vault: A Demonstration of the Disposal of High-Activity Solidified Wastes in Underground Salt Mines, ORNL-4555, 360 p.

2A.3 D. G. Brookins, 1976, "Shale as a Repository for Radioactive Waste: The Evidence from Oklo," Environmental Geology, Vol. 1, pp. 255-259.

2A.4 J. W. Forrester, 1961, Industrial Dynamics, Cambridge, Mass., M.I.T. Press, 464 p.

2A.5 J. W. Forrester, 1971, World Dynamics, Cambridge, Mass., Wright-Allen Press.

2A.6 I. J. Gruntfest, 1963, "Thermal Feedback in Liquid Flow; Plane Shear at Constant Stress," Trans. Soc. Rheology, Vol. 7, pp. 195-207.

2A.7 I. J. Gruntfest, 1968, The Role of Energy in Deformation, NASA Contractors Report CR-1039.

2A.8 H. C. Heard, 1976, "Comparison of the Flow Properties of Rocks at Crustal Conditions," Phil. Trans. Royl. Soc. Lond., A., Vol. 283, pp. 173-186.

2A.9 D. L. Meadows and D. H. Meadows, 1973, Toward Global Equilibrium: Collected Papers, Cambridge, Mass., Wright-Allen Press, 358 p.

2A.10 A. A. B. Pritsker, 1974, The GASP IV Simulation Language, New York, Wiley and Sons, 451 p.

2A.11 A. L. Pugh III, 1973, DYNAMO II User's Manual, 4th Edition Including DYNAMO II_F, Cambridge, Mass., M.I.T. Press, 92 p.

2A.12 H. R. Shaw, 1969, "Rheology of Basalt in the Melting Range," Jour. Petrology, Vol. 10, pp. 510-535.

2A.13 H. R. Shaw, 1965, "Comments on Viscosity, Crustal Settling and Convection in Granitic Magma," Amer. Jour. Sci., Vol. 263, pp. 120-152.

2A.14 H. R. Shaw and D. A. Swanson, 1970, "Eruption and Flow Rates of Flood Basalts; in E. H. Gilmour and D. Stradling (eds.) Proceedings of the Second Columbia River Basalt Symposium, Eastern Wash. State College Press, Cheney, WA, pp. 271-299.

2A.15 H. P. Taylor, J. R., 1975, "Stable Isotope Geochemistry," Revs. Geophys. and Space Phys., Vol. 13, pp. 102-107; pp. 159-163.

403 175

CHAPTER 3. MODEL OF THE TRANSPORT OF RADIONUCLIDES BY GROUNDWATER

3.1 Introduction

3.1.1 Nature of the Problem

Once radioactive waste has been sealed in a geologic repository for permanent isolation, any possible return to the biosphere of radionuclides contained in the waste would probably be by dissolution and transport of the nuclides by groundwater. Hence, it is imperative that a site with suitable hydrogeology be selected for waste isolation and that relevant site characteristics be evaluated by an appropriate methodology. The complexity of transport phenomena in geologic media over long periods of time is such that the problem can only be properly addressed by means of computer simulation (modeling). In addition to providing a predictive tool for radionuclide transport, such models can also form part of a methodology for assessing the risk of radioactive waste disposal. However, it should be recognized that modeling transport and assessing risk might require different approaches or even different models. A comprehensive radionuclide transport model, as discussed in the remainder of this chapter, strives for realism. Although such a model can be used in risk assessment, the large number of calculations required for risk analysis, time constraints, and other factors may make use of the comprehensive model less practical than the use of some simpler representation of a part of it. The comprehensive model is, nevertheless, essential to understand the processes that might affect the performance of the system and, hence, influence risk. Moreover, it is needed to determine meaningful boundary conditions and system characteristics for input into simpler model representations.

The problem of modeling radionuclide transport can be separated into three parts: (1) the source rate at which radionuclides are supplied to the transport medium -- i.e., groundwater; (2) the movement of groundwater with its dissolved nuclides through the geosphere; and (3) retardation effects, such as sorption, that impede movement of the radionuclides. The movement of groundwater through the geosphere is inherently a three-dimensional problem although a two- or one-dimensional simulation may provide an adequate representation in some cases.

Certain factors can be of importance to radionuclide migration in the vicinity of a deep, geologic repository. Because both domed and bedded salt are under consideration for waste disposal, the possible presence of salt and its potential effects on waste solubility, groundwater movement, and retardation must be considered. The generation of heat within the repository by radioactive decay may significantly influence both the carrier fluid and the structure of the geologic medium, thereby affecting radionuclide transport.

In principle, the problem of radionuclide transport by groundwater could be completely solved if it were possible to model the geologic region of the repository in sufficient detail and to know well enough the geophysical and geochemical processes that govern the transport of the radionuclides. Geologic modeling can be done reasonably well depending on the complexity of the situation and on the detail required. However, few data are available to treat specific situations at the desired quantitative level even though the general nature of physical and chemical processes that might affect geospheric transport are known reasonably well.

3.1.2 Background

Several geohydrological flow studies have been performed; however, there appear to be no studies which have included the coupled, three-dimensional transport of fluid, brine in non-dilute concentrations, heat, and trace constituents (radionuclides in this instance). The transport studies examined include those at Hanford, Washington; Oak Ridge, Tennessee; and Idaho Falls, Idaho. The latter work by J. B. Robertson[3.1] was particularly noteworthy in terms of both the spatial extent of the region modeled and the empirical data base. Robertson studied the groundwater transport of ^{90}Sr and ^{137}Cs near the Idaho National Engineering Laboratory. Considerable field data were available covering a period of 22 years. Using a two-dimensional flow model, he was able to fit the observed data and make predictions about future patterns of radionuclide movement. Even here, however, the model was limited by its dimensionality and by its exclusion of brine- and heat-transport processes.

The USGS Water Resources Division (WRD) in Denver recently sponsored the development of a model to represent liquid waste disposal in deep, saline aquifers.* The Survey Waste Injection Program (SWIP) is three-dimensional and solves the equation of flow, conservation of energy, and conservation of solute mass. Because SWIP represented state-of-the-art modeling of solute transport in groundwater, it was decided to use SWIP as the basis for the Sandia Groundwater Transport Model, and modify it to include radioactive decay and radionuclide sorption by geologic media. These modifications were made by INTERA under contract to Sandia Laboratories.

3.2 Model Structure

The SWIP model, in its original form, solves three differential equations simultaneously by a finite difference method. The differential equations describe the following:

1. Conservation of total liquid mass
2. Conservation of energy
3. Conservation of mass of a specific, possibly nontrace contaminant.

---

*This Survey Waste Injection Program (SWIP) was developed by INTERA, then a subsidiary of INTERCOMP of Houston, Texas.

403 157

The basic equation describing single-phase flow in a porous medium results from a combination of the continuity equation*

$$\underset{\text{Net Convection}}{\nabla \cdot \rho \underline{u}} + \underset{\text{Source}}{q'} = \underset{\text{Accumulation}}{-\frac{\partial}{\partial t}(\phi\rho)}$$

and Darcy's law in three dimensions

$$\underline{u} = -\frac{\underline{\underline{\kappa}}}{\mu} \cdot (\nabla p - \rho g \nabla Z)$$

$$\nabla \cdot \frac{\rho \underline{\underline{\kappa}}}{\mu} \cdot (\nabla p - \rho g \nabla Z) - q' = \frac{\partial}{\partial t}(\phi\rho) \ . \qquad (3.2.1)$$

The program also solves the energy balance equation which is defined as enthalpy-in less enthalpy-out equals change of internal energy,

$$\nabla \cdot \left(\frac{\rho \underline{\underline{\kappa}}}{\mu} H \cdot (\nabla p - \rho g \nabla Z)\right) + \nabla \cdot \underline{\underline{E}}_H \cdot \nabla T - q_L -$$

Net Energy Convection; Conduction; Heat Loss to Surrounding Strata

$$I'H - q_H = \frac{\partial}{\partial t}\left[\phi\rho U + (1-\phi)(\rho C_p)_R T\right] \qquad (3.2.2)$$

Enthalpy in with fluid source q'; Energy in without Fluid Input; Accumulation

The material balance for the solute leads to a concentration equation for material present in sufficient quantity to cause a density or viscosity effect as follows:

$$\nabla \cdot \left(\rho \hat{C} \frac{\underline{\underline{\kappa}}}{\mu} \cdot (\nabla p - \rho g \nabla Z)\right) + \nabla \cdot \rho \underline{\underline{E}}_C \cdot \nabla \hat{C} - q'\hat{C} = \frac{\partial}{\partial t}(\rho\phi\hat{C}) \ . \qquad (3.2.3)$$

Net solute Convection; Diffusion; Source; Accumulation

*Detailed definitions of all terms are given in the section on Nomenclature.

The SWIP program was modified to solve an additional equation for each of the radionuclides of radioactive chains considered important to our particular problem. This equation can be stated in terms of the conservation of mass of the species dissolved in the fluid phase and adsorbed on the rock medium, taking radioactive decay and generation from other radionuclides into account. Because radionuclides are likely to be present in aquifer fluids only in small quantities, it is assumed that fluid properties are independent of their concentration. The essential point of this assumption is that neither density nor viscosity of the fluids changes significantly with trace amounts of radionuclides; thus, the solution of the radioactive decay-generation-adsorption equation can be uncoupled from the density-dependent equations. This greatly simplifies the computational procedures.

A material balance of N radionuclides results in N component equations,

$$\underbrace{\nabla \cdot \left[\rho C_i \frac{\overline{\overline{k}}}{\mu} \cdot (\nabla p - \rho g \nabla Z)\right]}_{\text{Net component i convection}} + \underbrace{\nabla \cdot \rho \overline{\overline{E}}_c \cdot \nabla C_i}_{\text{Diffusion of component i}} - \underbrace{q_{c_i}}_{\text{Source of component i}} + \qquad (3.2.4)$$

$$\underbrace{\sum_{j=1}^{N} k_{ij} K_j \rho \phi C_j}_{\text{Generation of component i by decay of other isotopes}} - \underbrace{\sum_{k=1}^{N} k_{ki} K_i \rho \phi C_i}_{\text{Net decay of component i to other isotopes}} = \underbrace{\frac{\partial}{\partial t} (\phi \rho K_i C_i)}_{\text{Accumulation}}.$$

In the above,

$$k_{ki} K_i \rho \phi C_i = k_{ki} \rho \phi C_i + k_{ki} \rho_s (1-\phi) C_s ;$$

as k_{ki} is the decay constant for component i, this is an approximation to

$$\frac{\partial}{\partial t} (\phi K_i C_i) = \frac{\partial}{\partial t} (\phi \rho C_i) + \frac{\partial}{\partial t} \left[(1-\phi) \rho_s C_s\right].$$

The equilibrium adsorption constant K_i is equal to the quantity:

$$1 + \frac{B^{ij} d_j}{\phi} .$$

The system of equations 3.2.1 through 3.2.4, along with the equations describing fluid property dependence on pressure, temperature and concentration, describes the flow and transport of radionuclides in a groundwater system. This nonlinear system of equations is solved by dividing the geometric region of interest into a three-dimensional grid and developing finite difference approximations for the equations presented above.

The documentation for the modified computer program, designated Sandia Waste Isolation Flow and Transport (SWIFT), consists of the original report on the SWIP program[3.2] and the INTERCOMP report to Sandia Laboratories -- "Development of Radioactive Waste Disposal Model"[3.3] -- which describes the modifications to the original program. This second report also describes the more important features of the SWIP program.

3.3 Reference Site

3.3.1 General Description

The reference site referred to in Chapter 1 is entirely hypothetical, yet its physiographic setting and geologic and hydrologic properties are real in the sense that they were chosen as equivalent to those in several real regions in the U.S. Such a relatively complicated reference site is used in order to test the flow and transport models and to analyze the site in the same manner as real, potential repository sites.

The site is located in a symmetrical upland valley, half of which is shown schematically in Figure 3.3.1. The crest of the ridge surrounding the valley is at an elevation of 6000 feet, and the crest is a surface- and groundwater divide so that the only water moving in the valley falls in the valley itself. The valley is drained by a major river, River L, which is at elevation 2500 feet. Stream valleys tributary to River L exist, such as River U, but they are normally dry. The valley receives 40 inches of rainfall per year, of which 16 inches are lost by evapotranspiration and the remaining 24 inches recharge the ground water system.

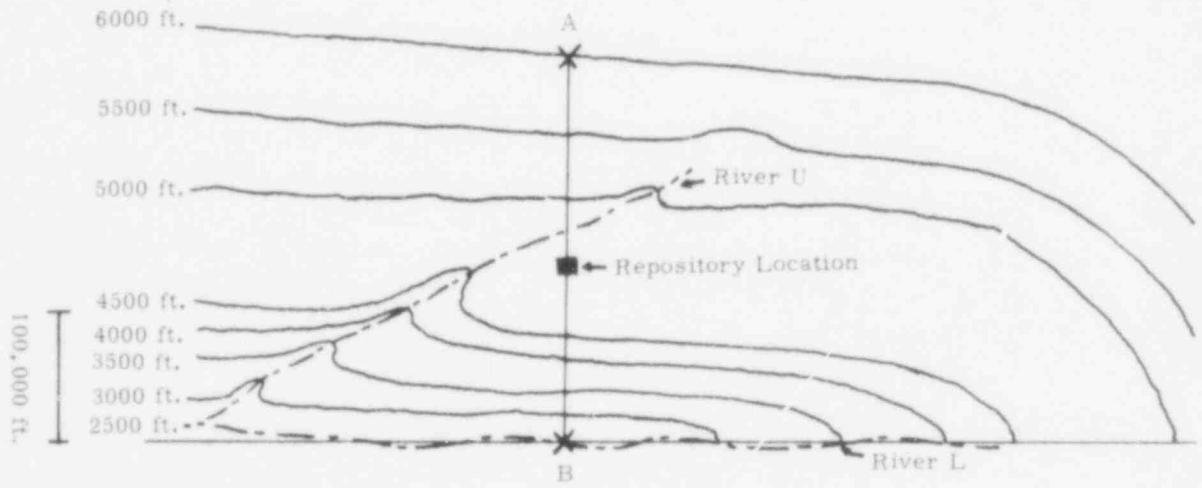

Figure 3.3.1. Map of Reference Site Area

The geology of the site is shown in cross section in Figure 3.3.2. The valley is underlain by crystalline bedrock which crops out only over a narrow width at the ridge crest surrounding the valley. This bedrock is assumed to be impermeable to groundwater flow. Above the bedrock is a sequence of sedimentary rock as shown in Figure 3.3.2. Detailed petrographic description of the sedimentary sequence given on Figure 3.3.2 is not relevant for the purpose of testing the models other than as indicated by tabulated properties. The values of hydraulic and thermal properties assumed are given in Tables 3.3.1 and 3.3.2 in report section 3.3.2 and in Table 2.4.2, section 2.4.1.

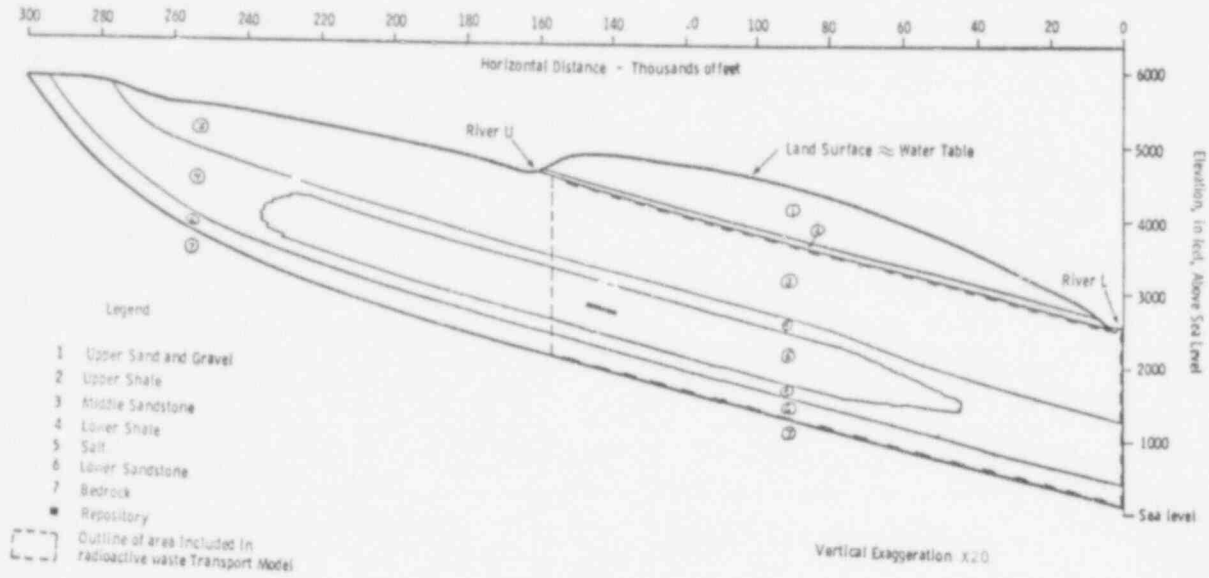

Figure 3.3.2. Geologic Cross-Section A-B Through Reference Site

3.3.2 Hydrology

The location of the repository was chosen to be far enough from the head of the valley that groundwater flow around the repository would be perpendicular to River L and to the valley axis. Thus the groundwater flow and radioactive waste transport models could be used in their two-dimensional modes to simulate the conditions around the repository. They were used in their two-dimensional mode here for speed and ease of computation only. In a real situation the three-dimensional configuration of flow and transport around a repository should be considered.

405 161

TABLE 3.3.1

Aquifer Properties Used in Radioactive Waste Transport Program and in USGS Flow Model

PROPERTY			UPPER SAND AND GRAVEL	UPPER SHALE	MIDDLE SANDSTONE	LOWER SHALE	SALT	REPOSITORY	LOWER SANDSTONE	BEDROCK	ENTERED ON CARD*
Symbol used on Fig. B & C	ft/da		1	2	3	4	5		6	7	
Hydraulic Conductivity											
Horizontal	ft/da		270	10^{-2}	50	10^{-2}	10^{-5}		40	N/A	R1-20, R1,21
Vertical	ft/da		27	10^{-5}	1.4	10^{-3}	10^{-6}		7	N/A	R1-20, R1-21
Porosity	fractional		0.3	0.3	0.3	0.3	0.03		0.3	N/A	R1-20, R1-21
Dispersivity											
Longitudinal	ft		———			500	———			N/A	R1-2
Transverse	ft		———			50	———			N/A	R1-2
Density - of solid rock	lb/ft^3	1/	———			170	———			N/A	R1-3
Thermal Conductivity of fluid solid medium	$\frac{Btu}{ft\text{-}da\text{-}°F}$										
Horizontal	$\frac{Btu}{ft\text{-}da\text{-}°F}$	1/	———			58.05	———			N/A	R1-2
Vertical	$\frac{Btu}{ft\text{-}da\text{-}°F}$	1/	———			49.34	———			40.6	R1-2,R1-13
Heat Capacity-of solid rock	$\frac{Btu}{ft^3\text{-}°F}$	1/	———			28.0	———			28.7	R1-1, R1-13
Molecular Diffusivity	ft^2/da		———			1.0×10^{-3}	———			N/A	R1-2
Compressibility of matrix	$(psi)^{-1}$					3.0×10^{-6}				N/A	R1-1

1/ Thickness weighted averages of properties of individual layers as specified for thermal conduction model.

*See Appendix 3A for list of data input cards

TABLE 3.3.2

Conversion Factors

QUANTITY		cgs units multiplied by	= English units used in RW7P		cgs units multiplied by	= SI units
FLUID PROPERTIES						
Density	grams/cm^3	x 62.428	= lb/ft^3	x	10^3	= kg/m^3
Compressibility	(bar)$^{-1}$	x 14.504	= (psi)$^{-1}$	x	10^{-5}	= (Pa)$^{-1}$ = 1 N/m^2; Pa = Pascal; N = Newton; 1N = 10^5 dynes)
Thermal Expansion	(°C)$^{-1}$	x 9/5	= (°F)$^{-1}$	x	1	= (°C)$^{-1}$ or (°K)$^{-1}$
Heat Capacity	$\frac{cal}{gm-°C}$	x 1.00	= $\frac{Btu}{ft-°F}$	x	(4.181×10^3)	= $\frac{J}{kg\ °C}$ (J = Joule; 1J = 4.181 cal at 20°C)
Viscosity	Centipoise		Centipoise	x	10^{-1}	= Pa sec
AQUIFIER AND ROCK PROPERTIES						
Hydraulic Conductivity	cm/sec	x 2.835×10^3	= ft/da	x	10^{-2}	= m/sec
Dispersivity	meters (m)	x 3.281	= ft	x	1	= m
Thermal Conductivity	$\frac{cal}{cm-sec-°C}$	x 5.805×10^3	= $\frac{Btu}{ft-da-°F}$	x	(4.181×10^2)	= $\frac{J}{m\ sec\ °C}$
Heat Capacity	$\frac{cal}{gm-°C}$	x 1.00 x Density $\frac{lb}{ft}$	= $\frac{Btu}{ft^3-°F}$	x	(4.181×10^3)	= $\frac{J}{kg\ °C}$
Molecular Diffusivity	cm^2/sec	x 7.363×10^{-4}	= ft^2/da	x	10^{-4}	= m^2/sec

The groundwater flow in the entire valley cross section shown in Figure 3.3.2 was simulated by the Albuquerque District Office of the U.S. Geological Survey, Water Resources Division with the commonly used finite difference model of Trescott.[3.4, 3.5] In the remainder of this section, this model is referred to as the USGS model. The finite difference grid used to represent the cross section through the repository is shown in Figure 3.3.3.

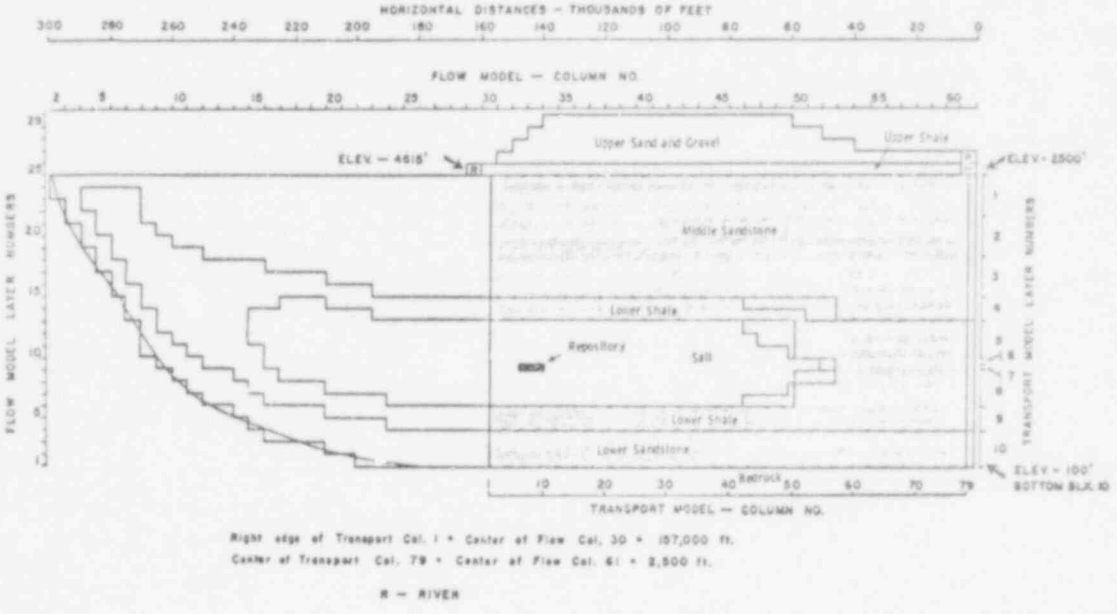

Figure 3.3.3. Reference Site as Gridded for Transport Calculations

The hydraulic properties of the rock units used in the USGS flow model and in the Groundwater Transport Model are given in Table 3.3.1. They are the properties of real rocks of the type assumed to make up the reference site, as given by Franke and Cohen.[3.6] The site described in Reference 3.6 does not contain salt. Therefore, the hydraulic conductivity and porosity of salt were arbitrarily assumed to be 10^3 and 10 times lower, respectively, than those of the lower shale bed. The effects of variations in the hydraulic properties of the rocks and salt on flow and transport in the system will be investigated. The values given in Table 3.3.1 are merely starting points for the purpose of testing the flow and transport models. The fluid properties required for the Groundwater Transport Model are given in Table 3.3.3.

Although most of the computer codes developed as part of this project use cgs or SI units for their input and output parameters, the transport program and USGS flow model require English units because they were developed from oil field and groundwater engineering codes. Although it is desirable to modify the transport code to accept cgs or SI units, at present it is being used with English units. Conversion factors are given in Table 3.3.2 to assist those used to thinking in cgs or SI units.

403 164

TABLE 3.3.3

Fluid Properties

PROPERTY	TEMPERATURE °C	TEMPERATURE °F	CONCENTRATION Wt. % NaCl	CONCENTRATION gmNaCl / ℓ soln	CONCENTRATION ℓbNaCl / ft³ soln	Relative	UNITS CgS	UNITS English	VALUE CgS	VALUE English	Reference	Input on Card*
Density - at 1 bar	25	77	0	0	0	0	gm/cm^3	lb/ft^3	0.9971	62.25	(1)	R1-3
Compressibility 1 to 100 bars	20-100	68-212	0	0	0	0	bar^{-1}	psi^{-1}	4.7×10^{-5}	3.2×10^{-6}	Calc. from (1)	R1-1
Thermal Expansion 1 to 100 bars	20-100	68-212	0	0	0	0	$°C^{-1}$	$°F^{-1}$	5.3×10^{-4}	2.9×10	Calc. from (1)	R1-1
Heat Capacity	20-100	68-212	0	0	0	0	$\frac{Cal}{gm-°C}$	$\frac{Btu}{lb/°F}$	1.00	1.00	(2)	R1-1
Density - at 1 bar	25	77	25	296		1.0	gm/cm^3	lb/ft^3	1.1851	73.98	(3)	R1-3
Viscosity: of pure water with temp.	15	59	0	0	0	0	cp			1.138	(4)	R1-7
	40	104	0	0	0	0	cp			0.6531	(4)	R1-9
	65	149	0	0	0	0	cp			0.4342	(4)	R1-9
	90	194	0	0	0	0	cp			0.3156	(4)	R1-9
of brine with conc.	15	59	5	51.7	3.23	0.2	cp			1.209	Calc. from	R1-8
	15	59	12.5	136	8.49	0.5	cp			1.320	(3) & (4)	R1-8
	15	59	20	229	14.3	0.8	cp			1.444		R1-8
	15	59	25	296	18.5	1.0	cp			1.532		R1-7
of brine with temp	25	77	25	296	18.5	1.0				1.260		R1-10
	35	95	25	296	18.5	1.0				1.055		R1-10
	42.5	108.5	25	296	18.5	1.0				1.004		R1-10

References: (1) Clark, S. P., Jr., ed, 1966, Handbook of Physical Constants;
(2) Weast, Robert C., ed, CRC Handbook of Chemistry and Physics, 59th edition, 1978-79.
(3) Potter, R. W., II and Brown, David L., 1977, The Volumetric Properties of Aqueous Sodium Chloride Solutions ... U.S. Geolog. Survey Bull. 1421-C
(4) Robinson, R. A. and Stokes, R. H., 1959, Electrolyte Solutions: Butterworths, London, Appendix 1.1 and 11.3.

*See Appendix 3A for list of data input cards

The following assumptions are made for flow modeling:

1. The bedrock underlying the sediments in the valley is impermeable and thus is a no-flow boundary.
2. The valley is symmetrical about its central axis, the line of River L. Thus, all discharge from the section modeled is to River L. and the vertical plane at River L is also treated as a no-flow boundary (plane of symmetry).
3. The elevation of River L, equivalent to the hydraulic head at the discharge point, is 2500 feet above sea level.
4. The surface of the entire region is recharged by infiltration at the constant rate of 24 inches per year.

In designing the ground-surface inclination of the reference site, the model was run to steady-state conditions with several different ground-surface slopes by varying the elevation of River U. It was desired that all the regional recharge should discharge to River L; i.e., River U should have as little flow as possible. A too steep slope would give heads that lie below the elevation of River U so that it would lose water to the groundwater system. A too shallow slope would give heads above the elevation of River U so that groundwater would discharge to and flow in River U. By trial and error, an elevation of 4615 feet for River U was chosen which gave essentially no recharge from or discharge to River U. The elevations of the water table elsewhere along the section are those calculated by the model at steady state. These elevations are those shown as the ground surface on Figure 3.3.2.

There are really two groundwater flow systems in the cross section. The upper system is restricted to the upper sand and gravel unit and upper clay unit. In the upper system, recharge between River U and River L flows and discharges to River L. The lower flow system is confined beneath the upper clay and is the system that influences the repository. The lower flow system receives all the recharge above River U which also discharges into River L.

In order to distinguish between these systems, the USGS flow model was gridded so that the discharge from each to River L was calculated separately. The results of the steady-state simulation can be summarized as follows:

Discharge to River L from upper flow system: 8.2×10^2 ft^3/da. ft
Discharge to River L from lower flow system: 7.5×10^2 ft^3/da. ft

Total discharge per 1 ft. length River L: 15.7×10^2 ft^3/da.

To assess the reasonableness of these values, the total discharge of River L at the repository section can also be calculated from the area of the valley and the assumed recharge rate of 2 ft/yr. Assuming the valley to be elliptical, its area above the repository is:

$$\pi/2 \times 390,000 \text{ ft} \times 580,000 \text{ ft} = 2.7 \times 10^{11} \text{ ft}^2.$$

With the recharge rate of 2 ft/yr, all discharging to River L, the flow of River L at point B in Figure 3.3.1 is:

$$2.7 \times 10^{11} \text{ ft}^2 \times 2 \text{ ft/yr} \times \text{yr}/365 \text{ da} = 1.5 \times 10^9 \text{ ft}^3/\text{da}.$$

From the groundwater flow model, the discharge from half the valley per foot of River L is 15.7×10^2 ft^3/da. If River L above the repository cross section received groundwater at this rate, the length of River L must be

$$(1.5 \times 10^9 \text{ ft}^3/\text{da})/(2 \times 15.7 \times 10^2 \text{ ft}^3/\text{da.ft}) = 4.8 \times 10^5 \text{ ft}.$$

This is less than the length of the valley itself (Figure 3.3.1), as it should be if the reference site plan and hydrology are consistent.

Because of the finite difference grid size limits in the Sandia Model (SWIFT), the entire cross section (Figures 3.3.2, 3.3.3) was not simulated. Only the lower flow system from River L to a distance of 157,500 feet along a line through the repository was simulated by SWIFT. The area and the finite difference grid used are shown in Figure 3.3.3. To compare the flow simulations by the USGS model and SWIFT, SWIFT was run to steady-state flow conditions. Constant boundary pressures were used along the left edge, taken from the USGS model results, and a well discharging at a head of 2500 feet in the upper right block was used to simulate the discharge to River L from the lower flow system. At steady state, the discharge from that well was 7.3×10^2 ft^3/da.ft, in agreement with the 7.5×10^2 ft^3/da.ft discharge from the lower flow system in the USGS model. Likewise, the heads in the lower right blocks of both models are in good agreement: 4093 feet in the SWIFT versus 4053 in the USGS model. Although a 40-foot difference in head may seem large, it is the hydraulic gradient which drives the flow. The vertical gradients (head/vertical distance) between the lower right block and the discharge point, River L, are

USGS model: (4053-2500)/2150 = 0.72

SWIFT: 4093-2500/2150 = 0.74.

3.3.3 Leach Rates for Solidified Waste

An input to the transport problem is the leach rate of radionuclides to the transport medium (i.e., groundwater). Leach rate is generally defined by some form of the following expression:[3.7]

$$R = \frac{a}{A_o} \frac{W}{St} \qquad (3.3.1)$$

where

a = amount of trace element leached during the period t,

A_o = amount of trace element originally in the sample,

W = weight of the sample (g),

S = effective surface area of the sample (cm^2),

t = duration of the leachant exposure period (days).

Thus, the units of R are grams of dissolved waste per cm^2 per day.

Certain elements tend to leach faster than others, at least during the initial phases of leaching. Typically, the fission products cesium and strontium are among the more leachable elements. At the present time, however, not enough consistent data are available for either glass or concrete to justify using different leach rates for different elements.

The rate of leaching from both glass and concrete is highest during the initial contact with water. The rate then decreases to a nearly constant value.[3.8] A functional time dependence that has been used for high-level waste glass to express this behavior is[3.7, 3.9]

$$R = At^{-1/2} + B \quad . \tag{3.3.2}$$

Initially, leaching from glass appears to be controlled by diffusion, which is the basis for the $t^{-1/2}$ term. For larger values of t, the constant term describes what is thought to be corrosion behavior. However, data describing the long-term behavior of glass are very scarce. The time-dependent leaching behavior of waste from concrete is even less studied than that of glass. However, from the data available,[3.10, 3.11] the time-dependent behavior of concrete appears to be similar to that of glass.

Once solidified wastes are emplaced in a repository, many factors combine to make the long-term leach behavior even more uncertain than the lack of consistent data would indicate. A fundamental difficulty is that the effective surface area of the waste is poorly known at the time of emplacement and less well known with time because changes in the surface area cannot be accurately predicted. After extended periods, a glass waste form may be devitrified and concrete may be reduced to sand and gravel. Moreover, different mechanisms may affect the availability of ions to the leachant. For example, the leaching of ions not strongly sorbed into the waste-form matrix may be diffusion controlled, whereas strongly sorbed ions may be leached through corrosion of the matrix. The rate of flow of leachant over the waste may also vary significantly over hundreds or thousands of years with consequent large changes in leach rate.

Because of the uncertainties involved in defining a representative leach rate, two simplifying assumptions are presently being made. First, all isotopes are assumed to leach at the same rate. Second, the waste is assumed to dissolve at a constant rate until dissolution is complete. We believe that these assumptions are reasonable, and that their use will lead to a meaningful study

of the sensitivity of risk to leach rate. We stress that these assumptions are preliminary. If the calculated risk should prove to be sensitive to these assumptions, SWIFT is sufficiently flexible that different assumptions about leach rates, or processes which control leach rates, can be incorporated.

As an example, an estimate is given of the dissolution time for a canister of high-level waste glass. The canister diameter is approximately 30 cm and is filled to a volume of 0.177 m^3 which implies a surface area

$$S_o = 2.5 \times 10^4 \text{ cm}^2.$$

However, the effective area is expected to be increased from cracking caused by physical and thermal shock. The effective surface area (S_E) is estimated to be[3.8]

$$S_E = 10 \times S_o = 2.5 \times 10^5 \text{ cm}^2.$$

The density of the glass is assumed to be 3 gm/cm^3, giving an initial mass (M_o) of 5.3×10^5 gm. The dissolution time is then estimated by

$$T_d = \frac{M_o}{R\, S_E} \quad . \tag{3.3.3}$$

Assuming $R = 10^{-5}$ gm/cm^2/day, $T_d \approx 600$ years. As previously stated we are assuming a constant dissolution rate. The example above simply provides a crude estimate for the dissolution time of glass for an assumed leach rate. Similar estimates can be made for other waste forms.

3.3.4 Selected Results

To illustrate the comprehensive nature of the SWIFT model as applied to the Reference Site, three items are presented. These are a sample input, flow results, and heat-transport results. Data input appropriate for a two-dimensional coupled pressure-temperature-radionuclide simulation for the Reference Site is shown as Table 3.3.4. This simulation, which has been performed, involved the tracking of 23 different radionuclides over a time span of 10^5 da. As might be expected there was a substantial storage requirement, which was at the upper limit of Sandia's CDC-6600 facility. The storage available for the model may be enlarged, however, by using the CDC-7600. For a simulation like this one in which there are more than four radionuclides, all radionuclide [illegible] on disk to lessen storage requirements. Another observation here pertains to the requirements. Central processor times of 15-30 minutes on the CDC-6600 are not unusual for a problem such as the one whose input appears in Table 3.3.4. The restart capability possessed by the code is therefore invaluable in minimizing computing costs.

TABLE 3.3.4

Transport Model Input for the Reference Site

```
INTERA MODEL - 79X10 GRID - PRESSURE ONLY - ISOTHERMAL
     USING USGS MODEL HEADS AT K=1 BOUNDARY 23 EL CHAIN IN REPOSITORY
   -2     1     0     0     0     1     0                                  M - 2
   79     1    10     2    23     1     0     2    23    10     0          M - 3
250CF99          1     2  13.68
245CM96          2     1 4711.
    1      .1321
242AM95M         3     0  192.
242AM95          4     11.9252 E-1
    3      1.
242CM96          6     14.4627 E-1
    4      .42
242PU94          5     2 3.79  E+5
    2      .3997          4        .18
238PU94          9     1 8.9   E+1
    6      1.
238U92           7     1 4.51  E9
    5      1.
234TH90          8     1 6.9932E-2
    7      1.
234PA91M        10     1 2.02+55-6
    8      1.
234PA91         11     1 7.7012E-4
   10      .001
234U92          12     3 2.47  E5
    9      1.             10       .999          11       1.
230TH90         13     1 8.    E4
   12      1.
226RA88         14     1 1600.
   13      1.
222RN86         15     1 1.0439E-2
   14      1.
218PO84         16     1 5.7993E-6
   15      1.
214PB82         17     1 5.3954E-3
   16      1.
214BI83         18     1 2.7455E-5
   17      1.
214PO84         19     1E.3376E-12
   18      1.
210PB82         20     1  21.
   19      1.
210BI83         21     1 1.1717E-2
   20      1.
210PO84         22     1 3.7782E-1
   21      1.
206PB82         23     1  0.
   22      1.
1.     E+001.0    E+001.324 E+01+1.     E+007.313 E+017.313 E+044.372 E+0+9.389 E+05
9.368 E+00+.439  E+00+.439  E+034.372 E+000.389 E+031.249 E+020.          1.243 E+05
9.368 E+02.499   E+021.249 E+039.368 E+042.488 E+02..049 E+059.368 E+04
 3.2   E-05 3.0   E-06 2.9   E-04 1.0        28.0                          P1- 1
 1.0   E-02 1.0   E-02 8.9   E-03 3.6056E+03 500.0     50.0        1.0  E-04R1- 2
 173.0       14.7        77.0        52.25       72.98                     P1- 3
    3     1     3     2                                                    R1- 6
 59.0        1.138       59.0        1.532                                 R1- 7
 0.2         1.209       0.9         1.320       0.6         1.444         R1- 8
 104.0       0.6531      149.0       0.4342      194.0       0.3156        R1- 9
 77.0        1.260       99.0        1.155       108.9       1.004         R1-10
-4498.90     68.0                                                         R1-11
 2500.00     58.0                                                         P1-11
    3     4                                                              P1-12
 5.0   E-03 29.7        7.0   E-03 28.7                                   P1-13
 103.0       207.0       300.0                                           R1-14
 100.0       200.0       400.0       800.0                               R1-15
```

403 170

TABLE 3.3.4 (cont)

```
58.0        0.0          -4498.9    0.0                                                    R1-15
    1000.       1500.       2000.       2000.       2000.       2000.       2000.R1-17
    2000.       2000.       2000.       2000.       2000.       2000.       2000.R1-17
    2000.       2000.       2000.       2000.       2000.       2000.       2000.R1-17
    2000.       2000.       2000.       2000.       2000.       2000.       2000.R1-17
    2000.       2000.       2000.       2000.       2000.       2000.       2000.R1-17
    2000.       2000.       2000.       2000.       2000.       2000.       2000.R1-17
    2000.       2000.       2000.       2000.       2000.       2000.       2000.R1-17
    2000.       2000.       2000.       2000.       2000.       2000.       2000.R1-17
    2000.       2000.       2000.       2000.       2000.       2000.       2000.R1-17
    2000.       2000.       2000.       2000.       2000.       2000.       2000.R1-17
    2000.       1000.                                                                  R1-17
      1.                                                                               R1-18
    333.3       333.3       333.3       200.0       300.0        50.0        50.0R1-19
    100.0       200.0       300.0                                                      R1-19
50.0        50.0        1.4         2.3        .012937864 0.0          -4498.9       R1-20
  1   79    1    1    1    3                                                          R1-26
   50.0        50.0        1.4         0.3                                           R1-21
  1   57    1    1    4    4                                                          R1-21
 1.E-02      1.E-02      1.E-03      0.3                                             R1-21
 58   79    1    1    4    4                                                          R1-25
   50.0        50.0        1.4         0.3                                           R1-26
  1   50    1    1    5    5                                                          R1-26
 1.E-06      1.E-06      1.E-06      0.03                                            R1-21
 51   79    1    1    5    5                                                          R1-21
 1.E-02      1.E-02      1.E-03      0.3                                             R1-21
 51   57    1    1    6    7                                                          R1-26
 1.E-06      1.E-06      1.E-06      0.03                                            R1-26
 58   79    1    1    6    7                                                          R1-26
 1.E-02      1.E-02      1.E+03      0.3                                             R1-26
 51   79    1    1    8    8                                                          R1-26
 1.E-02      1.E-02      1.E+03      0.3                                             R1-26
  1   79    1    1    9    9                                                          R1-26
 1.E-02      1.E-02      1.E-03      0.3                                             R1-26
  1   79    1    1   10   10                                                          R1-26
   40.0        40.0        7.0         0.3                                           R1-27
   4    3                                                                           R1-27
   1    1    1    1    1    1                                                        R1-28
1.0         20.39       68.0                                                        R1-28
   1    1    1    1    2    2                                                        R1-28
1.          164.76      68.0                                                        R1-28
   1    1    1    1    3    3                                                        R1-28
1.0         103.08      68.0                                                        R1-28
   1    1    1    1    4    4                                                        R1-28
1.0         453.39      68.0                                                        R1-28
   1    1    1    1    5    5                                                        R1-28
1.0         663.59      68.0                                                        R1-28
   1    1    1    1    6    6                                                        R1-28
1.0         721.07      68.0                                                        R1-28
   1    1    1    1    7    7                                                        R1-28
1.0         790.61      68.0                                                        R1-28
   1    1    1    1    8    8                                                        R1-28
1.0         799.79      68.0                                                        R1-28
   1    1    1    1    9    9                                                        R1-28
1.0         953.34      68.0                                                        R1-28
   1    1    1    1   10   10                                                        R1-28
1.0        1039.94      68.0                                                        R1-28
   0    0    1                                                                      I-1
   7   10    1    1    7    7 1.306E-02                                            I-4.1
   7   10    1    1    7    7 1.044E+05                                            I-4.2
```

TABLE 3.3.4 (cont)

```
   7   10    1    1    7    7 1.981E-99                                                I-4,3
   7   10    1    1    7    7 1.881E+00                                                I-4,4
   7   10    1    1    7    7 7.313E+02                                                I-4,5
   7   10    1    1    7    7 1.281E+05                                                I-4,6
   7   10    1    1    7    7 6.563E+05                                                I-4,7
   7   10    1    1    7    7 1.175E+06                                                I-4,8
   7   10    1    1    7    74.519E-038                                                I-4,9
   7   10    1    1    7    7 0.0                                                      I-4,10
   7   10    1    1    7    7 0.0                                                      I-4,11
   7   10    1    1    7    7 1.275E+05                                                I-4,12
   7   10    1    1    7    7 1.937E+01                                                I-4,13
   7   10    1    1    7    7 1.394E-02                                                I-4,14
   7   10    1    1    7    70.0                                                       I-4,15
   7   10    1    1    7    70.0                                                       I-4,16
   7   10    1    1    7    70.0                                                       I-4,17
   7   10    1    1    7    70.0                                                       I-4,18
   7   10    1    1    7    70.0                                                       I-4,19
   7   10    1    1    7    7 4.606E-05                                                I-4,20
   7   10    1    1    7    7 0.0                                                      I-4,21
   7   10    1    1    7    7 7.629E-07                                                I-4,22
   7   10    1    1    7    7 0.0                                                      I-4,23

   1    1    1    0    0    0    0    0                                               R2- 1
   1 0.5                                                                             R2- 2
   5                                                                                 R2-4
1.      E3                                                                           R2-5
   1   79    1    1    1   -1                                                        R2- 7-1
   1000.  1.0001          66.0         0.0
   2    9    1    7    7    1                                                        R2- 7-1
1000.0                                                                               R2- 7-2
   3    9    1    3    3    1
   1600.0
   4   36    1    3    3    1
   1000.0
   5   12    1    3    3    1                                                        R2- 7-1
1000.0                                                                               R2- 7-2

10.0       10.0
   0    0    1   -1    1  011    0  000    0    0    0                              R2-13
   0    0    0    0    0    0    0    0                                             R2- 1
1.000E+03                                                          1.000E+03
   0    0    1   -1    1  011    1  000    0    0    1                              R2-13
   0    0    0    0    0    0    0    0                                             R2- 1
1.000E+04                                                          1.000E+04
   0    0    1   -1    1  011    1  000    0    0    1                              R2-13
   0    0    0    0    0    0    0    0                                             R2- 1
1.000E+05                                                          1.000E+05
   0    0    1   -1    1  011    1  000    0    0    1                              R2-13
   0    0    0    1    0    0    0    0                                             R2- 1
```

The flow portion of the program will be used to illustrate the flexibility of the model. A replotted version of the program output, in terms of pressure heads over the Reference Site, is given as Figure 3.3.4B. To produce the results in Figure 3.3.4A, the same input conditions were used except that an assumed thermal stress cracking was allowed to give a U-tube effect in the region of the repository. As can be seen, this effect (implemented by changing the porosity in the U-tube area) dramatically changed the head and, thus, the flow pattern.

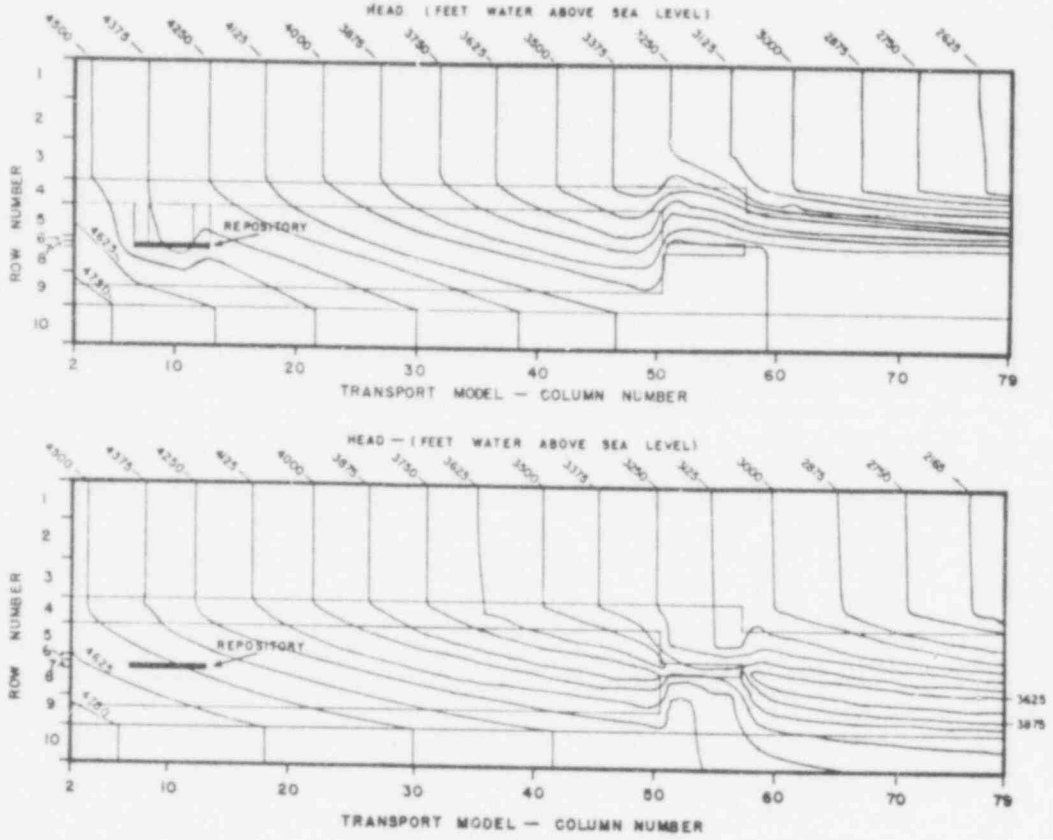

Figure 3.3.4. Calculated Pressure Heads Near the Reference Site

A final example is provided by the input of the thermal source in the repository (Figure 3.3.5). SWIFT was run out to 6504 years, and maps were prepared of the Reference Site. This was done in the two-dimensional 10 x 79 grid block setup (Figure 3.3.3) in two ways. For one, the porosity was set to zero so that only conductive heat transfer was effective. For the other, the normal flow was permitted so that both conductive and convective heat transfer operated.

Of interest is the fact that both results are similar out to about 75 years, although higher temperatures are reached in the purely conductive mode. At later times, dramatic differences exist due to flow and the resulting convective transfer. First, the temperatures are lower throughcut with flow, and second, the temperature rise at the surface was significant only with pure conductive transfer.

403 1-3

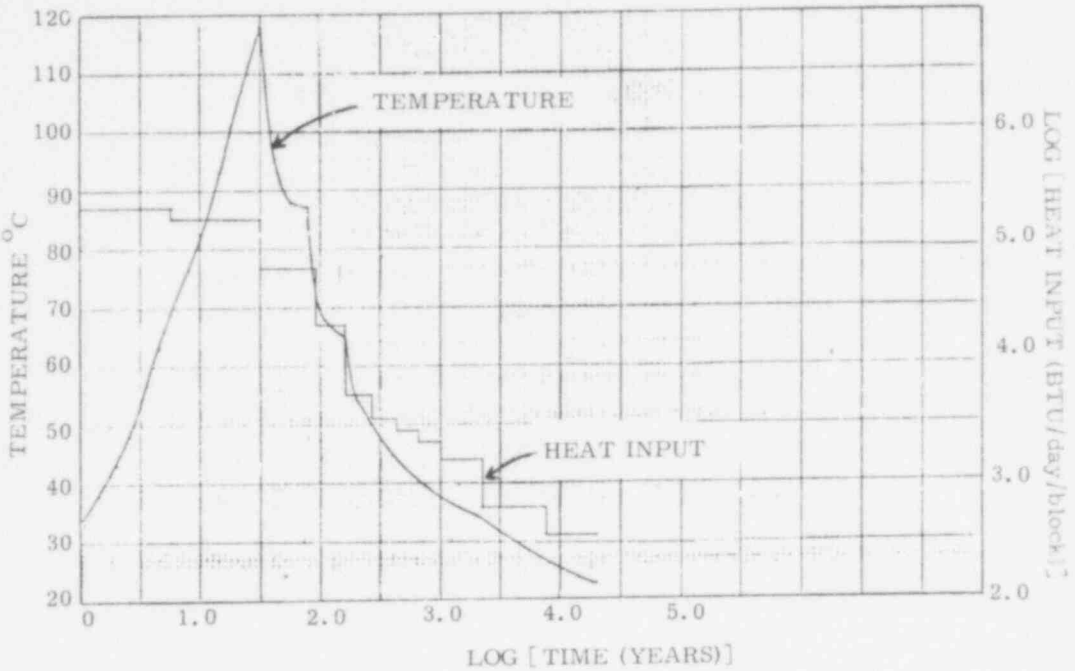

Figure 3.3.5. Thermal Input to Transport Model and Resulting Temperature at Grid Site (9, 1, 7)

These results are illustrated by Figures 3.3.6, 3.3.7, and 3.3.8. Figure 3.3.6 gives the numerical code to temperature correspondence for the maps in Figures 3.3.7 and 3.3.8, which are plotted for a time of about 400 years. It is obvious from the maps that the temperature is affected by convective flow. These results indicate types of analysis that can be performed with SWIFT.

MAP LEGEND

HORIZONTAL GRID BLOCK RANGE, FROM 2 TO 79
VERTICAL GRID BLOCK RANGE, FROM 1 TO 10

DEPENDENT VARIABLE RANGE	MAP CHARACTER
0. - .675E+02	
.625E+02 - .675E+02	1
.650E+02 - .675E+02	
.675E+02 - .700E+02	2
.700E+02 - .725E+02	
.725E+02 - .750E+02	3
.750E+02 - .775E+02	
.775E+02 - .800E+02	4
.800E+02 - .825E+02	
.825E+02 - .850E+02	5
.850E+02 - .875E+02	
.875E+02 - .900E+02	6
.900E+02 - .925E+02	
.925E+02 - .950E+02	7
.950E+02 - .975E+02	
.975E+02 - .100E+03	8
.100E+03 - .102E+03	
.102E+03 - .105E+03	9
.105E+03 - .107E+03	
.107E+03 - .110E+03	0

HORIZONTAL GRID VECTOR .175E+04 .355E+04 .655E+04 .795E+04 .955E+04 .115E+05 .135E+05 .155E+05 .175E+05
.215E+05 .235E+05 .255E+05 .275E+05 .295E+05 .315E+05 .335E+05 .355E+05 .375E+05 .395E+05
.415E+05 .435E+05 .455E+05 .475E+05 .495E+05 .515E+05 .535E+05 .555E+05 .575E+05 .595E+05
.615E+05 .635E+05 .655E+05 .675E+05 .695E+05 .715E+05 .735E+05 .755E+05 .775E+05 .795E+05
.815E+05 .835E+05 .855E+05 .875E+05 .895E+05 .915E+05 .935E+05 .955E+05 .975E+05 .995E+05
.101E+06 .103E+06 .105E+06 .107E+06 .109E+06 .111E+06 .113E+06 .115E+06 .117E+06 .119E+06
.121E+06 .123E+06 .125E+06 .127E+06 .129E+06 .131E+06 .133E+06 .135E+06 .137E+06 .139E+06
.141E+06 .143E+06 .145E+06 .147E+06 .149E+06 .151E+06 .153E+06 .155E+06
VERTICAL GRID VECTOR .167E+03 .550E+03 .833E+03 .110E+04 .135E+04 .152E+04 .157E+04 .175E+04 .220E+04

Figure 3.3.6. Temperature Range Represented by Map Characters in Temperature Maps

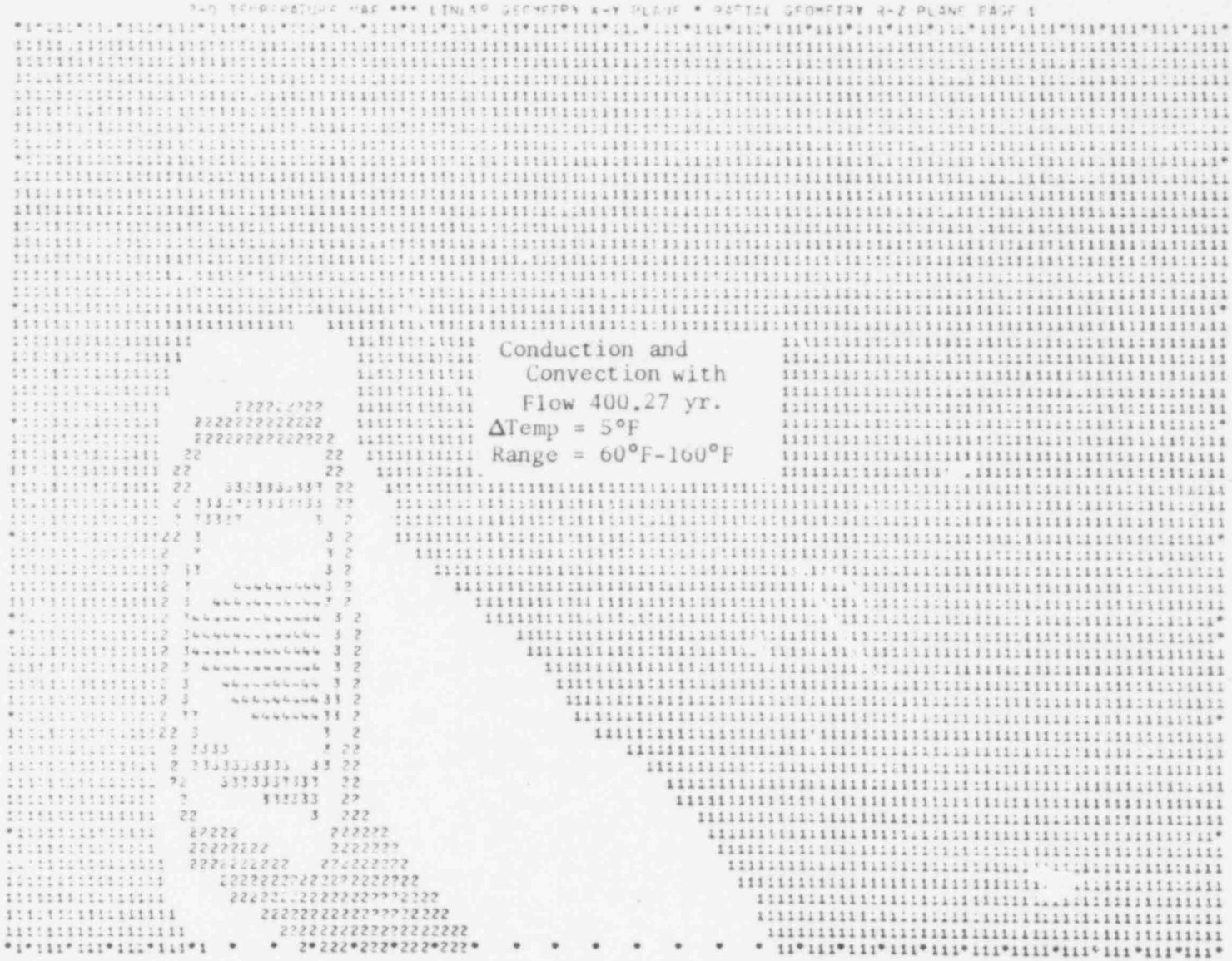

Figure 3.3.7. Temperature Map for Conduction and Convection

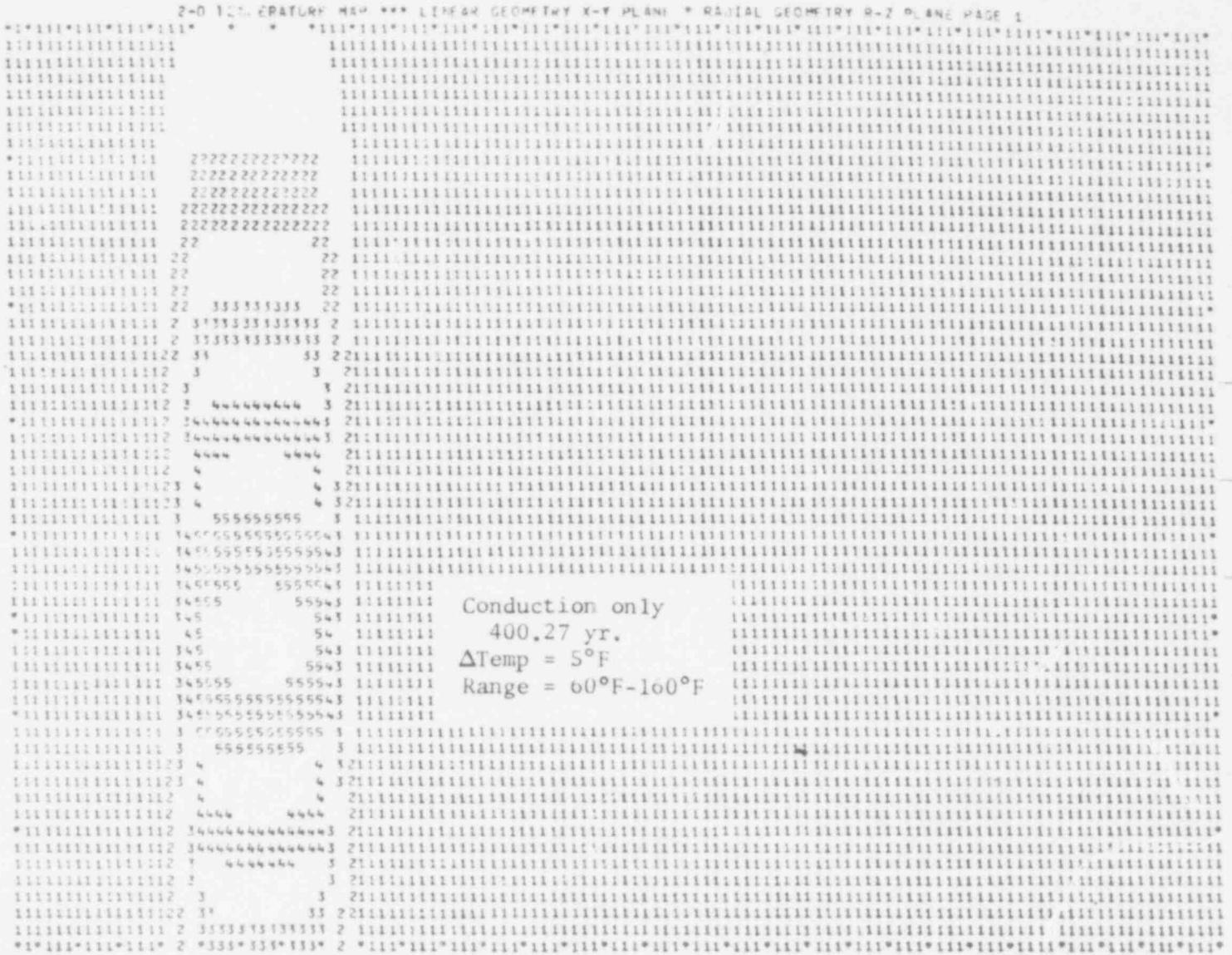

Figure 3.3.8. Temperature Map for Conduction Only

To date, the Transport Model has been verified hydrologically by comparison with a USGS geohydrology code that has been accepted by the scientific community. It has also been used for a number of thermal calculations.

3.4 Limitations and Future Improvements

The major limitations noted to date in the model are associated with numerical dispersion and oscillatory instability. These problems are most severe for large simulation times ($\sim 10^6$ years†) and large flow distances (10's of miles†). In the time domain one can usually overcome these problems if one is interested primarily in the peak concentrations. Predetermined amounts of numerical dispersion can be permitted consistent with preserving the desired accuracy of the peak concentration.

In the space domain the restriction is related to the physical dispersivity. For example, in a one dimensional problem using the less restrictive centered-in-space approach one obtains $\Delta x \leq 2\alpha$. Thus, as α decreases, spatial discretization becomes finer, and therefore computer time- and storage-requirements increase. Even for physically reasonable values of α these computer requirements can become intolerable. This problem is most acute in the case of sensitivity and risk analyses where many computations will probably be necessary. In the short term it may be desirable to use numerical and analytical models in a tandem mode in which the former is used for the near field transport and the latter is used for the far field transport. In contrast to numerical models, analytical models are restricted to constant material properties. Ultimately, therefore, it would be desirable to offer, as an option, a numerical integration technique which is specially adapted to advection-dominated transport. Possibilities include the method of characteristics, higher-order finite difference, and two-point upstream weighting.

In its present form, the model uses English units. Conversion to a more accepted set of units (e.g., SI) is desirable. The output of the model is presented primarily in tabular form. Because this results in large quantities of printout, more efficient methods of displaying output need to be developed.

The model currently uses distribution coefficients (Kd's) to represent sorption. It may be desirable to make Kd a function of salinity and to make the solubility of the radionuclides a function of both salinity and temperature.

---

† These times and distances are merely suggestive. The actual values, of course, depend on the characteristics.

403 177

3.5 NOMENCLATURE

C	-	concentration of the radioactive/trace component in fluid phase
$\hat{C}$	-	concentration of the inert contaminant
C_S	-	concentration of the radioactive/trace component in adsorbed state
$\underline{\underline{E}}_C$	-	dispersivity tensor (hydrodynamic + molecular)
$\underline{\underline{E}}_H$	-	thermal conductivity tensor
g	-	acceleration due to gravity
H	-	fluid enthalpy
$\underline{\underline{k}}$	-	permeability tensor
k	-	rate of decay
K	-	equilibrium adsorption constant
K_d	-	adsorption distribution constant
ℓ	-	distance between adjacent grid block centers
p	-	pressure
q'	-	fluid source rate (withdrawal)
q_L	-	rate of heat loss
q_H	-	rate of energy withdrawal
t	-	time
T	-	temperature
$\underline{u}$	-	velocity vector
U	-	internal energy
V	-	grid block pore volume
Z	-	height above a reference plane

Greek Letters

ϕ	-	porosity
μ	-	viscosity
ρ	-	fluid density
ρ_S	-	formation density
ρ_B	-	bulk density of rock and fluid
τ	-	radioactive decay half life

Subscripts

c	-	component (mass)
H	-	heat (energy)
R	-	rock (formation)
w	-	water (fluid)

References

3.1 Robertson, J. B., "Digital Modeling of Radioactive and Chemical Waste Transport i.. the Snake River Plain Aquifer at the National Reactor Testing Station, Idaho," National Technical Information Service, Washington, D.C., May, 1974.

3.2 INTERCOMP Resource Development and Engineering Inc., "Development of Model for Calculating Disposal in Deep Saline Aquifers, Parts I and II," PB-236903, National Technical Information Service, Washington, D.C., 1976.

3.3 INTERCOMP Resource Development and Engineering Inc., "Development of Radioactive Waste Disposal Model," Prepared for Sandia Laboratories, Albuquerque, New Mexico, May, 1977.

3.4 Trescott, Peter C., Documentation of Finite Difference Model for Simulation of Three-Dimensional Groundwater Flow, U.S. Geol. Survey, Open File Report 75-438, 1975.

3.5 Trescott, P. C. and Larson, S. P., Supplement to Open File Report 75-438 (Trescott, 1975), U.S. Geol. Survey Open File Report 76-571, 1976.

3.6 Franke, O. L. and Cohen, Philip, "Regional Rates of Groundwater Movement on Long Island, New York," U.S. Geol. Survey Prof. Paper 800-C, p. C271-277, 1972.

3.7 Mendel, J. E., A Review of Leaching Test Methods and the Leachability of Various Solid Media Containing Radioactive Wastes, BNWL-1765, 1973.

3.8 Mendel, J. E., "High-Level Waste Glass," Nuclear Technology, 32, 1977.

3.9 Determination of Performance Criteria for High-Level Solidified Nuclear Waste, LLL-NUREG-1002 (Draft), 1976.

3.10 Moore, J. G.; Godbee, H. W., Kibbey, A. H., and Joy, D. S., Development of Cementitious Grouts for the Incorporation of Radioactive Wastes, Part I, ORNL-4962, 1975.

3.11 Moore, J. G., Development of Cementitious Grouts for the Incorporation of Radioactive Wastes, Part 2, ORNL-5142, 1976.

APPENDIX 3A

List of Input Data Cards

Reference No.	Enter
M-1	Title
M-2	Control Parameters
M-3	Grid system dimensions
RO-1	Radioactive component identification, half-life and chain description
M-4, M-5	Time at which next set of recurrent data are to be entered for a restart run
R1-1 to R1-3	Fluid and aquifer properties
R1-4 to R1-5	Wellbore model data
R1-6	Number of entries in viscosity and temperature tables
R1-7 to R1-10	Viscosity data
R1-11	Temperature vs depth table
R1-12	Number of overburden and underburden blocks
R1-13	Overburden and underburden properties
R1-14 to R1-15	Overburden and underburden block dimensions
R1-16	Initial pressure at a reference depth
R1-17 to R1-19	Grid block dimensions for a linear geometry aquifer
R1-20	Transmissivity and porosity data for a linear geometry, homogeneous aquifer
R1-21	Heterogeneous aquifer data
R1-22	Radial geometry aquifer dimensions
R1-23	Radial geometry aquifer properties
R1-24 to R1-25	Data for dividing a radial geometry aquifer into regions of constant logr
R1-26	Aquifer description (transmissibilities, pore volume, depth and thickness) modification data
R1-27	Selection of aquifer influence function representation
R1-28	Aquifer influence coefficients for pot and steady-state aquifer representations
R1-29	Control parameters for Carter-Tracy aquifer representation
R1-30	Aquifer influence coefficients for Carter-Tracy aquifer representation
R1-31	Average or "effective" aquifer properties for Carter-Tracy calculations
R1-32	User specified aquifer influence functions
R1-33	Modification of aquifer influence coefficients
I-1	Control parameters for initializing concentrations (including number of radioactive components) and natural flow

Reference No.	Enter
I-2	Initial concentrations
I-3	Resident aquifer fluid velocity
I-4	Radioactive component concentration data
R2-1	Control parameters for entering recurrent data
R2-2	Solution technique
R2-3	Wellbore calculation iteration parameters
R2-4	Number of wells
R2-5 and R2-6	Well rates
R2-7	Well description
R2-8	Surface pressures at the wellbores
R2-9	Number of radioactive source/sinks
R2-10	Radioactive source data
R2-11	Numerical solution iteration parameters
R2-12	Time change, time step data
R2-13	Output control
R2-14 to R2-17	Contour maps data
P-1	Number of wells for which plots are desired
P-2 to P-4	Data for plots
M-1 to M-7	Maps from restart records

CHAPTER 4. PATHWAYS TO MAN MODEL

4.1 Introduction

4.1.1 The Model

The Pathways to Man Model is the bridge between the Groundwater Transport Model and the Dosimetry Model. The purpose of the model is to represent the physical and biological processes that result in the transport of nuclides through the earth's surface environment and in man's eventual exposure to these nuclides. For each nuclide, the Groundwater Transport Model provides the following input to the Pathways to Man Model:

1. Concentration of nuclide in aquifer discharge
2. Rate of aquifer discharge
3. Location of aquifer discharge.

In turn, the Pathways to Man Model provides the following input to the Dosimetry Model:

1. Rate of nuclide ingestion
2. Rate of nuclide inhalation
3. Physical data needed to calculate external exposure.

The Pathways to Man Model is not intended as a model for a specific site. Instead, it is a model (or, more correctly, a collection of models) that can be modified to represent different candidate disposal sites. Many factors are involved in determining the characteristics of a particular disposal site, and it must be possible to incorporate these into any model used to predict the results of a nuclide release at that site. Factors that affect the distribution of a nuclide release include surface topography, surface and near-surface hydrology, climatic conditions, and location (or locations) of the release. Other factors that affect the importance of the release include population distribution, agricultural practices, and dietary patterns. Characteristics such as the preceding can vary greatly between disposal sites and, indeed, within the area surrounding a specific site. In the following, a model is presented which can be adapted by the user to the characteristics of the particular site under consideration.

In representing a process, it is important to select a model and a time scale which are appropriate for the situation under consideration. For the transport of nuclides to man, there are two processes involved with distinctly different time scales. The first process is the long-term distribution and accumulation of nuclides in the environment. Nuclide release to, distribution through, and removal from the environment will generally be very slow. It could take from hundreds to thousands of years for a nuclide release to reach its maximum concentration or distribution. Such movement must be represented by a model which emphasizes the dominant features in nuclide distribution over an extended time period. The second process is the movement of nuclides

from the environment to man. Here, the time scale is much shorter, and movement must be represented by a model which emphasizes the dominant features in the food chain leading to man. Therefore, the Pathways to Man Model is divided into two submodels. One of these, the Environmental Transport Model, represents the long-term distribution and accumulation of nuclides in the environment. The other, the Transport to Man Model, represents the movement of nuclides from the environment to man. The relationship of the submodels is shown in Figure 4.1.1.

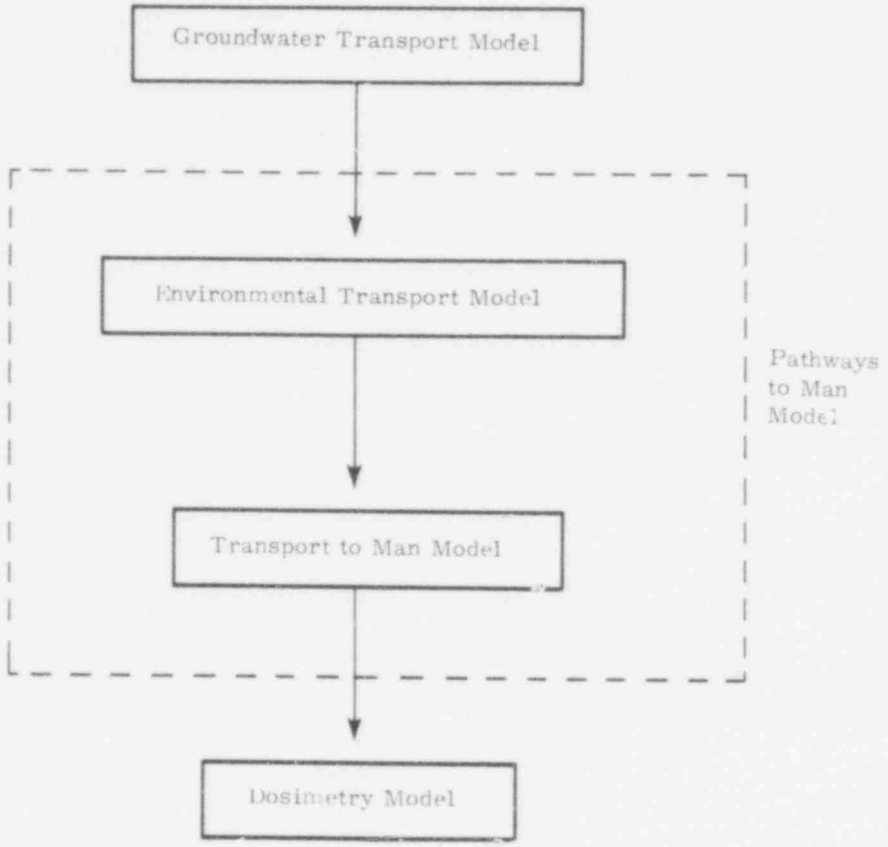

Figure 4.1.1. Division of Pathways to Man Model

4.1.2 The Environmental Transport Model

Many requirements are placed on the Environmental Transport Model. It must be able to represent the diverse features which influence the movement of nuclides through the surface environment. Such features include water flow patterns, climatic conditions, chemical properties of soil, sediment or water, erosion rates, agricultural practices, and the existence of sinks that tend to remove nuclides from the biosphere. It must be sufficiently adaptable to represent both the area initially affected by a nuclide release and the total area eventually affected by such a release. This requires flexibility with respect to the diversity and the size of the area modeled. It must be able to represent a number of concurrent processes which take place at different rates and to predict the eventual outcome of these interacting processes. Such need exists since the accumulation and distribution of nuclides in and through the environment is a lengthy process involving both

nuclide decay and many interacting forms of physical transport. The preceding requirements and many others result from the diversity of both potential disposal sites and possible patterns of nuclide release. The result is that it is not possible to present one fixed model for the surface transport of nuclides. Instead, a model is presented that allows and, indeed, requires user participation to fit it to the particular situation under consideration.

In the Environmental Transport Model, nuclide movement is represented with a compartment model. With this approach, nuclides in the area under consideration are divided into a number of "compartments," and then nuclide movement between these compartments is represented by a system of differential equations. The basic idea is to place nuclides which are in physical regions with different characteristics (hydrologic, climatic, chemical, ...) in different compartments and then to determine the distribution which results from the various possible nuclude movements between these compartments. Such movement could result from the physical transport of a nuclide from one region to another region or from the decay of a nuclide to its daughter. Solution of the system of differential equations which represents these movements, yields nuclide distribution in the area under consideration.

The flexibility of this approach comes from the freedom of the user in selecting the compartments and the rates of nuclide movement between the compartments. These are selected for the particular site, the particular pattern of nuclide discharge, and the particular time span under consideration.

A detailed description of the Environmental Transport Model is contained in Section 4.2. There, an explanation of what is meant by compartment and compartment model is presented. Further, a technique for determining the compartments needed to model a nuclide discharge is presented in Section 4.3.

4.1.3 The Transport to Man Model

As with the Environmental Transport Model, many requirements are placed on the Transport to Man Model. It must be adaptable to the numerous factors that determine both the area affected by a nuclide release and the consumption of food produced within this area. The areas affected by a nuclide release can vary greatly in size and, in turn, support a limited food production, no food production, or a great variety of food production. Similarly, a population living in or near an area affected by a nuclide release may receive some, none, or all of its food from this area. Further, individuals may have widely varying dietary habits.

To represent this diversity, a model based on simple food chains and concentration factors is presented. With this approach, food chains which originate in an affected area and lead to man are determined. The nuclide concentration in an affected food type is then determined by the use of concentration factors. The amount of nuclide consumed follows from the amount of food consumed and the nuclide concentration in that food. This approach is adaptable as it allows the model user

to determine the type, amount, and origin of food consumed by a population. Such determinations are made on the basis of the Environmental Transport Model, which indicates the area affected by a release and the resultant nuclide concentrations in water and soil within that area. Further, the amount of each nuclide inhaled is determined from the amount of nuclide-containing soil suspended in the air. External exposure is not calculated in the Transport to Man Model. Instead, information on environmental nuclide concentration is provided by the Environmental Transport Model to the Dosimetry Model, where such calculations are made.

A detailed description of the Transport to Man Model is contained in Section 4.4. Further, possible food chains leading to man are discussed and selected tables of concentration factors are presented.

4.2 Environmental Transport Model

4.2.1 Compartment Models

As discussed in the introduction to this chapter, a general and adaptable model is needed to represent the transport and distribution of nuclides through the environment. It must be possible to fit the model to the surface environment of different candidate disposal sites and to adapt it to the surface discharge patterns that are indicated by the Groundwater Transport Model. Further, the capability must exist to incorporate areas into the model which are not initially affected by a nuclide release but may eventually be affected because of surface transport.

To permit such flexibility, a compartment model is used to represent environmental transport. With this type of model, nuclides in different areas are placed in different compartments, and the nuclide distribution which results from movements between these compartments is then determined. Specifically, the user divides the nuclides involved into a suitable number of compartments, determines the rate of nuclide flow between these compartments, and then represents the movement of nuclides by a system of differential equations in which each unknown function denotes the amount of a nuclide in a compartment. The exact number and form of these compartments as well as the nuclide movements between them must be determined by the model user on the basis of a careful assessment of the problem to be solved. Factors influencing such an assessment include hydrologic, ecologic, climatic, and demographic characteristics of the region being modeled, chemical and physical properties of the nuclides involved, and detail and accuracy desired in model predictions. External input of nuclides into the region modeled from the Groundwater Transport Model or some other source can take place into any or all of the compartments. Indeed, it is assumed that the need to properly represent such input will influence compartment selection.

Some comment with respect to the use of the word "compartment" is needed to avoid confusion. This expression is not necessarily used in reference to containment in a physical area. When nuclides are referred to as being in a particular compartment, it means that they belong to a particular set. A movement between compartments denotes a change in set membership and not

necessarily a change in physical location. Physical location may be used to determine if a nuclide is in a compartment. In such a situation, atoms of the same nuclide might be placed in different compartments on the basis of their physical location; a change in compartment membership would correspond to a change in physical location. However, other criteria may also enter in. For example, each nuclide in a decay chain might be placed in a different compartment; then, decay would result in the movement of a nuclide out of one compartment and into another compartment even though there was no change in physical location.

In general, if M compartments are selected, then there are M functions $f_i(t)$, $i = 1, 2, \ldots, M$, such that $f_i(t)$ represents the amount of nuclide present in compartment i at time t. Flows between compartments and out of the system are assumed to be linear. That is, if i and j are distinct integers between 1 and M, then there exists a nonnegative constant a_{ij} such that the rate of nuclide flow from compartment i to compartment j at time t is given by $a_{ij}f_i(t)$. Further, if i is an integer between 1 and M, then there exists a nonnegative constant k_i such that the rate of nuclide flow from compartment i to locations out of the system at time t is given by $k_i f_i(t)$. For convenience, the constants a_{ij} and k_i are referred to as rate constants. Finally, for each compartment, there is a function $R_i(t)$ which represents the rate of nuclide input to that compartment from the Groundwater Transport Model or some other source. The resultant system of differential equations for nuclide transport is

$$f_i'(t) = R_i(t) + \sum_{j=1}^{i-1} a_{ji} f_j(t) - \left[k_i + \sum_{\substack{j=1 \\ j \neq i}}^{M} a_{ij} \right] f_i(t) + \sum_{j=i+1}^{M} a_{ji} f_j(t) \qquad (4.2.1)$$

for $i = 1, 2, \ldots, M$, where the convention

$$\sum_{j=1}^{0} a_{ji} f_j(t) = \sum_{j=M+1}^{M} a_{ji} f_j(t) = 0$$

is adopted for notational convenience.

Mathematically, no serious complications in representation or solution are introduced if the coefficient a_{ij} are considered to be functions of time rather than constants. Then, the rate of movement at time t from compartment i to compartment j would be $a_{ij}(t)f_i(t)$. Whether the coefficients are assumed to be constants or functions of time, the real problem is determining values for them which are appropriate for the particular situation being modeled. For convenience, the coefficients are referred to as constants in this report. However, in a given situation, it is the modeler's responsibility to decide if these coefficients should be treated as constants or as

functions of time. Unfortunately, although it is easy to argue that the coefficients should be functions, it is much more difficult to obtain the environmental information needed to define them in such a manner. Thus, in deciding how to define the coefficients, it is necessary to consider both the computational results desired and the environmental information available. The preceding remarks also apply to the coefficients k_i.

Compartment models have been widely studied and used; many readers are undoubtedly familiar with them. An extensive literature is available, and additional background can be found in reviews by Atkins,[4.1] Shipley and Clark,[4.2] Rescigno and Segre,[4.3] Rescigno and Beck,[4.4] Sheppard,[4.5] Jacquez,[4.6] Bernhard,[4.7] Bernhard et al,[4.8] and Funderlic and Heath.[4.9] The series on systems analysis and ecology edited by Patten[4.10] contains numerous studies employing compartment models.

4.2.2 Related Transport Studies

There are many models for the environmental transport of nuclides. A recent paper by Hoffman et al.[4.11] lists 83 computer codes that have been developed to assess the impact of nuclides released to the environment. A review is also provided by Strenge et al.[4.12] However, most models for environmental nuclide transport are designed to represent atmospheric transport. For geologic waste disposal, such transport is of limited importance. It is believed that the environmental transport of nuclides will be water dominated. Thus, models for water-related transport of nuclides are of primary interest.

A review of the existing water transport models indicates that they have been constructed to represent releases from nuclear facilities. Here, releases are essentially from point sources and involve nuclides with relatively short half-lives. The primary interest is to determine dilution due to radioactive decay or movement through increasing volumes of water. Limited emphasis is placed on potential accumulation of nuclides in the environment. Although single nuclide decay is considered, there is no treatment of decay chains. To insure that predicted water concentrations are conservative, there usually is no treatment of nuclide sorption by solids. For nuclides with short half-lives, this is probably acceptable since nuclides attached to stationary sediments can be considered in a sink from which they are soon removed by decay. The important point is not to underestimate their concentration in water. However, for nuclides with long half-lives, this ignores a potential area of concentration. Discharges are generally assumed to go directly into water, where the associated water system acts much as a pipe with little nuclide movement between the system and parallel areas of possible overbank deposition. Again, this is probably acceptable for nuclides with short half-lives but is questionable for nuclides with long half-lives that can be selectively deposited due to sorption on sediments. Since nuclide releases are assumed to go directly into a homogeneous water system and to remain there, these models are constructed with little capacity to incorporate environmental diversity.

A model which represents the movement of nuclides discharged from a geologic waste facility must be able to predict the cumulative results of a slow and possibly very small release rate which involves nuclides with long half-lives and radioactive daughters. Such releases would not necessarily enter large water bodies with extensive potential for dilution or turnover. Indeed, there is considerable possibility that such releases would occur into small or intermittent water bodies. Release could and probably would occur in a diffuse manner and in one or more areas. A large or small area might be affected by a release. This applies to both the area initially affected by the discharge of a nuclide-bearing aquifer and the total area eventually affected because of surface transport.

Because of considerations of the type presented in the two preceding paragraphs, it was decided that existing environmental transport models were not suitable for the transport problems that arise when the geologic disposal of nuclear waste is considered. As has already been discussed, the decision was made to use compartment models to represent environmental transport since such models can be adjusted to include many situations that are not (and probably do not need to be) included in existing models for the transport of reactor effluent.

For comparison, several related studies are discussed. Computational procedures used by the Nuclear Regulatory Commission to determine the distribution of nuclides released to aquatic environments are presented in several publications.[4.13,4.14] The models included in these publications are not constructed to represent the situations that are encountered in modeling the long-term consequences of nuclide release from geologic disposal sites. Included in the character of these models are (a) releases begin at fixed and known points, (b) partial differential equations are used to determine concentration gradients in the receiving body of water, (c) the region affected by a release is assumed to be homogeneous, and (d) although decay is included, there is no treatment of extended decay chains. The emphasis is on representing the dilution of a release. Long-term consequences (i.e., nuclide reconcentration) are not considered. Thus, there is no treatment of sorption, buildup in sediments, or migration in and out of stream channels.

In the Reactor Safety Study,[4.15] an extensive methodology is developed to determine the consequences of reactor accidents. However, the situation there is very different from the one with which we are concerned: (a) Release is essentially instantaneous and from a single point source, (b) release is airborne, and (c) nuclides with relatively short half-lives are dominant. In contrast, the following characteristics are associated with geologic waste disposal: (a) Release to the environment takes place over a long period of time and possibly over an extended area, (b) release is waterborne, and (c) nuclides with long half-lives are involved.

Of the environmental transport codes, the greatest similarity probably exists between the HERMES code[4.16] and the Environmental Transport Model. In HERMES, releases are considered from many sources in a diverse region. River systems are divided into homogenous sections and flow is assumed to be from section to section. A finite different model is used to represent transport. Unfortunately, the description of the water transport model (Reference 4.15 pp 73-80) lacks detail, and it is difficult to determine exactly what assumptions and models underlie the code's construction.

Another similar approach is presented by Booth.[4.17] By linking a sequence of the four compartment models used by Booth, one could produce a model similar to the Environmental Transport Model.

4.2.3 An Example

A simple compartment model involving transport of a single nuclide is presented for illustration. The nuclide is assumed to be present in three compartments as is schematically represented in Figure 4.2.1. This could correspond to a number of different physical situations. For example, the situation represented might be a lake, where the nuclides dissolved in lake water are in Compartment 1, the nuclides attached to suspended sediments are in Compartment 2, and the nuclides in sediments deposited on the lake bottom are in Compartment 3. As another example, the situation represented might be a river valley, where the nuclides in the river channel are in Compartment 1, the nuclides in the river flood plain are in Compartment 2, and the nuclides in the shallow ground water beneath the river and its flood plain are in Compartment 3.

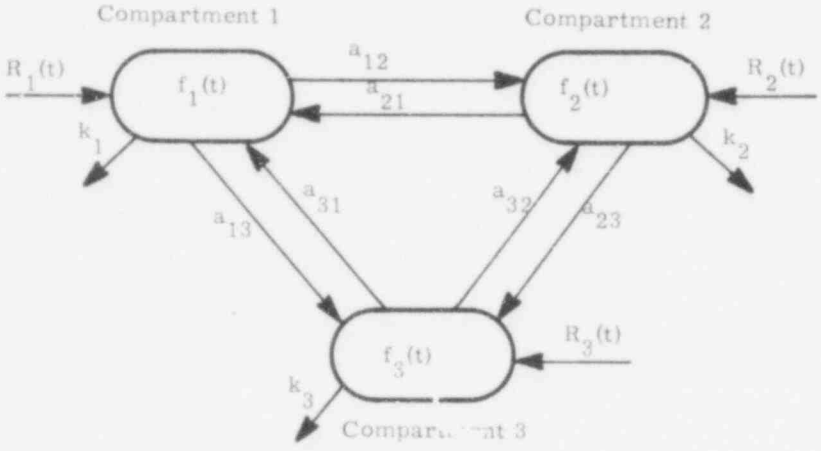

Figure 4.2.1. A Compartment Example for a Single Nuclide

In the example diagrammed in Figure 4.2.1, $f_1(t)$, $f_2(t)$, and $f_3(t)$ represent the amount of nuclide at time t in Compartments 1, 2, and 3, respectively. Further, $a_{12}f_1(t)$ and $a_{13}f_1(t)$ represent the rate of movement at time t from Compartment 1 to Compartments 2 and 3, and $k_1f_1(t)$ represents the rate of movement from Compartment 1 out of the system under consideration. For example, the movement represented by $k_1f_1(t)$ might be due to downstream movement or radioactive decay. The rate constants a_{21}, a_{23}, a_{31}, a_{32}, k_2, and k_3 and the corresponding rates $a_{21}f_2(t)$, $a_{23}f_2(t)$, $a_{31}f_3(t)$, $a_{32}f_3(t)$, $k_2f_2(t)$, and $k_3f_3(t)$ have similar meanings. The functions $R_1(t)$, $R_2(t)$, and $R_3(t)$ represent rates of nuclide input for Compartments 1, 2, and 3 from a source outside the system being modeled. Normally, this source would be the Groundwater Transport Model. The system of differential equations representing the situation portrayed in Figure 4.2.1 is

$$f_1'(t) = R_1(t) - (a_{12} + a_{13} + k_1)f_1(t) + a_{21}f_2(t) + a_{31}f_3(t)$$

$$f_2'(t) = R_2(t) + a_{12}f_1(t) - (a_{21} + a_{23} + k_2)f_2(t) + a_{32}f_3(t) \qquad (4.2.2)$$

$$f_3'(t) = R_3(t) + a_{13}f_1(t) + a_{23}f_2(t) - (a_{31} + a_{32} + k_3)f_3(t) .$$

For simplicity, this example has been presented with only three compartments. For most situations, it is anticipated that a greater number of compartments will be needed for adequate representation.

4.2.4 Compartment Models with Decay

Thus far, no reference has been made to the treatment of decay chains. Since the Environmental Transport Model is used to represent the long-term accumulation and distribution of nuclides, it is necessary to consider such chains. To ignore them over extended periods of time could result in misrepresentations of nuclide transport. Fortunately, it is relatively easy to incorporate decay chains into the compartment model framework. This is accomplished by considering compartments that contain different nuclides and allowing two types of movement between the compartments: movement due to physical transport and movement due to decay.

Specifically, the representation of decay chains is achieved in the following manner. First, the compartmentalization needed to model the physical transport of a single nuclide is determined. Then, this compartmentalization is replicated for each nuclide in the decay chain. Thus, if M compartments are needed to represent the movement of a single nuclide and there are N nuclides in the decay chain, then N replicates of the original M compartments are formed. This produces a total of MN compartments. For each compartment needed to model the transport of a single nuclide there are now N compartments, where each of these replicated compartments corresponds to one nuclide in the decay chain under consideration. There is physical movement for each nuclide between the various compartments which correspond to that nuclide. These movements can be represented by appropriate rate constants. However, when decay occurs, there is movement from the compartment containing the parent nuclide to the corresponding compartment containing the daughter nuclide. Here, the rate constant is the decay constant of the parent nuclide. There has been no physical movement, but there is a change in compartment membership since a different nuclide is now present. When all of these interactions are incorporated into a single system of differential equations, a system of the same general form as that represented in Eq. 4.2.1 is produced with the exception that there are now MN equations rather than M equations.

4.2.5 An Example with Decay

The treatment of decay chains is illustrated by expanding the example diagrammed in Figure 4.2.1. For convenience, assume the same physical setting is being modeled. Further, assume a decay chain containing two nuclides is under consideration. The three compartments

needed to represent the movement of a single nuclide are replicated for the two nuclides in the decay chain. This produces the six compartments diagrammed in Figure 4.2.2. In this figure, each of the flows present in Figure 4.2.1 is represented by a solid arrow. However, it should be recognized that corresponding rate constants are not necessarily the same for corresponding flows of the two nuclides since different nuclides can have different chemical and physical properties. In addition to physical movement between compartments associated with a particular nuclide, there is also movement due to decay between compartments associated with the different nuclides. This movement is represented by a dashed line in Figure 4.2.2. Specifically, the decay of a nuclide in Compartment 1 results in the movement of a nuclide from Compartment 1 to Compartment 4, the decay of a nuclide in Compartment 2 results in the movement of a nuclide from Compartment 2 to Compartment 5, and the decay of a nuclide in Compartment 3 results in the movement of a nuclide from Compartment 3 to Compartment 6.

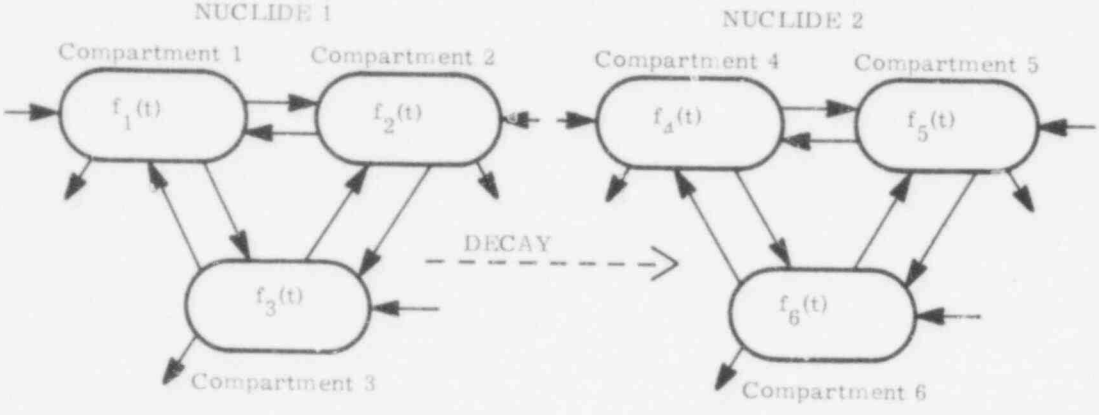

Figure 4.2.2. A Compartment Example for a Decay Chain with Two Nuclides

The system of differential equations representing the situation portrayed in Figure 4.2.2 has the same form as the system in Eq 4.2.1. Here, i runs from 1 to 6 since there are six compartments. Many of the rate constants in this representation are zero. When this is taken into account, the system of equations simplifies to

$$
\begin{aligned}
f_1'(t) &= R(t) - (a_{12} + a_{13} + a_{14} + k_1)f_1(t) + a_{21}f_2(t) + a_{31}f_3(t) \\
f_2'(t) &= R_2(t) + a_{12}f_1(t) - (a_{21} + a_{23} + a_{25} + k_2)f_2(t) + a_{32}f_3(t) \\
f_3'(t) &= R_3(t) + a_{13}f_1(t) + a_{23}f_2(t) - (a_{31} + a_{32} + a_{36} + k_3)f_3(t) \\
f_4'(t) &= R_4(t) + a_{14}f_1(t) - (a_{45} + a_{46} + k_4)f_4(t) + a_{54}f_4(t) + a_{64}f_6(t) \\
f_5'(t) &= R_5(t) + a_{25}f_2(t) + a_{45}f_4(t) - (a_{54} + a_{56} + k_5)f_5(t) + a_{65}f_6(t) \\
f_6'(t) &= R_6(t) + a_{36}f_3(t) + a_{46}f_4(t) + a_{56}f_5(t) - (a_{64} + a_{65} + k_6)f_6(t) \ .
\end{aligned}
\tag{4.2.3}
$$

403 192

As before, a_{ij} represents the rate constant for the movement of a nuclide from Compartment i to Compartment j. The compartments corresponding to Nuclide 1 and Nuclide 2 are coupled together by the decay of Nuclide 1 to Nuclide 2. This coupling is affected by the rate constants a_{14}, a_{25}, and a_{36}, which link Compartments 1, 2, and 3 to Compartments 4, 5, and 6, respectively. If there was no decay connecting Nuclide 1 and Nuclide 2, then these constants would be zero and the system in Eq. (4.2.3) would reduce to two independent systems, each of the form in Eq (4.2.2).

More complicated situations can be handled in a similar manner. With simple modifications, this method of compartment construction can be extended to longer decay chains and to branched decay chains. Such constructions are discussed in greater detail in Section 4.3.

4.2.6 Advantages and Disadvantages of Compartment Models

There are many advantages associated with the use of compartment models. These models are adaptable. The user can construct a model on the basis of the diversity of the region under consideration. Changes in regional characteristics can be represented by suitable compartmentalization. If necessary, time-dependent rates of change and nuclide input can be incorporated into the model. These models are widely studied and many individuals are familiar with them. Numerical methods exist to solve the differential equations that arise. The asymptotic behavior of such equations is known.

There are also disadvantages associated with the use of compartment models. They treat the nuclides in each compartment as being distributed in a "homogeneous" manner. Thus, it is difficult to represent continuously varying nuclide distributions. There may be numerical problems with the system of differential equations used to represent transport; in particular, the system may be stiff. Finally, it is necessary to determine the compartments and define the rates of flow between them.

The necessity of determining the compartments and the associated rate constants for nuclide flow between the compartments is a major problem. So far, it has been proposed that compartment models be used to represent the environmental transport of nuclides but no method for this determination has been presented. Without such a method, the value of the proposal to use the model is greatly reduced. A technique for determining the needed compartmentalization is presented in the next section. It is not suggested that this technique is general enough to cover all possible situations. However, it should be sufficiently general and flexible to model the surface flow of nuclides in most of the situations that it will be encountered in the study of geologic waste disposal.

4.3 A Technique for Compartment Definition

4.3.1 Need for Technique

As indicated in Section 4.2, compartment models are very flexible. By proper definition of compartments and flow rates between compartments, many different situations can be represented

by the same mathematical model. However, to obtain this representation the modeler must be able to define the compartments and the associated flows. The utility of compartment models for representing nuclide transport would be greatly reduced if such definitions had to be developed independently for each situation considered. Though the variability between potential disposal sites is too great to define a single, well-structured model which fits all possible situations, it is possible to present a technique for adapting the basic compartment model to different situations. One such technique is presented in this section; however, other techniques are certainly possible.

The basis of the technique is a method for systematically defining the compartments and the flows between the compartments. In particular, the region to be modeled is divided into a number of distinct geographic areas and various movements of water and solid material between these areas are defined. Further, it is assumed that nuclides are uniformly distributed in each of these geographic areas and that movements of water and solid material are responsible for nuclide transport into and out of these areas. From the preceding assumptions and the possible movements of water and solid material, a system of differential equations representing nuclide transport is then derived. The application of the technique requires significant user participation; otherwise it would be too rigid to incorporate both the physical diversity of the area being modeled and the data needs of the modeler. Though the technique does not free the user from responsibility in the definition of compartments, it does add structure and guidance to the process.

The technique for compartment definition presented in this section was selected for two reasons. First, it can be used to develop models of many different situations. Second, its data requirements are reasonable. With regard to data requirements, it is emphasized that this technique does not develop a model to predict the movement of water and solid material. Instead, it assumes that the directions and magnitudes of such movements are known and then uses their values to determine the movement and distribution of nuclides. Values for movements of water and solid material must be determined from additional models, empirical data, educated guesses or other sources. It is felt that decoupling the model for nuclide transport from models for water and sediment transport adds to both the simplicity and the flexibility of the technique.

The technique is developed under certain assumptions (See Section 4.3.8) about the nature of nuclide movement; for a given situation, these assumptions may or may not be satisfied. The user cannot employ the technique blindly and assume that, if the required information is supplied, then meaningful predictions concerning nuclide transport will be produced. For each situation to which the technique is applied, the assumptions that underlie its construction must be satisfied. If these assumptions are not satisfied, then the setting to which the technique is applied must be reformulated so that they are satisfied. The technique is constructed to permit many modifications to make the developed model consistent with the setting under consideration. However, it is possible that the technique will not apply to a given situation; if so, some other method must be used to define the needed compartmentalization. Indeed, since no model can fit all potential situations, it is possible that a compartment model will not be appropriate for a particular situation; then, some other modeling technique will have to be used. Fortunately, compartment models together with the

technique for compartment definition now presented provide an approach of wide application for the representation of nuclide transport. Even if a situation can be represented ultimately by a model more appropriate for its particular characteristics, compartment models and the technique presented here for compartment definition provide a means of producing an initial representation and assessment of nuclide transport.

The following outlines the remainder of Section 4.3. In Sections 4.3.2 and 4.3.3, a technique is presented for defining compartments and potential nuclide movements between compartments. In Sections 4.3.4, 4.3.5, and 4.3.6, the information requirements of the technique are listed. In Sections 4.3.7 through 4.3.12, the system of differential equations representing nuclide movement is derived. Finally, in Section 4.3.13, the computer program which implements the technique is discussed briefly.

4.3.2 Basis of Technique

The basis of the technique is a hierarchical division of the area potentially affected by the discharge of a contaminated aquifer. This division is derived from water flow patterns and other factors influencing the surface and near-surface movement of nuclides. The area is divided into a number of nonintersecting, three-dimensional, geographic zones. Further, each zone is divided into the following nonintersecting subzones:

1. Groundwater
2. Soil
3. Surface water
4. Sediment.

The region designated by the zone is the union of the regions that constitute its four subzones. Further, each of the subzones is assumed to have two phases:

1. Liquid (water)
2. Solid (a material that sorbs nuclides).

A zone and its associated subzones are selected so that each subzone can be considered "uniform" in some sense. This is because nuclide flows through the system are considered to take place from subzone to subzone and, in deriving a representation for these flows, it is assumed that nuclides are evenly distributed in each subzone and that physical and chemical properties are uniform throughout each subzone. The nuclides are assumed to move between various subzones in a zone. Further, the same general pattern of movement between subzones is assumed to take place within each zone. However, nuclide movement from zone to zone is assumed to occur only from surface-water subzone to surface-water subzone. As will be shown, these assumptions enable one to systematically construct a representation of the movement of nuclides through a given area.

Two examples of zone selection are presented in Figures 4.3.1 and 4.3.2. As has been emphasized, the selection of the zones is the responsibility of the user and depends on the site being modeled.

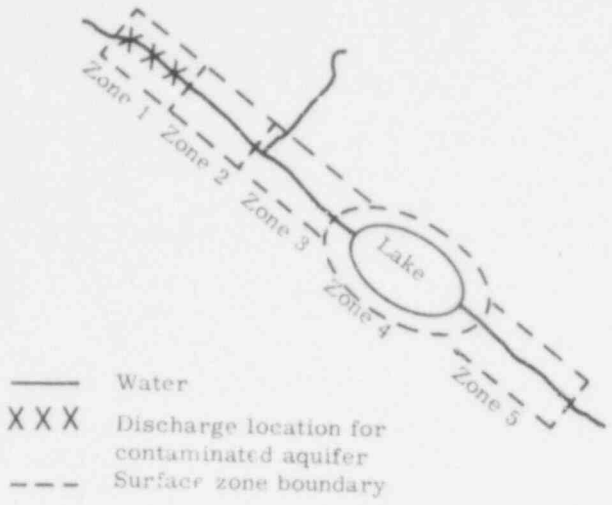

Figure 4.3.1

Zone Selection Example with Five Zones. Each zone corresponds to a stretch of river. The nuclides enter with the discharge of a contaminated aquifer in or near the stream and then travel down the stream system. The zones are selected to correspond to changes in the hydrologic properties of the stream system. The zones hug the river since most nuclides would stay in the river or in the river's sediments and flood plain.

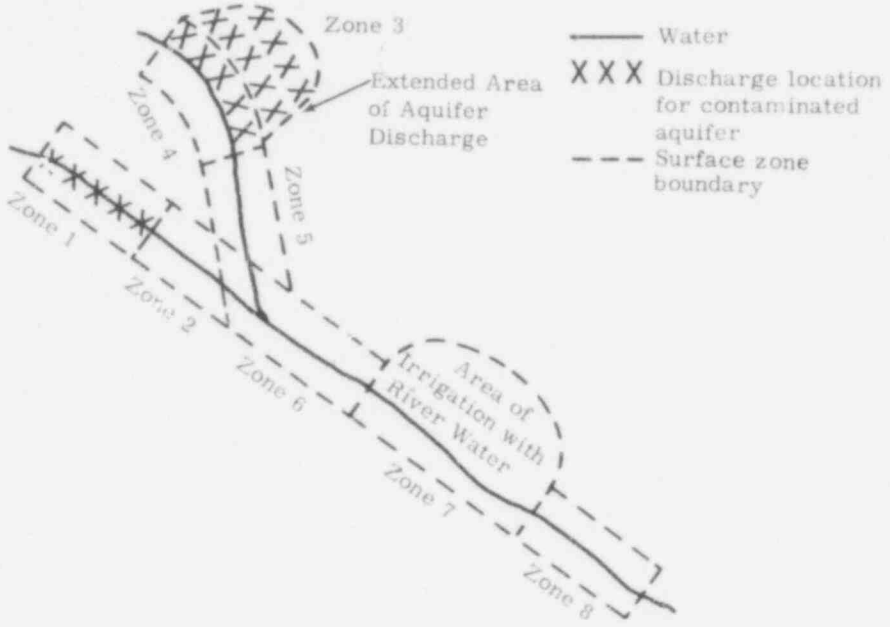

Figure 4.3.2. Zone Selection Example with Eight Zones. Zones 1, 2, 4, 5, 6, and 8 correspond to stretches of river. Zone 3 encompasses an area of surface aquifer dishcarge and Zone 7 encompasses a stretch of river plus an adjacent area of land which is being irrigated with river water.

The subzone classifications of groundwater, soil, surface water, and sediment are intended to be suggestive. No attempt is made to give them precise meanings. The regions that they designate vary with the situation being modeled. The division of a zone into subzones is shown schematically in Figure 4.3.3, where arrows represent directions of movement for water and solid material between the subzones of a zone. Nuclide movement should follow the same pattern since it is these flows that dominate nuclide transport.

403 196

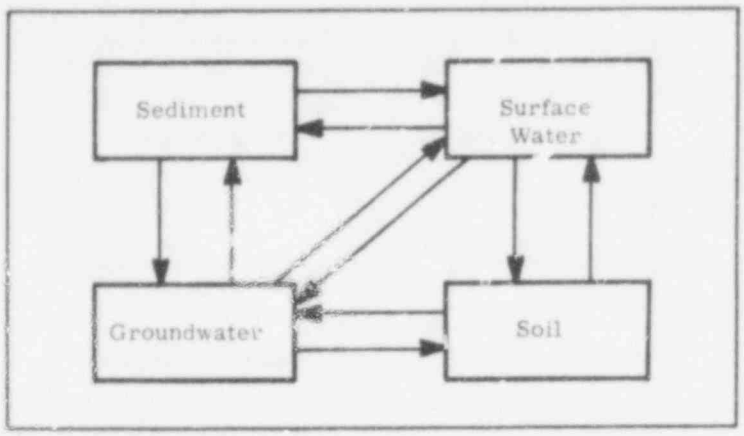

Figure 4.3.3. Division of a zone into Subzones. Arrows represent potential directions of movement for water and solid material between the subzones of a zone. Nuclide movement should follow the same pattern since it is these flows that dominate nuclide transport.

The general concept designated by each subzone follows. The soil subzone represents the top earth layer. This might be anything from the first few centimetres of surface soil and litter to the first few metres or more of surface material. The ground water subzone is the region lying beneath the soil subzone and possibly beneath the surface water subzone. Thus, the top of the groundwater subzone is essentially defined by the bottom of the soil subzone. The depth of this subzone is whatever is appropriate for the situation being considered. The surface water subzone represents water that is free to move on the zone's surface. Thus, it might refer to a lake, a river, or an estuary. The sediment subzone is material deposited beneath the surface water subzone. Generally, one is not interested in all such depositional material but rather in that material which is capable of sorbing significant amounts of nuclides.

However, the subzones can also be used in manners that bear little relation to their given names. Indeed, it is possible that the use of these names should be dropped. For example, another interpretation is to use the groundwater subzone to represent a second soil layer. Yet another interpretation is to use the groundwater subzone to represent a second sediment layer and to use the soil subzone to represent a third sediment layer. Such representations are possible by suitable selection of the parameters that define the subzones and the flows between them. But, regardless of how the subzones are interpreted, they are treated the same mathematically by the Environmental Transport Model. It is also possible that a given situation might be represented most appropriately with only the surface water and sediment subzones or only the soil, surface water, and sediment subzones. Indeed, a useful extension of the Environmental Transport Model and the computer programs which implement it would be to permit the user to define the number of subzones per zone, to name the subzones, and to select the movements of water and solid between the subzones.

All subzones have a liquid and a solid phase between which the nuclides present in the subzone are partitioned. Thus, the sediment subzone includes not only the solid material deposited beneath the surface water but also the water associated with that material. Similarly, the surface water subzone includes not only free water but also particulate matter suspended in and moving with that water.

With the technique presented in this section, a flow pattern for nuclides is derived from specific information about each subzone. Thus, when a particular situation is modeled, the zones and subzones must be carefully defined and certain required information determined. At this point, the subzones are defined in some unequivocal manner. In doing this, it is necessary to define not only how many zones there are and what their physical boundaries are, but also what is represented by each subzone within a zone. These definitions are generally based on the chemical and physical characteristics of the area being modeled plus other considerations such as quality and form of input from the Groundwater Transport Model, the length of time that surface processes are to be modeled, and the degree of detail desired in calculation results.

Various flows of water and solid material can take place into and out of the subzones. Since water is the major erosional force in most situations, solid materials tend to move in the same direction as water, though generally not at the same rate. It is these flows that move nuclides through a given zone and out of that zone into other zones. Indeed, it is the need to properly represent these flows within whatever time scale is being considered that determines how the zones and subzones are defined in a particular situation. The possible directions of flow between subzones of a given zone are represented in Figure 4.3.3. All flows can involve both water and solid material. However, it is anticipated that flows into and out of the groundwater subzone will normally involve only water. This is because water moving through a porous medium such as soil or rock usually carries little, if any, suspended material. Exceptions are possible; for example, the solid material in the ground water subzone might be in the process of weathering into one of the other subzones. The division of flows between water and solid material is important since nuclides tend to be sorbed on solid material. There is no link indicated between the sediment subzone and the soil subzone in Figure 4.3.3 because material moving between these two subzones must pass through either the surface water subzone or the groundwater subzone as an intermediate step.

Flows between zones involve both water and solid material and are assumed to take place only from the surface water subzone of one zone to the surface water subzone of another zone. Such a pattern of movement is consistent with the assumption that water is the dominant erosional force. This relationship is shown schematically in Figure 4.3.4. Note that the same flows are taking place within each zone but the only link between zones is from surface water subzone to surface water subzone. In describing a zone, it is necessary to specify the zone receiving its outflow. A single zone may receive the outflow of one or more zones.

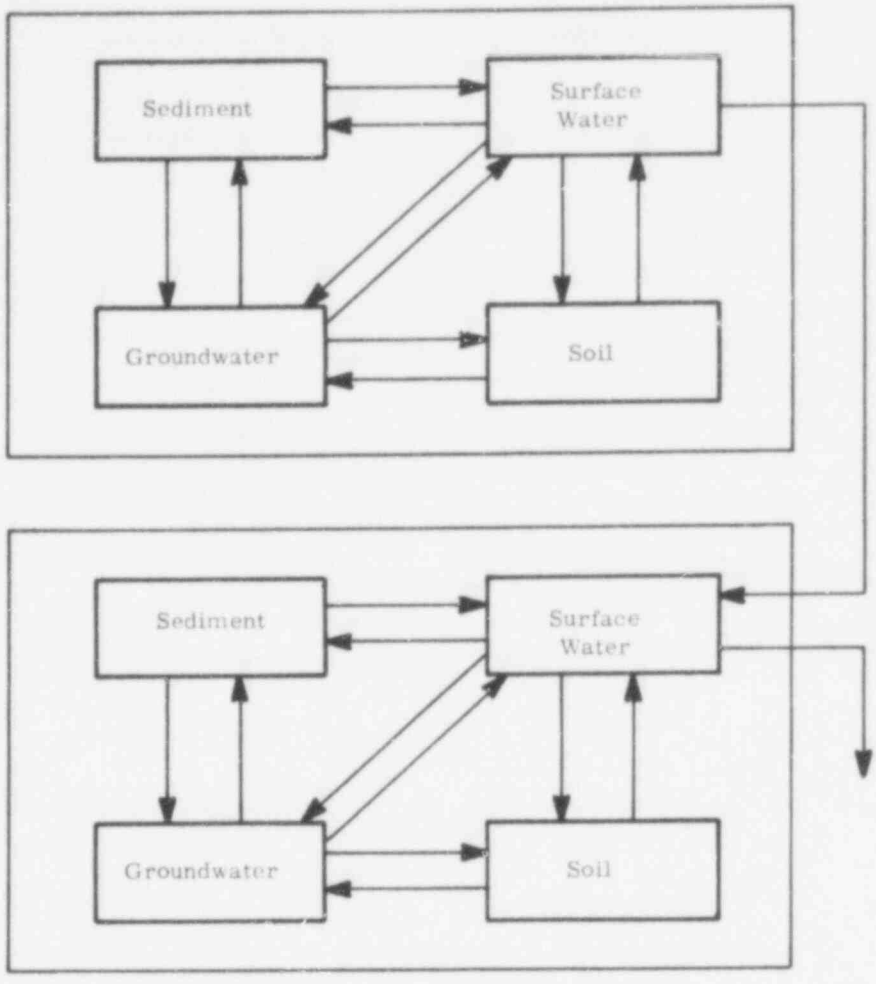

Figure 4.3.4. Interconnecting Flow Between Zones

Some explanation is needed as to why there is no built-in connection between adjacent groundwater subzones. The omission is made for several reasons. First, the Environmental Transport Model represents surface and near-surface transport. It is not intended to represent extensive groundwater transport. Second, most shallow groundwater discharges in the drainage basin that it orginates in. Third, once a contaminated discharge has reached the surface, it is doubtful if its reentry into the groundwater system would cause significant changes in its distribution pattern. (The reader is reminded that another model is used to represent groundwater flow.) Finally, as is discussed later, the Environmental Transport Model has a mechanism built into it whereby additional connections between subzones can be added. Thus, if it is decided that connections between groundwater subzones (or, indeed, between any subzones) are important, then these connections can be easily added to the model.

One additional type of flow out of subzones is also possible. This is the movement of water and solid material out of a subzone and out of the system under consideration. This amounts to movement from a subzone to a sink in that any nuclides associated with the material in this flow

are removed from the system. For example, such a flow might be the movement of water from the groundwater subzone to an area of sufficient depth or remoteness that any nuclides dissolved in the water are unlikely to reenter the biosphere. In Figure 4.3.5, the representation for flows within a zone presented in Figure 4.3.3 is expanded to include flows from subzones to sinks. Here, arrows leaving the box indicate movement of water and solid material out of the system. A similar expansion is also possible for Figure 4.3.4.

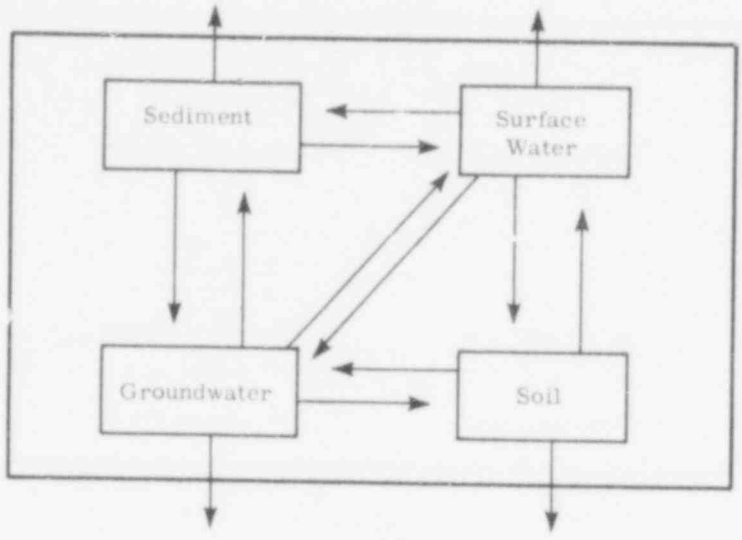

Figure 4.3.5. Physical Flows Out of Subzones. Arrows represent potential directions of movement for water and solid material between the subzones of a zone and out of that zone to a sink. The representation given in Figure 4.3.4 for interconnecting flows between zones can be expanded in a similar manner to include movements out of the system.

Thus far, nothing has been said with respect to flows of material which might move nuclides into the system. The purpose of the model under development is to represent the movement and dispersion of nuclides released to the environment. Therefore, the model is constructed so that an arbitrary (i.e., user-defined) rate of nuclide input is possible into one or more subzones. This rate would normally be determined from the Groundwater Transport Model. Then, the distribution these nuclides which results from the previously discussed movements of water and solid material is determined.

Because of the dominant influence of water in nuclide transport, it is anticipated that the drainage basin (or appropriate subdivisions thereof) will be the basic physical feature underlying the selection of zones in most situations. This is not to imply that each zone will be a complete drainage basin; this is probably not the case. Rather, the intent is to emphasize that water flow patterns and drainage basins are expected to be the unifying factor in the selection of zones for most situations. However, in some situations water flow patterns may not be relevant to the selection of

zones; in such cases, the method of defining compartments presented in this section probably will not apply.

4.3.3 Definition of Compartments

The compartments and associated flow patterns for nuclides are determined in the following manner. If a single nuclide is under consideration, then a compartment is formed for each subzone, and the nuclides in a subzone are assumed to be in the compartment associated with that subzone. The movement of the nuclide into and out of compartments is assumed to have the same pattern as the movement of water and solid material into and out of subzones. Such a situation is represented in Figure 4.3.6 for the movement of a nuclide through a system of M zones, where zone J feeds into zone J + 1 for J = 1, 2, ..., M - 1. In this figure, the dotted lines represent loss of nuclide due to decay. A similar representation is possible for the situation where there is intersecting flow between zones (i.e., two or more zones feeding into the same zone).

The reader is reminded of the distinction between compartments and subzones. Compartments refer to certain sets of nuclides. When a movement takes place between compartments, it does not necessarily mean that there has been a change in physical location. On the other hand, subzones refer to particular physical regions. This distinction is important in the treatment of decay chains, where a given subzone has a compartment associated with it for each nuclide in the decay chain.

If a chain of N nuclides is under consideration, then the compartments and physical flow patterns needed to describe the movement of a single nuclide are replicated N times. If M zones are being used (four subzones each), this produces 4 M compartments for each nuclide and a total of 4 MN compartments for the chain. The physical movement of a nuclide through the 4 M compartments associated with it follows the same pattern of movement shown by the flows of water and solid material through the subzones. However, when decay occurs, the nuclide moves from the compartment associated with the parent to the corresponding compartment associated with the daughter. Such a situation is represented in Figure 4.3.7 for the movement of a chain of N nuclides through a system of M zones. As in Figure 4.3.6, solid lines represent directions of physical movement and dotted lines represent loss of nuclide by decay.

403 201

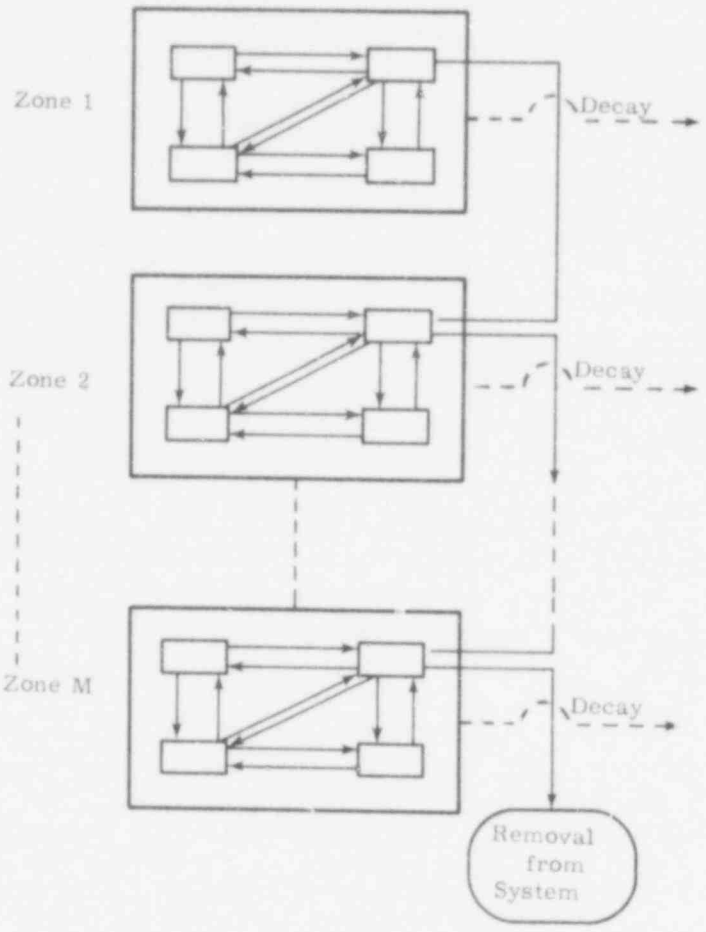

Figure 4.3.6. Compartments and Flows Associated with the Movement of a Single Nuclide Through a System of M Zones. Since a decay chain is not considered in this example, each subzone has one compartment associated with it. Solid lines represent physical flows of nuclides, and dotted lines represent decay. With the exception of the surface water subzone of Zone M, arrows which represent possible physical flows out of the system are omitted. See Figure 4.3.5. Decay acts to remove nuclides from every compartment. It is emphasized that compartment refers to the set of nuclides in a subzone and not to the subzone itself.

403 202

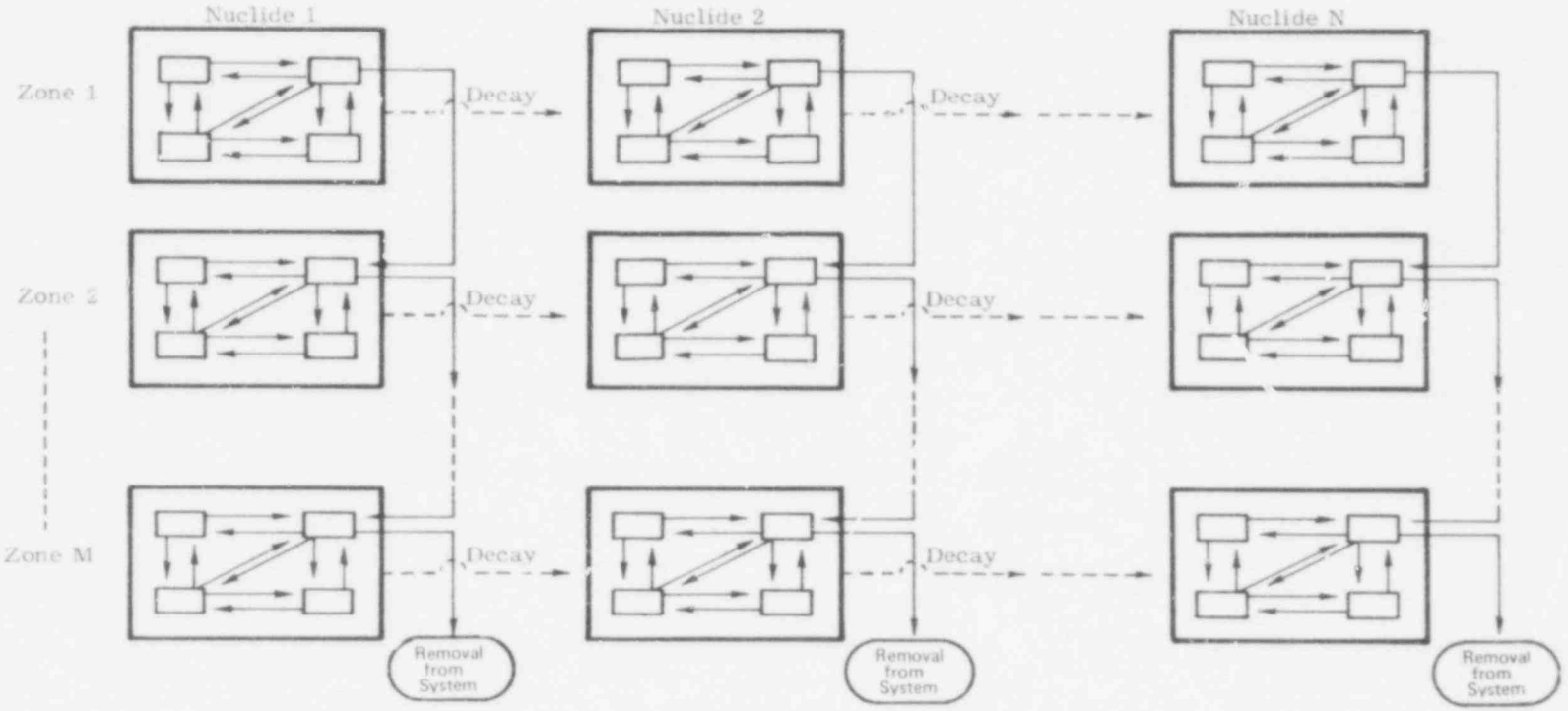

Figure 4.3.7. Compartments and Flows Associated with the Movement of a Chain of N Nuclides Through a System of M Zones. Each subzone has N compartments associated with it. Each nuclide has 4 M compartments associated with it. Solid lines represent physical flows of nuclides, and dotted lines represent decay. With the exception of the surface water subzone of Zone M, arrows which represent possible physical flows out of the system are omitted. See Figure 4.3.5. A numbering system for the compartments is presented in Figure 4.3.8, and a more explicit representation for decay is presented in Figure 4.3.9.

The zones are numbered I = 1, 2, ..., M, and the nuclides in a decay chain are numbered J = 1, 2, ..., N. Further, the numbers K = 1, 2, 3, and 4 are used to represent the subzones groundwater, soil, surface water, and sediment, respectively. The compartments associated with M zones and N nuclides are numbered so that compartment L, where

$$L = 4N(I - 1) + 4(J - 1) + K \ ,$$

is the compartment associated with the presence of Nuclide J in Subzone K to Zone I. This representation is shown in Figure 4.3.8.

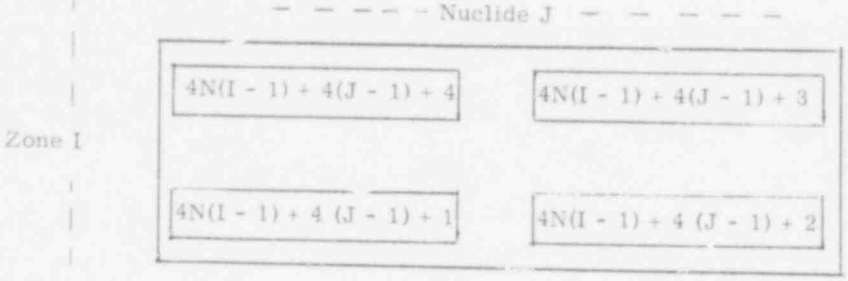

Figure 4.3.8. Numbering of Compartments. For M Zones and N Nuclides, the Number 4N(I - 1) + 4(J - 1) + K is assigned to the compartment associated with the presence of Nuclide J in Subzone K of Zone I.

When a nuclide decays, it stays in the same subzone but changes compartments. In particular, if Nuclide J is in Compartment L and decays to Nuclide J + 1, then the daughter is in Compartment L + 4. More generally, if Nuclide J decays to Nuclide K, then the daughter is in Compartment L + 4(K - J). The pattern of movement between compartments due to decay is represented in Figure 4.3.9.

Zones and nuclides are numbered so that surface water flows from a zone with a lower number to a zone with a higher number and so that decay occurs from a nuclide with a lower number to a nuclide with a higher number with this convention. Compartmentalization can be represented in a systematic manner similar to that shown in Figure 4.3.7, where movement down the page corresponds to physical flow through the area being modeled and movement across the page corresponds to radioactive decay.

In Figure 4.3.7 no branching is represented in either physical flow or decay. Such branchings cause no problems and produce representations of essentially the same form as that shown in Figure 4.3.7. As part of the Environmental Transport Model, a computer program is supplied to determine the compartmentalization associated with a given collection of zones and a given decay chain. Here the input includes the flows of water and solid material between subzones and the decay patterns of the chain. From this information and certain additional information about the subzones,

all compartments and associated rates of flow are determined. If branchings occur, they are properly incorporated into the compartments and the flows between compartments.

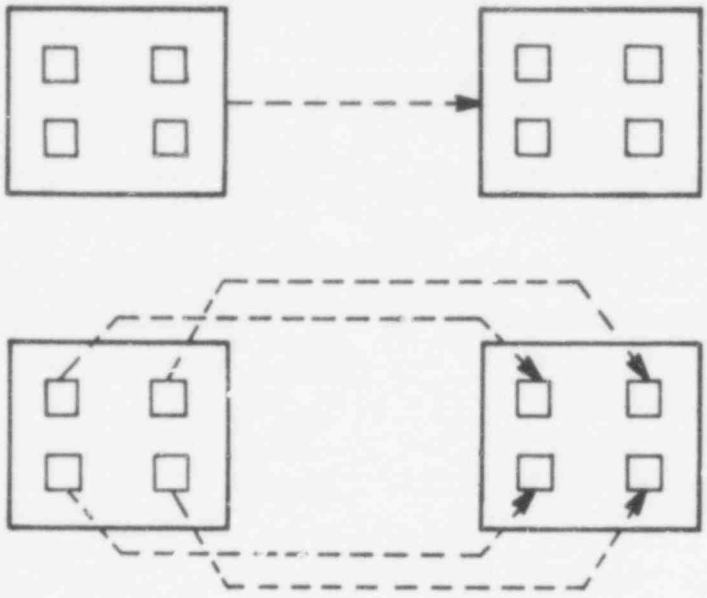

Figure 4.3.9. Representation of Decay. The representation for movement between compartments due to decay in the upper diagram is an abbreviation for the more detailed representation below it. The nuclides are staying in the same subzones but changing compartments. The lines representing physical flow are omitted to reduce clutter.

The technique for defining the compartments and the flows between compartments has now been presented. However, only potential directions have been determined for nuclide flow. The actual values (i.e., rate constants) for these flows have not been determined. Since these flows depend on properties of the subzones, additional information is required before they can be defined. The physical information needed to define each subzone is presented next. Then, under certain assumptions as to the nature of the transport processes, the rates of nuclide movement between the compartments defined in this section are derived. Whenever possible, the notation used in the following sections is consistent with the notation used in computer programs which implement the technique under presentation.

4.3.4 Data Requirements for Subzones

The basic physical information required for each subzone is listed in this section. These physical characteristics of the various subzones are used in determining rates of nuclide movement. For convenience, this information is presented for each subzone through the use of an array of the form Z(P, K, I), where I denotes the zone, K denotes the subzone and P denotes the particular physical characteristic being defined.

For Zone I, the following information is required on the groundwater subzone (i.e., Subzone K = 1):

Z(1, 1, I) = volume of water in subzone (units: L)

Z(2, 1, I) = mass of solids in subzone (units: kg)

Z(3, 1, I) = rate of water outflow from subzone to soil subzone (units: L/yr)

Z(4, 1, I) = rate of solid outflow from subzone to soil subzone (units: kg/yr)

Z(5, 1, I) = rate of water outflow from subzone to surface water subzone (units: L/yr)

Z(6, 1, I) = rate of solid outflow from subzone to surface water subzone (units: kg/yr)

Z(7, 1, I) = rate of water outflow from subzone to sediment subzone (units: L/yr)

Z(8, 1, I) = rate of solid outflow from subzone to sediment subzone (units: kg/yr)

Z(9, 1, I) = rate of water outflow from subzone to a sink (units: L/yr)

Z(10, 1, I) = rate of solid outflow from subzone to a sink (units: kg/yr).

The solids represented in Z(2, 1, I) are those solids which are important in sorbing nuclides. If part of the solids in the subzone were of little importance in sorbing nuclides, then it would be appropriate to omit their mass from the mass expressed in Z(2, 1, I). Similarly, the solids represented in Z(4, 1, I), Z(6, 1, I), Z(8, 1, I), and Z(10, 1, I) are solids which are important in sorbing nuclides. The rates represented in Z(P, 1, I) for P = 3, 4, ..., 10 refer to gross rates of outflow, not the difference between inflow and outflow. This distinction is important since material moving into and material moving out of the subzone can contain different nuclide concentrations. The diversity of potential flows out of the subzone is provided for flexibility. It is possible, and indeed probable, that in a given situation some of these flow rates will be zero. For example, it is anticipated that flows of solid material out of the groundwater subzone will usually be zero. The preceding comments also apply to similar information on other subzones.

For Zone I, the following information is required on the soil subzone (i.e., Subzone K = 2):

Z(1, 2, I) = volume of water in subzone (units: L)

Z(2, 2, I) = mass of solids in subzone (units: kg)

Z(3, 2, I) = rate of water outflow from subzone to groundwater subzone (units: L/yr)

Z(4, 2, I) = rate of solid outflow from subzone to groundwater subzone (units: kg/yr)

Z(5, 2, I) = rate of water outflow from subzone to surface water subzone (units: L/yr)

Z(6, 2, I) = rate of solid outflow from subzone to surface water subzone (units: kg/yr)

Z(7, 2, I) = rate of water outflow from subzone to a sink (units: L/yr)

Z(8, 2, I) = rate of solid outflow from subzone to a sink (units: kg/yr).

403 206

For Zone I, the following information is required on the surface water subzone (i.e., Subzone K = 3):

Z(1, 3, I) = volume of water in subzone (units: L)

Z(2, 3, I) = mass of solids in subzone (units: kg)

Z(3, 3, I) = rate of water outflow from subzone to groundwater subzone (units: L/yr)

Z(4, 3, I) = rate of solid outflow from subzone to groundwater subzone (units: kg/yr)

Z(5, 3, I) = rate of water outflow from subzone to soil subzone (units: L/yr)

Z(6, 3, I) = rate of solid outflow from subzone to soil subzone (units: kg/yr)

Z(7, 3, I) = rate of water outflow from subzone to sediment subzone (units: L/yr)

Z(8, 3, I) = rate of solid outflow from subzone to sediment subzone (units: kg/yr)

Z(9, 3, I) = rate of water outflow from subzone to surface water subzone in Zone INTZ(I) (units: L/yr)

Z(10, 3, I) = rate of solid outflow from subzone to surface water subzone in Zone INTZ(I) (units: kg/yr)

Z(11, 3, I) = rate of water outflow from subzone to a sink (units: L/yr)

Z(12, 3, I) = rate of solid outflow from subzone to a sink (units: kg/yr)

INTZ(I) = number of zone into which the surface water subzone of Zone I discharges.

For Zone I, the following information is required on the sediment subzone (i.e., Subzone K = 4):

Z(1, 4, I) = volume of water in subzone (units: L)

Z(2, 4, I) = mass of solids in subzone (units: kg)

Z(3, 4, I) = rate of water outflow from subzone to groundwater subzone (units: L/yr)

Z(4, 4, I) = rate of solid outflow from subzone to groundwater subzone (units: kg/yr)

Z(5, 4, I) = rate of water outflow from subzone to surface water subzone (units: L/yr)

Z(6, 4, I) = rate of solid outflow from subzone to surface water subzone (units: kg/yr)

Z(7, 4, I) = rate of water outflow from subzone to a sink (units: L/yr)

Z(8, 4, I) = rate of solid outflow from subzone to a sink (units: kg/yr).

4.3.5 Data Requirements for Decay Chain

In addition to the basic physical information on the subzones, certain basic information is also required for each decay chain considered. This information is represented by elements of the arrays HLIFE(J), ATW(J), and NDAUGHT(J), where

HLIFE(J) = half life of Nuclide J (units: yr)

ATW(J) = atomic weight of Nuclide J

NDAUGHT(J) = number of daughter products for Nuclide J.

In the computer program which implements this model, NDAUGHT(J) is permitted to be 0, 1, or 2. Further, for a nuclide with one or more daughters, it is necessary to know what the daughters are and what fraction of the original nuclide decays to each of the daughters. It is assumed that the decay chain is numbered J = 1, 2, ..., N, where N denotes the total number of nuclides in the decay chain and the numbering is selected so that decay is always from a nuclide with a smaller number to a nuclide with a larger number. For K = 1, ..., NDAUGHT(J), the array element IDAUGHT(J, K) denotes the integer in this numbering of the decay chain corresponding to the Kth daughter of Nuclide J, and the array element FDAUGHT(J, K) denotes the fraction of Nuclide J decaying to this daughter. The elements of the array IDAUGHT are arranged so that

$$J < \text{IDAUGHT}(J, 1) < \text{IDAUGHT}(J, 2),$$

where only the first inequality applies if NDAUGHT(J) = 1.

4.3.6 Additional Data Requirements

In the two preceding sections, information is listed that depends either on the subzones or on the decay chain. Certain required information depends on both the subzones and the nuclides in the decay chain.

The first such information needed is the rate of nuclide input into each subzone from sources external to the surface system being modeled in the Environmental Transport Model. Normally, this would be the input from the Groundwater Transport Model. Array elements of the form RIN(L) are used to represent the rate of nuclide input into Compartment L. If there are N nuclides and

$$L = 4N(I - 1) + 4(J - 1) + K,$$

then RIN(L) represents the rate of input of Nuclide J into Subzone K of Zone I. For simplicity in treating decay chains, the amount of a nuclide in a compartment is expressed as the number of atoms present. Thus, the units for RIN(L) are atoms/yr. Normally, these rates of input are decided on as part of the process used in selecting the zones and subzones. Indeed, the proper representation of such inputs is one of the important considerations in defining the zones and subzones.

The second such information needed pertains to the partitioning of nuclides between the liquid and solid phases of a subzone. Such partitioning is represented through the use of KD values, which are assumed to depend on both the nuclide and the subzone under consideration. Suppose a particular system has two phases, water and solid. Suppose also that

A = amount of nuclide in system (units: atoms)
AS = amount of nuclide in system sorbed to solids (units: atoms)
AW = amount of nuclide in system dissolved in water (units: atoms)
MS = mass of solid in system (units: kg)
VW = volume of water in system (units: L).

Then, the KD value (distribution coefficient) is defined to be the proportionality constant

$$KD = \frac{\text{conc. of nuclide sorbed on solids}}{\text{conc. of nuclide dissolved in water}} = \frac{AS/MS}{AW/VW} .$$

The units for the KD value are L/kg and are independent of the units used in measuring the amount of nuclide present. For background on the use and derivation of KD values, the reader is referred to a report by Borg et al, (Reference 18, pp 130-152).

In the Environmental Transport Model, a different KD value can be specified for each nuclide and each subzone. The KD value for Nuclide J in Subzone K of Zone I is represented by the array element KD(K, J, I). Detailed information on the variation of KD values is difficult to obtain. In many situations, the KD values may not be known well enough to assign a particular nuclide a different KD value in each subzone.

4.3.7 Partitioning of Nuclides

The existence of KD values is important because it enables one to determine the partitioning of a nuclide between the liquid and solid phases of a system. This partitioning is significant in representing the movement of a nuclide since the nuclide moves with the phase that it is associated with and the rate of movement of the liquid and solid phases can differ greatly. This division is particularly important because of the capability of some solids to sorb nuclides. This produces very large KD values, which indicates that the concentration of nuclides sorbed to solids is much greater than the concentration of nuclides dissolved in water.

403 209

A derivation of the partitioning of a nuclide between the liquid and solid phases of a system is given below. This partitioning is used extensively in determining the rates of nuclide flow between the compartments used in the Environmental Transport Model. Notation is the same as that presented in Section 4.3.6 before the definition of KD value.

Assume A, MS, VW, and KD are known for the system under consideration. Now, AS and AW are determined. Since

$$KD = [AS/MS][AW/VW]^{-1} \text{ and } A = AS + AW,$$

we have that

$$[KD][MS] = [AS][VW][AW]^{-1} \text{ and } AW = A - AS.$$

Thus,

$$[KD][MS] = [AS][VW][A - AS]^{-1},$$

$$[KD][MS][A] - [KD][MS][AS] = [AS][VW],$$

$$[KD][MS][A] = \{[KD][MS] + VW\} AS,$$

and hence

$$AS = \left\{\frac{[KD][MS]}{[KD][MS] + VW}\right\} A. \qquad (4.3.1)$$

Further,

$$AW = A - AS = \left\{1 - \frac{[KD][MS]}{[KD][MS] + VW}\right\} A. \qquad (4.3.2)$$

The relations in Eqs (4.3.1) and (4.3.2) represent the desired partitioning.

4.3.8 Flows Between Compartments

The information needed to determine the compartments, the directions of flow between the compartments, and the associated rate constants for these flows has been presented for a system of M zones and decay chain of N nuclides. All information and relations that have been discussed are assumed to be known. The resultant flows of nuclides are now derived. This is accomplished by systematically going through the compartments and determining the following information for each compartment: (1) every nuclide flow out of the compartment, (2) the compartment receiving each of these flows, and (3) the rate constant for each of these flows. This process is simplified in that all compartments derived from groundwater subzones have similar patterns of

403 210

outflow. In like manner, the compartments derived from each of the other subzones also have similar patterns of outflow. This permits the needed flows and rate constants to be derived in a repetitive manner. Once the preceding information for each compartment is known, it is relatively easy to construct the system of differential equations that represents the movement of nuclides through the surface region being modeled.

Three basic assumptions underlie these derivations. First, it is assumed that the nuclides are uniformly distributed through each subzone and are partitioned between the liquid and solid phases on the basis of their KD values for that subzone. A derivation for this partitioning is presented in Section 4.3.7. Second, it is assumed that the flow of water and solid material between subzones or out of the system is the only mechanism involved in the physical transport of nuclides. Third, it is assumed that all nuclides associated with a phase, liquid or solid, remain with that phase in movements between subzones or out of the system. In essence, each subzone is treated as a uniformly mixed "vessel" in which the nuclides are partitioned between the liquid and solid phase on the basis of distribution coefficients and such that nuclides can be carried between these "vessels" or out of a "vessel" and out of the system only by movements of water or solid material. For a given situation and a given selection of zones and subzones, these assumptions may or may not be satisfied. The model will produce calculated results whether the basic assumptions are satisfied or not. Thus, it is necessary for the model user to understand both the model and the system being modeled in order to decide in what manner, if any, the use of the model is justified.

For notational convenience in the following derivations, the array element L(K, J, I) is used to denote the integer

$$4(I - 1)N + 4(J - 1) + K ,$$

and the array element A(K, J, I) is used to denote the amount of nuclide in compartment L(K, J, I). As has been noted before, the amount of a nuclide is measured in atoms to simplify the treatment of decay chains. Recall that Compartment L(K, J, I) is the compartment associated with the presence of Nuclide J in Subzone K of Zone I.

4.3.9 Flows Associated with Groundwater Subzones

In the following, the flows and associated rate constants are determined for the movement of Nuclide J out of Compartment L(1, J, I). To determine the rate constants, it is necessary to know the concentration of Nuclide J in the water phase and in the solid phase of the groundwater subzone of Zone I. These concentrations are given by

$$CW = \frac{\text{amount of nuclide dissolved in water}}{\text{volume of water}}$$

$$= \frac{(1 - S)\, A(1, J, I)}{Z(1, 1, I)}$$

403 21

and

$$CS = \frac{\text{amount of nuclide sorbed to solids}}{\text{mass of solids}}$$

$$= \frac{S[A(1, J, I)]}{Z(2, 1, I)} ,$$

where CW is selected to represent concentration in water (units: atoms/L), CS is selected to represent concentration in solid material (units: atoms/kg) and

$$S = \frac{[KD(1, J, I)][Z(2, 1, I)]}{[KD(1, J, I)][Z(2, 1, I)] + Z(1, 1, I)}$$

(units: dimensionless). The validity of this partitioning follows from the equalities in Eqs (4.3.1) and (4.3.2).

The flows that take place out of Compartment L(1, J, I) are now listed and the associated rate constants are derived.

a. Flow from Compartment L(1, J, I) to Compartment L(2, J, I), i.e., from groundwater subzone to soil subzone:

$$\begin{aligned}
\text{Rate of flow} &= (\text{conc. in water})(\text{rate of water flow}) \\
&\quad + (\text{conc. in solids})(\text{rate of solid flow}) \\
&= [CW][Z(3, 1, I)] \\
&\quad + [CS][Z(4, 1, I)] \\
&= \left[\frac{(1 - S)\, A(1, J, I)}{Z(1, 2, I)}\right] Z(3, 1, I) \\
&\quad + \left[\frac{S[A(1, J, I)]}{Z(2, 1, I)}\right] Z(4, 1, I) \\
&= \left[\frac{(1 - S)\, Z(3, 1, I)}{Z(1, 1, I)} + \frac{(S)\, Z(4, 1, I)}{Z(2, 1, I)}\right] A(1, J, I) .
\end{aligned}$$

Thus, the desired rate constant is

$$\frac{(1 - S)\, Z(3, 1, I)}{Z(1, 1, I)} + \frac{(S)\, Z(4, 1, I)}{Z(2, 1, I)}$$

(units: 1/yr).

b. Flow from Compartment L(1, J, I) to Compartment L(3, J, I), i.e., from groundwater subzone to surface water subzone:

The derivation is similar to that presented in (a) above. The desired rate constant is

403 212

$$\frac{(1 - S)\, Z(5, 1, I)}{Z(1, 1, I)} + \frac{(S)\, Z(6, 1, I)}{Z(2, 1, I)}$$

(units: 1/yr).

c. Flow from Compartment L(1, J, I) to Compartment L(4, J, I), i.e., from groundwater subzone to sediment subzone:

The derivation is similar to that presented in (a) above. The desired rate constant is

$$\frac{(1 - S)\, Z(7, 1, I)}{Z(1, 1, I)} + \frac{(S)\, Z(8, 1, I)}{Z(2, 1, I)}$$

(units: 1/yr).

d. Flow from Compartment L(1, J, I) to a sink, i.e., from groundwater subzone to an area outside the region being modeled:

The derivation is similar to that presented in (a) above. The desired rate constant is

$$\frac{(1 - S)\, Z(9, 1, I)}{Z(1, 1, I)} + \frac{(S)\, Z(10, 1, I)}{Z(2, 1, I)}$$

(units: 1/yr).

If Nuclide J has no daughters, then there are no more flows to be determined. If the number of daughters is not equal to zero, then there are one or two additional flows to be determined as shown in (e) below.

e. Flow from Compartment L(1, J, I) to Compartment L(1, J', I), where $1 \le K \le$ NDAUGHT(J) and J' = IDAUGHT(J, K), i.e., decay from Nuclide J to Nuclide IDAUGHT(J, K):

The desired rate constant is obtained from the half-life of Nuclide J and the fraction of that nuclide decaying to nuclide IDAUGHT(J, K). The value produced is

$$[FDAUGHT(J, K)]\,[\ln(2.0)]\,[HLIFE(J)]^{-1}$$

(units: 1/yr).

4.3.10 Flows Associated with Soil Subzones

In the following, the flows and associated rate constants are determined for the movement of Nuclide J out of Compartment L(2, J, I). To determine the rate constants, it is necessary to know

the concentration of Nuclide J in the water phase and in the solid phase of the soil subzone of Zone I. These concentrations are given by

$$CW = \frac{\text{amount of nuclide dissolved in water}}{\text{volume of water}}$$

$$= \frac{(1 - S)\, A(2, J, I)}{Z(1, 2, I)}$$

and

$$CS = \frac{\text{amount of nuclide sorbed to solids}}{\text{mass of solids}}$$

$$= \frac{S\,[A(2, J, I)]}{Z(2, 2, I)} \quad ,$$

where CW is selected to represent concentration in water (units: atoms/L), CS is selected to represent concentration in solid material (units: atoms/kg), and

$$S = \frac{[KD(2, J, I)]\,[Z(2, 2, I)]}{[KD(2, J, I)]\,[Z(2, 2, I)] + Z(1, 2, I)}$$

(units: dimensionless). The validity of this partitioning follows from the equalities in Eqs (4.3.1) and (4.3.2).

The flows that take place out of Compartment L(2, J, I) are now listed and the associated rate constants are derived.

a. Flow from Compartment L (2, J, I) to Compartment L(1, J, I), i.e., from soil subzone to groundwater subzone:

$$\begin{aligned}
\text{Rate of flow} &= (\text{conc. in water})\,(\text{rate of water flow}) \\
&\quad + (\text{conc. in solids})\,(\text{rate of solid flow}) \\
&= [CW]\,[Z(3, 2, I)] \\
&\quad + [CS]\,[Z(4, 2, 1)] \\
&= \left[\frac{(1 - S)\, A(2, J, I)}{Z(1, 2, I)}\right] Z(3, 2, I) \\
&\quad + \left[\frac{S[A(2, J, I)]}{Z(2, 2, I)}\right] Z(4, 2, I) \\
&= \left[\frac{(1 - S)\, Z(3, 2, I)}{Z(1, 2, I)} + \frac{(S)\, Z(4, 2, I)}{Z(2, 2, I)}\right] A(2, J, I) \quad .
\end{aligned}$$

403 214

Thus, the desired rate constant is

$$\frac{(1 - S)\ Z(3, 2, I)}{Z(1, 2, I)} + \frac{(S)\ Z(4, 2, I)}{Z(2, 2, I)}$$

(units: 1/yr).

b. Flow from Compartment L(2, J, I) to Compartment L(3, J, I), i.e., from soil subzone to surface water subzone:

The derivation is similar to that presented in (a) above. The desired rate constant is

$$\frac{(1 - S)\ Z(5, 2, I)}{Z(1, 2, I)} + \frac{(S)\ Z(6, 2, I)}{Z(2, 2, I)}$$

(units: 1/yr).

c. Flow from Compartment L(2, J, I) to a sink, i.e., from soil subzone to an area outside the region being modeled:

The derivation is similar to that presented in (a) above. The desired rate constant is

$$\frac{(1 - S)\ Z(7, 2, I)}{Z(1, 2, I)} + \frac{(S)\ Z(8, 2, I)}{Z(2, 2, I)}$$

(units: 1/yr).

If Nuclide J has no daughters, then there are no more flows to be determined. If the number of daughters is not equal to zero, then there are one or two additional flows to be determined as shown in (d) below.

d. Flow from Compartment L(2, J, I) to Compartment L(2, J', I), where $1 \leq K \leq$ NDAUGHT(J) and J' = IDAUGHT(J, K), i.e., decay from Nuclide J to Nuclide IDAUGHT(J, K):

The desired rate constant is obtained from the half life of Nuclide J and the fraction of the nuclide decaying to Nuclide IDAUGHT(J, K). The value produced is

$$[\text{FDAUGHT}(J, K)]\ [\ln(2.0)]\ [\text{HLIFE}(J)]^{-1}$$

(units: 1/yr).

4.3.11 Flows Associated With Surface Water Subzones

In the following, the flows and associated rate constants are determined for the movement of Nuclide J out of Compartment L(3, J, I). To determine the rate constants, it is necessary to know the concentration of Nuclide J in the water phase and in the solid phase of the surface water subzone of Zone I. These concentrations are given by

$$CW = \frac{\text{amount of nuclide dissolved in water}}{\text{volume of water}}$$

$$= \frac{(1 - S)\, A(3, J, I)}{Z(1, 3, I)}$$

and

$$CS = \frac{\text{amount of nuclide sorbed to solids}}{\text{mass of solids}}$$

$$= \frac{S\,[A(3, J, I)]}{Z(2, 3, I)} \quad ,$$

where CW is selected to represent concentration in water (units: atoms/L), CS is selected to represent concentration in solid material (units: atoms/kg), and

$$S = \frac{[KD(3, J, I)]\,[Z(2, 3, I)]}{[KD(3, J, I)]\,[Z(2, 3, I)] + Z(1, 3, I)}$$

(units: dimensionless). The validity of this partitioning follows from the equalities in Eqs. (4.3.1) and (4.3.2).

The flows that take place out of Compartment L(3, J, I) are now listed and the associated rate constants are derived.

a. Flow from Compartment L(3, J, I) to Compartment L(1, J, I), i.e., from surface water subzone to groundwater subzone:

$$\text{Rate of flow} = (\text{conc. in water})\ (\text{rate of water flow}) + (\text{conc. in solids})\ (\text{rate of solid flow})$$

$$= [CW]\,[Z(3, 3, I)] + [CS]\,[Z(4, 3, I)]$$

$$= \frac{(1 - S)\, A(3, J, I)}{Z(1, 3, I)}\ Z(3, 3, I) + \frac{S\,[A(3, J, I)]}{Z(2, 3, I)}\ Z(4, 3, I)$$

$$= \left[\frac{(1 - S)\, Z(3, 3, I)}{Z(1, 3, I)} + \frac{(S)\, Z(4, 3, I)}{Z(2, 3, I)}\right] A(3, J, I) \quad .$$

403 216

Thus, the desired rate constant is

$$\frac{(1 - S)\ Z(3, 3, I)}{Z(1, 3, I)} + \frac{(S)\ Z(4, 3, I)}{Z(2, 3, I)}$$

(units: 1/yr).

b. Flow from Compartment L(3, J, I) to Compartment L(2, J, I), i.e., from surface water subzone to soil subzone:

The derivation is similar to that presented in (a) above. The desired rate constant is

$$\frac{(1 - S)\ Z(5, 3, I)}{Z(1, 3, I)} + \frac{(S)\ Z(6, 3, I)}{Z(2, 3, I)}$$

(units: 1/yr).

c. Flow from Compartment L(3, J, I) to Compartment L(4, J, I), i.e., from surface water subzone to sediment subzone:

The derivation is similar to that presented in (a) above. The desired rate constant is

$$\frac{(1 - S)\ Z(7, 3, I)}{Z(1, 3, I)} + \frac{(S)\ Z(8, 3, I)}{Z(2, 3, I)}$$

(units: 1/yr).

d. Flow from Compartment L(3, J, I) to Compartment L(3, J, INTZ(I)), i.e., from the surface water subzone of Zone I to the surface water subzone of Zone INTZ(I):

The derivation is similar to that presented in (a) above. The desired rate constant is

$$\frac{(1 - S)\ Z(9, 3, I)}{Z(1, 3, I)} + \frac{(S)\ Z(10, 3, I)}{Z(2, 3, I)}$$

(units: 1/yr).

e. Flow from Compartment L(3, J, I) to a sink, i.e., from surface water subzone to an area outside the region being modeled:

The derivation is similar to that presented in (a) above. The desired rate constant is

$$\frac{(1 - S)\, Z(11, 3, I)}{Z(1, 3, I)} + \frac{(S)\, Z(12, 3, I)}{Z(2, 3, I)}$$

(units: 1/yr).

If Nuclide J has no daughters, then there are no more flows to be determined. If the number of daughters is not equal to zero, then there are one or two additional flows to be determined as shown in (f) below.

f. Flow from Compartment L(3, J, I) to Compartment L(3, J', I), where $1 \le K \le$ NDAUGHT(J) and J' = IDAUGHT(J, K), i.e., decay from Nuclide J to Nuclide IDAUGHT(J, K):

The desired rate constant is obtained from the half life of Nuclide J and the fraction of that nuclide decaying to Nuclide IDAUGHT(J, K). The value produced is

$$[(\text{FDAUGHT}(J, K)]\,[\ln(2.0)]\,[\text{HLIFE}(J)]^{-1}$$

(units: 1/yr)

4.3.12 Flows Associated With Sediment Subzones

In the following, the flows and associated rate constants are determined for the movement of Nuclide J out of Compartment L(4, J, I). To determine the rate constants, it is necessary to know the concentration of Nuclide J in the water phase and in the solid phase of the sediment subzone of Zone I. These concentrations are given by

$$\text{CW} = \frac{\text{amount of nuclide dissolved in water}}{\text{volume of water}}$$

$$= \frac{(1 - S)\, A(4, J, I)}{Z(1, 4, I)}$$

and

$$\text{CS} = \frac{\text{amount of nuclide sorbed on solids}}{\text{mass of solids}}$$

$$= \frac{S[A(4, J, I)]}{Z(2, 4, I)} ,$$

where CW is selected to represent concentration in water (units: atoms/L), CS is selected to represent concentration in solid material (units: atoms/kg), and

$$S = \frac{[KD(4, J, I)]\,[Z(2, 4, I)]}{[KD(4, J, I)]\,[Z(2, 4, I)] + Z(1, 4, I)}$$

(units: dimensionless). The validity of this partitioning follows from the equalities in Eqs (4.3.1) and (4.3.2).

403 218

The flows that take place out of Compartment L(4, J, I) are now listed and the associated rate constants are derived.

a. Flow from Compartment L(4, J, I) to Compartment L(1, J, I), i.e., from sediment subzone to groundwater subzone:

$$\begin{aligned}\text{Rate of flow} &= (\text{conc. in water})(\text{rate of water flow}) \\ &\quad + (\text{conc. in solids})(\text{rate of solid flow}) \\ &= [CW][Z(3, 4, I)] \\ &\quad + [CS][Z(4, 4, I)] \\ &= \frac{(1 - S)\, A(4, J, I)}{Z(1, 4, I)}\, Z(3, 4, I) \\ &\quad + \frac{(S)\,[A(4, J, I)]}{Z(2, 4, I)}\, Z(4, 4, I) \\ &= \left[\frac{(1 - S)\, Z(3, 4, I)}{Z(1, 4, I)} + \frac{(S)\, Z(4, 4, I)}{Z(2, 4, I)}\right] A(4, J, I) \quad .\end{aligned}$$

Thus, the desired rate constant is

$$\frac{(1 - S)\, Z(3, 4, I)}{Z(1, 4, I)} + \frac{(S)\, Z(4, 4, I)}{Z(2, 4, I)}$$

(units: 1/yr).

b. Flow from Compartment L(4, J, I) to Compartment L(3, J, I), i.e., from sediment subzone to surface water subzone:

The derivation is similar to that presented in (a) above. The desired rate constant is

$$\frac{(1 - S)\, Z(5, 4, I)}{Z(1, 4, I)} + \frac{(S)\, Z(6, 4, I)}{Z(2, 4, I)}$$

(units: 1/yr).

c. Flow from Compartment L(4, J, I) to a sink, i.e., from sediment subzone to an area outside the region being modeled:

The derivation is similar to that presented in (a) above. The desired rate constant is

$$\frac{(1 - S)\, Z(7, 4, I)}{Z(1, 4, I)} + \frac{(S)\, Z(8, 4, I)}{Z(2, 4, I)}$$

403 219

(units: 1/yr).

If Nuclide J has no daughters, then there are no more flows to be determined. If the number of daughters is not equal to zero, then there are one or two additional flows to be determined as shown in (d) below.

d. Flow from Compartment L(4, J, I) to Compartment L(4, J', I), where $1 \le K \le$ NDAUGHT(J) and J' = NDAUGHT(J, I), i.e., decay from Nuclide J to Nuclide IDAUGHT(J, K):

The desired rate constant is obtained from the half life of Nuclide J and the fraction of that nuclide decaying to Nuclide IDAUGHT(J, K). The value produced is

$$[\text{FDAUGHT}(J, K)]\,[\ln(2.0)]\,[\text{HLIFE}(J)]^{-1}$$

(units: 1/yr).

4.3.13 Implementation of Technique

The preceding technique for defining compartments and rates of flow is implemented through a sequence of subroutines in the Environmental Transport Model. The first of these is the subroutine COEF. For a system of M zones and a decay chain of N nuclides, this subroutine systematically goes through the associated 4 MN compartments and determines in the manner just outlined the following information for every compartment: (1) each outflow from the compartment, (2) the compartment receiving each outflow, and (3) the rate constant for each outflow. Then, COEF is followed by the subroutines ALTER and ADD. The subroutine ALTER provides the user with the opportunity to alter any of the information concerning flows between compartments that have been determined in COEF, and the subroutine ADD provides the user with the opportunity to add any additional flows between the compartments that are needed but not included in the flows constructed in COEF. Next, the subroutine EQ takes the user-defined external nuclide input rates for the compartments and the flows between compartments from subroutines COEF, ALTER, and ADD and constructs the resultant system of 4 MN linear differential equations which represents the movement of the nuclides.

Once the system of differential equations for the transport of the nuclides is obtained, it must be solved. A technique for the solution of this system is not constructed as an integral part of the Environmental Transport Model. Instead, a solution for the system is obtained by calling on a user-supplied solver for differential equations. Currently a solver for stiff, banded systems of differential equations which is available at Sandia Laboratories is being used. Documentation for this code is provided by Hindmarsh.[4.19,4.20] However, any appropriate code for solving differential equations could be used.

The solution of the differential equations produced in the Environmental Transport Model yields the concentration of each nuclide in each subzone. By obtaining solutions for these equations at different times, the temporal and spatial distribution of the nuclides can be determined. It is these patterns of nuclide distribution and concentration that are used as input to the Transport to Man Model.

403 220

4.4 Transport to Man Model

4.4.1 The Approach

Once the environmental distribution and concentration of nuclides are determined by use of the Environmental Transport Model, it is necessary to use the Transport to Man Model to determine the amount of nuclides reaching man by inhalation or ingestion. The amount of nuclides inhaled is determined from the amount of suspended soil material in the air. The underlying assumption is that the concentration of nuclides in suspended material is the same as the concentration of nuclides in nearby soil. The determination of the amount of nuclides ingested is more complicated.

Nuclide ingestion is determined by using models based on concentration factors. Nuclide concentrations are calculated along various food pathways leading to man. The amount of nuclides ingested then follows from the amount of food consumed and the concentrations of nuclides in that food. The computational methods are modifications of models currently employed by the Nuclear Regulatory Commission to calculate doses to man from the release of reactor effluents.[4.21,4.22] These models are used in the HERMES code[4.6,4.23] and additional discussions of them can be found in articles by Soldat et al,[4.24] Baker et al,[4.25] and Soldat.[4.26] Related models are discussed in Booth,[4.17] Watts,[4.27] Booth et al,[4.28] Booth and Kaye,[4.29] Killough et al,[4.30] and Bramati.[4.31] The article by Hoffman et al provides a review of computer models currently available to represent environmental nuclide transport.[4.11]

There are two important features that favor basing the Transport to Man Model on concentration factors. First, this approach is adaptable. There are too many possible food systems leading to man to present one all-encompassing model. Possible pathways to man range from those associated with the various common agricultural systems to more exotic possibilities such as the seaweed-man food chain which is of local importance in England and the lichen-reindeer-man food chain in the Arctic. By using concentration factors to represent the movement of nuclides in specific food chains, it is possible to tailor the Transport to Man Model to the food chains which are important in a particular situation. Also, the model can be readily adapted to determine the effects of different diets and of diets which contain food from areas of varying nuclide concentrations (i.e., zones). In the following, five generic food types that culminate pathways leading to man are discussed: drinking water, aquatic food, plants, milk, and meat. It is possible that some food types would not be involved in a given situation; they could then be omitted from consideration. It is also possible that the pathways to man culminating in these five food types would not cover all possibilities in a specific situation. However, it is anticipated that calculations similar to those presented can handle most situations.

Second, information needed to implement the approach is either available or in the process of becoming available. This does not imply that the variation of concentration factors is fully understood or that they are empirically known for all potential disposal sites. However, concentration factors have been widely studied and such studies are continuing. Thus, implementation of the model should not be prevented by unfillable data needs.

The individual models which constitute the Transport to Man Model are now presented. The inhalation model is presented first and then the ingestion models are presented. Finally, a brief discussion of external exposure is provided.

4.4.2 Inhalation

For each nuclide, the following provides the amount of that nuclide inhaled as the result of its suspension in the atmosphere:

$$\begin{pmatrix}\text{amt. of nucl.}\\ \text{inhaled per yr}\end{pmatrix} = \begin{pmatrix}\text{nucl. conc.}\\ \text{in atmos.}\end{pmatrix} \begin{pmatrix}\text{inhalation}\\ \text{rate}\end{pmatrix}$$

$$\begin{pmatrix}\text{nucl. conc. in atmos.}\end{pmatrix} = \begin{pmatrix}\text{conc. of suspended}\\ \text{material}\end{pmatrix} \begin{pmatrix}\text{nucl. conc. in}\\ \text{suspended material}\end{pmatrix} .$$

Units:

$$\text{Ci/yr} = (\text{Ci/L})\,(\text{L/yr})$$
$$\text{Ci/L} = (\text{kg/L})\,(\text{Ci/kg}) .$$

For most situations, it is anticipated that suspended material will be derived from local soil. Inhalation rates are provided in Tables 4.IV and 4.V. Since nuclides must reach the surface and then be suspended before inhalation, this probably will not be an important pathway. This model is not intended for the treatment of gaseous products; however, this problem has been widely studied and such models are available.

4.4.3 Treatment of Decay

In calculating the amount of nuclides ingested, no allowance is made for decay. Since decay is included in the Environmental Transport Model and in the Dosimetry Model, the only need for decay in the Transport to Man Model is to account for the reduction in radioactivity during the production or storage of a food type. This is not considered for two reasons. First, if a nuclide has a long half-life, then a consideration of decay produces a negligible change in concentration during the time of food production and storage. Second, if a nuclide has a short half-life, it should be in equilibrium with a longer lived parent. Time spans of more than a year are unusual in the production or storage of a food product. In most situations, the time span would be much less.

4.4.4 Ingestion of Water

For each nuclide, the following provides the amount of that nuclide ingested from the consumption of water:

$$\begin{pmatrix}\text{amt. of nucl.}\\ \text{ingested per yr}\end{pmatrix} = \begin{pmatrix}\text{nucl. conc.}\\ \text{in water}\end{pmatrix} \begin{pmatrix}\text{water treatment}\\ \text{removal factor}\end{pmatrix} \begin{pmatrix}\text{rate of water}\\ \text{ingestion}\end{pmatrix} .$$

Units:

$$\text{Ci/yr} = (\text{Ci/L})\,(\text{dimensionless})\,(\text{L/yr}) .$$

403 272

As indicated by the name, the water treatment removal factor is the fraction of disaolved nuclides removed by water treatment. Additional discussion of this pathway is given by Soldat (Reference 4.26, p. 543).

4.4.5 Ingestion of Aquatic Food

For each nuclide, the following provides the amount of that nuclide ingested from the consumption of aquatic foods:

$$\begin{pmatrix}\text{amt. of nucl.}\\ \text{ingested per yr}\end{pmatrix} = \begin{pmatrix}\text{nucl. conc.}\\ \text{in water}\end{pmatrix}\begin{pmatrix}\text{conc.}\\ \text{factor}\end{pmatrix}\begin{pmatrix}\text{rate of}\\ \text{ingestion}\end{pmatrix} .$$

Units:

$$\text{Ci/yr} = (\text{Ci/L})\,(\text{L/kg})\,(\text{kg/yr}) .$$

The concentration factor (units: L/kg) is defined by

$$\frac{\text{conc. of nucl. in aquatic food type}}{\text{conc. of nucl. in water}} .$$

Whenever possible, site-specific values for concentration factors should be used. Table 4.4.1 lists a compilation of concentration factors prepared by the Nuclear Regulatory Commission which might be used in the absence of such information (Reference 4.21, Table A.8, p. 1.109-31). Additional discussion of this pathway is given by Soldat (Reference 4.26, p. 543). Included in this pathway are food types such as fish, crustaceans, shellfish, and aquatic plants. In this as in other pathways, food weight refers to wet weight.

4.4.6 Ingestion of Plants

For each nuclide, the following provides the amount of that nuclide ingested from the consumption of plant material:

$$\begin{pmatrix}\text{amt. of nucl.}\\ \text{ingested per yr}\end{pmatrix} = \begin{pmatrix}\text{conc. of nucl.}\\ \text{in plant}\end{pmatrix}\begin{pmatrix}\text{rate of}\\ \text{ingestion}\end{pmatrix}$$

$$\begin{pmatrix}\text{conc. of nucl.}\\ \text{in plant}\end{pmatrix} = \begin{pmatrix}\text{conc. of nucl.}\\ \text{in soil}\end{pmatrix}\begin{pmatrix}\text{conc.}\\ \text{factor}\end{pmatrix} + \begin{pmatrix}\text{conc. due to}\\ \text{foliar deposition}\end{pmatrix} .$$

Units:

$$\text{Ci/yr} = (\text{Ci/kg})\,(\text{kg/yr})$$

$$\text{Ci/kg} = (\text{Ci/kg})\,(\text{dimensionless}) + \text{Ci/kg} .$$

The concentration factor (units: dimensionless) is defined by

$$\frac{\text{conc. of nucl. in plant}}{\text{conc. of nucl. in soil}} .$$

403 223

TABLE 4.4.1

Concentration Factors*
(Ci/kg per Ci/L)

	FRESHWATER			SALTWATER		
ELEMENT	FISH	INVERTEBRATE	PLANT	FISH	INVERTEBRATE	PLANT
H	9.0E-01	9.0E-01	9.0E-01	9.0E-01	9.3E-01	9.3E-01
HE	1.0E 00	1.0E 00	1.0E 00	1.0E 00	1.0E 00	1.0E 00
LI	5.0E-01	4.0E 01	3.0E 00	5.0E-01	3.0E-01	3.0E 00
BE	2.0E 00	1.0E 01	2.0E 01	2.0E 02	2.0E 02	1.0E 03
B	2.2E-01	5.0E 01	2.2E 00	2.2E-01	4.4E-01	2.2E 00
C	4.6E 03	9.1E 03	4.6E 03	1.8E 03	1.4E 03	1.8E 03
N	1.5E 05	1.5E 05	1.3E 04	6.0E 04	1.7E 04	1.0E 04
O	9.2E-01	9.2E-01	9.2E-01	9.6E-01	9.6E-01	9.6E-01
F	1.0E 01	1.0E 02	2.0E 00	3.6E 00	3.6E 00	1.4E 00
NE	1.0E 00	1.0E 00	1.0E 00	1.0E 00	1.0E 00	1.0E 00
NA	1.0E 02	2.0E 02	5.0E 02	6.7E-02	1.9E-01	9.5E-01
MG	5.0E 01	1.0E 02	1.0E 02	7.7E-01	7.7E-01	7.7E-01
AL	1.0E 01	6.3E 01	4.2E 02	1.0E 01	6.0E 01	6.0E 02
SI	2.5E 00	3.5E 01	1.3E 02	1.0E 01	3.3E 01	6.7E 01
P	1.0E 05	2.0E 04	5.0E 05	2.9E 04	3.0E 04	3.0E 03
S	7.5E 02	1.0E 02	1.0E 02	1.7E 00	4.4E-01	4.4E-01
CL	5.0E 01	1.0E 02	5.0E 01	1.3E-02	1.9E-02	7.6E-02
AR	1.0E 00	1.0E 00	1.0E 00	1.0E 00	1.0E 00	1.0E 00
K	1.0E 03	8.3E 02	6.7E 02	1.1E 01	5.6E 00	2.6E 01
CA	4.0E 01	3.3E 02	1.3E 02	5.0E-01	1.3E 01	5.0E 00
SC	2.0E 00	1.0E 03	1.0E 04	2.0E 00	1.0E 04	1.0E 05
TI	1.0E 03	3.0E 03	5.0E 02	1.0E 03	1.0E 03	2.0E 03
V	1.0E 01	3.0E 03	1.0E 02	1.0E 01	5.0E 01	1.0E 02
CR	2.0E 02	2.0E 03	4.0E 03	4.0E 02	2.0E 03	2.0E 03
MN	4.0E 02	9.0E 04	1.0E 04	5.5E 02	4.0E 02	5.5E 03
FE	1.0E 02	3.2E 03	1.0E 03	3.0E 03	2.0E 04	7.3E 02
CO	5.0E 01	2.0E 02	2.0E 02	1.0E 02	1.0E 03	1.0E 03
NI	1.0E 02	1.0E 02	5.0E 01	1.0E 02	2.5E 02	2.5E 02
CU	5.0E 01	4.0E 02	2.0E 03	6.7E 02	1.7E 03	1.0E 03
ZN	2.0E 03	1.0E 04	2.0E 04	2.0E 03	5.0E 04	1.0E 03
GA	3.3E 02	6.7E 02	1.7E 03	3.3E 02	6.7E 02	1.7E 03
GE	3.3E 03	3.3E 01	3.3E 01	3.3E 03	1.7E 04	3.3E 02
AS	1.0E 02	4.0E 01	3.0E 03	3.3E 02	3.3E 02	1.7E 03
SE	1.7E 02	1.7E 02	[illegible]0E 03	4.0E 03	1.0E 03	1.0E 03
BR	4.2E 02	3.3E 02	[illegible]0E 01	1.5E-02	3.1E 00	1.5E 00
KR	1.0E 00	1.0E 00	[illegible]	1.0E 00	1.0E 00	1.0E 00
RB	2.0E 03	1.0E 03	[illegible]	8.3E 00	1.7E 01	1.7E 01
SR	3.0E 01	1.0E 02	5.0E [illegible]	2.0E 00	2.0E 01	1.0E 01
Y	2.5E 01	1.0E 03	5.0E [illegible]3	2.5E 01	1.0E 03	5.0E 03
ZR	3.3E 00	6.7E 00	1.0E 03	2.0E 02	8.0E 01	1.0E 03
NB	3.0E 04	1.0E 02	8.0E 02	3.0E 04	1.0E 02	3.0E 02
MO	1.0E 01	1.0E 01	1.0E 03	1.0E 01	1.0E 01	1.0E 01
TC	1.5E 01	5.0E 00	4.0E 01	1.0E 01	5.0E 01	4.0E 03
RU	1.0E 01	3.0E 02	2.0E 03	3.0E 00	1.0E 03	2.0E 03
RH	1.0E 01	3.0E 02	2.0E 02	1.0E 01	2.0E 03	2.0E 03
PD	1.0E 01	3.0E 02	2.0E 02	1.0E 01	2.0E 03	2.0E 03
AG	2.3E 00	7.7E 02	2.0E 02	3.3E 03	3.3E 03	2.0E 02
CD	2.0E 02	2.0E 03	1.0E 03	3.0E 03	2.5E 05	1.0E 03
IN	1.0E 05	1.0E 05	1.0E 05	1.0E 05	1.0E 05	1.0E 05
SN	3.0E 03	1.0E 03	1.0E 02	3.0E 03	1.0E 03	1.0E 02
[illegible]	1.0E 00	1.0E 01	1.5E 03	4.0E 01	5.0E 00	1.5E 03
[illegible]	4.0E 02	1.0E 05	1.0E 02	1.0E 01	1.0E 05	1.0E 03
[illegible]	1.5E 01	5.0E 00	4.0E 01	1.0E 01	5.0E 01	1.0E 03

*This table is taken from an NRC publication (Reference 4.21, Table A-8, p. 1.109-31). Documentation is provided there.

224
403

TABLE 4.4.1
(cont)

	FRESHWATER			SALTWATER		
ELEMENT	FISH	INVERTEBRATE	PLANT	FISH	INVERTEBRATE	PLANT
XE	1.0E 00	1.0E 00	1.0E 00	1.0E 00	1.0E 00	1.0E 00
CS	2.0E 03	1.0E 02	5.0E 02	4.0E 01	2.5E 01	5.0E 01
BA	4.0E 00	2.0E 02	5.0E 02	1.0E 01	1.0E 02	5.0E 02
LA	2.5E 01	1.0E 03	5.0E 03	2.5E 01	1.0E 03	5.0E 03
CE	1.0E 00	1.0E 03	4.0E 03	1.0E 01	6.0E 02	6.0E 02
PR	2.5E 01	1.0E 03	5.0E 03	2.5E 01	1.0E 03	5.0E 03
ND	2.5E 01	1.0E 03	5.0E 03	2.5E 01	1.0E 03	5.0E 03
PM	2.5E 01	1.0E 03	5.0E 03	2.5E 01	1.0E 03	5.0E 03
SM	2.5E 01	1.0E 03	5.0E 03	2.5E 01	1.0E 03	5.0E 03
EU	2.5E 01	1.0E 03	5.0E 03	2.5E 01	1.0E 03	5.0E 03
GD	2.5E 01	1.0E 03	5.0E 03	2.5E 01	1.0E 03	5.0E 03
TB	2.5E 01	1.0E 03	5.0E 03	2.5E 01	1.0E 03	5.0E 03
DY	2.5E 01	1.0E 03	5.0E 03	2.5E 01	1.0E 03	5.0E 03
HO	2.5E 01	1.0E 03	5.0E 03	2.5E 01	1.0E 03	5.0E 03
ER	2.5E 01	1.0E 03	5.0E 03	2.5E 01	1.0E 03	5.0E 03
TM	2.5E 01	1.0E 03	5.0E 03	2.5E 01	1.0E 03	5.0E 03
YB	2.5E 01	1.0E 03	5.0E 03	2.5E 01	1.0E 03	5.0E 03
LU	2.5E 01	1.0E 03	5.0E 03	2.5E 01	1.0E 03	5.0E 03
HF	3.3E 00	6.7E 00	1.0E 03	2.0E 02	2.0E 01	2.0E 03
TA	3.0E 04	6.7E 02	8.0E 02	3.0E 04	1.7E 04	1.0E 03
W	1.2E 03	1.0E 01	1.2E 03	3.0E 01	3.0E 01	3.0E 01
RE	1.2E 02	6.0E 01	2.4E 02	4.8E 00	6.0E 01	2.4E 02
OS	1.0E 01	3.0E 02	2.0E 02	1.0E 01	2.0E 03	2.0E 03
IR	1.0E 01	3.0E 02	2.0E 02	1.0E 01	2.0E 03	2.0E 03
PT	1.0E 02	3.0E 02	2.0E 02	1.0E 02	2.0E 03	2.0E 03
AU	3.3E 01	5.0E 01	3.3E 01	3.3E 01	3.3E 01	3.3E 01
HG	1.0E 03	1.0E 05	1.0E 03	1.7E 03	3.3E 04	1.0E 03
TL	1.0E 04	1.5E 04	1.0E 05	1.0E 04	1.5E 04	1.0E 05
PB	1.0E 02	1.0E 02	2.0E 02	3.0E 02	1.0E 03	5.0E 03
BI	1.5E 01	2.4E 01	2.4E 01	1.5E 01	2.4E 01	2.4E 01
PO	5.0E 02	2.0E 04	2.0E 03	3.0E 02	5.0E 03	2.0E 03
AT	1.5E 01	5.0E 00	4.0E 01	1.0E 01	5.0E 01	4.0E 03
RN	1.0E 00	1.0E 00	1.0E 00	1.0E 00	1.0E 00	1.0E 00
FR	4.0E 02	1.0E 02	8.0E 01	3.0E 01	2.0E 01	2.0E 01
RA	5.0E 01	2.5E 02	2.5E 03	5.0E 01	1.0E 02	1.0E 02
AC	2.5E 01	1.0E 03	5.0E 03	2.5E 01	1.0E 03	5.0E 03
TH	3.0E 01	5.0E 02	1.5E 03	1.0E 04	2.0E 03	3.0E 03
PA	1.1E 01	1.1E 02	1.1E 03	1.0E 01	1.0E 01	6.0E 00
U	2.0E 00	6.0E 01	5.0E-01	1.0E 01	1.0E 02	6.7E 01
NP	1.0E 01	4.0E 02	3.0E 02	1.0E 01	1.0E 01	6.0E 00
PU	3.5E 00	1.0E 02	3.5E 02	3.0E 00	2.0E 01	1.0E 03
AM	2.5E 01	1.0E 03	5.0E 03	2.5E 01	1.0E 03	5.0E 03
CM	2.5E 01	1.0E 03	5.0E 03	2.5E 01	1.0E 03	5.0E 03
BK	2.5E 01	1.0E 03	5.0E 03	2.5E 01	1.0E 03	5.0E 03
CF	2.5E 01	1.0E 03	5.0E 03	2.5E 01	1.0E 03	5.0E 03
ES	1.0E 01	1.0E 02	1.0E 03	1.0E 01	1.0E 01	6.0E 01
FM	1.0E 01	1.0E 02	1.0E 03	1.0E 01	1.0E 01	6.0E 01

Whenever possible, site-specific and plant-specific values for concentration factors should be used. Table 4.4.2 lists a compilation of concentration factors prepared by the Nuclear Regulatory Commission which might be used in the absence of specific data (Reference 4.21, Table C-5, p. 1.109-56). Included in this pathway are food types such as fruits, vegetables, and grain.

Foliar deposition is assumed to be due to sprinkler irrigation. The concentration of nuclide retained on or in a plant as the result of sprinkler irrigation is determined by solving a differential equation which represents the change in this concentration as the difference in the rate at which the nuclide is contaminating the plant and the rate at which the nuclide is being removed by weathering. This equation is

$$\frac{dC(t)}{dt} = d(t) - \lambda C(t) \quad ,$$

where

C(t) = concentration of nuclide on plant (units: Ci/kg)

d(t) = rate of nuclide deposition (units: Ci/kg-yr)

λ = rate constant for removal by weathering (units: 1/yr) .

With the initial condition C(0) = 0 and the assumption that d(t) has a constant value d, the preceding equation has the solution

$$C(t) = (d/\lambda)(1 - e^{-\lambda t}) \quad ,$$

which provides the concentration due to foliar deposition for the basic equations.

The weathering half-life is taken to be 14 days. This yields a value for λ of 18.1 yr^{-1}. It is pointed out that $1 - e^{-\lambda t}$ approaches 1 rapidly. With t = 1/6 yr, the value is 0.95, and with t = 1/4 yr, the value is 0.99. Thus, the length of time for irrigation is probably not critical. The deposition rate d is given by

$$d = \frac{r[CW][I]}{Y} \quad ,$$

where

r = fraction of deposited nuclides retained on crops, taken to be 0.25 (units: dimensionless)

CW = concentration of nuclide in irrigation water (units: CI/L)

I = irrigation rates (units: L/m^2-yr)

Y = agricultural yield (units: kg/m^2-yr) .

The values presented for λ and r are widely used and appear to come from a study by Milbourn and Taylor.[4.32]

403 226

TABLE 4.4.2

Stable Element Concentration Factors*

ELEM	B_{iv} VEG/SOIL	$F_{m(Cow)}$ MILK(D/L)	F_f MEAT(D/KG)	ELEM	B_{iv} VEG/SOIL	$F_{m(Cow)}$ MILK(D/L)	F_f MEAT(D/KG)
H	4.8E 00	1.0E-02	1.2E-02	SB	1.1E-02	1.5E-03	4.0E-03
HE	5.0E-02	2.0E-02	2.0E-02	TE	1.3E 00	1.0E-03	7.7E-02
LI	8.3E-04	5.0E-02	1.0E-02	I	2.0E-02	6.0E-03	2.9E-03
BE	4.2E-04	1.0E-04	1.0E-03	XE	1.0E 01	2.0E-02	2.0E-02
B	1.2E-01	2.7E-03	8.0E-04	CS	1.0E-02	1.2E-02	4.0E-03
C	5.5E 00	1.2E-02	3.1E-02	BA	5.0E-03	4.0E-04	3.2E-03
N	7.5E 00	2.2E-02	7.7E-02	LA	2.5E-03	5.0E-06	2.0E-04
O	1.6E 00	2.0E-02	1.6E-02	CE	2.5E-03	6.0E-04	1.2E-03
F	6.5E-04	1.4E-02	1.5E-01	PR	2.5E-03	5.0E-06	4.7E-03
NE	1.4E-01	2.0E-02	2.0E-02	ND	2.4E-03	5.0E-06	3.3E-03
NA	5.2E-02	4.0E-02	3.0E-02	PM	2.5E-03	5.0E-06	4.8E-03
MG	1.3E-01	1.0E-02	5.0E-03	SM	2.5E-03	5.0E-06	5.0E-03
AL	1.8E-04	5.0E-04	1.5E-03	EU	2.5E-03	5.0E-06	4.8E-03
SI	1.5E-04	1.0E-04	4.0E-05	GD	2.5E-03	5.0E-06	3.6E-03
P	1.1E 00	2.5E-02	4.6E-02	TB	2.5E-03	5.0E-06	4.9E-03
S	5.9E-01	1.8E-02	1.0E-01	DY	2.5E-03	5.0E-06	5.3E-03
CL	5.0E 00	5.0E-02	8.0E-02	HO	2.5E-03	5.0E-06	4.4E-03
AR	6.0E-01	2.0E-02	2.0E-02	ER	2.5E-03	5.0E-06	4.0E-03
K	3.7E-01	1 E-02	1.2E-02	TM	2.5E-03	5.0E-06	4.4E-03
CA	3.6E-02	8.0E-03	4.0E-03	YB	2.5E-03	5.0E-06	4.0E-03
SC	1.1E-03	5.0E-06	1.6E-02	LU	2.5E-03	5.0E-06	4.4E-03
TI	5.4E-05	5.0E-06	3.1E-02	HF	1.7E-04	5.0E-06	4.0E-01
V	1.3E-03	1.0E-03	2.3E-03	TA	6.3E-03	2.5E-02	1.6E 00
CR	2.5E-04	2.2E-03	2.4E-03	W	1.9E-02	5.0E-04	1.3E-03
MN	2.9E-02	2.5E-04	8.0E-04	RE	2.5E-01	2.5E-02	8.0E-03
FE	6.6E-04	1.2E-03	4.0E-02	OS	5.0E-02	5.0E-03	4.0E-01
CO	9.4E-03	1.0E-03	1.3E-02	IR	1.3E 01	5.0E-03	1.5E-03
NI	1.9E-02	6.7E-03	5.3E-03	PT	5.0E-01	5.0E-03	4.0E-03
CU	1.2E-01	1.4E-02	8.0E-03	AU	2.5E-03	5.0E-03	8.0E-03
ZN	4.0E-01	3.9E-02	3.0E-02	HG	3.9E-01	3.8E-02	2.6E-01
GA	2.5E-04	5.0E-05	1.3E 00	TL	2.5E-01	2.2E-02	4.6E-02
GE	1.0E-01	5.0E-04	2.0E 01	PB	6.3E-02	6.2E-04	2.9E-04
AS	1.0E-02	6.0E-03	2.0E-03	BI	1.5E-01	5.0E-04	1.3E-02
SE	1.3E 00	4.5E-02	1.5E-02	PO	1.5E-01	3.0E-04	1.2E-02
BR	7.6E-01	5.0E-02	2.6E-02	AT	2.5E-01	5.0E-02	8.0E 00
KR	3.0E 00	2.0E-02	2.0E-02	RN	3.5E 00	2.0E-02	2.0E-02
RB	1.3E-01	3.0E-02	3.1E-02	FR	1.0E-02	5.0E-02	2.0E-02
SR	1.7E-02	8.0E-04	6.0E-04	RA	3.1E-04	8.0E-03	3.4E-02
Y	2.6E-03	1.0E-05	4.6E-03	AC	2.5E-03	5.0E-06	6.0E-02
ZR	1.7E-04	5.0E-06	3.4E-02	TH	4.2E-03	5.0E-06	2.0E-04
NB	9.4E-03	2.5E-03	2.8E-01	PA	2.5E-03	5.0E-06	8.0E 02
MO	1.2E-01	7.5E-03	8.0E-03	U	2.5E-03	5.0E-04	3.4E-04
TC	2.5E-01	2.5E-02	4.0E-01	NP	2.5E-03	5.0E-06	2.0E-04
RU	5.0E-02	1.0E-06	4.0E-01	PU	2.5E-04	2.0E-06	1.4E-05
RH	1.3E 01	1.0E-02	1.5E-03	AM	2.5E-04	5.0E-06	2.0E-04
PD	5.0E 00	1.0E-02	4.0E-03	CM	2.5E-03	5.0E-06	2.0E-04
AG	1.5E-01	5.0E-02	1.7E-02	BK	2.5E-03	5.0E-06	2.0E-04
CD	3.0E-01	1.2E-04	5.3E-04	CF	2.5E-03	5.0E-06	2.0E-04
IN	2.5E-01	1.0E-04	8.0E-03	ES	2.5E-03	5.0E-06	2.0E-04
SN	2.5E-03	2.5E-03	8.0E-02	FM	2.5E-03	5.0E-06	2.0E-04

*This table is taken from an NRC publication (Reference 4.21, Table C-5, p. 1.109-56). Documentation is provided there.

4.4.7 Ingestion of Animal Products

For each nuclide, the following provides the amount of that nuclide ingested from the consumption of animal products (milk or meat):

$$\text{amt. of nucl. ingested} = \begin{pmatrix}\text{nucl. conc. in}\\ \text{animal prod.}\end{pmatrix}\begin{pmatrix}\text{rate of}\\ \text{ingestion}\end{pmatrix}$$

$$\begin{pmatrix}\text{nucl. conc. in}\\ \text{animal product}\end{pmatrix} = \left[\begin{pmatrix}\text{rate of nucl. ingestion}\\ \text{from feed}\end{pmatrix} + \begin{pmatrix}\text{rate of nucl. ingestion}\\ \text{from water}\end{pmatrix}\right] \cdot \begin{bmatrix}\text{conc.}\\ \text{factor}\end{bmatrix} .$$

Units*:

$$\text{Ci/yr} = (\text{Ci/kg})\,(\text{kg/yr})$$

$$\text{Ci/kg} = [(\text{Ci/day}) \div (\text{Ci/day})]\,[\text{day/kg}] .$$

The concentration factor (units: day/kg or day/L) is defined by

$$\frac{\text{conc. of nucl. in animal product}}{\text{intake of nucl. per day}} .$$

Whenever possible, site-specific and animal-specific values for concentration factors should be used. Table 4.4.2 lists a compilation of concentration factors prepared by the Nuclear Regulatory Commission which might be used in the absence of specific data (Reference 4.21, Table C-5, p. 1.109-56).

The concentration of nuclides in plant material consumed by animals is determined by the use of the equations presented earlier. Table 4.4.3 contains feed and water consumption rates for cattle used by the Nuclear Regulatory Commission (Reference 4.21, Table A-10, p. 109-34).

4.4.8 External Exposure

The Dosimetry and Health Effects Model contains dose factors to convert from environmental nuclide concentrations to individual organ exposures (units: mrem/hr per pCi/m^3 for air submersion, mrem/hr per pCi/m^2 for surface exposure, and mrem/hr per pCi/L for water submersion). The Environmental Transport Model yields nuclide concentrations in soil, sediment, and water. Thus, nuclide concentration in water is produced directly by the model. However, nuclide concentration per unit air volume and nuclide concentration per unit surface area are not produced directly.

At present, no technique to approximate these values is provided; instead, their calculation is left to the discretion of the model user. For example, nuclide concentration in air might be obtained by supposing a certain concentration of airborne soil or sediment (units: mg/m^3) then,

---

*For milk, the units would involve litres rather than kilograms.

nuclide concentration in air (units: pCi/m^3) would follow from nuclide concentration in the associated soil or sediment (units: Ci/kg). As another example, surface concentration (units: pCi/m^2) might be produced either by assuming all nuclides to a certain depth are concentrated on the surface and all others are inconsequential or by performing the radiation transport calculations to reduce a volume source to an equivalent surface source.

4.4.9 Implementation of Transport to Man Model

In deciding what to include in an ingestion study, one must return to the zones of the original transport model and consider factors such as nuclide concentration, food types produced, and population patterns. It is possible that some zones might be of relatively little importance in determining ingestion patterns. For example, some zones might be of importance in the transport of nuclides but of relatively little importance in the production of food materials. Thus, determining or projecting site-specific patterns of food consumption is necessary. Indeed, the capability to handle such information was one of the factors for basing the Transport to Man Model on concentration factors. For reference, Tables 4.4.4 and 4.4.5 contain consumption rates used by the Nuclear Regulatory Commission in the absence of site-specific information (Reference 4.21, Table A-2, p. 1.109-19; Table D-1, p. 1.109-64).

TABLE 4.4.3

Animal Consumption Rates*

Animal	Feed or Forage (kg/day [wet weight])	Water (L/day)
Milk cow	50 (pasture grass)	60
Beef cattle	50 (stored feed grain)	50

*This table is taken from an NRC publication (Reference 4.21, Table A-10, p. 1.109-34). Documentation is provided there.

TABLE 4.4.4

Recommended Usage Rates for the Maximum Exposed Individual in Lieu of Site-Specific Data

Pathway	Child	Teen	Adult	Units
Fruits, vegetables, and grain	520.0	630.0	520	kg/yr
Leafy vegetables	26.0	42.0	64	kg/yr
Milk	330.0	400.0	310	L/yr
Meat and poultry	41.0	65.0	110	kg/yr
Fish (fresh or salt)	6.9	16.0	21	kg/yr
Seafood	1.7	3.8	5	kg/yr
Drinking water	510.0	510.0	730	L/yr
Shoreline recreation	14.0	67.0	12	hr/yr
Boating	29.0	52.0	52	hr/yr
Inhalation	2700.0	5100.0	7300	m^3/yr

[a] This table is taken from an NRC publication (Reference 4.21, Table A-2, p. 1.109-19). Documentation is provided there.

TABLE 4.4.5

Recommended Usage Rates for the Average Individual in Lieu of Site-Specific Data

Pathway	Child	Teen	Adult	Units
Fruits, vegetables, and grain	200.00	240.00	190.0	kg/yr
Milk	170.00	200.00	110.0	[a] L/yr
Meat and poultry	37.00	59.00	95.0	kg/yr
Fish	2.20	5.20	6.9	kg/yr
Seafood	0.33	0.75	1.0	kg/yr
Drinking water	260.00	260.00	370.0	[a] L/yr
Shoreline recreation	9.50	47.00	8.3	hr/yr
Inhalation	2700.00	5100.00	7300.0	m^3/yr
External exposure from deposited airborne radioactive materials	8760.00	8760.00	8760.0	hr/yr

[a] This table is taken from an NRC publication (1, Table D-1, p. 1.109-64). Documentation is provided there.

403 230

In using the preceding relations to calculate nuclide ingestion, considerable variation is possible. For example, each zone might have individuals with different dietary habits. Variation could be in types of food consumed, amount of food consumed, or agricultural practices used to produce food. Some of the pathways might have to be used several times for a given individual. Thus, one individual might consume three different types of aquatic food, two different classes of plant material, and four different types of animal products. Each of these could require a separate application of the appropriate pathways model with a different concentration factor. One individual might possibly consume food produced in several different zones, each with a different nuclide concentration in solid or water.

Some comment is needed about the type of computer model that can or should be developed for the preceding pathway models. Certainly one could attempt to construct a very general model, where 'general' means capable of representing many different situations. However, possible variability in food chains, diets, sources of diet, and population distributions would result in many requirements for flexibility. But, since the ingestion models are easy to program, there is much to be said for a relatively simple computer model that requires some additional programming to represent situations with special requirements. Then it would not be necessary to develop, maintain, and understand a large and complicated model with many seldom-used features. Further, by suitable user programming, such a model can be tailored to the exact situation under consideration. This latter approach has been adopted.

A computer model has been written to implement the calculations in the Transport to Man Model. This model includes all the pathways in the Transport to Man Model and can represent a number of different situations. However, it is not intended to be all-encompassing; situations exist to which it does not apply. Generally, it has the following properties: It calculates dose by inhalation or ingestion in each of the zones of the Environmental Transport Model. The following food types can be considered in each zone: drinking water, fish, invertebrates, plants, milk, and beef. For each zone, the user supplies an arbitrary number of food consumers with different dietary patterns and the code calculates the amount of each nuclide ingested by each individual. Further, the user can specify for each individual whether drinking water is from the groundwater or the surface water subzone, whether agricultural water is from the groundwater or the surface water subzone, and whether irrigation is used. Food is assumed to be consumed in the same zone in which it is produced.

4.5 Conclusion

4.5.1 Review of Pathways to Man Model

The Pathways to Man Model is divided into two parts: the Environmental Transport Model and the Transport to Man Model. This division is made because the processes and time scales

involved in the movement of nuclides through the environment and in the movement of nuclides from the environment to man can be radically different. By subdividing the Pathways to Man Model, it is possible to emphasize the processes and time scales which are important in each situation.

A compartment model is used for the Environmental Transport Model. In such a model, the area under consideration is divided into a suitable number of compartments, nuclide movements between these compartments are determined, and a system of differential equations is used to represent these movements. The solution of this system of equations yields time-dependent nuclide distribution through the environment. This modeling approach is adaptable, well-known, and numerically tractable.

To employ a compartment model, it is necessary to define the compartments, the nuclide movements, and the resultant system of differential equations. To facilitate this, an algorithm based on water flow patterns is presented for use in the development of these definitions. Although this technique may not always be applicable, it can be used to develop models of many different patterns of nuclide release and transport. The basic idea underlying its construction is the division of the area potentially affected by a nuclide release into a number of geographic zones. Further, it is assumed that similar processes take place within each zone, that certain movements of water and solid material are possible within and between zones and that nuclide movements are determined by the movements of water and solid material. The system of equations representing nuclide transport is then derived from linking a suitable number of these user-defined zones. A computer program has been written to implement this approach to transport equation derivation.

The Transport to Man Model is based on concentration factors. In this approach, the amount of a nuclide ingested by an individual is determined from the amount and type of food consumed by that individual and the concentration of the nuclide in each food type consumed. The concentration of a nuclide in a particular food type is determined from the multiplication of an appropriate concentration factor by the nuclide concentration in the medium which produced the food type. This approach is flexible, widely studied, and mathematically simple. A computer program has been written to implement the model.

The purpose of the Pathways to Man Model is to provide a methodology which can be used to assess the results of nuclide releases from different potential waste repositories and under diverse sets of environmental conditions. It is felt that the two models which constitute the Pathways to Man Model provide such a methodology. The Environmental Transport Model together with the technique presented for compartment definition can be used to obtain an assessment of nuclide transport through a variety of observed or postulated environments into which nuclides might be released from a waste repository. Similarly, the Transport to Man Model can be used to obtain an assessment of the nuclides reaching man in a variety of observed or postulated environments. In the preceding two statements, reference is made to postulated environments as a reminder that current environmental

conditions cannot be assumed to continue unchanged when releases from waste repositories are considered; within the time scales involved in such modeling, significant climatic, hydrologic, and ecologic changes are not only possible but probable. Though no claim is made that the methodology in the Pathways to Man Model is optimum for, or even applicable to, all release scenarios, it is our belief that it can be meaningfully applied to many, if not most, such scenarios.

4.5.2 Future Work on Pathways to Man Model

Although the Environmental Transport Model and the Transport to Man Model are well advanced in their development, work remains to be done on them. The models are discussed in this report in some detail but limited descriptions are given of the computer programs which implement them. Once these programs are complete, users' manuals will be written for them. At present, the programs are close to completion.

Decisions must be made as to the proper treatment of variability in the data used in the derivation of the nuclide transport equations. In preceding sections, data such as water flow rates and amounts of suspended sediment have been treated as if they had constant values. Such is certainly not the case. Methods must be devised to properly incorporate this natural variability into the results of the Environmental Transport Model. With regard to this, sensitivity studies on this model are underway and will continue. Such studies should yield information on the importance of parameters and parameter variations.

Although the computer programs which implement the Environmental Transport Model and the Transport to Man Model have been exercised on hypothetical sites, they have not been used to model a real site. It is important to initiate such a modeling project in the near future, to select a well-known hydrologic system and use these models to predict the results of a hypothetical nuclide release to this system. By selecting a well-known system, it is possible to work with physically realistic values for input data. Further, by working with such real data, it should be possible to recognize many potential problems and complications that are not apparent from artificially constructed situations. It is hoped that the treatment of a real hydrologic system will give insight into an acceptable treatment of the variability inherent in such a system.

As mentioned earlier, techniques for sensitivity analysis are under development. The study of a natural hydrologic system would provide an excellent setting in which to present and demonstrate these results.

References

4.1. G. L. Atkins, Multicompartment Models for Biological Systems, Methuen, London, 1969.

4.2. R. A. Shipley and R. E. Clark, Tracer Methods for In Vivo Kinetics, Academic Press, New York, 1972.

4.3. A. Rescigno and G. Segre, Drug and Tracer Kinetics, Ginn (Blaisdell), Boston, 1966.

4.4. A. Rescigno and J. S. Beck, "Compartments," Foundations of Mathematical Biology, Vol. II, R. Rosen, Ed., Academic Press, New York, pp 255-322, 1972.

4.5. C. W. Sheppard, Basic Principles of the Tracer Method, Wiley, New York, 1962.

4.6. J. A. Jacquez, Compartmental Analysis in Biology and Medicine, American Elsevier, New York, 1972.

4.7. M. Bernhard, "The Utilization of Simple Models in Radioecology," Marine Radioecology, OECD, Paris, pp 129-63, 1972.

4.8. M. Bernhard, A. Bruschi, and F. Moller, "Use of Compartmental Models in Radioecological Laboratory Studies," Design of Radiotracer Experiments in Marine Biological Systems, IAEA, Vienna, pp 241-89, 1975.

4.9. R. E. Funderlic and M. T. Heath, Linear Compartment Analysis of Ecosystems, ORNL-IBP-71-4, Oak Ridge National Laboratory, August 1971.

4.10. B. C. Patten, editor, Systems Analysis and Simulation in Ecology, Vol. I-IV (Vol. I, 1971, Vol. II, 1972, Vol. III, 1975, Vol. IV, 1976) Academic Press, New York.

4.11. F. O. Hoffman et al, "Computer Codes for the Assessment of Radionuclides Released to the Environment," Nuclear Safety, Vol. 18, pp 343-54, 1977.

4.12. D. L. Strenge et al, Review of Calculational Models and Computer Codes for Environmental Dose Assessment of Radioactive Releases, ERDA Report BNWL-B-454, Battelle Pacific Northwest Laboratories, June 1976.

4.13. "Estimating Aquatic Dispersion of Effluents from Accidental and Routine Reactor Releases for the Purpose of Implementing Appendix I," U.S. NRC Regulatory Guide, Office of Standards Development, Regulatory Guide 1.113, May 1976.

4.14. "Draft Liquid Pathway Generic Study," U.S. NRC, Division of Site Safety and Environmental Analysis, NUREG-0140, September 1976.

4.15. U.S. NRC, Reactor Safety Study: An Assessment of Accident Risks in U.S. Commercial Nuclear Power Plants, NUREG-75/014 (WASH-1400), October 1975.

4.16. J. F. Fletcher and W. L. Dotson (compilers), HERMES-A Digital Computer Code for Estimating Regional Radiological Effects from the Nuclear Power Industry, USAEC Report HEDL-TME-71-168, Hanford Engineering Development Laboratory, 1971.

4.17. R. S. Booth, "Systems Analysis Model for Calculating Radionuclide Transport Between Receiving Water and Bottom Sediments," Environmental Toxicity of Aquatic Radionuclides: Models and Mechanisms, Proceedings of the 8th International Conference on Environmental Toxicity, June 2-4, 1975, University of Rochester, Rochester, NY, Ann Arbor Science, pp 133-63, 1976.

4.18. I. Y. Borg et al, Information Pertinent to the Migration of Radionuclides in Ground Water at the Nevada Test Site, Part 1: Review and Analysis of Existing Information, UCRL-52078, Lawrence Livermore Laboratory, May 25, 1976.

4.19. A. C. Hindmarsh, GEAR...Ordinary Differential Equation System Solver, UCID-30001 Rev. 3, Lawrence Livermore Laboratory, December 1974.

4.20. A. C. Hindmarsh, GEARB...Solution of Ordinary Differential Equations Having Banded Jacobian, UCID-30059 Rev. 1, Lawrence Livermore Laboratory, March 1975.

4.21. "Calculation of Annual Doses to Man from Routine Releases of Reactor Effluents for the Purpose of Evaluating Compliance with 10 CFR Part 50, Appendix I," U. S. NRC Regulatory Guide, Office of Standards Development, Regulatory Guide 1.109, March 1976.

4.22. J. Kastner and J. S. Bland, "Assessment of Doses in the Environment for Liquid Releases from Nuclear Power Reactors," Impacts of Nuclear Releases into the Aquatic Environment, IAEA, Vienna, pp 405-13, 1975.

4.23. J. K. Soldat, Modeling of Environmental Pathways and Radiation Doses from Nuclear Facilities, USAEC Report, BNWL-SA-3939, Battelle Pacific Northwest Laboratories, NTIS, October 1971.

4.24. J. K. Soldat et al, Models and Computer Codes for Evaluating Environmental Radiation Doses, USAEC Report BNWL-1754, Battelle Pacific Northwest Laboratories, 1974.

4.25. D. A. Baker et al, FOOD - An Interactive Code to Calculate Internal Radiation Doses from Contaminated Food Products, ERDA Report BNWL-SA-5523, Battelle Pacific Northwest Laboratories, 1976.

4.26. J. K. Soldat, "Aquatic Exposure Pathways - Potential Exposure of Man from Environmental Transport of Waste Nuclides," International Symposium on the Management of Wastes from the LWR Fuel Cycle, Denver, July 11-16, 1976, pp 539-53.

4.27. J. R. Watts, "Modeling and Radiation Doses from Chronic Aqueous Releases," presented at Health Physics Society Annual Meeting, San Francisco, June 27-July 2, 1976, ERDA Report CONF-760652-1, Savannah River Laboratory, NTIS, 1976.

4.28. R. S. Booth, S. V. Kaye, and P. S. Rohwer, "Systems Analysis Methodology for Predicting Dose to Man from a Radioactively Contaminated Terrestrial Environment," Radionuclides in Ecosystems, Proceedings of the Third National Conference on Radioecology, Oak Ridge, TN, May 10-12, 1971, USAEC Report CONF-710501-P2, pp 877-93, Oak Ridge National Laboratory, NTIS, 1971.

4.29. R. S. Booth and S. V. Kaye, A Preliminary Systems Analysis Model of Radioactivity Transfer to Man from Deposition in a Terrestrial Environment, USAEC Report ORNL-TM-3135, Oak Ridge National Laboratory, NTIS, October 1971.

4.30. G. G. Killough et al, A Methodology for Calculating Radiation Doses from Radioactivity Released to the Environment, ORNL-4992, 1976.

4.31. L. Bramati et al, VADOSCA: A Simple Code for the Evaluation of Population Exposure Due to Radioactive Discharges, Proceedings of the Third International Congress of the International Radiation Protection Association, Washington, DC, September 9-14, 1973, USAEC Report CONF-730907-P2, NTIS, pp 1072-77., 1973.

4.32. G. M. Milbourn and R. Taylor, "The Contamination of Grasslands with Radioactive Strontium I. Initial Retention and Loss," Radiation Botany, Vol. 5, p 337, 1965.

CHAPTER 5. DOSIMETRY AND HEALTH EFFECTS

5.1 Dosimetry

The purpose of this section is to discuss the models used to convert the dose from radionuclides inhaled and ingested to dose commitments to specific organs of the body. The dose to different organs is needed to compute the health effects discussed in the next section.

The doses received from the radionuclides inhaled and ingested are expected to be of a very low level, comparable to natural background irradiations. The dose will be received at a very low dose rate protracted over an individual's lifetime. The nuclides that dominate waste disposal initially have both low and high linear energy transfer (LET), although the long-lived isotopes are primarily high LET.

The basic model used for the dosimetry is the ICRP-2 model.[5.1,5.2] The first component of that model is the rate of change in the radioactive burden $B_{ik}(t)$ of the k^{th} organ at time t from the i^{th} radionuclide inhaled or ingested. The model used is given by

$$\frac{dB_{ik}(t)}{dt} + \lambda_{ik}(t - t_b)B_{ik}(t) = I_i(t - t_b, t)f_{ik}(t - t_b) \quad ,$$

expressed in Ci/year, where

λ_{ik} = effective elimination rate of nuclide i from organ k

I_i = yearly intake rate (Ci/year) of the i^{th} nuclide

f_{ik} = fraction of the i^{th} nuclide absorbed in the k^{th} organ

t_b = time of birth and $t - t_b$ is the age of the individual at time t.

The model describes the rate of change in the radioactive burden to an organ as the uptake rate (intake rate I_i times the fraction absorbed f_{ik}) minus the discharge rate (proportional to the existing burden $\lambda_{ik} B_{ik}$).

The values of λ, I, and f have been generated using an adult model. As will be discussed later, the closer proximity of organs in a child is approximately offset by the lower intake and more rapid metabolism. Consequently we take $\lambda_{ik}(t) = \lambda_{ik}$ and $f_{ik}(t) = f_{ik}$.

With the additional assumption that intake will be a constant over the lifetime of an individual ($I_i(t) \equiv I$), the above equation can be solved to get

$$B_{ik}(t) = \frac{e^{-\lambda_{ik}t} I_i f_{ik}}{\lambda_{ik}} \left(e^{\lambda_{ik}t} - 1\right) \mu Ci \quad .$$

The cumulative dose in rems, $D_{ik}(t)$, satisfies the equation,

$$\frac{dD_{ik}(t)}{dt} = \frac{51\ B_{ik}(t)\ E_{ik}(t - t_b)}{m_k(t - t_b)} \quad ,$$

where

$$51 \approx \frac{(3.2 \times 10^9 \text{ disintegrations/year/}\mu Ci)\ (1.6 \times 10^{-6} \text{ erg/MeV})}{(100 \text{ erg/gram of tissue/rad})}$$

E_{ik} = effective absorbed energy (MeV) of the i^{th} nuclide in the k^{th} organ

M_k = mass (g) of the k^{th} organ.

This equation can also be solved to get

$$D_{ik}(t) = \frac{51\ E_{ik} I_i f_{ik}}{m_k \lambda_i^2 k} \left(\lambda_{ik} t + e^{-\lambda_{ik}t} - 1\right) \text{ rems} \quad .$$

the actual dose commitment to organ k as a result of ingesting radionuclide i at the rate I_i for t years.

The actual quantity of interest is the dose factor, i.e., the increment in dose for a given year with unit intake of 1 μCi/year. The dose factor is given by

$$DF_{ik}(t) = D_{ik}(t) - D_{ik}(t - 1)$$

$$= \frac{51\ E_{ik} f_{ik}}{m_k \lambda_{ik}^2} \left(\lambda_{ik} + e^{-\lambda_{ik}t} - e^{-\lambda_{ik}(t-1)}\right) \quad .$$

The dose factor is typically given for the 50^{th} year, as a compromise value, so that

$$DF_{ik} = D_{ik}(50) - D_{ik}(49) \quad .$$

Since the total dose is linear in the dose rate, the dose to the k^{th} organ during a given year can be computed as $I_i DF_{ik}$, which solves the dosimetry problem. A data base has been created which gives dose factors for 305 radionuclides by 11 organs.

403 237

It should be noted that an alternative solution to the ICRP-2 model sometimes appears.[5.3] This solution is obtained by noting that

$$\frac{D_{ik}(t) - D_{ik}(t-1)}{1} \simeq \frac{dD_{ik}(t)}{dt}$$

$$= \frac{51 E_{ik} f_{ik}}{m_k \lambda_{ik}} \left(1 - e^{-\lambda_{ik} t}\right) .$$

Then letting $\tau_{ik} = (\ln 2/\lambda_{ik})$ be the effective half life,

$$DF_{ik}(t) = \frac{74 E_{ik} \tau_{ik} f_{ik}}{m_k} \left(1 - e^{-\ln 2 \cdot t/\tau_{ik}}\right) .$$

The interesting aspect of the latter solution is that the dose factor, the increment in cumulative dose in the t^{th} years due to consuming 1 μCi/year for t years, is equivalent to the cumulative dose in t years obtained from consuming 1 μCi the first year. While there is little biological significance in this result, it is a very convenient device for computing dose factors with programs such as INREM[2] which only outputs cumulative doses.

There are many uncertainties and approximations in the derivation of the formulas given above. It is important to discuss some of the possible errors.

The ICRP-2 model is itself a tractable simplification of a complicated system and it would be easy to point out inadequacies in the model. However, variation in the physiological characteristics of individuals in a population and a lack of data make the parameters (λ_{ik}, f_{ik}, E_{ik}, and m_k) a much greater source of variation. Even with accurate values of these parameters and an accurate model, the nonlinearities of the dose factor to these parameters, together with human variation, would make dosimetry an impossible task. So a reference man must be assumed with statistical errors (at least) recognized.

The assumption of an adult model is also a convenient simplification. More detailed studies have revealed, however, that the effect of the closer proximity of the organs to each other in an infant are approximately offset by lower consumption and higher metabolism.[5.4] So again human variation and uncertainty of the parameters introduce more serious errors than those that arise from the use of an adult model.

Under the assumption of continual consumption of a nuclide, there will always be a fraction of the body burden that is circulating and not yet in the critical organ (to which it is ascribed by f_{ik}).[5.5] In time this total body dose equivalent ("en route") may contribute a fair fraction of the dose independent of the "deposited" fraction accumulation. This provides another source of error.

The very low dose rates to be encountered from waste disposal also offer another problem in the use of the ICRP-2 model. The assumption is made that the fraction absorbed (f_{ik}) is independent of dose and dose rate. At very low concentrations, however, the uptake fraction may be larger than we now assume since the possibility of aggregation and chelation may be limited.[5.5] This effect alone can make previously considered conservative assumptions about health effects not conservative at all.

A parameter that exists in the ICRP-2 model but which is not apparent in the final formulation is the quality factor (QF) which reflects the degree of homogeneity to which a radionuclide will deposit within an organ, and the possibility of producing [illegible] spots of increased risk. Considerable uncertainty exists with respect to this factor as well.[5.1, 5.6]

The ICRP-2 model also assumes an average energy per disintegration. This assumption has been necessary to make results tractable. Considerations of molecular biology as to the interaction of living cells with ionizing radiations make the nonlinear effect of energy level quite apparent. This, again, must be viewed as adding a stochastic error to the result.

Previous studies[5.7] have shown that the dose factors are accurate to within a factor of 2. The stochastic errors were assumed to have a log normal distribution with a standard deviation of 0.35.

New dosimetry models and computer codes which are more accurate than existing ones are presently in development. As more sophisticated computer codes become available, it only remains to update the dose factors DF_{ik} in the data base.

5.2 Health Effects

The low doses expected from nuclear waste disposal would exclude acute effects, but pose chronic problems. Estimates of three kinds of adverse health effects that low doses of radiation could produce are considered: developmental and teratogenic effects, genetic effects, and somatic effects (chiefly carcinogenic).

5.2.1 Developmental and Teratogenic Effects

The developing fetus is exposed to radiation as a result of inhalation and ingestion of radioactive material by the mother for 9 months. At very low doses and dose rates, the total dose accumulated by the fetus will be quite small. In addition, even though the fetus is sensitive to the effects of radiation in some stages of development, these stages are sharply limited in time.

The most pessimistic case for embryotoxicity can be calculated from an estimated threshold dose of 10 rads of acute radiation.[5.3] If the 10 rads were protracted over a 9-month period of gestation and the first year of life, a daily dose of about 15 mrad would result. The conservatism of this estimate is pointed up by the fact that the lowest dose of protracted external radiation for which confirmed deleterious effects have been reported is slightly over 1 rad per day throughout late gestation and early postnatal life.[5.8]

On the basis of the anticipated doses, we expect no measurable developmental and teratogenic effects of radionuclides from waste disposal.

5.2.2 Genetic Effects

Many national and international groups (BEIR, NCRP, ICRP) revise from time to time our understanding of the genetic risks to human populations from ionizing radiation. The following estimates of genetic effects of low levels of radiation due to ingestion and inhalation of radioactive isotopes released from disposed nuclear waste are based on their work.

Mutations – changes in the genetic formation – can occur at any time in any cell of the body. Geneticists, however, are concerned primarily with mutations that occur in the genes and chromosomes of germ cells, sperm and eggs, or the cells from which they are derived. Sperm and egg cells, after fertilization, give rise to the individuals of the next and later generations.

Mutations arising in nongerminal or somatic cells are limited to expression in the individual and cannot be transmitted to future generations. They are nevertheless of considerable importance, in that there is a compelling body of evidence linking the induction of many cancers to mutation induction.

All forms of genetic change are known to occur spontaneously, i.e., in the absence of known causative agents. They also can be produced by various physical agents, such as ultraviolet light and ionizing radiation, and by chemical agents. Whether or not naturally occurring mutagens in our environment are responsible for the "spontaneous" mutation rate is moot. Certainly no single agent can readily be implicated as the sole cause. Present evidence indicates that natural background radiation levels are able to account for only part of the spontaneous incidence.

Although there is no definitive proof that any single mutant human individual resulted from exposure of the parents to a known mutagen (radiation or chemical) and thus no direct proof that these agents are indeed mutagenic in man, radiation has been demonstrated to be mutagenic in so many organisms that it seems very unlikely that it is not mutagenic in man.

Three major principles of particular relevance to human risk estimates have emerged from studies of induced mutation.[5.3]

1. Radiation or other mutagens appear to produce genetic changes that are qualitatively the same as those that occur naturally. Different mutagens, however, may not increase all types of mutations at the same rate.
2. At low doses and low dose rates of low-LET radiation, mutations are induced in direct proportion to the dose. No threshold dose is evident in the experiments testing this.

3. In the low dose range of irradiation to which human populations are normally exposed from natural background or man-made sources, the rate at which the dose is received will not affect the yield of induced mutations. The same type and quantity of mutations will result if the dose is received all at once or spread out over weeks, months, or even years.

The BEIR report by the National Academy of Science[5.8] serves as a guiding source for radiological protection. We, therefore, use the BEIR recommendations in this study as presented in Table 5.2.1.

TABLE 5.2.1

Estimated Effects of 5 rem per Generation on a Population of One Million Live Births (from Reference 5.8)

Disease Classification	Current Incidence	Effect of 5 rem per Generation		
		First Generation	Equilibrium	Generations to Equilibrium
Dominant diseases	10,000	50 - 500*	250 - 2500	5
x-linked recessive diseases	400	0 - 15*	10 - 100	6
Recessive diseases	1,500	Very few	Very slow increase	-
Chromosomal anomalies				
Unbalanced rearrangements	1,000	60	75	2-3
Aneuploidy	4,000	5	5	0
Congenital anomalies	15,000			
Abnomalies expressed later	10,000	5 - 500	50 - 5000	10
Constitutional and degenerative diseases	15,000			
TOTAL	56,900	120 - 1100	390 - 7700	

*Based on a doubling dose of 20 - 200 rem.

403 241

5.2.3 Somatic Effects

The dose magnitudes and dose rates which would result from release of nuclear waste to the human environment are expected to be quite low. The acute effects of radiation exposure are considered to be phenomena of much larger doses and are not considered in this report. However, should further analysis indicate that certain low-probability/high-consequence events (e.g., massive meteorite impact) are significant contributors to risk, the health effects model will be expanded to include consideration of acute radiation effects. For various reasons, we confine our attention of somatic effects to carcinogenicity.

There is no conclusive data representing the relationship between ionizing radiation and latent cancer fatalities at the low dose and dose rates discussed here. Evaluation of the potential risk at such levels must depend, therefore, on extrapolation from observations at higher doses and dose rates. Because the dose-rate characteristic of background radiation (approximately 100 mrem per year) is several orders of magnitude lower than the lowest rates at which carcinogenic effects have been documented unequivocally, the extrapolation involves assumptions that are highly questionable in our present state of knowledge.

Among the major factors complicating the extrapolation is uncertainty about the shapes of the incidence/dose curves for cancers of different types, about the relevant mechanisms of carcinogenesis, and about the influence of biological and physical variables (e.g., spatial and temporal distribution of the radiation dose, age at irradiation, sex, and physiological state) that have been observed to affect the induction of malignancy at higher dose rates in human and animal populations.[5.3,5.9] The problem is further complicated by the multiplicity and diversity of effects through which radiation is thought to influence the probability of cancer development.

The combined effects of the various types of radiation-induced carcinogenic changes must depend heavily on the dose, dose rate, quality of radiation, and other variables; hence, it is not surprising that the incidence/dose relationship has been observed to vary with these factors. The relationship differs quantitatively, however, from one type of cancer to another, and in no instance are the parameters known well enough to enable confident prediction of the carcinogenic effects to be expected at the low dose rates associated with background radiation levels.

Some of the effects are likely to be minimal or absent at low doses and low dose rates. Disturbances in hormonal regulation and impairment of immunological defenses require extensive killing of cells unlikely at a low dose rate. Other types of effects also should be reduced in frequency per rad at low doses and dose rates because of the action of various processes, at least in the case of low-LET radiation, as well as existing evidence of multistage mechanisms of carcinogenesis[5.10,5.11] giving rise to a "shoulder effect." Furthermore, if the time required to accumulate a given dose is a sufficient fraction of the life span, then, in the absence of age-dependent changes in susceptibility, the carcinogenecity per rad of the total cumulative dose can be expected to diminish because the latent period for carcinogenesis will ultimately exceed the life expectancy of some members of the population at risk.

It may be concluded, therefore, from all available data that, for carcinogenic effects, just as for the induction of mutations, chromosome aberrations, cell-killing, teratogenic effects, and most other effects on mammalian cells and tissues, the dose/response curves for low-LET radiation will tend to be concave upward. Characteristically the curves tend to increase in slope with increasing dose and dose rate until they reach the point where, with high doses accumulated at high dose rates, they pass through a maximum and eventually turn downward, owing presumably to excessive cell-killing or other forms of injury. In comparison, the dose/response curves for high-LET radiation tend to be steeper, more nearly linear, and less dependent on dose rate.[5.3,5.8,5.11]

Because of these variations in the biological effectiveness of radiation with changes in the spatial and temporal distribution of dose, various weighting factors have been introduced for use in risk estimation. These include the QF which has long been used to adjust for differences in LET.[5.3,5.12] More recently, other dose-effectiveness factors for carcinogenic effects have been based largely on empirical observations of radiation carcinogenesis in experimental animals; they are concordant with the data on man and with the bulk of radiobiological experience on the induction of mutations, chromosome aberrations, cell-killing, cell transformation in culture, and other effects that may be involved in carcinogenesis.

Weighting factors have been proposed which range in magnitude from 0.2, for doses of less than 10 rads or for larger doses received at dose rates of less than 1 mrad per minute, to 1.0 for doses of 200 rads or more received at dose rates in excess of 1 mrad per minute.[5.3,5.12]

For each type of cancer which might ensue as a result of radiation exposure from nuclear waste, we have formed three estimates of the absolute risk per one million man rems per year: a lower bound estimate, a central estimate, and an upper bound estimate. This approach is similar to approaches previously used by NRC[5.12] and NAS.[5.3]

5.2.4 Central Estimate

As noted before, the usual approach[5.3,5.8,5.12] to relate dose effects to dose is to use a linear response for high-LET radiations and a linear response weighted by dose effectiveness factor for low-LET radiations. Using the dose effectiveness factors of NRC[5.12] with less than a rad per day, the dose effectiveness factor is 0.2. Consequently, the dose (in rems) used to compute the central estimate of risk is given by

$$\text{Dose} = \text{high-LET dose} + 0.2\ \text{low-LET dose} .$$

Hypothetically, the dose so computed could be used directly with the absolute risk factors computed by the BEIR Committee,[5.8] given in Table 5.2.2, or by NRC,[5.12] given in Table 5.2.3. However, both tables give age-specific risks and so the population must be partitioned into age groups: In utero, 0 to 9.9 years, 10 to 19.9 years and 20+ years. While there is no way to predict the effects of future changes in longevity, etc, on the age distribution of the U.S. population, it would require large shifts to significantly alter these numbers. Hence, using the 1974 population,[5.12] we use:

Age (yr)	Percentage
In utero	1.1
0 - 9.9	16.0
10 - 10.9	19.6
20+	63.3

The risk factors used by NRC[5.12] were then age-adjusted to yield the central factors given in Table 5.2.4.

TABLE 5.2.2

Values Assumed by BEIR Committee[5.3,5.8] in Estimating Risks of Low-Level Irradiation

Type of Cancer	Age at Time of Irradiation (yrs)	Latent Period (yrs)	Plateau Period (yrs)	Risk Estimate	
				Absolute (death/10^6 yr/rem)	Relative (% incr. in deaths/rem)
Leukemia	In utero	0	10	25	50
	0 - 9.0	2	25	2	5
	10+	2	25	1	2
Lung	10+	15	30[a]	1.3	0.3
GI tract, including stomach	10+	15	30[a]	1	0.2
Breast	10+	15	30[a]	1.5[b]	0.8
Bone	10+	15	30[a]	0.2	1
All other[c]	In utero	0	10	25[d]	50
	0 - 9.9	15	30[a]	1[e]	2
	10	15	30[a]	1	0.1

[a]Remaining life expectancy stated as an alternative plateau period.

[b]Includes males and an assumed 50% cure rate.

[c]Includes thyroid and skin. It is noteworthy that the mortality from thyroid cancer was inferred to be low, as compared with the morbidity from the disease, which was estimated to approximate 1.6-9.3 case/10^6/yr/rem in persons irradiated during childhood.

[d]"All other" denotes all cancers except leukemia.

[e]"All other" denotes all cancers except those specified in table.

403 244

TABLE 5.2.3

Risk Factors for Cancer Mortality
(Type of Cancer and Age at Irradiation)
(From References 5.8, modified as appropriate, and 5.12)

Type of Cancer and Age at Irradiation	Latency (yr)	Plateau (yr)	Risk[a]
Leukemia:			
In utero	0	10	15
0 - 9.9 years	2	25	2
10+ years	2	25	1
Lung cancer:			
10+ years	15	30	1.3
Gastrointestinal tract, stomach:			
10+ years	15	30	0.6
Rest of gastrointestinal tract:[b]			
10+ years	15	30	0.2
Pancreas:[c]			
10+ years	15	30	0.2
Breast cancer:[d]			
10+ years	15	30	1.5
Bone cancer:			
0 - 19.9 years	10	30	0.4
20+ years	10	32	0.2
Other cancers:[e]			
In utero	0	10	15
0 - 9.9 years	15	30	0.6
10+ years	15	30	1

[a] Number of deaths per million population per year per rem

[b] Including the lower bowel

[c] See text

[d] Includes male population correction

[e] Includes all other cancers; corrects for juvenile bone cancers; assumes fetal leukemia risk equals that for all other cancers.

5.2.5 Lower Bound Estimate

Considerable literature exists which indicates the possible existence of dose thresholds and of quadratic dose response function, essentially giving thresholds for very low doses (see Reference 5.12, Section GI.4 for a review). These lower bounds are normally taken as applied only to low LET radiations. However, the "linear hypothesis" certainly has not been proven for high-LET radiations, and several reports indicate nonlinear dose response functions for ^{226}Ra - ^{228}Ra in man and ^{226}RA in dogs.[5.9,5.11] Reference 5.11 indicates good reconciliation with the data using a three-stage (initiation, promotion type) model. At very low doses, the three stages will present a "shoulder" much like that of a three-hit model in classic target theory. Also increases in the latent period have been observed for decreased doses for neutron irradiation.[5.13] In general, the linear model is held to be a conservative or overestimate of incidence. Consequently, the quadratic

model of Mays[5.14] used by NRC[5.12] was also used here for a lower bound, but for all radiation. The coefficients of the lower bound quadratic model are given in Table 5.2.4.

TABLE 5.2.4

Risk Factors for Cancer Mortality
(Lower, Central, and Upper Bound Estimates)

Type of Cancer	Lower Bound[a]	Central Estimate	Upper Bound
Leukemia	.004	30.4	537.4
Lung	.03	32.3	571
Stomach	.06	14.9	263.4
Rest of alimentary canal	.02	5	88.4
Pancreas	.02	5	88.4
Bone	.03	8.1	143.2
All other[b]	.09	29.4	519.7

[a] From Reference 5.12

[b] Excludes thyroid

5.2.6 Upper Bound Estimate

For a variety of reasons it has been indicated that, for high-LET in particular, the linear extrapolation to low doses and dose rates underestimates the risk.[5.15] Several explanations have been advanced, among them the possibility mentioned in the dosimetry section of this report that the fraction of a radionuclide absorbed in an organ may be greater at low doses and dose rates. A second possibility is that, since it is accepted that at very high doses and dose rates the incidence will begin to decrease owing possibly to increased cell toxicity and excess cell-killing, if the data is collected (unknowingly, since no other data may be available) beyond the peak response, an underestimate can be obtained. Also, there is considerable evidence, for neutrons at least, that RBE will increase with decreased dose.

With these considerations in mind, a dose model,

$$\text{Risk} = a\,(\text{dose})^{1/n},$$

was considered. From the watch-dial-painter study (see Reference 5.8, Figure C.1), a value for n of 2 was selected. The upper bound is then given by a square root model equivalent to the quadratic lower bound of Mays[5.14] (using the dose factor of 0.016). The coefficients of the upper bound are also given in Table 5.2.4.

403 246

References

5.1. ICRP Publ. 2, Report of Committee II on Permissible Dose for Internal Radiation, Pergamon Press, New York, 1959.

5.2. G. G. Killough, P. S. Rohwer, and W. D. Turner, INREM-A Fortran Code Which Implements ICRP-2 Models of Internal Radiation Dose to Man, ORNL-5003, Oak Ridge, TN, 1975.

5.3. Drinking Water and Health, National Research Council, Advisory Center on Toxicology, Safe Drinking Water Committee, National Academy of Sciences, Washington, DC, 1977.

5.4. W. S. Snyder, personal communication, 1977.

5.5. M. Goldman, personal communication, 1977.

5.6. R. E. Alexander, Risk of Radiation Induced Cancer From the Systematic Deposition of Plutonium, U.S. Nuclear Regulatory Commission, Washington, DC, 1976.

5.7. R. G. Cuddihy, personal communication, 1977.

5.8. BEIR Report, The Effects on Populations of Exposure to Low Levels of Ionizing Radiation, Report of the Advisory Committee on the Biological Effects of Ionizing Radiations, Division of Medical Sciences, National Academy of Sciences, National Research Council, Washington, DC, 1972.

5.9. M. Goldman, L. S. Rosenblatt, N. W. Heatherington, and M. P. Finkel, "Scaling Dose, Time, and Incidence of Radium-Induced Osteosarcomas of Mice and Dogs to Man," Radionuclide Carcinogenesis, Proceedings of the Twelfth Annual Hanford Biology Symposium, Richland, WA, May 10-12, 1972, published 1973.

5.10. W. J. B. Ashley, "The Two "Hit" and Multiple "Hit" Theories of Carcinogenesis," British J. of Cancer 23, pp 313-28, 1969

5.11. J. M. Marshall and P. G. Groer, "A Theory of the Induction of Bone Cancer by Alpha Radiation: A Summary," The Health Effects of Plutonium and Radium, W. S. S. Jee, ed, J. W. Press, Salt Lake City, UT, 1976.

5.11a Ionizing Radiation: Levels and Effects, United Nations Scientific Committee on the Effects of Atomic Radiations (report on E 72 IX 18), United Nations, New York, 1972.

5.12. Reactor Safety Study, Appendix VI, Wash-1400, U. S. Nuclear Regulatory Commission, Washington, DC, 1975.

5.13. R. D. Evans, "Radium in Man," Health Physics 27, pp 497-510, 1974.

5.14. C. W. Mays, R. D. Lloyd, and J. M. Marshall, "Malignancy Risk to Humans from Total Body X-Ray Irradiation," presented at the International Congress, Radiological Protection Assn., Washington, DC, September 9-14, 1973.

5.15. J. M. Brown, "Linearity vs Non-Linearity of Dose Response for Radiation Carcinogenesis," Health Physics 31, pp 231-45, 1976.

403 247

CHAPTER 6. SUMMARY

The four models which form the basis of the risk assessment methodology are presented in Figure 6.1. The Local Waste Release Model represents events and processes which occur in the near vicinity of the repository. This model treats releases due to events and processes initiated by the presence of the repository (self-induced releases) and releases due to events and processes which are independent of the repository (externally induced releases). Herein release means the movement of radionuclides away from the underground, engineered facility which constitutes the repository. Self-induced release mechanisms are treated by simulating the time-dependent evolution of the system consisting of the radioactive waste, the repository and the host rock. Externally induced releases are treated by simple, probabilistic models. The processes of primary concern are those which lead to contact between the waste and circulating groundwater. As currently conceived, the outputs of this model are time-dependent probabilities and rates of local waste release.

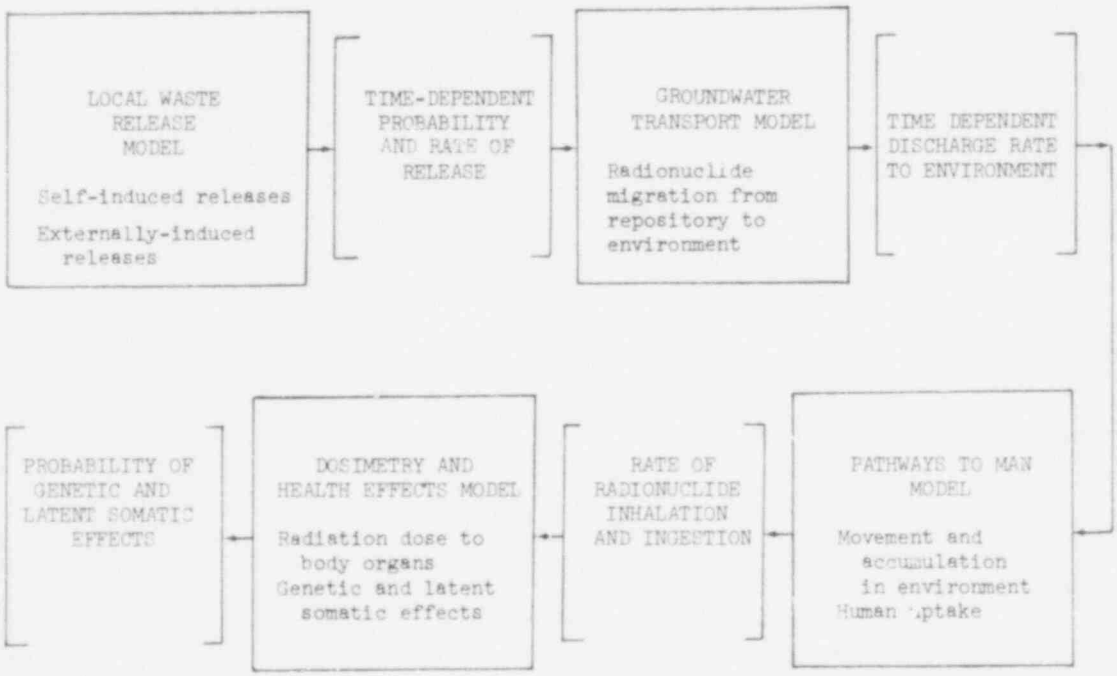

Figure 6.1. Models for Site Evaluation. The larger squares represent models in the risk assessment methodology. The smaller lettering in these squares provides an indication of what the model represents. The smaller bracketed squares represent the output of the preceding model and the input to the next model.

403 248

For a waste release to circulating groundwater, the Groundwater Transport Model represents radionuclide movement from the repository to a surface discharge location. This model includes groundwater flow, radioactive decay, and radionuclide sorption. Surface discharge modes include surface aquifer discharge and aquifer discharge through a well. The output of this model is time-dependent nuclide discharge rates at preselected points in the surface environment. Although other release modes to the surface environment are considered in the Local Waste Release Model, groundwater transport is considered the most important process in the potential movement of radionuclides from the repository to the surface environment.

The Pathways to Man Model uses the surface discharge rates generated by the Groundwater Transport Model as input and from this represents the long-term movement of radionuclides through the environment and determines their accumulation in soil, water, and sediments. Once environmental concentrations are determined, human radionuclide uptake is calculated through the use of concentration ratios and simple food chains. The output of the Pathways to Man Model is time-dependent rates of radionuclide ingestion and inhalation.

In turn, the output of the Pathways to Man Model is used as input to the Dosimetry and Health Effects Model. This model determines radiation dose to sensitive body organs. From this, probabilities of genetic effects and latent somatic effects are estimated.

A collection of models and the manner in which the output from one model provides input to the next are represented in Figure 6.1 However, in addition to these needed models, a risk or consequence methodology must provide a statistical design to measure, propagate, and assess the variability and uncertainity associated with model input parameters.

Such a statistical design has been developed and will be presented in a later report. Fundamental to this statistical design is the use of scenarios, which provides a method for (1) grouping and organizing assumptions of the subsurface and surface conditions under which calculations will be performed and (2) assuring that a reasonable range of possible conditions has been represented. Briefly, such a scenario involves assumptions about the following: (1) engineered features and radioactive waste inventory of the repository, (2) stratigraphy, hydrology, and physico-chemical properties of the rock strata that bound the site, (3) the surficial hydrologic and geomorphic features of the region surrounding the site and the environmental receptors associated with those features, and, (4) modes of human exposure to radionuclides.

The model structure shown in Figure 6.1 suggests that a scenario can be broken into subscenarios involving assumptions about (1) local waste release (R), (2) radionuclide transport in groundwater (T), and (3) environmental movement and human uptake (P). To cover a reasonable range of possible conditions, a variety of assumptions will be required. Thus, many R, T, and P subscenarios may be needed. A scenario is a three-tuple $(R_i R_j \ldots, T_k T_\ell \ldots, P_u P_v \ldots)$ of combinations of R's, T's, and P's. Event trees will be used to display scenarios. The event

will be used to display scenarios. The event tree shown in Figure 6.2 illustrates the use of subscenarios to form scenarios. In this illustration we have two R, one T, and three P subscenarios.

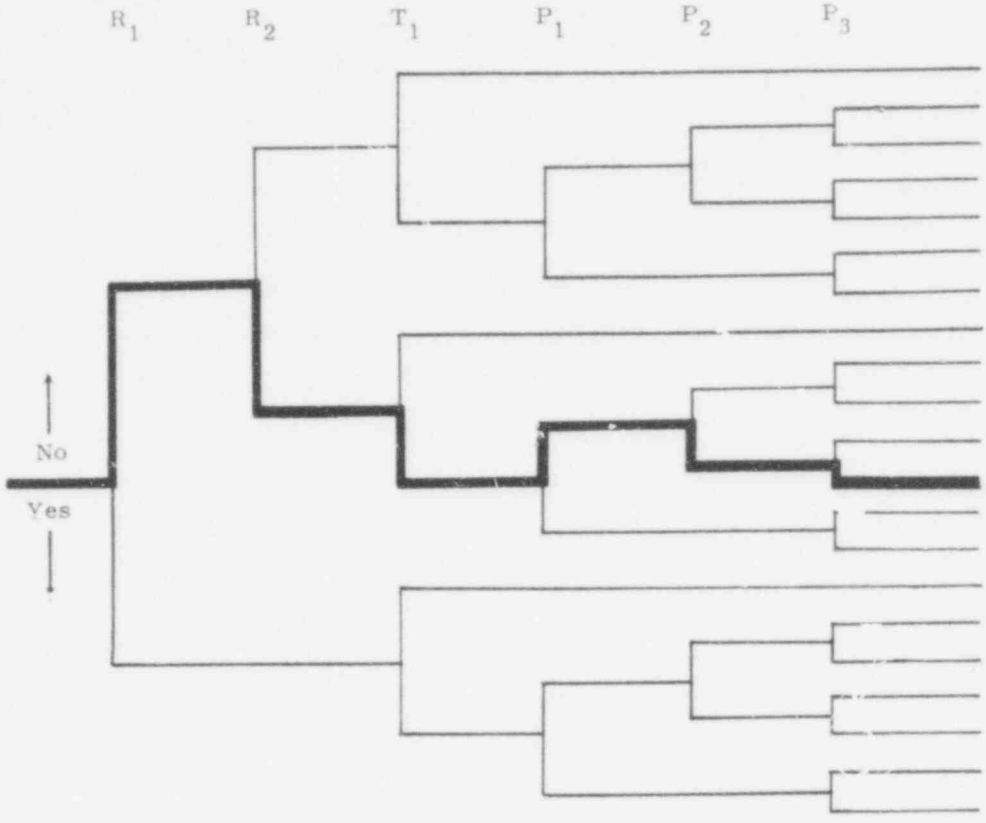

Figure 6.2 Example of the Use of an Event Tree to Display Scenarios

Any path through the event tree would define a scenario. The darkened path through the event tree in Figure 6.2 would define the scenario (R_2, T_1, P_2P_3). Such an event tree should reflect the presence of dependencies. For example, the event tree in Figure 6.2 indicates that if R_1 occurs, R_2 cannot occur, or if P_1 occurs, P_2 cannot occur.

A statistical design for risk analysis has been developed which uses scenarios as discussed above and which has the following properties: (1) scenarios can be ranked in relative importance; (2) input variables can be ranked in relative importance; (3) probabilities of the assumed scenarios are not intrinsically part of the design; i.e., the sensitivity of risk to the subscenario probabilities can be studied without rerunning the consequence calculations; and (4) the effects of different probability distributions on input variables can be examined without rerunning the consequence calculations.

DISTRIBUTION:

U.S. Nuclear Regulatory Commission
(105 copies for RW)
Division of Document Control
Distribution Services Branch
7920 Norfolk Avenue
Bethesda, MD 20014

ACRS Subcommittee on Waste Management (25)
U.S. Nuclear Regulatory Commission
Washington, DC 20555
Attn: R. E. McKinley
H-1016

U.S. Nuclear Regulatory Commission (9)
Office of Nuclear Material Safety & Safeguards
Washington, DC 20555
Attn: C. Smith, Director, 958-SS
Division of Fuel Cycle & Material Safety (8)
For: M. Bell, Chief, Low Level Waste Br., 396-SS
J. Bunting, Jr., A/D for Waste Mngt, 396-SS
H. Lowenberg, A/D for Oprs & Tech., 396-SS
J. Martin, A/D for Fuel Cycle Safety & Licensing, 396-SS
D. Nussbaumer, A/D for Matl Safety & Licensing, 396-SS
R. Boyle, High Level & Transuranic Waste Br., 396-SS
J. Malaro, Chief, High Level & Transuranic Waste Br, 674-SS
S. Schreurs, High Level & Transuranic Waste Br., 396-SS

U.S. Nuclear Regulatory Commission (17)
Probabilistic Analysis Staff
Office of Nuclear Regulatory Research
3106 MNBB
Washington, DC 20555
Attn: A. Buhl, Director
M. Cullingford (14)
P. McGrath, Deputy Director
W. Vesely

U.S. Nuclear Regulatory Commission (3)
Office of Standards Development
NL 5650
Washington, DC 20555
Attn: R. Baker
E. Conti
C. Roberts

U.S. Congress
Office of Technical Assessment
Washington, DC 20510
Attn: T. Cotton

U.S. Department of Energy (2)
B-107
Washington, DC 20545
Attn: C. Heath, Actg Director, Div. of Waste Isolation
S. Meyers, Director, Office of Nuclear Waste Management

U.S. Department of Interior (5)
U. S. Geologic Survey
345 Middlefield Road
Menlo Park, CA 94025
Attn: H. R. Shaw

403 251

DISTRIBUTION (cont):

U.S. Department of Interior (3)
U.S. Geologic Survey
P.O. Box 25046
Denver Federal Center
Denver, CO 80225
Attn: D. Leap, Nuclear Hydrology Project, WRD, MS 416
W. S. Twenhofel, Chief, Special Projects Branch
R. Waddell, Nuclear Hydrology Project, WRD, MS 416

U.S. Department of Interior (5)
U.S. Geologic Survey
National Center
Reston, VA 22092
Attn: F. J. Pearson

U.S. Environmental Protection Agency
Office of Radiation Programs
AW-459
Washington, DC 20464
Attn: D. Egan

Allied General Nuclear Services
P. O. Box 847
Barnwell, SC 29812
Attn: A. L. Ayers
Assistant to the President

American Nuclear Energy Council
1750 K Street, NW, Suite 300
Washington, DC 20006
Attn: A. G. Randol, III

The Analytical Sciences Corp.
6 Jacob Way
Reading, MA 01867

Texas Tech University
College of Business Administration
P. O. Box 4320
Lubbock, TX 79409
Attn: W. J. Conover

Texas Tech University
Department of Mathematics
P. O. Box 4319
Lubbock, TX 79409
Attn: J. M. Davenport

General Electric Company
175 Curtner Avenue, MC 851
San Jose, CA 95125
Attn: A. B. Carson

Harvard University
Pierce Hall, Room 115
Cambridge, MA 02134
Attn: M. Stack

403 252

DISTRIBUTION (cont):

Harvard University
Physics Department
Cambridge, MA 02138
Attn: R. Wilson

Intera Environmental Consultants (3)
11511 Katy Freeway
Suite 630
Houston, TX 77079
Attn: R. Lantz
S. Pahwa
M. Reeves

Los Alamos Technical Associates
P. O. Box 410
1553 Myrtle Street
Los Alamos, NM 87544
Attn: S. E. Logan

Natural Resources Defense Council, Inc.
2345 Yale Street
Palo Alto, CA 94306
Attn: T. Lash

Nuclear Fuel Services
6000 Executive Blvd., Suite 600
Rockville, MD 20852
Attn: W. H. Lewis

Radiation Research Association
3550 Hulen Street
Fort Worth, TX 76107
Attn: R. M. Rubin

Science Applications, Inc.
1200 Prospect Street
P.O. Box 2351
La Jolla, CA 92037
Attn: L. Simmons

Science Applications, Inc.
1385 George Washington Way
P.O. Box 857
Richland, WA 99352
Attn: M. J. Szulinski

Swedish Embassy
600 New Hampshire Avenue, NW
Washington, DC 20037
Attn: Lars G. Larsson

Quadrex Corporation
1700 Dell Avenue
Campbell, CA 95008
Attn: I. Wall

403 253

DISTRIBUTION (cont):

The University of Arizona
Department of Hydrology and Water Resources
Tucson, AZ 85721
Attn: D. R. Davis

University of California
Chemical, Nuclear, and Thermal Engineering Dept.
5532 Boelter Hall
Los Angeles, CA 90024
Attn: G. Apostolakis

University of Pittsburg
Physics Department
Pittsburgh, PA 15260
Attn: B. Cohen

University of Rhode Island
Graduate School of Oceanography
Kingston, RI 02881
Attn: G. R. Heath

University of Tennessee
Department of Nuclear Engineering
Knoxville, TN 37916
Attn: J. B. Fussell

Woods Hole Oceanographic Institution
Woods Hole, MA 02543
Attn: C. D. Hollister

Environmental Evaluation Group
320 East March Street
P. O. Box 968
Santa Fe, NM 87583
Attn: R. Holland

Chalmers University of Technology
Goteborg
Sweden
Attn: Jan Rudberg

GSF - Institut fur Tieflagerung
Wissenschaftliche Abteilung
D-3392 Clausthal-Zellerfeld
Berliner Strasse 2
West Germany
Attn: L. Dole

Duetsche Gesellschaft für Wiederaufarbeitung von
Kernbrennstoffen mbH
Bünteweg 2, 3000 Harnover 71
West Germany
Attn: D. R. Proske

Hitachi Shipbuilding and Engineering Co., Ltd.
Plant and Machinery Design Office
3-40 Sakurajina 1-Chome
Konoshana-Ku
Osaka, SS4
Japan
Attn: A. Onodera

403 254

DISTRIBUTION (cont):

Theoretical Physics Division
Building 8.9
AERE Harwell, Oxfordshire
OX 11 ORA
England
Attn: D. Hodgkinson

Nuclear Chemistry and Reactor Division
Hahn-Meitner - Institut fur Kunforschung - Berlin
D-1000 Berline -39
Glienecken Strasse 100
West Germany
Attn: H. W. Levi

OECD Nuclear Energy Agency
38 Boulevard Suchet
75016 Paris
France
Attn: F. Gera

Boite Postale No. 48
92260 Fontenay-Aux Roses
France
Attn: P. Pages

Studsvik Energiteknik AB
Reactor Systems and Nuclear Safety
S-6111 82 KYKOPING
Sweden
Attn: L. Devell

Royal Institute of Technology
Dept. Land Improvement and Drainage
S-10044 Stockholm 70
Sweden
Attn: R. Thunuik

Physikalisch-technische Bundesanstalt
Bundesallee 100
D-3300 Braunschweig
West Germany
Attn: H. Rothemeyer

Bundesanstalt für Geowissenschaften und Rohstoffe
Stillweg 2
D-3000 Hannover 51
West Germany
Attn: K. Tietze

Kärnbränslesäkerhet
Fack
S-102 40 Stockholm 5
Sweden
Attn: T. Papp

Battelle-Pacific Northwest Laboratories (2)
P.O. Box 999
Richland, WA 99352
Attn: H. C. Burkholder
K. Schneider

403 255

DISTRIBUTION (cont):

Lawrence Livermore Laboratory (2)
P.O. Box 808
Mail Code L 156
Livermore, CA 94550
Attn: R. Heckman
A. Kaufman

Oak Ridge National Laboratory
P.O. Box X
Oak Ridge, TN 37830
Attn: R. E. Brooksbank, Bldg 3019

Savannah River Laboratory (2)
Aiken, SC 29801
Attn: J. T. Buckner
M. L. Hyder

1223 R. R. Prairie
1223 R. G. Easterling
1223 R. L. Iman (5)
1418 M. S. Tierney (3)
2330 E. Barsis
4400 A. W. Snyder
4410 D. J. McCloskey
4411 M. Berman
4412 J. W. Hickman
4412 G. J. Kolb
4413 N. R. Ortiz
4413 D. C. Aldrich
4413 J. E. Campbell (15)
4413 R. M. Cranwell
4413 F. Donath (5)
4413 J. C. Helton (5)
4413 B. S. Langkopf
4413 S. J. Niemczyk
4414 G. B. Varnado
4415 D. A. Dahlgren
4416 R. T. Dillon (5)
4500 E. H. Beckner
4510 W. D. Weart
4511 G. E. Barr
4511 L. R. Hill
4514 M. L. Merritt
4514 J. P. Brannen
4530 R. W. Lynch
4537 A. R. Lappin
4538 R. C. Lincoln
4538 S. Sinnock
4538 H. D. Stephens
4541 L. W. Scully
4541 H. C. Shefelbine
4723 W. P. Schimmel
4737 L. C. Bartel
5521 M. G. Marietta
5533 A. J. Chabai
5611 W. H. Ling
5613 L. B. Hostetler
5636 J. K. Cole
5641 H. T. Davis (3)

403 256

DISTRIBUTION (cont):

8252 P. K. Lovell
Attn: T. Devlin
8320 T. S. Gold (2)
8330 G. W. Anderson
Attn: P. D. Gilder
8266 E. A. Aas
3141 T. L. Werner (5)
3151 W. L. Garner (3)
For DOE/TIC (Unlimited Release)
DOE/TIC (25)
(For R. P. Campbell, 3172-3)

403 257

Org.	Bldg.	Name	Rec'd by *	Org.	Bldg.	Name	Rec'd by *

* Recipient must initial on classified documents